International Energy Agency (IEA) Greenhouse Gas (GHG) Weyburn-Midale CO_2 Monitoring and Storage Project

Final Technical Report

Project start date: October 1, 2010

Project end date: September 30, 2015

Principal authors:

Norm Sacuta

Aleana Young

Kyle Worth

December 22, 2015

DOE Award Number: DE-FE0002697

Petroleum Technology Research Centre

220, 6 Research Drive

Regina, Saskatchewan, Canada

S4S 7J7

info@ptrc.ca

(306) 787-7497

Disclaimer

Abstract

The IEAGHG Weyburn-Midale CO_2 Monitoring and Storage Project (WMP) began in 2000 with the first four years of research that confirmed the suitability of the containment complex of the Weyburn oil field in southeastern Saskatchewan as a storage location for CO_2 injected as part of enhanced oil recovery (EOR) operations. The first half of this report covers research conducted from 2010 to 2012, under the funding of the United States Department of Energy (contract DE-FE0002697**),** the Government of Canada, and various other governmental and industry sponsors. The work includes more in-depth analysis of various components of a measurement, monitoring and verification (MMV) program through investigation of data on site characterization and geological integrity, wellbore integrity, storage monitoring (geophysical and geochemical), and performance/risk assessment. These results then led to the development of a Best Practices Manual (BPM) providing oilfield and project operators with guidance on CO_2 storage and CO_2-EOR. In 2013, the USDOE and Government of Saskatchewan exercised an optional phase of the same project to further develop and deploy applied research tools, technologies, and methodologies to the data and research at Weyburn with the aim of assisting regulators and operators in transitioning CO_2-EOR operations into permanent storage. This work, detailed in the second half of this report, involves seven targeted research projects – evaluating the minimum dataset for confirming secure storage; additional overburden monitoring; passive seismic monitoring; history-matched modelling; developing proper wellbore design; casing corrosion evaluation; and assessment of post CO_2-injected core samples. The results from the final and optional phases of the Weyburn-Midale Project confirm the suitability of CO_2-EOR fields for the injection of CO_2, and further, highlight the necessary MMV and follow-up monitoring required for these operations to be considered permanent storage.

Table of Contents

Executive Summary

Saskatchewan is home to the Weyburn and Midale oilfields, which together contain the largest amount of injected anthropogenic CO_2 in the world. Approximately 30 million tonnes (Mt) of CO_2 are already stored in these two reservoirs, with an additional 2.8 Mt added annually in the course of CO_2 enhanced oil recovery (CO_2-EOR). In 2000, the Canadian government and the research organization Petroleum Technology Research Centre in Regina, Saskatchewan launched the IEAGHG Weyburn-Midale CO_2 Monitoring and Storage research project. It was a research program endorsed and sponsored by the International Energy Agency Greenhouse Gas R&D Programme (IEAGHG) and funded in part by the U.S. Department of Energy (DE-FE0002697). It was also endorsed by the Carbon Sequestration Leadership Forum. The project was an international collaboration which brought together Canada, the U.S., the European Community, and Japan, as well as numerous other industrial and government sponsors. The research program integrated research studies with the $2 billion commercial EOR and storage operations of Cenovus Energy and Apache Canada at the Weyburn and Midale oil fields in the Williston Basin, Saskatchewan.

Phase One of the project was completed between 2000 and 2004, prior to the start of this USDOE grant number, and is referenced but not covered in this USDOE report. Research was completed in four themes: geological characterization; prediction, monitoring, and verification of CO_2 movement; CO_2 storage capacity and distribution predictions and the application of economic limits; and long-term risk assessment of the storage site.

This report covers the Final Phase (Base) and Final Phase (Optional) of the research project (the former initiated in 2005 and completed in 2012, the latter begun in 2013 and completed in 2015) as outlined in DE-FE0002697's Statement of Project Objectives. Findings on the Base Phase are presented in the following four technical themes:

1. Site characterization and geological integrity
2. Wellbore integrity
3. Storage monitoring (geophysical and geochemical)
4. Performance/risk assessment

Advanced measurement and monitoring methods were used to inform databases that were then used to create advanced models to demonstrate the security of the containment complex for storing CO_2 at the Weyburn-Midale fields.

Site characterization successfully examined the two main components of the study area – namely the stability of the seals above the reservoir (both the immediate anhydrite caprock and the subsequent aquitard layers above it) and the oil field into which the CO_2 was being injected. The long-term integrity of the containment seal was determined to be sound based on the

measurement and monitoring of geochemical and geomechanical data and its impact on the deformation of the caprock, which incrementally widens and narrows microfractures during periods of pressure increase and decrease, respectively. Close integration of site characterization, modelling, and monitoring programs were important to achieving a defensible predictive capability in the modelling work.

Wellbore integrity work involved looking at new well design considerations, well remediation and conversion methods, well abandonment considerations and, in the long term, well integrity monitoring. The results of the WMP wellbore work – which included examining an older well in the field that had been under CO_2 exposure for many years – illustrated that it is crucial to identify all wells which might potentially come into contact with CO_2, and that prior to injection these wells should be identified and the previous completion and drilling information examined. This is particularly true for wells in the area that might penetrate the caprock.

The data from geochemical analyses in the project documented the progressive movement away, in the reservoir, from baseline conditions as CO_2 injection progressed. None of these chemical changes in the reservoir were seen to affect the caprock above the field, assuring the safe storage of CO_2. Equally, the surface monitoring of ground water at over sixty locations and soil gases, which were compared over the 12 years of the project to baselines taken before the project began and to a control site outside the injection area, demonstrated that containment of the CO_2 in the reservoir was occurring. Passive seismic monitoring throughout the project with a surface array and with downhole tools illustrated that no significant seismic events occurred. The largest induced seismicity was – 1, and attributed less to the injection of CO_2 and, rather, to the resulting increased movement of fluids and oil towards the production wells.

Finally, performance/risk assessment work conducted in the Final Phase of the WMP indicated that the storage of CO_2 in the field was within acceptable boundaries of risks compared to other industrial scale projects. A ranking of scenario severities and likelihoods was conducted using the RISQUE method, and key assets identified through interviews and meetings with local residents.

The results from the Final Phase of the WMP, which came to an end in 2012, culminated in the publication of a Best Practices Manual (BPM) entitled *Best Practices for Validating CO_2 Geological Storage: Observations and Guidance from the IEAGHG Weyburn-Midale CO_2 Monitoring and Storage Project* (Hitchon, 2012). The Optional phase of the WMP (2013 to 2015) expands on the lessons learned from and summarized in the BPM by further developing and deploying applied research tools, technologies, and methodologies to Saskatchewan CO_2-EOR and storage commercial operations, with specific attention paid to CO_2-EOR fields that may be transitioning to CO_2-storage.

This Optional Phase was named *Saskatchewan CO_2 Oilfield Use for Storage and EOR Research Project* (SaskCO_2USER), and conducted applied research for commercial applications in high priority areas of CO_2-EOR operations that could be relevant to future recognition of CO_2 geological storage. Research was undertaken by North American and European organizations, which provided an international context to findings for commercialized applications. The research reported here advanced the rich datasets generated from the Weyburn and Midale fields to better inform prospective CO_2-EOR operators, government regulators and service providers on how to maintain the safety and integrity of CO_2 storage, improve the efficiency of CO_2-EOR operations, and limit liabilities and risks during operations.

Sections 6 through 12 of this report covers work in the Final Optional Phase, grounded in seven key research areas:

1. Overburden monitoring
2. Casing corrosion
3. Passive seismic monitoring
4. Well design
5. Minimum data sets
6. History-matched modelling
7. Geology

While these seven research areas were considered distinct, significant collaboration and overlap between projects occurred. This aided researchers in achieving the goal of providing recommendations for CO_2-EOR operators looking to transition to permanent storage of CO_2. While the Weyburn Midale field was used in the project, results described herein can be applied to other CCUS projects with adjustments made for differences in site locations and site-specific regulations.

Additional overburden monitoring work examined and ranked the best technologies available for overburden monitoring of CO_2-EOR sites, and what components of a storage site (wellbores, caprock, etc.) require monitoring to assure long term storage. Pulsed-neutron logging can measure whether CO_2 leakage is occurring above the formation. Wells remain the highest potential leakage routes, and performing cement bond logs as baselines early in a well's life will be useful for later examinations as wells age. The most useful imaging for locating CO_2 in the subsurface remains 3D seismic monitoring of the plume. The monitoring technology ranking provided may aid in the creation of a monitoring plan for other CO_2 storage projects. It affords an operator a method of objectively comparing monitoring technologies to address specific needs related to site-specific risks, regulatory regimes, and economics.

The casing corrosion work looked at two characteristic corrosion scenarios in five case study wells. The first was where corrosion is more prevalent in the lower wellbore near production

perforations and the other involved more widespread corrosion closer to the surface. It is possible that different corrosion mechanisms other than water- and/or CO_2-initiated pathways were involved in each of the five studied wells. In all cases, the rate of casing corrosion increased near the lower sections of the well near the existing production perforations. Additional research monitoring time-lapse casing corrosion and cement integrity under varying operating conditions is critical to understanding not only the factors that influence corrosion and cement degradation under field conditions but to quantify the rates and probability at which they occur. While several factors influencing wellbore integrity were discovered in this study, completion methods play a critical role in mitigating their impact. More laboratory analyses will be required to fully investigate and pinpoint the key corrosion mechanisms involved.

Additional passive seismic analyses were also done in the Optional Phase. Researchers analyzed one year of data from the three broadband stations deployed at the Weyburn Midale field. No local seismic events were detected during the monitoring period. Indeed, the USGS and CNSN catalogues did not detect any events within 300 km of the site during the monitoring period, and no regional events were detected on the array. The only earthquakes picked up by the array were tele-seismic arrivals from large, global events. In-situ stress conditions at the Weyburn-Midale field were also examined in relation to preexisting literature. These conditions were used to estimate the optimum orientation of a fault for it to be reactivated by injection, requiring a pore pressure increase of 10MPa above hydrostatic to re-activate such a fault. Pore pressures at Weyburn have not exceeded such values, which may account for the fact that no large, induced events have occurred in this area.

Well design work in the Optional Phase successfully outlined the design and costing of CO_2-EOR wells drilled or converted to injectors. The project highlighted key well design requirements, operational procedures and proper material selection to construct wells in CO_2-EOR and storage reservoirs that have a high degree of wellbore integrity for all phases of the well's potential life cycle. For example, operational procedures to maximize fluid containment reliability within the injection zone including tubular connection selection options were developed, and options for future horizontal well designs and investigative techniques of minimizing potential risk of losing seal against sour CO_2 laden fluids were built.

Minimum dataset recommendations were developed in the Optional Phase through modelling the reservoir flow system, and predicting storage capacity and monitoring CO_2 migration so as to meet a certain level of risk assessment. The analyses included examining the formation petrophysical properties that are most sensitive to the CO_2 geological storage prediction and migration monitoring; establishing a large spatial range of data acquisition that captures the potential CO_2 migration range, which is normally larger than the storage complex; developing the smallest spatial resolution of sampling measurements, determined from local geologic and

petrophysical heterogeneity and anisotropy; and, establishing the smallest temporal span of data acquisition for the purpose of reservoir monitoring.

Additional history matching experiments were conducted as part of the Optional Phase, using inversion of time-lapse seismic data from the Weyburn field for permeability and porosity. The experiments were conducted on a sector model for a single well pattern carved out of a larger coarse-grid model containing 9 patterns. These additional modelling results results show that in all cases the updated models were able to reproduce the synthetic measurements with much greater accuracy than before history matching, with reasonable values for the permeability and porosity updates since the initial modeling done prior to 2012. The addition of production data produced a compromise result in terms of the fit to the seismic maps and to the well data. These history matching experiments compared favourably with earlier reported approaches and suggest continued refinement of history matching models should provide a useful tool for operators developing CO_2-EOR scenarios.

Finally, examination of core samples from the Weyburn field that have been under long-term exposure to CO_2 provided a means of determining the effect of injected CO_2 on the rock framework and the pore space in the reservoir. Two pressure observation wells with extensive cores were recently drilled in the Weyburn field, providing a unique situation to observe the influence of 15 years of injected CO_2 on the mineralogy and rock properties of the reservoir. Comparing the recently drilled wells to wells that were drilled prior to CO_2 injection revealed the effects of injected CO_2 on the reservoir matrix. The analytical techniques that were utilized to determine if the injected CO_2 has impacted the reservoir include QEMSCAN to determine the mineralogy and porosity, SEM images, and cathodoluminescent analysis. It was found that the volume of pore space did not consistently change from the pre-CO_2 wells to the post CO_2 wells; the post CO_2 injection wells did not have the same overgrowth and appeared “clean.” Investigating the internal structure of the calcite crystals (still progressing) will determine if they formed after CO_2 injection or if they were already present.

1.0 Introduction and Background

In 2000, the Canadian government and the research organization Petroleum Technology Research Centre (PTRC) located in Regina, Saskatchewan, launched the IEAGHG Weyburn-Midale CO_2 Monitoring and Storage Project (WMP). It was endorsed and sponsored by the International Energy Agency Greenhouse Gas R&D Programme, the Government of Canada, and the U.S. Department of Energy (DOE) along with other industry and government sponsors. It was also endorsed by the Carbon Sequestration Leadership Forum (CSLF). The project was an international collaboration which brought together researchers from Canada, the U.S., the European Community, and Japan, as well as numerous other industrial and government researchers.

The intent of the research program was to enhance the knowledge base and understanding of CO_2 geologic sequestration conducted with enhanced oil recovery (EOR) operations, and to understand controlling conditions and processes such as site suitability, reservoir capacity, reactive transport, storage integrity, wellbore performance, risk assessment, and effective monitoring and validation techniques. The research program integrated studies with the $2 billion commercial EOR and storage operations of Cenovus Energy and Apache Canada at the Weyburn and Midale oil fields in the Williston Basin in southeast Saskatchewan. Storage of CO_2 in these two fields up to December 2015 is estimated to have reached just under 30 Mt, with about 2.8 Mt of anthropogenic CO_2 being added annually. The CO_2 in this project was and is still being captured from the Great Plains Synfuel plant in Beulah, North Dakota and pipelined 320 km north to the Weyburn and Midale fields.

The tasks discussed in this final report detail the work completed in the Final Phase (Base) of the Weyburn-Midale project (USDOE funding beginning October 2010) and in the Final Phase (Optional) of the program between 2013 and the end of 2015 (Saskatchewan CO_2 Oilfield Use for Storage and EOR Research – SaskCO_2USER) as outlined in the DE-FE0002697 "Scope of Project".

The Final Phase (Base) of the Weyburn-Midale project, ending in 2012, conducted research in the following four technical themes: site characterization and geological integrity; wellbore integrity; storage monitoring (geophysical and geochemical); and performance/risk assessment. The ultimate objective of the WMP's final phase was to support research in these four technical themes and to support efforts necessary to integrate results and data into comprehensive scientific documents available to the public. This occurred in 2012 with the publication of a *Best Practices for Validating CO_2 Geological Storage: Observations and Guidance from the IEAGHG Weyburn-Midale CO_2 Monitoring and Storage Project*, henceforth referred to as BPM in this report (Hitchon, 2012) and in 2013 with the publication of a special supplement of the International Journal of Greenhouse Gas Control (Wildgust and Tontiwachwuthikul, 2013).

In 2014, work began on the Optional Phase of research arising out of the final phase of WMP by expanding upon the lessons summarized in the BPM and further developing and deploying applied research tools, technologies, and methodologies to Saskatchewan CO_2-EOR and storage oil fields commercial operations, with the aim of assisting regulators and operators in transitioning CO_2-EOR operations into permanent storage. This phase, referred to in this report as "Saskatchewan CO_2 Oilfield Use for Storage and EOR Research" or SaskCO_2USER, had seven key research projects including: evaluating the minimum dataset for confirming secure storage; overburden monitoring; passive seismic monitoring; history-matched modelling; proper wellbore design; casing corrosion evaluation; and assessment of post CO_2-injected core samples. The SaskCO_2USER project conducted this research using field-based data collected during the first twelve years of research in the WMP (2000-2012) and final results are reported here. A special supplement in the International Journal of Greenhouse Gas Control will be appearing in the fall of 2016.

2.0 Weyburn-Midale Final Phase – Geological Characterization and Storage Performance Predictions

In 2004, the first phase of the Weyburn-Midale Project published a summary report (Wilson and Monea, 2004) identifying the regional hydrogeology of the Midale Beds, the location of the Weyburn/Midale oilfield. The field (which is broken into the two named units but are in fact the same formation) is located within the Williston Basin, sedimentary rock across the southern Canada prairie and the northern USA. The oil-bearing beds are made up of carboniferous (Mississippian) carbonate deposits, about 30m thick, and the reservoir rests about 1.4 km below surface.

The first phase of the WMP identified the reservoir's trapping mechanism as a dense layer of anhydrite up to 11m thick immediately above the oil reservoir. This caprock was determined to be an effective natural seal to prevent the migration of fluids upwards. The initial phase of research also suggested that further storage integrity is provided by the presence of the overlying Watrous Formation – a mixed sequence of anhydritic shales and silts.

2.1 Geological Characterization – Approach and Methodology

Further work on characterization during the final phase of the WMP included refinement of the geological model at both local and regional scales. This included a better resolved stratigraphy, incorporation of additional wellbores (see Figure 1) and assessment of regional hydrogeochemistry, hydrogeology and groundwater flow systems. A major component of this final phase work was the use of invasion percolation modelling of potential leakage pathways –

providing an important reference for risk assessment and identification of priority wellbores (Wildgust et al., 2013).

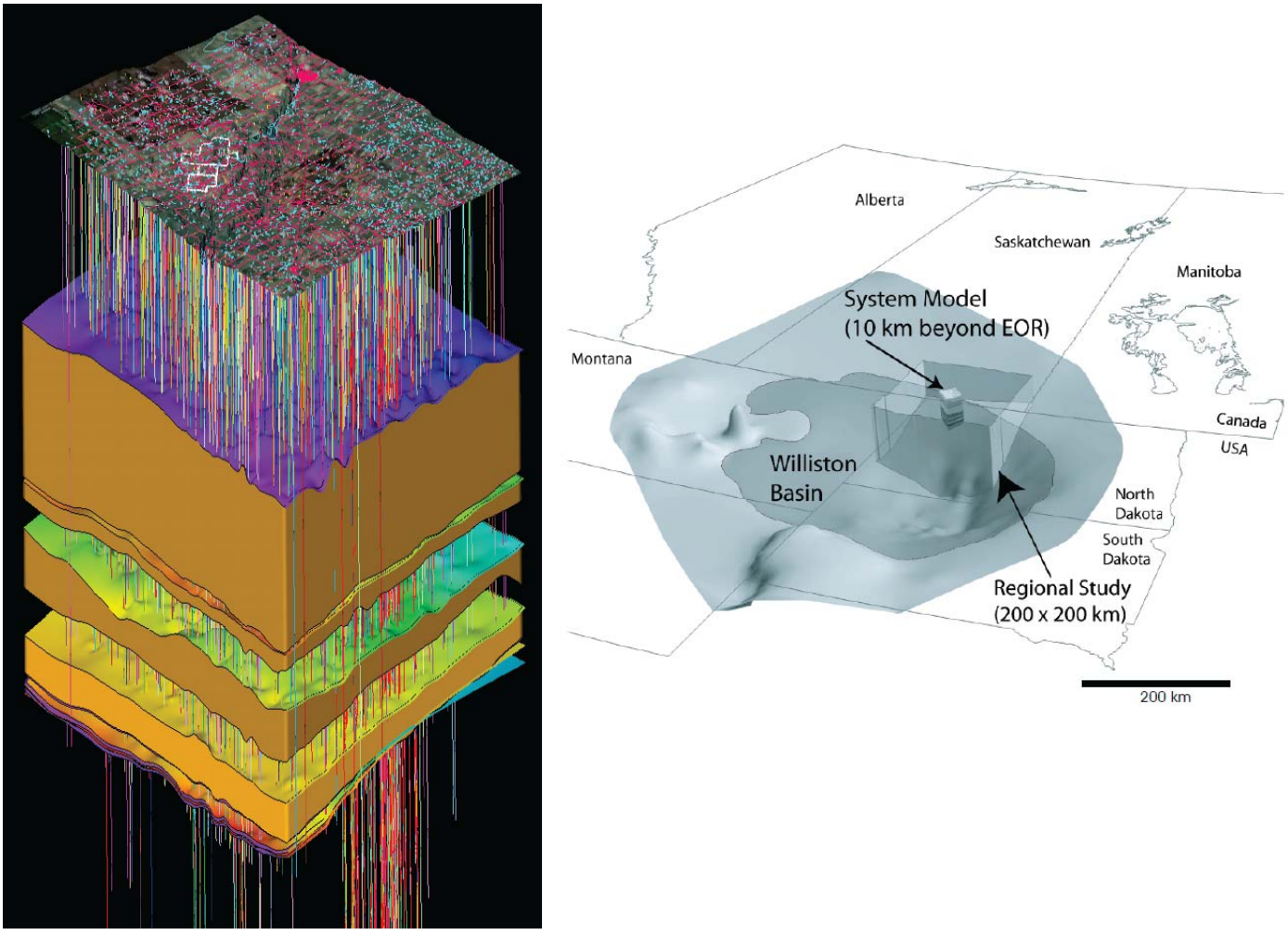

Figure 1 – a) Schematic of the final phase geological model showing the digital elevation of the topographic surface and all well penetrations (about 800) used to create the final model and b) location of the Weyburn field and study area in southwestern Canada and in relation to north central United States (Rostron et al., 2012).

Characterization work also expanded through the analysis and comparison of the Weyburn field to a natural analogue (naturally occurring accumulation of CO_2) within Palaeozoic strata of the Williston Basin located 400 km southwest of the field (see Figure 2). The natural analogue used for comparison to the Weyburn field – the Duperow Formation – was shown to be very similar

to the Midale Beds in terms of whole rock chemistry, mineralogy, mineral chemistry and porosity distribution.

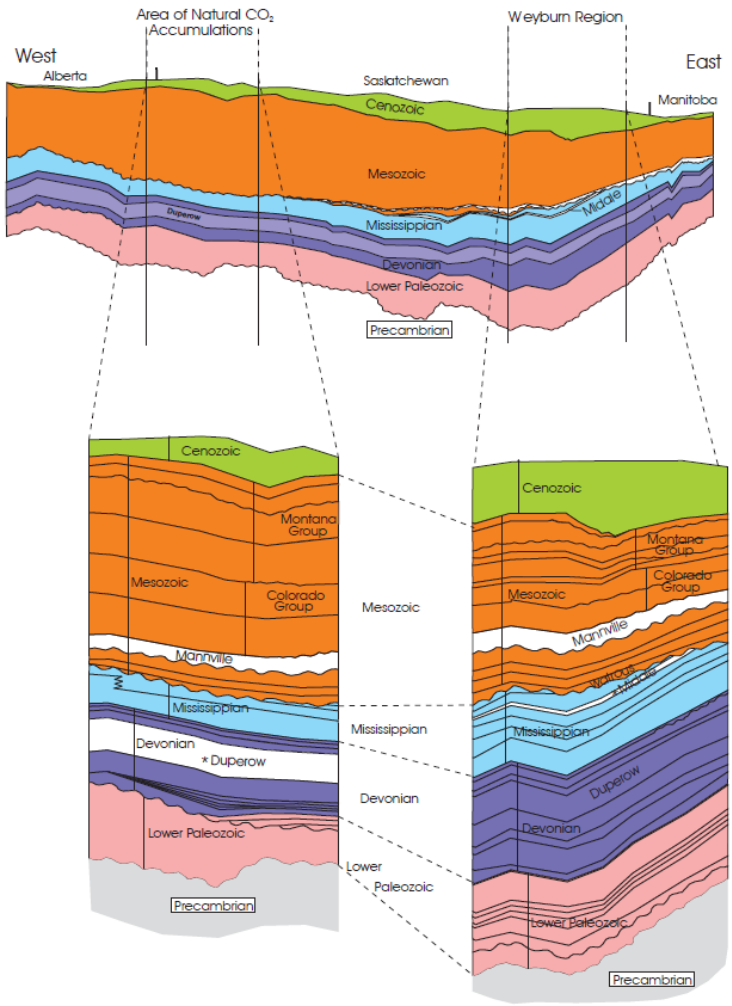

Figure 2 – Comparison of the geological setting between the natural analogue site in southwestern Saskatchewan and the Weyburn Injection site. The extracted geological columns indicate the broad similarity of geological settings in both (Rostron et al., 2012).

The comparison between the natural analogue location and the Weyburn field indicated the suitability of the injection location for long-term safe storage, both from a geochemical and geophysical perspective:

> …anhydrite-rich evaporites, sometimes containing authigenic K-feldspar, form aquitards which, in the case, of the Duperow appear to have prevented loss of CO_2 over a time frame that may extend as long as 50 million years (cf, Lake and Whittaker, 2006). The stratigraphic sequences and observed mineral assemblages in both the Mississippian

> and Devonian carbonate-evaporite strata in the Williston basin are similar to that of the Madison Limestone, where CO_2 storage for ~50 m.y, in the absence of mineral trapping…. Clearly, carbonate-evaporite sedimentary sequences are capable of long-term CO_2 storage based on hydrodynamic and solubility trapping alone for substantial periods of time. (Ryerson et al., 2013)

Additional work was also conducted in the areas of containment and hydrogeology. The former included examining the hydraulic properties of the seals above the reservoir, which helped to determine the properties of the primary seal (Midale Evaporite) and larger seal (Watrous Formation) and their suitability for containing the injected CO_2. Examining the hydrogeology of the aquifers above these principal seals was done to determine – should a leak occur from the main containment area – what the flow rate and direction of CO_2 movement would be since both of these are controlled by the hydrogeology of the layers above the containment zone (Rostron et al., 2012). Ultimately, this hydrological work helped to identify the preferential pathways for cross formation fluid flow, provided an assessment of the competence of low-permeability strata (i.e. the aquitards), characterized the hydrochemistry of each aquifer, and provided all the hydrological data to be used in predictive modelling and risk assessment work (Rostron et al., 2012).

The geomechanics and geochemistry of the containment structure were also examined as a part of the site characterization and containment work; these are examined more fully in the Section 4.0 of this report. In terms of geomechanics and geophysics, the potential implications of pressure buildup as CO_2 is injected into the reservoir were a focus of research. Key data types examined to alleviate these concerns included geophysical logs, small scale hydraulic fracture tests, and the examination of core samples in laboratory programs such as triaxial compression tests (Rostron et al., 2012). Geochemical compositions of the formation waters were completed to understand water-rock and well cement-rock interactions and determine if these interactions maintained the integrity of storage. These chemistries were also studied to identify and trace migrating formation fluids. Ultimately, much of this data was then complied and applied to the completion of storage performance predictions through numerical modeling and the development of an effective reactive transport model (Johnson and Rostron, 2012).

2.2 Geological Characterization – Results and Recommendations

Arising from the site characterization and modelling work done in the WMP, a number of recommendations have been brought forward, and are described in more depth in the "Characterization" and "Storage Performance Predictions" sections of the BPM (Hitchon, 2012). The main recommendations and results are paraphrased here.

Geological characterization of the Weyburn study area was constrained, as all potential storage sites are, by data distribution in the stratigraphic unit with the minimum information, in other words, the deepest zero-flow boundary (in the case of the Weyburn field, the Precambrian basement). All strata from this boundary to the surface were mapped, although not in the same detail. For other storage projects, it is recommended that as much mapping detail as possible be used at the beginning, since it is not known if 'lumping' of such data will be required later (Rostron et al., 2012) particularly for modelling work.

The geological framework of the characterization included standard features such as maps of stratigraphic surfaces and bed thickness, as well as cross-sections. These were developed from well logs and seismic information. Faults, fracture zones, joints and other lineaments received particular attention as possible conduits for fluid flow (natural or induced) (Rostron et al, 2012). In the Weyburn area, structures resulting from salt dissolution proved to be important. When applying these findings to other sites, however, the issue could be faults associated with salt domes. Being able to detail the geological history of a project's area of study, and the impact of that history on rocks and the containment zone is of key importance.

The geological models constructed from the data available at Weyburn was designed to fit into numerical modelling (in the case of this project, invasion percolation modelling) in order to conduct potential leakage scenarios and to test variations in CO_2 injection rates and locations.

Hydrogeological characterization was completed in both hydrostratigraphy and hydrochemistry. The former examined the properties of the aquifers, aquitards and aquicludes, and the latter the properties of formation waters. The program examined these two areas of hydrogeology through different means:

(1) the geological framework
(2) measurements of such properties of the rocks as permeability and porosity, obtained from drill stem tests, core analysis, and pump tests, and
(3) analysis of major, minor, and trace elements, and of stable isotopes in formation water. (Rostron et al., 2012).

In any storage project, identifying the seals above the storage area and their safety/stability is critical. This was done in the WMP through

(1) core analysis of shales and other rocks, to determine permeability and porosity
(2) vertical pressure gradient plots
(3) steep gradients in permeability and salinity distribution maps
(4) fracture mapping, using seismic AVO Analysis, and
(5) comparison with natural analogues such as nearby reservoirs with high-CO_2 natural gases. (Rostron et al., 2012).

It is particularly important to identify the characteristics of not just the primary seal (which is directly above the injection zone) but also the ultimate seal (which should be regionally extensive). This should be supplemented with a study of the regional stress field, to determine the nature and magnitude of the horizontal stresses in the containment zone (Rostron et al., 2012).

Reactive modelling was used to compile much of the data collected in the geochemical and geophysical analyses work done in the site characterization to simulate the transfer processes among fluids and the rock mass (both aquifer properties and minerals). The models illustrate the impact of reaction-dependent changes in reservoir porosity and permeability, with respect to the integrity of the reservoir and seals, and extrapolate into the future. The invasion percolation models used in the WMP differ significantly in behaviour from traditional Darcy flow simulations, in that the simulation is dependent upon threshold and capillary pressures, rather than permeability and viscosity (Johnson and Rostron, 2012). In percolation models, the work at Weyburn showed that pooling of CO_2 could determine both vertical and lateral breach points as a function of threshold pressure.

Ultimately, proving the safe containment of CO_2 at the Weyburn site was at the root of the characterization and geological containment work completed in the WMP. The long-term integrity of the containment seal was determined to be sound based on the measurement and monitoring of geochemical and geomechanical data and its impact on the deformation of the caprock, which incrementally widens and narrows microfractures during periods of pressure increase and decrease, respectively (Johnson and Rostron, 2012). Close integration of site characterization, modelling, and monitoring programs proved important to achieving a defensible predictive capability in the modelling work. In particular, continuous minimization of discrepancies between predicted and measured results through refined modelling and monitoring (successful history matching) proved essential for long-term forecasting of containment integrity and also validated the reliability and accuracy of modeling CO_2 partitioning and distributions in the Weyburn field (Uddin et al., 2013).

3.0 Weyburn-Midale Final Phase – Wellbore Integrity

Over 4000 wells exist in the WMP's final phase study area, both active and enclosed wells, drilled and in operation at various points since the field began operating in the mid-1950s. At approximately 40 km by 50 km, the study area represents a well density consistent with many other oilfield operations in North America of similar ages and sizes. Because the site began operations in the 1950s, almost forty years before CO_2-EOR operations began, wells have been constructed and enclosed to varying standards that have developed over this period. As a

result, wellbores represent the most likely pathways to the surface for potential leaks of CO_2 (as well as other substances in the reservoir) and were determined to be major areas of focus in the final phase of the WMP research program.

3.1 Wellbore Integrity – Approach and Methodology

The first task was to identify the parameters most likely to affect the integrity of wells, and this was in part determined through an investigation of the available well records. Cementing, debonding between casings and the wall rock, and channelling in the cement itself were all identified and possible containment risks and important areas of study (Wildgust and Tontiwachwuthikul, 2013).

Final phase research focussed on access granted by Cenovus Energy (the EOR operators at Weyburn) to one of the older wells in the field – a 1957 well that had been exposed extensively to CO_2. To fully examine this well, the WMP commissioned a specially adapted downhole tool to conduct pressure testing of the cement sheath of the well, and to obtain core samples (see Figure 3).

Figure 3 – On the left is a close view of cement, within the coring bit, after it was retrieved from the well. Right, is the modified version of Penatrator's MaxPERF tool. The lower half of the tool (dark part near the bottom) contains a milling bit, which was used to mill through the casing. (Photo courtesy of PTRC and Chris Hawkes)

This tool provided important information on the hydraulic characteristics of the well and the integrity of the cement. Several additional tools were also used in the field trials at the well, including a Schlumberger Isolation Scanner, Schlumberger Sonic Scanner, Baker Atlas High-Resolution Vertilog™ , a Schlumberger Reservoir Saturation Tool (RST), and the Expro borehole camera to image 'perforations' and cement sampling holes, in order to assess the geometry of these penetrations (Hawkes and Gardner, 2012).

The purpose of wellbore research was two-fold. The first was to use the sample well to investigate the effect of CO_2 on the existing wells in the Weyburn field and determine their effectiveness at maintaining containment. But an equally important goal arising from the field research was a set of recommendations detailing the methods to be used for securing well integrity when building new wells in CO_2-EOR projects, as well as remediating and converting existing and/or abandoned wells in existing CO_2 fields (Hawkes and Gardner, 2012). See Figure 4 for a cross section of the test well.

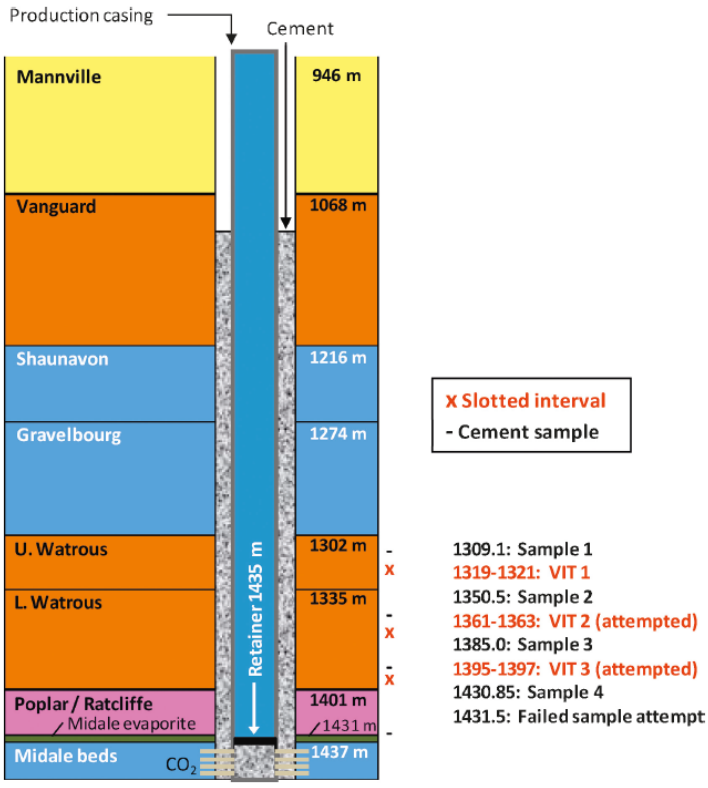

Figure 4 – Well construction diagram for the lower portion of the test well. Approximate depths of slotted intervals and cement sampling are shown. (Hawkes and Gardner, 2013)

The field test program was broken into four key elements:

(1) Cased-hole logging to assess casing and cement.
(2) Vertical interference (pressure transient) tests to assess the hydraulic properties of the cemented annulus within the Watrous Formation; i.e., to assess the potential for fluids to migrate along the cemented annulus and damage the site's regional seal.
(3) Cement sampling, to directly verify the presence of cement (as inferred from non-destructive logs) and to provide samples for laboratory analysis.
(4) Supplementary tests to assist in geological characterization of the site; specifically, small-scale hydraulic fracture (mini-frac) tests to assess minimum in situ stress magnitudes in the Watrous Formation, and water sampling in the Gravelbourg Formation (a saline aquifer overlying the Watrous Formation) in order to fill a gap in the project's database of pore water compositions. (Hawkes and Gardner, 2013)

Additional studies in the program (Deisman et al., 2013 and Choi et al., 2013) provide details on the new tools used in the field testing program above, and on the potential effects of corrosion on the steel casings of wells that are not cemented adequately to keep such casings from direct contact with CO_2.

3.2 Wellbore Integrity – Results and Recommendations

Findings and recommendations were identified in five key areas: well integrity assessment; new well design considerations; well remediation and conversion; well abandonment considerations; and, well integrity monitoring. These results are provided in more detail in the BMP (Hitchon, 2012).

In terms of well integrity assessment, the results of the WMP wellbore work illustrated that it is crucial to identify all wells which might potentially come into contact with CO_2, and that prior to injection these wells should be identified and the previous completion and drilling information examined. This is particularly true for all wells in the area that might penetrate the caprock (whether those wells are for oilfield production, or for access to deeper formations underlying the oilfield in question). Once the wells have been identified it is recommended that they be ranked in the order of importance for monitoring and investigation, in particular abandoned wells, which should have their cement plugs and sheathes investigated (Hawkes and Gardner, 2013).

New wellbores – both into existing CO_2-EOR fields and into those that anticipate CO_2 injection in the future – will require different things depending on the qualities of the CO_2 being injected, and the compounds already in the reservoir. What is most important is the effectiveness and quality of the casing cement job, and the project also identified that surface casing provides an additional protection over the life of the well, particularly for maintaining the integrity of

ground water sources. Wells used for CO_2 injection (as opposed to oil production wells) should use CO_2 resistant cement formulations right across the whole injection zone. While the CO_2 itself may be mostly void of moisture, thus lessening the chances of affecting the integrity of the cement, the storage zone itself (the oil field) may already have significant moisture or acids present. This means resistant cement should be used throughout the injection zone (Hawkes and Gardner, 2012).

In existing CO_2-EOR operations such as the Weyburn and Midale fields, well remediation and conversion of wells drilled prior to the beginning of injection are of main concern. A risk assessment of the wells in questions might indicate that remediation may be required prior to the commencement of CO_2 injection, or could be deferred depending on the time it takes for the CO_2 plume to reach the wellbores. In some CO_2-EOR operations, older production wells may be considered by operators as CO_2 injection wells, but these wells may not be cemented all the way to surface It is recommended that if these wells are to be used for injection, remedial operations focus on the injection zone only.

In wells that have been abandoned or enclosed in a CO_2-EOR field, the quality of cementing is of the greatest concern. Plugs must be set across the reservoir caprock with all enclosed wells, to assure that the CO_2 does not leave the containment zone. The WMP wellbore research also concluded that it is highly desirable to extend those plugs across the intermediate porous zones adjacent to the sealing zones (Hawkes and Gardner, 2012) Most importantly, an evaluation of the cement sheath in a well casing is the first step to determining what might be required in enclosing a well (the well tools used in the WMP are good examples of effective tools that could be used to examine such sheathing).

Finally, on-going well integrity monitoring is important in CO_2-EOR operations. Oilfield operations, whether using CO_2 or not, usually conduct monitoring in and around wells for natural gas, sour gas, and other emissions. For CO_2-EOR operations, it is recommended that new CO_2 injection wells conduct baseline studies for:

(1) logs for zonal isolation, cement evaluation, and casing inspection
(2) tests for soil gas migration, and
(3) a surface-casing vent flow test, both for hydrocarbons and CO_2, with carbon isotopes on all gas components containing carbon. (Hawkes and Gardner, 2012).

Monitoring programs at CO_2-EOR fields will vary depending on the initial testing done prior to injection, since meaningful comparisons with post-injection data can only be made if effective baselines have been completed. Any post-closure monitoring will vary significantly project to project, and depend on the depth of the storage location and how close wells and affiliated operations are to significant populations.

4.0 Weyburn-Midale Final Phase – Storage Monitoring

Much of the most important fundamental research conducted in the WMP's final phase focussed on geophysical and geochemical monitoring of the reservoir and overburden. The project examined the shallow ground water system, soil horizons (including, specifically soil gas), the formation water and the oil in the reservoir (Johnson and Rostron, 2012). This kind of data is particularly important for setting baselines for the project (which began its measurement and monitoring program in 2000) and comparing those data with additional measurement that occurred over the intervening years when injection was occurring. In one particular case where a local farming family near Weyburn claimed CO_2 was leaking onto their land and ground water in 2010, baseline results and a comparison with additional soil gas and ground water measurement results taken on the farm, were definitive in proving the CO_2 injected at Weyburn remained securely in place (Trium, 2011; Sherk et al., 2011; Romanak et al., 2013; Beaubien et al., 2013).

4.1 Storage Monitoring – Approach and Methodology (Geochemical Analyses)

With respect to ground water sampling, more than 60 wells in the area of interest were examined for their water chemistry. Local potable wells were examined prior to CO_2 being injected in 2000, and sampled at six times in the life of the project, up to 2011, to monitor for any changes in chemistry (SO_4, HCO_3, Na, Ca, Mg Cl and K were all measured). Figure 5 illustrates results for a typical well in the region.

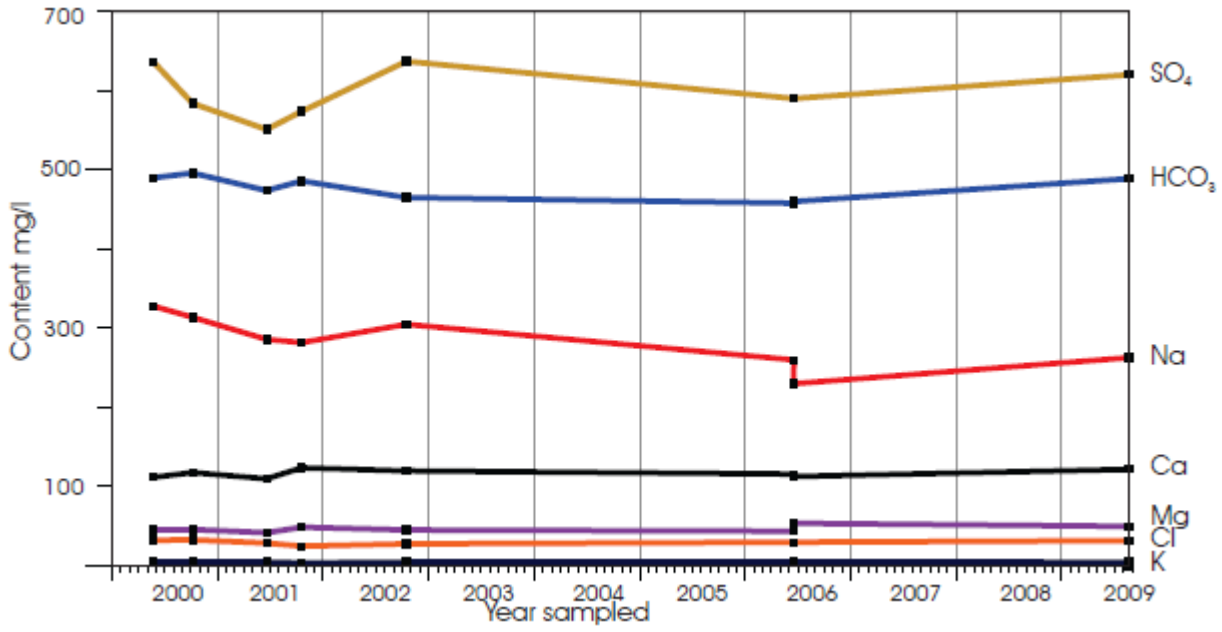

Figure 5 – Water sampling results taken at seven different intervals, plotted as a comparison (Johnson and Rostron, 2012)

The quality of ground water in the Weyburn-Midale area is highly variable, and many of the water wells, prior to injection of CO_2 into the oil field, had components that exceeded Drinking Water Standards from Saskatchewan Environment. Most importantly, what the ongoing measurements indicated was that there were no significant increases in CO_2 or HCO_3, illustrating that breakthrough of CO_2 to the surface had not occurred (Johnson and Rostron, 2012).

A second important component of the ongoing monitoring above the injection zone included soil gas monitoring. Soil gas measurements are an effective means of determining if CO_2 from the containment zone is leaking into the biosphere, but such measurement and monitoring must take into consideration the time of year when measurement were done (which will have varying results depending on seasons and weather conditions) and the specific topology of study areas:

> Continuous monitoring at specific locations may be necessary to track variations in soil gas concentrations, isotopic signatures, or surface fluxes that fingerprint CO_2. These fingerprints may be transient due to changes in pressure, temperature, soil moisture, precipitation, and wind, and might be missed by discontinuous measurements. Determination of carbon isotopes on gas components can often be used effectively to identify the source of CO_2. (Johnson and Rostron, 2012)

Several components were measured during the soil pas program. These included:

(1) soil gas content of CO_2, oxygen, argon, light hydrocarbons, helium, and radon
(2) stable and radiogenic carbon isotopes
(3) surface CO_2 fluxes, and
(4) near-surface atmospheric CO_2 content. (Johnson and Rostron, 2012)

Measurement techniques included discontinuous single depth measurement, discontinuous depth-profile measurements, and (particularly where environmental conditions might be highly variable) continuous monitoring. For a full description of these individual methods, please see the BPM (Hitchon, 2012).

In the case of soil gas measurements, a test control location (the Minard Farm) outside of the injection zone was used throughout the testing period. Tests were conducted yearly between 2000 and 2006, and again in 2011. Figures 6 and 7 provide comparisons between measurements at the control site and other measurement locations throughout the injection area. Note that the 2011 results shown in Figure 6 also included the Kerr farm, the location where local residents alleged a leak of CO_2 to the surface. The results clearly indicate that the soil gas measurements were not unusual and, in fact, were consistent with those taken above and outside the injection area, indicative of naturally occurring CO_2.

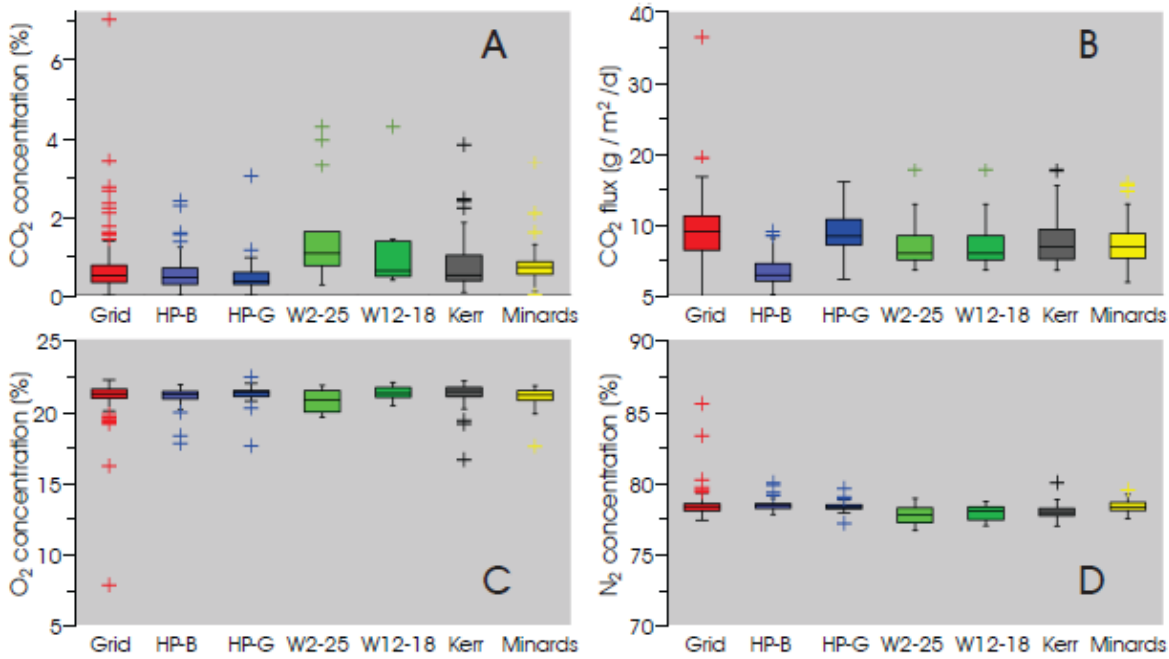

Figure 6 – Comparison of soil gas samples for 2011, including A) CO_2 %, B) CO_2 flux (G/m2/d), C) oxygen % and D) nitrogen (%).(Johnson and Rostron, 2012)

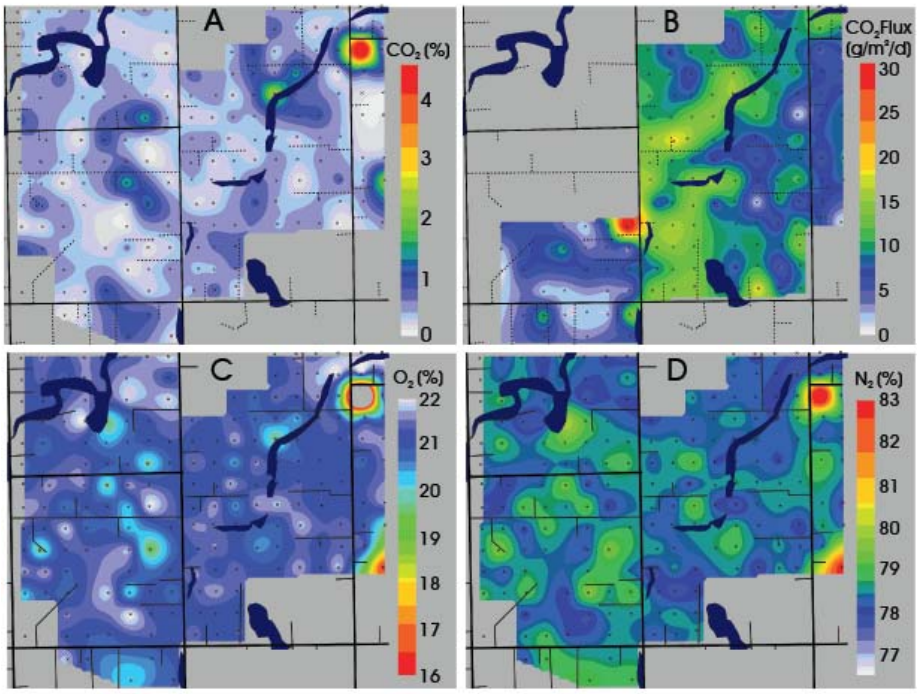

Figure 7 – Maps of the soil gas content (measured in 2011) at the Minard Farm control site. A) CO_2 (%), B) CO_2 flux ($g/m_2/d$), C) oxygen (%), and D) nitrogen (%). Dark blue areas are surface water bodies. These grids are compared and contrasted with grids at test sites above the injection zone.

In addition to the surface geochemical monitoring, the project also examined reservoir fluids, including formation water and gases. This was done to evaluate how "CO_2 partitioning occurs among the hydrocarbon, aqueous and mineral phases" in the reservoir (Johnson and Rostron, 2012). In turn, this information becomes important for modeling and forecasting the processes that help keep CO_2 stored in aquifers (such as hydrodynamics, solubility and mineral trapping). Alkalinity, downhole pH, calcium and stable isotopes were all examined. Figure 8 illustrates the changes in alkalinity in the Weyburn reservoir over the years of CO_2 injection. Such information, as well as pH levels, is important for determining, for example, fluid effects on wellbores and their casing.

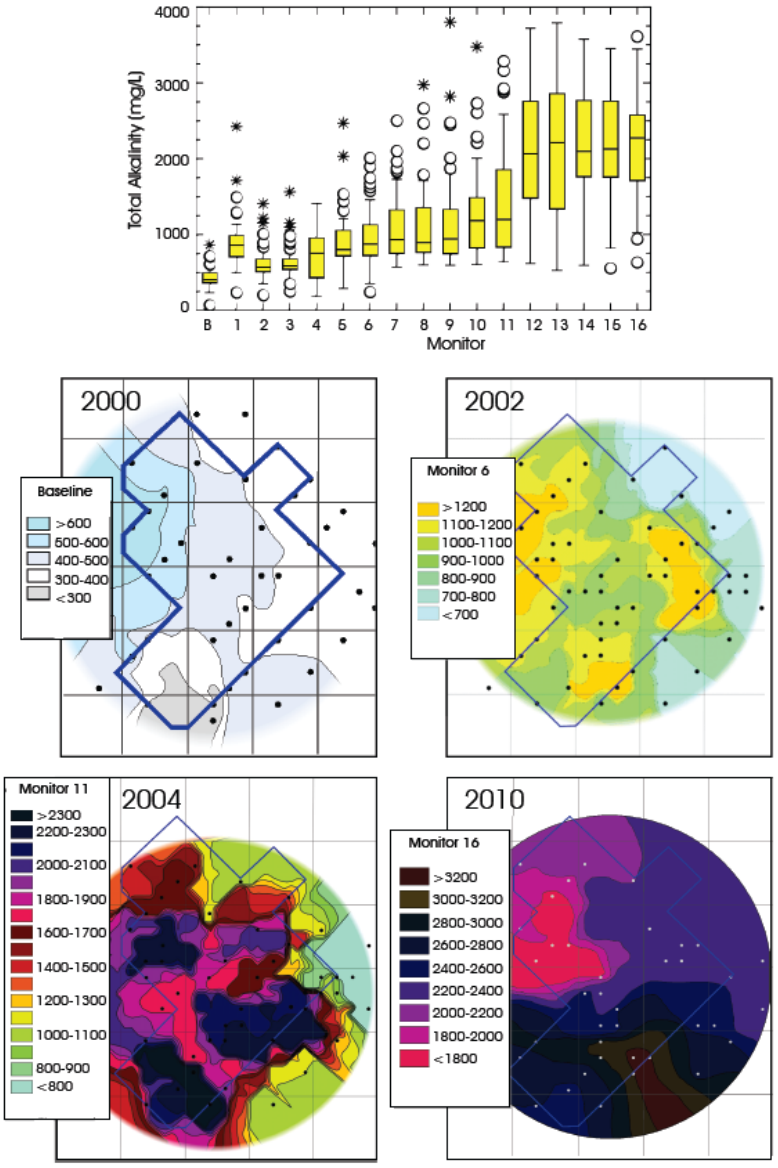

Figure 8 – Changes in alkalinity in the Weyburn Field (mg/L) over a decade of injection. (Johnson and Rostron, 2012)

4.2 Storage Monitoring – Approach and Methodology (Geophysical Analyses)

The WMP's geophysical monitoring provided an effective way to track the distribution of CO_2, and the associated pressure plume in the Weyburn field. It also provided the means by which deformation of the storage container (caprock and secondary seals) could be catalogued.

Surface-based 3D seismic methods provided the best means of monitoring the distribution of CO_2 over a large area in the subsurface, with a combination of AVA intercept (I) and gradient (G) used to distinguish CO_2 saturation from pressure-related effects (White, 2012). Downhole seismic techniques tested during the project included continuous downhole passive seismic monitoring to detect microseismicity, and active source downhole seismic methods to acquire high resolution subsurface images.

The geophysical monitoring in the project had five main objectives (White, 2012):

(1) Tracking the CO_2 plume within the primary storage reservoir.
(2) Detecting migration of CO_2 above the primary reservoir seal.
(3) Providing constraints on perturbations in the subsurface pressure field.
(4) Assessing the significance of injection-related microseismicity with respect to the integrity of the CO_2 storage container and potential effects on surface infrastructure.
(5) Continuing calibration of the geological model used for predictive modelling.

Two of the major successes of the geophysical testing at Weyburn were the results from downhole passive seismic monitoring methods used to measure the induced seismicity at the site in relation to CO_2 injection, and the use of 3D time-lapse seismic surveys to investigate the decreases in acoustic impedance observed near the CO_2 injection wells. For the latter, Figure 9 shows the regions of negative amplitude difference associated with the effects of CO_2 injection and oil production (2002, 2004 and 2007 readings specifically).

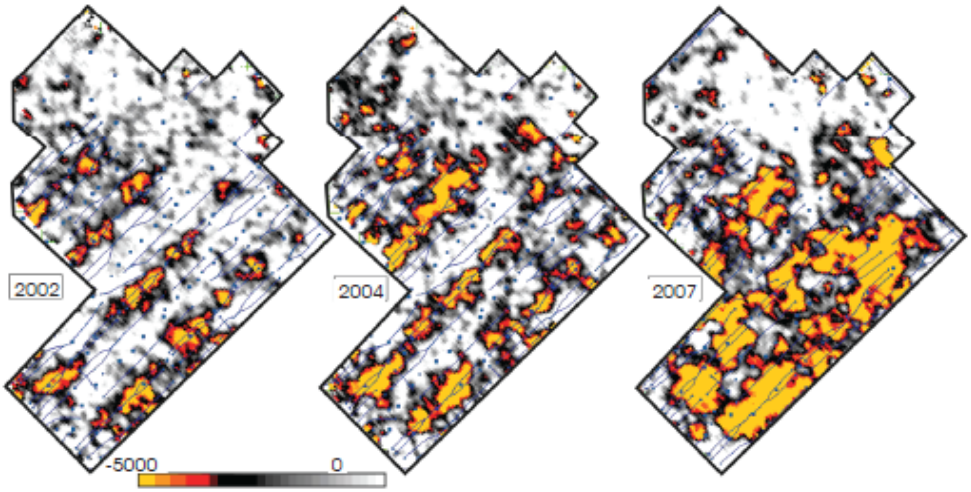

Figure 9 – Maps of seismic amplitude difference for the Weyburn field.

Microseismic measurement at the site indicated that a majority of the seismic events had magnitudes ranging between -3.0 and -1.0, and that their main occurrences were located near production wells, perhaps indicating that the seismic events were less a result of CO_2 injection and more likely related to the production and increased flow of oil. Microseismic event locations did correlate "with the time-lapse seismic amplitude anomaly (indicating the presence of CO_2 or an increase in pore pressure)", but there "did not appear to be a systematic correlation of seismic events with CO_2-related anomalies" (White, 2012). Figure 10 shows the locations and sizes of microseismic events.

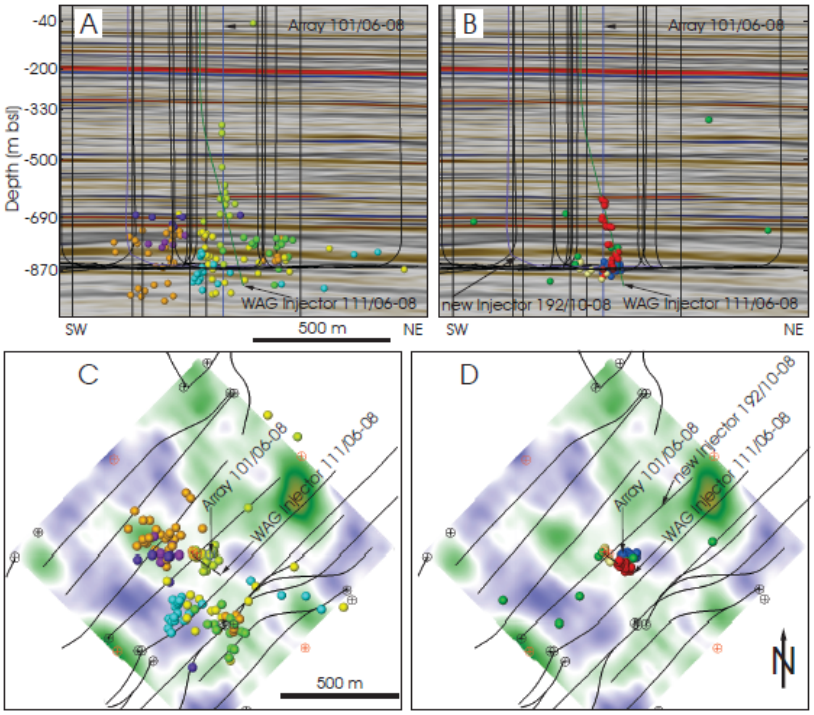

Month	Field Activity	Microseismicity / Symbol
0 to 5	Pre-injection period incl. completion of 121/06-08 vertical injection well	· 30 events · tight cluster associated with completion of 121/06-08 injection well · others are diffuse about production wells 191/09-08 and 191/10-08
4	Start-up of water injection	· increased noise shuts down array
5	Switch to CO_2 injection	· 12 events prior to start of CO_2
7	Production well 191/09-08 shut-in	· 15 events
9 to 11	Increased CO_2 injection rate	· 34 events
26 to 86	Unknown	· 18 events · 20 events over 4 hours · 9 sporadic events
73	Shut-in of 102/06-08 injector for later abandonment	· 52 events occur 4 days later
86	Drilling of new horizontal injector (192/10-08)	· 9 events
87	Completion and perforation shots in 111/06-08 observation well	· 32 events

Figure 10 -- Vertical section view of microseismic events recorded from: A. August, 2003 to January, 2006, and B. from January 2006 to December 2010. C. and D. Plan view of the same events. The 2004 minus 2000 time-lapse seismic amplitude difference map for the reservoir interval (from 3D surface seismic) forms the coloured backdrop. Green-to-orange and blue background colours represent negative and positive amplitude changes, respectively (White, 2012).

The WMP integrated data from 3D seismic, reservoir geochemical monitoring and production/injection data using reactive transport modelling and geostatistical techniques. Application of amplitude versus-offset-and-azimuth techniques to seismic data provided a method for interpreting and mapping anisotropy in the caprock, with good correlation to core measurements (Wildgust and Tontiwachwuthikul, 2013).

Other methods considered and tested in the geophysical analysis of the Weyburn site are discussed elsewhere in more detail (White, 2012; White, 2013 a, b) including their success or failures. The technologies examined for possible application at the site included InSAR, long-electrode electrical resistance tomography (LEERT), time-lapse gravity measurements, and forward seismic modelling.

4.3 Storage Monitoring – Results and Recommendations

Geochemical monitoring and geophysical monitoring were proven to be a critical component of the WMP. The data from geochemical analyses documented the progressive movement away, in the reservoir, from baseline conditions as CO_2 injection progressed. Equally, the surface monitoring of ground water and soil gases demonstrated that containment of the CO_2 in the reservoir was occurring, and the changes recorded in the deep formation were not happening in the surface measurements, which indicated no changes resulting from CO_2-EOR operations. The surface geochemical baseline work also proved to be of critical import in disproving claims of CO_2 leakage made in 2011 and studied by four three separate groups (Trium, 2011; Romanak et al., 2011; Romanak et al, 2013; Beaubien et al., 2013).

The WMP highlighted that for soil gas and ground water measurements, a survey before the injection of CO_2 begins in any storage project is of critical importance, since the baseline data provide the basis of comparison for all results measured after injection has begun. Also of critical import in the measurements taken throughout a monitoring program is to acknowledge the differences that will exist when measurements are taken in different seasons and in different biosphere environments. These variations will also play a significant role in determining baselines for measurements and in the comparison of baseline results to any subsequent survey.

A key observation arising from ground water measurements is that sampling the same wells throughout the program often proved difficult. The Weyburn area does not have many potable wells that meet drinking water standards, leading to many farmers and residents abandoning the wells originally measured by the project in favour of new water sources. This meant some wells could not be retested. As a result, project researchers suggest that new projects avoid this potential problem by “developing a dedicated monitoring network of small-diameter wells

strategically located throughout the study area" (Johnson and Rostron, 2012) in order to avoid having to access abandoned wells over a prolonged testing period.

Downhole fluid testing (reservoir fluids) required the same baseline testing prior to injection beginning. The project found that changes in formation water happened slowly following initial arrival of the CO_2 plume, mostly because of the slow kinetics of water-mineral interactions (Johnson and Rostron, 2012). Compared to the analysis of surface geochemical readings, interpretation of the reservoir data versus anticipated results is usually straightforward and related to CO_2 migration and CO_2–oil–formation water–rock interactions. Unlike surface readings, where the environment makes temporal variations due to natural processes quite significant, variations in the deep subsurface are more subtle (Johnson and Rostron, 2012).

Finally, geochemical analyses at Weyburn found that close integration of site characterization, modelling, and monitoring programs through iterative inter-program feedback was essential to facilitate continuous optimization of monitoring activities (Johnson and Rostron, 2012).

As mentioned, the geophysical work at Weyburn involved monitoring the subsurface distribution of the CO_2, along with the pressures associated with the plume and looking for any possible pressure-induced damage of the containment complex. A number of considerations should be made by any CO_2-storage project in determining its geophysical measurement program, including "rock type (clastic or carbonate), porosity, depth, thickness, and resident pore fluids, as well as the quantity of CO_2 to be injected, the expected areal extent of the CO_2 plume, the surface infrastructure or physiography, and the number of wells in the field" (White, 2012).

Several downhole monitoring technologies were used in the WMP. Use of passive seismic monitoring suggested that the method is not particularly well suited for directly tracking the CO_2 plume, but the downhole passive seismic monitoring provided a better sensitivity to the measuring of microseismic events during and after injection (White, 2012). For downhole arrays, greater horizontal location accuracy can be provided by deploying arrays in more than a single well. Multiple wells will provide better location of events in the reservoir and help with evaluating the stresses being placed on containment. Going one step further, crosswell and VSP provide a means of acquiring subsurface images with even better resolution. The project also found that surface-based 3D seismic proved to be the most effective means of monitoring the subsurface distribution of CO_2 (White, 2013b).

5.0 Weyburn-Midale Final Phase – Performance/Risk Assessment

When the WMP began in 2000, risk assessment processes for the storing of CO_2 in the subsurface were mostly non-existent. In the first phase of the project (2000-2004) the site characterization work and its examination of storage performance through modeling and other

methods, as well as existing well regulations for oil and gas, were seen as adequate for providing confidence in the capabilities of the reservoir to safely contain the injected CO_2.

With the development of best practices and advances in risk assessment methods, the final phase of the WMP developed a comprehensive risk assessment program for the site, seeking to provide assurance to the general public and to government sponsors/regulators that the Weyburn field could securely store 30MT of CO_2 in the present and going forward over many thousands of years.

5.1 Performance/Risk Assessment – Approach and Methodology

The final phase risk assessment work at Weyburn took into account a number of areas of concern: human health and safety, the environment and security of the biosphere above the injection zone, the safety of operations and systems involved in the CO_2-EOR injection and storage – and perhaps most importantly for regulators and governments – identifying the factors that might affect future operations and storage such as availability of CO_2, reservoir capacity and changes in economic conditions (Chalaturnyk, 2012).

The risk assessment process developed and followed on the risk assessment standards for CO_2 storage developed in Canada by the Canadian Standards Association through a panel that included some of the research scientists involved with the work done in the WMP – in fact, the project was instrumental in helping to set standards for CO_2 risk assessment going forward. That risk management process (CSA Z741-11) is indicated in Figure 11.

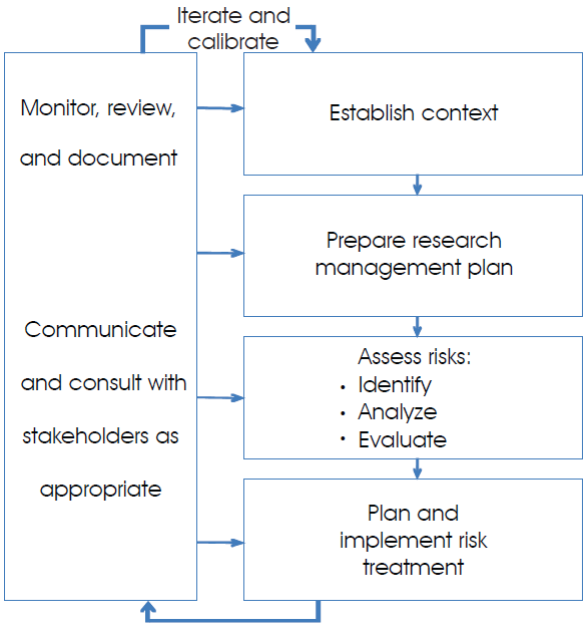

Figure 11 – Schematic of the risk management process for CO_2 geological storage (Canadian Standards Association, 2012)

This risk assessment work was based on the deliberations of an expert panel that met three times in workshops between 2007 and 2010, and that helped investigate different scenarios by which migration of CO_2 might occur to the biosphere. Many different scenarios were put forth, and a risk ranking system was developed to assist participants in determining the likelihood of the scenarios put forth (see Table 1).

Qualitative Description	Order of Magnitude Annual Probability	Basis
Certain	1 (or 0.999, 99.9%)	Certain, or as near to as makes no difference
Almost certain	0.2–0.9	One or more incidents of a similar nature have occurred here
Highly probable	0.1	A previous incident of a similar nature has occurred here
Possible	0.01	Could have occurred already without intervention
Unlikely	0.001	Recorded recently elsewhere
Very unlikely	1×10^{-4}	It has happened elsewhere
Highly improbable	1×10^{-5}	Published information exists, but in a slightly different context
Almost impossible	1×10^{-6}	No published information on a similar case

Table 1 – Guide to assist participants in ranking the likelihood of events to occur (Chalaturnyk, 2012)

Of key importance in the risk assessment process was consultations with local stakeholders above and near the containment zone/oil field. These included local landowners, residents of communities in the area including the City of Weyburn, and local elected officials. Meetings were held with those local stakeholders in 2009 and in 2011 to help identify assets that were particularly of concern to members of the community. Identifying what assets might be affected by the highest ranked containment risks developed through the risk assessment process was important for maintaining community support for the project and explaining effectively to community members how the perceived project risks could and were being mitigate to protect those most valued assets.

Several scenarios were examined during workshops with the expert panel. The methodology used in determining the risk for each scenario is detailed elsewhere (RISQUE methodology, see Bowden and Rigg, 2004 and Bowden et al., 2013 a,b), but the main features of the methodology include:

Stage 1. Establish the context.

Stage 2. Identify the risk.

Stage 3. Analyse the risk.

Stage 4. Develop risk management strategies.

Stage 5. Implement a risk management strategy.

When ranking and quantifying risk events, the RISQUE method allows for defining a risk quotient through multiplying the likelihood that an event will occur by its severity (or consequence) should it occur (Chalaturnyk, 2012). For example, while a large meteorite strike on the oilfield might have a very high, catastrophic consequence, it has an extremely low likelihood of occurrence. Therefore the overall risk quotient would be very low.

5.2 Results and Recommendations – Performance/Risk Assessment

The principal risks identified with containing the CO_2 in the Weyburn reservoir were identified, ranked by the expert panel and are listed in Figure 12.

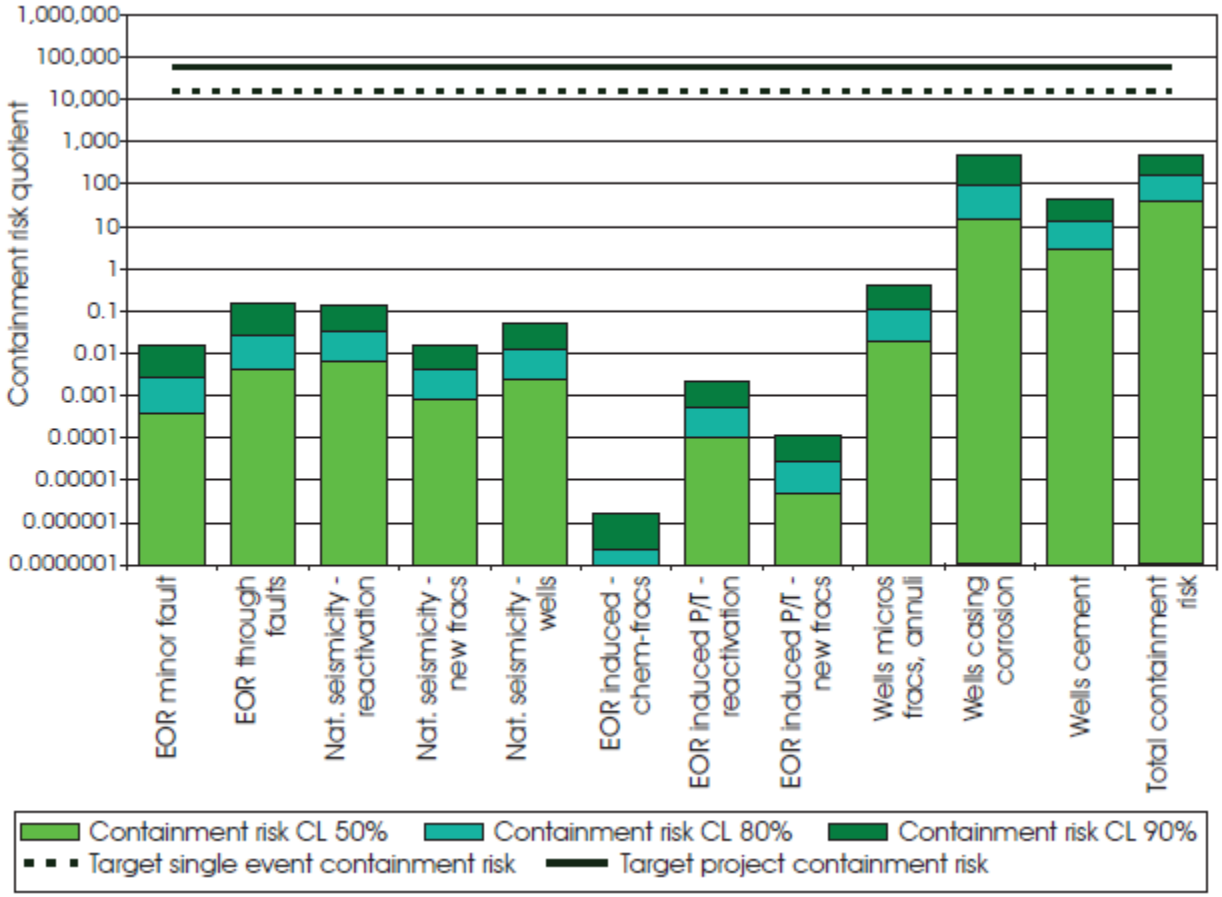

Figure 12 – Comparison of event containment risk (Chalaturnyk, 2012).

Risk quotients are identified for each of the risk events identified by the expert panel. Chalaturnyk (2012) provides the following assessment of the figure above:

The right hand column represents the total containment risk quotient for the project. The graph shows the risk quotients on a log scale and therefore each horizontal gridline on the graph represents an order of magnitude difference from the lines above and below. The different shades of the green bars on the graph represent the risk quotients at different levels of confidence. The 50% confidence level (CL 50%) estimate represents an optimistic assessment of the risk quotient, or one that will be exceeded in 50% of cases. The CL 95% represents a conservative estimate of risk (one that will only be exceeded in 5% of cases), and the CL 80%, a level that is typically used by organizations in planning. The magnitude of the difference between the CL 95% and CL 50% estimates represents the degree of uncertainty in the consequence and/or likelihood estimates.

The column on the right side of the risk profile shows that the total containment risk (calculated as the sum of all individual risk events to the left) is around two orders of magnitude lower than the target acceptable level of containment risk (indicated by the solid green horizontal line). All individual risk events pose acceptable risk with respect to the defined target, with wells generally posing the highest risk to containment. The highest risk event ('well-casing corrosion') still presents a relatively low risk, being about 10 to 30 times less than the target risk for single events (indicated by the dashed green horizontal line).

Risk assessment work completed in the WMP indicated that the storage of CO_2 in the Weyburn field, and all associated risks identified, were within acceptable boundaries of risk comparable to other industrial projects.

The process for identifying unplanned events in relation to CO_2 geological storage, and determining what could happen as a result of those events, required, in the words of the investigators "a different mindset from that typically required for performance assessments" in other industries (Chalaturnyk, 2012). This was in part because the injection of CO_2 for permanent storage is a relatively recent phenomenon, and the WMP was at the leading edge of developing a process for proper risk assessment.

The risk assessment done in the WMP was conducted in tandem with the detailed geological characterization of the site, the geochemical and geophysical work and the investigation of wellbore integrity; for most projects going forward, risk assessment work should begin ahead of such work, and involve ongoing cycles of review as the other work progresses, updating information as it becomes available (Chalaturnyk, 2012).

6.0 SaskCO_2USER (WMP Optional Phase) – Overburden Monitoring

The objective of overburden monitoring in the Optional Phase was to provide insight into the deployment of cost-effective monitoring for CO_2-EOR operators through an investigation of

regulatory regimes and identified risks. Technologies and processes were ranked and strategies developed based on risk-principles, with end goals of cost-efficiency and monitoring effectiveness. Schlumberger Carbon Services was awarded the study of and reporting on overburden monitoring. This project used available data from the twelve years of research at the Weyburn and Midale fields to identify potential pathways for CO_2 leakage. An in-depth review of previous work helped determine potential leakage pathways. Likely pathways for CO_2 migration from CO_2-EOR reservoirs include geologic pathways such as faults or through fracture networks, heterogeneous seals, or along wellbores.

6.1 Overburden Monitoring – Approach and Methodology

The objective of overburden monitoring was to provide insight into technologies and strategies for deploying cost-effective monitoring for CO_2-EOR operators and demonstrating storage performance. The goal was to create a methodology for evaluating monitoring technologies and quantifying their utility vis-à-vis identified risks (severity vs. likelihood). While this project was specific to the Weyburn-Midale field, the methodology used is applicable to other CO_2-EOR operators. The strategies developed in this project are risk based, and designed to allow for the efficient allocation of resources while monitoring the highest risk potential leakage pathways in formations, faults, and wellbores above the storage reservoir/storage complex. The primary objectives or risks related to CO_2 storage were identified as:

- Containment of the injected quantity
- Conformance of the site to expected performance
- Assurance that CO_2 injection will not endanger health, safety, or the natural environment.

Containment is focused on verifying that the injected CO_2 is contained within the storage reservoir and confirming that it has not migrated laterally or vertically out of the reservoir. Although it is considered to be unlikely for this project, the integrity of any storage complex can be potentially compromised by faults, fractures, inadequate caprock, or unforeseen conditions. The mechanical integrity of wells, both old and new, is an additional source of risk. Integrity monitoring is designed for early detection of compromised performance to ensure corrective steps can be taken. Quantifying the amount of injected CO_2 is very difficult under almost any risk scenario. No single monitoring technology can provide an accurate and unequivocal estimate of CO_2 under all risk scenarios. The approach to this practical challenge is to apply multiple technologies so that all targets are monitored for indication of leakage. Within this project, the technologies were selected and ranked based on proven usefulness for assessing CO_2 storage performance, both inside and outside of the storage complex. Technologies also had to be accessible at a reasonable cost.

Conformance is focused on verifying that the quantity of CO_2 injected can be measured with accuracy at the surface. This quantity is then used to determine how much CO_2 is present in the storage complex until monitoring technologies indicate otherwise. Conformance monitoring is also focused on demonstrating to regulators and other stakeholders that the development of the CO_2 plume is safe and predictable. Indicators like injection pressure, reservoir pressure and CO_2 plume development are measured with those technologies. Results are used to verify, calibrate, and update geologic models and predictive reservoir simulations. As more monitoring data becomes available, the pressure and CO_2 plume development become more predictable. Many techniques that address conformance also address integrity through the evidence of results within the storage zone and negative results outside of it.

Assurance monitoring is critical to CO_2 projects. As CCS and CCUS projects are relatively novel, and often poorly understood by some stakeholders, assurance monitoring is required to demonstrate that CO_2 injection has no adverse effects on health, safety, and/or the environment. As discussed, integrity monitoring is used to provide early detection in the unlikely event of CO_2 escape from the storage complex. Comparatively, assurance monitoring is designed to monitor for potential impacts at the surface and near surface. If the CO_2 plume develops as predicted, assurance monitoring techniques will yield null results, indicating that the CO_2 is contained and not detectable at or near the surface.

Evidently, risk management and monitoring are closely associated in CCUS projects. This project combined analysis of the efficacy of monitoring techniques across these three levels, with risk assessments – identifying the highest risk areas and linking them directly to real-world monitoring technologies. The technologies selected are well established and known to be effective, suitable for commercial application. The technologies were sorted into three primary categories: containment, conformance, and assurance. Each was then grouped by target, i.e. caprock integrity, groundwater, natural seismicity, etc.

A review of all previous WMP data related to risk assessment, leakage scenarios, and monitoring was completed, including:

- Data and results from previous risk assessments
- Well integrity data from the Weyburn-Midale field
- Previous invasion percolation theory-based simulation results for potential leakage pathways
- Current EOR monitoring plans applicable to the field and past deployments of technologies.

The primary deliverable, a ranking of monitoring techniques, was ultimately produced. This product used the Weyburn-Midale field as a case study. A methodology was developed to quantify the benefit of each monitoring technology based on that technology's ability to

provide monitoring for each and various risk scenarios. Twenty nine technologies were considered. All of the recommended monitoring techniques were evaluated in regard to risk, cost-benefit, and technical applicability. All technologies were considered vis-à-vis regulatory requirements across jurisdictions. These technologies were then ranked in a matrix. This matrix was also evaluated in regards to annual monitoring costs in regards to both the technology schedule and the unit cost of each deployment. Those with high cost and low benefit were disregarded.

This project established that risk assessment can be used to identify wells for mitigation and monitoring. While not all impact and likelihood categories can be monitored, many can. Within CO_2 -EOR fields, individual wells can be identified and selected for monitoring. The selection of technologies should use technologies that monitor individual wells (such as logging and in-well sensors) as well as technologies that provide area coverage for categories of risk (such as dedicated monitoring wells). Conclusions in regards to high risk areas and technology recommendations were made. The ranking of monitoring technologies can aid in the creation of monitoring plans for CCUS projects. While this ranking was specific to the Weyburn-Midale field, it is adaptable to other CO_2 -EOR fields interested in converting from CCUS to CO_2 -EOR, with adjustments made on a site-specific basis. The ranked technologies will also assist operators in meeting regulatory requirements by allowing a minimum selection of technologies that meet operational and regulatory requirements.

The project was divided into five tasks:

1. Review of previous work
2. Physical characteristics of leakage pathways
3. Review of emerging regulatory regimes
4. Ranking of monitoring techniques
5. Converting a CO_2 -EOR project to CCUS guidance notes.

Task 1 involved an in-depth review of previous work performed in the WMP. This was carried out to gain a more complete understanding of risks, likely monitoring targets, and technologies currently in use. This review also allowed for the identification of existing gaps and/or newly identified risks. The review of this data provided a detailed understanding of well integrity specifically. Each well has been assessed for risk of potential leakage based on a set of well risk related criterion.

Task 2 involved the review and characterization of leakage pathways, and the review of the modelled leakage plumes. The invasion percolation model was reviewed to identify targets for the application of monitoring efforts. Due to the limitations of this model a mass reduction was also conducted on the model results to assess the monitoring targets during several stages of plume development, simulating the continued activity of CO_2 injection in the field. As per these

modelling studies, the most likely pathways for potential migration and leakage of CO_2 from the storage reservoir/complex were identified for risk assessment purposes. These models guided the development of a monitoring technology ranking which can be deployed to measure for CO_2 plume development and/or potential leakage. This technology ranking was designed to help regulators select monitoring technologies that are cost-effecting and appropriate to the level of risk and the regulatory requirements identified in Task 3.

Task 3 compared a number of regulatory regimes in Canada and the United States. The regimes considered were:

- Existing CO_2 -EOR monitoring requirements in Saskatchewan and Alberta
- New regulatory framework for CCS in Alberta
- Existing CO_2 -EOR monitoring requirements for selected US states including Texas and Wyoming
- Environmental Protection Agency (EPA) Class VI regulations and guidance for CO_2 storage
- CCS best practices and guidance documents.

These comparisons were made to identify deficiencies in the existing EOR monitoring plan and to ensure any recommendations for a CCUS Monitoring Plan would be compliant with regulatory requirements and objectives.

Task 4 reviewed and ranked a variety of monitoring techniques. Numerous techniques are available that can theoretically be applied to check for leakage in and overlying storage reservoirs, and measure plume development. Similarly, various technologies exist for monitoring wellbore integrity above the reservoir. This student reviewed techniques applicable to the storage reservoir, caprock and strata above the reservoir, including shallow groundwater, surface water bodies, and soils. With the data and studies form the previous phases of WMP, this project reviewed various techniques and ranked them using a cost-effective equation with factors such as the ability of a technique to reduce risk, satisfy regulations, likelihood of success, etc. this ranking system also considered the technical performance requirements. These rankings were used to winnow technologies, outline deployment strategies, prepare a schedule and eliminate technologies considered least effective.

In Task 5, all work performed in Tasks 1 – 4 was evaluated to develop a monitoring implementation strategy to allow the technology ranking and methodology to be used to develop a monitoring plan that would meet the requirements of CCUS operators and allow these operators to claim CO_2 storage credits in the EOR fields.

6.2 Overburden Monitoring – Results and Recommendations

Task 1 – Review of Previous Work

Previous work was reviewed in consideration of risk assessment, leakage scenarios, and monitoring. The BPM from the WMP (Hitchon, 2012) was reviewed along with data and results including:

1. Data and results from the previous risk assessments;
2. Welly integrity data from the Weyburn-Midale field
3. Previous invasion percolation theory based simulations results for potential leakage pathways
4. Current EOR monitoring plans applicable to CO_2-EOR and past deployment of technologies.

Risk assessments were used to identify risks for the project to input into the ranking of monitoring technologies. Data and reports considered included:

- Weyburn Project, Geosphere Risk Assessment (URS, 2010b)
- Weyburn Project, Biosphere Risk Assessment (URS, 2010a)
- Development and Application of Bow Tie Risk Assessment Methodology for Carbon Geological Storage Projects, PhD Thesis (Irani, 2012)
- Best Practices for Validating Geological CO_2 Storage (Hitchon, 2012).

The Weyburn-Midale field currently has 177 CO_2 injection wells, both horizontal and vertical. 118 of these wells have a record of CO_2 injection.

Well integrity was identified as the biggest risk area for leakage pathways and illustrates areas of higher risk. This may need to be addressed by a future monitoring strategy. The risk assessment reviewed covered all 1424 wells in the field. These wells were evaluated on the basis of features, events and processes (FEPs), related to the likelihood of occurrence or the impact of a risk. The likelihood score values are displayed in Table 2 and Table 3. Likelihood categories were scored between A and E, with A as low (least likely) and E as high (most likely).

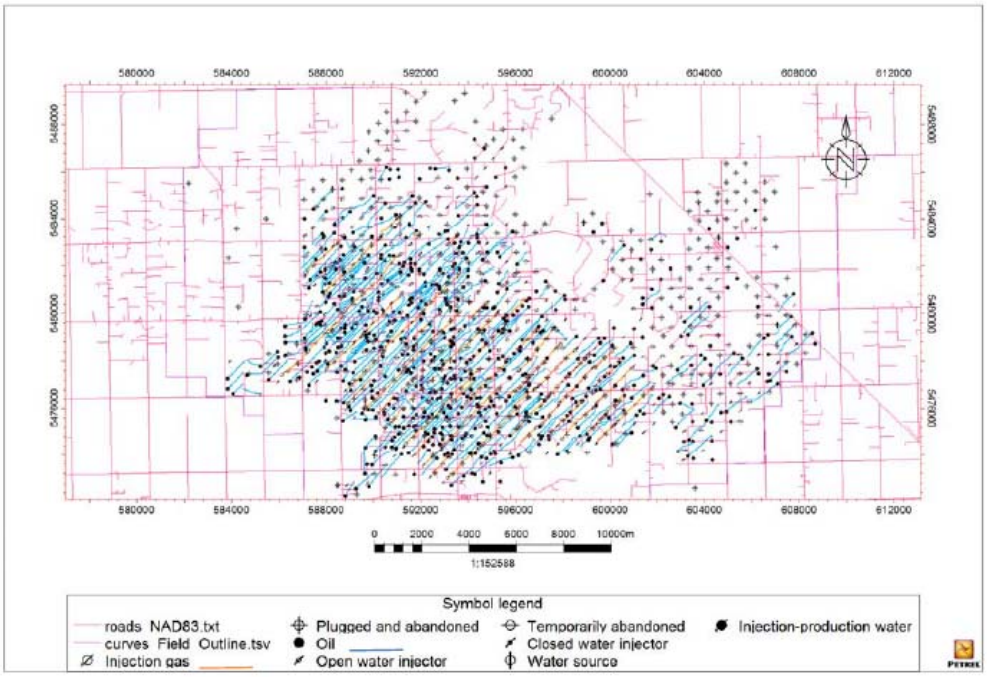

Figure 13 – Weyburn-Midale field well map

LIKELIHOOD CATEGORY	Criteria	Score
Well Deviation	Slant wells	C
	Horizontal	B
	Unknown	B
	Vertical	A
History of GM and SCVF	Serious	E
	Non-serious only	D
	Not Tested	C
	None	A
Suspension Status	Inactive Not Suspended	E
	Risky - not downhole compliant	D
	Caution > 10 y Non-Compliant Suspension	C
	Low > 10 yrs	B
	Low < 10 yrs	A
	Caution < 10 yrs	A
Cement Top	Very Low	E
	Unknown	D
	Low	C
	Moderate	B
	Above Surface Casing Shoe	A
Casing Failure History	Unrepaired	E
	Yes	E
	Unknown	C
	Repaired	C
	Probable	B
	None	A
	Not likely	A
	No	A
Age	Unknown	E
	Spud between 1975 and 1985	E
	Spud Pre-1975	D
	Spud between 1986 and 1997	C
	Spud after 1997	A
Depth	Unknown	D
	>=2000 mKB	C
	>1000 <2000 mKB	B
	<=1000 mKB	A

Table 2 – Likelihood categories, criteria, and associated scores

Other Relevant Factors	Criteria	Score
Cement Quality	Excellent + Very Good meters of Cement 0 - 100 meters (Trouble)	E
	Excellent + Very Good meters of Cement > 100 meters (above Midale)	D
	Excellent + Very Good meters of Cement > 150 meters (above Watrous)	C
	Excellent + Very Good meters of Cement > 500 meters (above Manville)	B
	Excellent + Very Good meters of Cement > 800 meters (about Upper Colorado)	A
Casing Quality	Any penetrations	E
	Casing Anomoly, Poor Casing (leak) from SPINNER	E
	Any Class 4 (1,2,3&4) 60 - 80% wall loss	D
	Poor or Poor Casing or Poor Casing (possible leak) from SPINNER	D
	Any Class 3 (1,2&3) 40 - 60% wall loss	C
	Okay from SPINNER	C
	Any Class 2 (1&2) 20 - 40% wall loss	B
	All Class 1 joints or 0 to 20% internal wall loss	A

Table 3 – Other relevant factors, categories, criteria, and associated scores.

Most of the likelihood categories were evaluated for the full number of wells; however, casing quality was evaluated for 84 wells, suspension status for 179 wells, and cement quality for 39. The assessment undertaken assumed that higher scores in the FEPs lead to a higher likelihood or outcome. The impact categories (Table 4) were evaluated on a numeric scale between one (1) and five (5) with one (1) indicating the least potential impact and five (5) indicating the highest potential impact.

Impact Category	Criteria	Score
Well Type	H_2O Injection	5
	CO_2 Injection	5
	CO_2 Injection	5
	H_2O Disposal	5
	Flowing Oil	4
	Med. Risk Gas	3
	Non-Flowing Oil	3
	Low Risk	2
	Low Risk Oil H_2S < 50 m/mkm	1
	Low Risk Gas	1
	pressure obs.	1
Neighbors	<= 500 km	5
	> 500 m < 1 KM	3
	> 1 KM	1
Water Source	<= 1 km	5
	> 1 km < 2 km	3
	> 2 km	1
Environmentally Sensitive Area	<= 100 m	5
	> 100 m < 1 km	3
	> 1 km	1
Aquifer Protection	Non-saline water aquifer	5
	Not protected	5
	Unknown	4
	Base of Groundwater Protected	2
	Aquifer protected	1

Table 4 – Impact categories, criteria, and associated scores.

The database of +1,400 wells was evaluated using the categories identified in Table 4 to develop risk for each well using a combination of the likelihood and impact categories. Possible risk scores ranged from 1A (least risky) to 5E (most risky). No wells received the lowest risk ranking. All wells scored between 4A and 5E. Table 5 shows the number of wells at each risk level.

Rank	Number of wells
4	877
3	421
2	125
1	0

Table 5 – Number of wells in the data base assigned to each risk rank.

The technology review was conducted to establish a starting point for the monitoring technology ranking and understandings of what risks were already addresses from both a CO_2-EOR and a CCS perspective. The current monitoring program was reviewed in the context of moving the project from CO_2-EOR to being able to claim credit for CO_2 storage under CCUS regulations with a focus on the following areas:

- Potential for additional long-term monitoring requirements;
- Overall ability to monitor the formations above the injection reservoir;
- Ability to detect leakage through the wellbores;
- Ability to monitor potential geologic leakage pathways;
- Ability to meet Saskatchewan regulatory requirements.

Geophysical monitoring technologies were considered. The following were employed:

- Downhole: passive seismic, cross-well seismic, vertical seismic profile.
- Surface based seismic: 3D seismic
- Other: technologies such as inferometric synthetic aperture radar (InSAR), Long Electrode Electrical Resistance Tomography (LEERT), time-lapse gravity, and forward seismic modelling.

The previous invasion percolation model was reviewed to try and establish the monitoring targets in the leakage area. Older reports and data were reviewed including Cavanagh's (2013) report, and associated data archive. A mass reduction was also performed to highlight what the plumes could potential look like over time to allow for a schedule to be developed based on the efficacy of techniques.

This model review was not intended to newly simulate the CO_2 plumes, and as such Task 2 assumed the previous invasion percolation based simulation results as a potential CO_2 distribution. In this simulation work, applied fracture scenarios are hypothetical and neither real nor empirical data for wells or near-well aquitard conditions are available to test these scenarios. In addition, no CO_2 dissolution into bring was assumed. Task 2 considered this previously simulated CO_2 migration through fractures associated with the well path as CO_2 plumes in the overlying aquifers after a long-term leakage. These simulated leakage results are not representing actual leakage but providing potential CO_2 plumes which can be applied in this work to demonstrate the developed workflow in characterizing CO_2 plumes and ranking monitoring techniques. See Figures 14, 15 and 16.

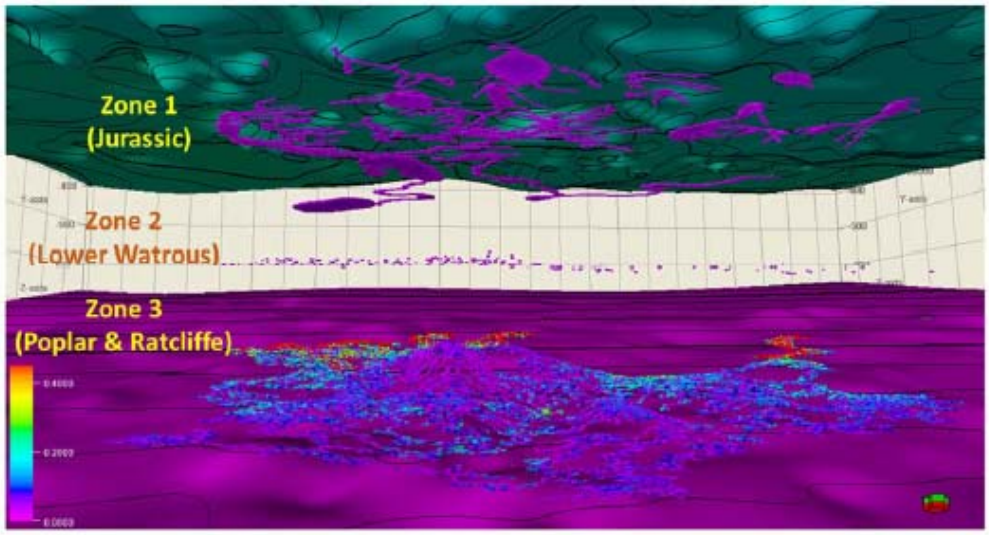

Figure 14 – Point of data of CO_2 saturation imported form the data archive of Cavanagh (2013).

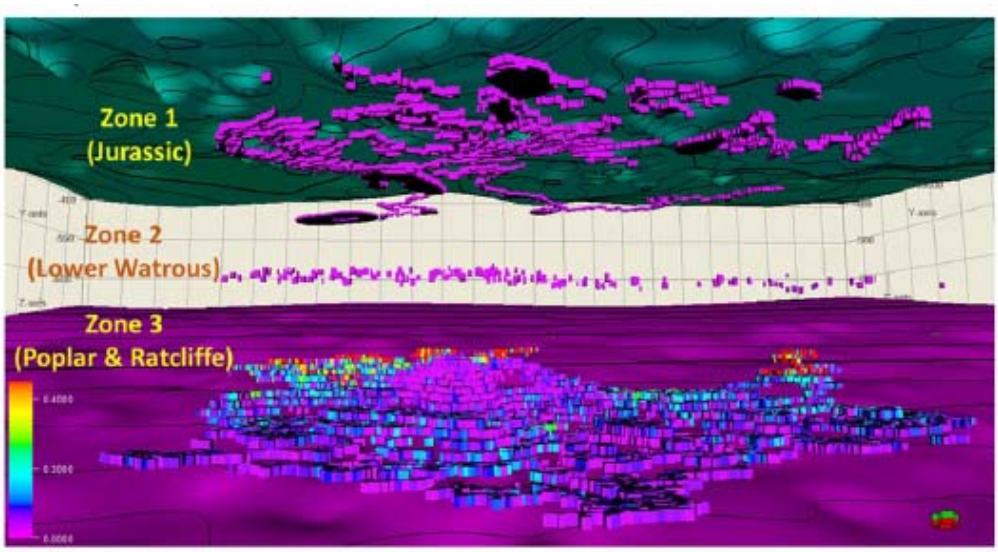

Figure 15 – 2D plan view of each plume, indicating the plume characteristics in each zone.

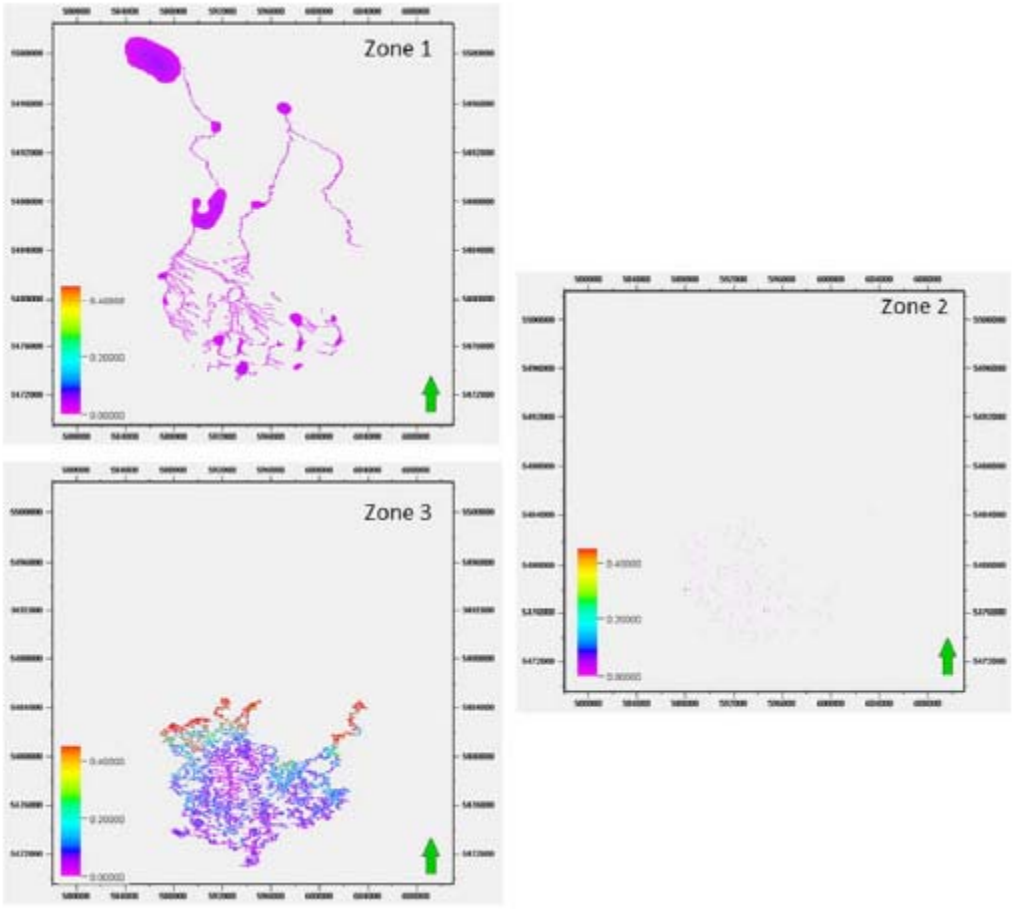

Figure 16 – 2D plan view of plumes in each zone

Wellbore leakage was identified as the highest risk area for this project. Wellbore leakage can occur along annuli between the casing and cement, the cement and formation, through defects in cement, or through the pore network of the cement in the annulus. The low values of cement permeability lead to annuli and defects in the wellbeing the primary pathways within a well for CO_2 migration. The average annuli permeability have been studied by Gasda et al. (2013). The results showed the well annulus to be two to three orders of magnitude larger than cement permeability. See Table 6.

Original Paper	Estimated Wellbore permeability	Measured Cement permeability
(Crow, Carey, Gasda, Williams, & Celia, 2010)	1.7 mD	0.0001 – 0.032 mD
(Duguid, et al., 2013) 46-TPX-10 Well	170 mD	0.0001 – .449 mD
(Duguid, et al., 2013) CC1 Well	25 mD	0.001 – 4.63 mD

Table 6 – Well and cement permeabilities describing potential leakage pathway characteristics

Task 2 - Physical characteristics of leakage pathways

With respect to the characterization of CO_2 plumes due to leakage, previously simulated plumes were investigated with the quantitative measures such as CO_2 plume average size, number closers, tortuosity (surface area per cluster), and coordination number. These measures have been used to measure the special patter or connectivity for the lithofacies and adopted here to characterize the CO_2 plumes.

As each plume migration and distribution in a site may require a different monitoring strategy, the different plume characteristics from 3 different zones (Jurassic; Lower Watrous; Poplar & Radcliff) were explored. CO_2 plumes of each geologic zone shown below would require corresponding monitoring strategies according the plum characteristics. Therefore, in Task 4, the ranking of monitoring techniques accounts for these different plume characteristics under each geological zone.

		Zone 1 (Jurassic)	Zone 2 (Lower Watrous)	Zone 3 (Poplar & Ratcliffe)
Mean Length (m)	$\bar{\Gamma}_x$	373.9	70.9	448.0
	$\bar{\Gamma}_y$	330.3	51.7	301.0
	$\bar{\Gamma}_z$	6.2	5.0	7.1
Total no. of CO_2 nodes		15,959	253	21,011
Total no. of CO_2 clusters		375	172	245
No. of nodes in the largest cluster		4,407	4	9,264
(surface area/volume)		0.4	0.44	0.417
No. of nodes in 2nd largest cluster		2,331	4	2,240
(surface area/volume)		0.4	0.44	0.418
Coordination No.		3.17	0.66	2.73

Table 7 – Characterization of CO_2 plumes

A major detraction from invasion percolation based simulation is the lack of transient plume outcome. Only the final result (after long time periods) is provided. Therefore, in regard to developing a monitoring strategy, there is a lack of information in the early times which is of equal importance for developing the strategy. Due to this limitation, the aforementioned mass reduction and analysis were applied. The mass removal explored here was applied to

demonstrate the temporal evolution of a CO_2 plume and thus the need to monitor accordingly. This indicates the need for monitoring strategies to evolve over time.

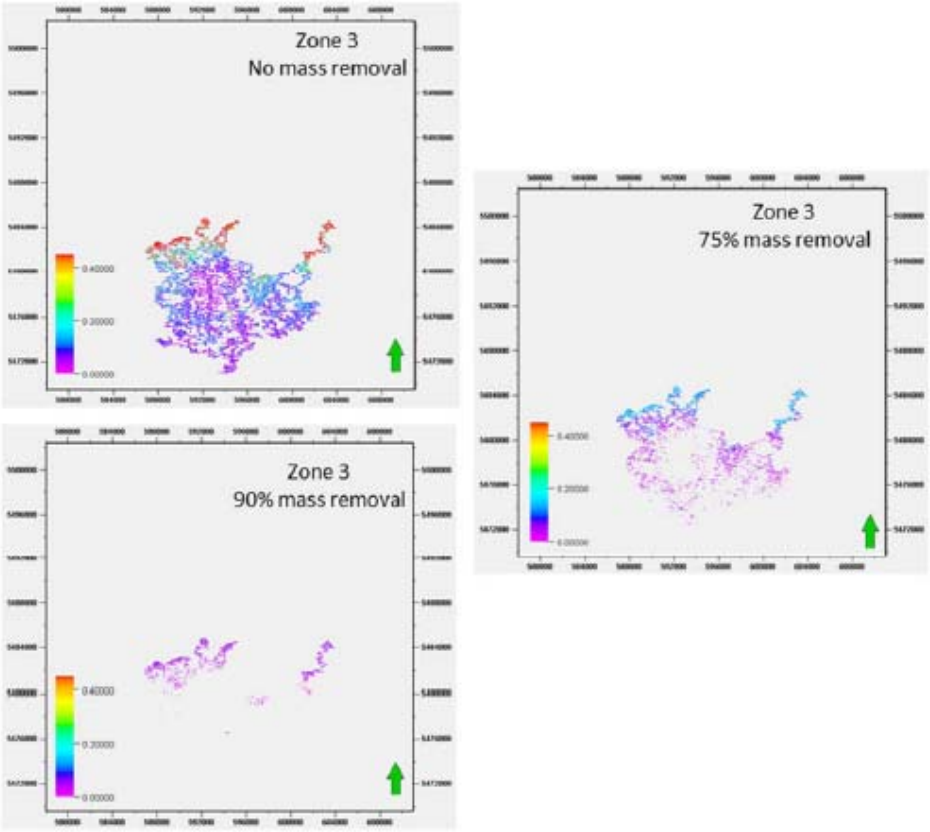

Figure 17 – 2D plan view of CO_2 distribution in Zone 3 (Poplar and Radcliffe) after 75% and 90% mass reduction

		No Mass Removal	75% Mass Removal	90% Mass Removal
Mean Length (m)	$\overline{\Gamma}_x$	448.0	124.5	140.7
	$\overline{\Gamma}_y$	301.0	85.7	94.0
	$\overline{\Gamma}_z$	7.1	5.2	5.1
Total no. of CO_2 nodes		21,011	6,723	2,224
Total no. of CO_2 clusters		245	1,450	376
No. of nodes in the largest cluster		9,264	235	175
(surface area/volume)		0.417	0.42	0.428
No. of nodes in 2nd largest cluster		2,240	207	166
(surface area/volume)		0.418	0.424	0.423
Coordination No.		2.73	1.93	2.09

Table 8 – Spatial connectivity measures of CO_2 plumes after mass reduction in Zone 3

Task 3 - Review of emerging regulatory regimes

CO_2-EOR and CO_2 storage projects are similar, however, they differ in regards to how CO_2 is accounted for, and therefore, are regulated differently. For this bilateral project, both U.S. and Canadian regulations were examined. The regulations reviewed were:

- Existing CO_2 -EOR monitoring requirements in Saskatchewan and Alberta
- New regulatory framework for CCS in Alberta
- Existing CO_2 -EOR monitoring requirements for selected US states including Texas and Wyoming
- Environmental Protection Agency (EPA) Class VI regulations and guidance for CO_2 storage
- CCS best practices and guidance documents.

Comparing these regimes was challenging, as regulations are emerging. Subsequently, specific requirements are not always stated. The regulations reviewed were those available as of January 2015. Each document was written differently and has its own requirements in regards to monitoring technology requirements and a straight forward comparison is difficult and cumbersome. The majority of documents indicate each site is different and that specific technologies cannot be dictated. However, they do require that evidence be provided to support required conclusions on conformance, containment, and assurance monitoring. There are very few places in which a specific technology was requested. The matrix provided in Table 9 is a summary of the regulatory and CCUS guidance document review for Canada and the U.S. contexts.

- Vertically technologies are grouped by conformance, containment, and assurance.
- Horizontally, the applicable regulatory requirements and guiding documents are listed and organized by country, state, and/or province.
- Two codes are used: S= specifically required technology and I= monitoring target was specifically required; however, no technology was specified.

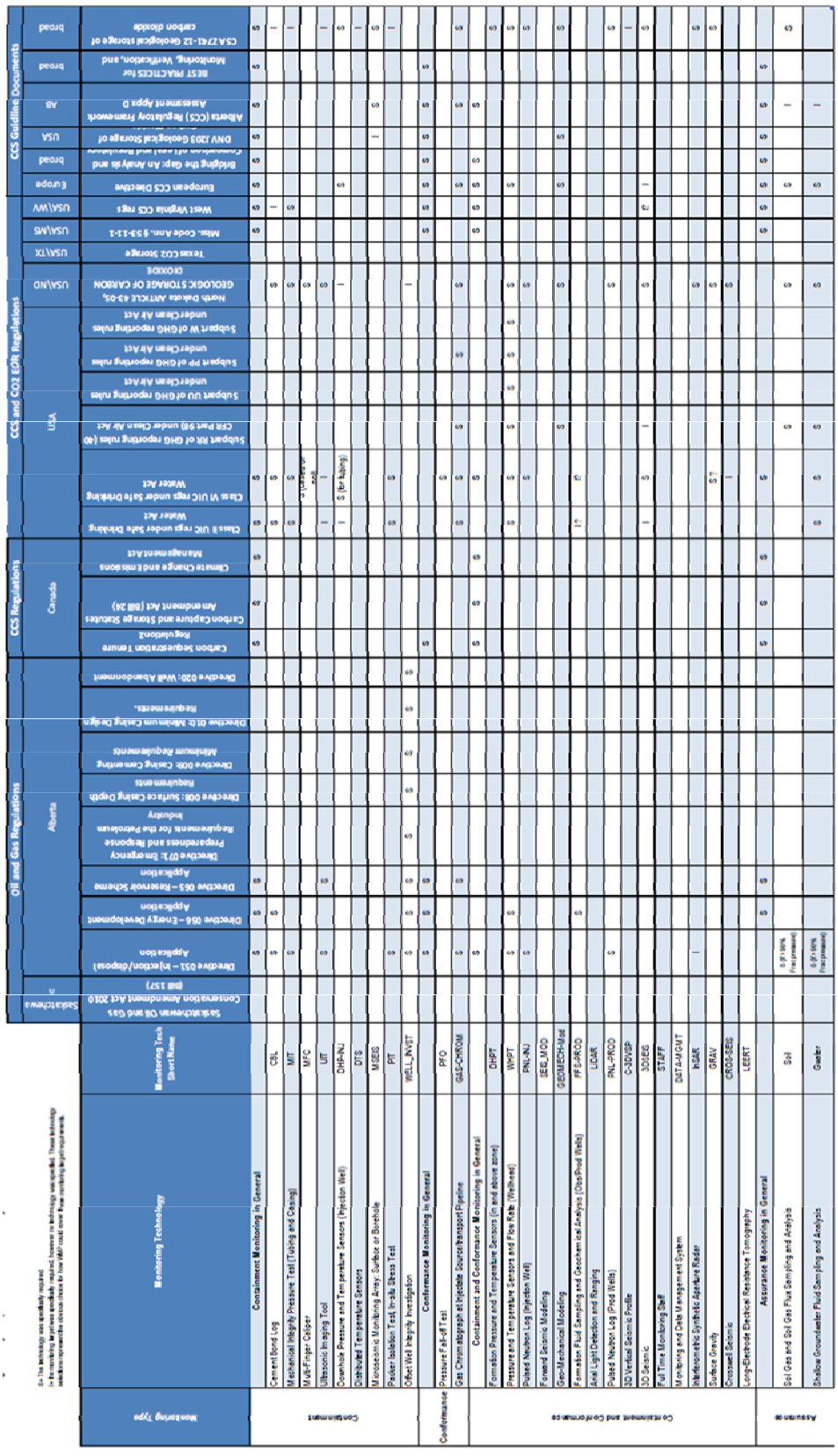

Table 9 – Regulatory requirements, summary matrix

Task 4 - Ranking of monitoring techniques

Multiple risk assessments were completed in the past. The primary driver for the development of this ranking was the identified risk scenarios and associated risk ratings. The following data was reviewed for this risk assessment task:

- Weyburn Project, Geosphere Risk Assessment (URS, 2010b)
- Weyburn Project, Biosphere Risk Assessment (URS, 2010a)
- Development and Application of BowTie Risk Assessment Methodology for Carbon Geological Storage Projects, PhD Thesis (Irani, 2012)
- Best Practices for Validating Geological CO_2 Storage (Hitchon, 2012).

For each risk category, the risk scenario is discussed below (conformance and containment/assurance), and each associated risk scenario has a quantified risk quotient which is an expression of likelihood and consequence.

Conformance: conformance of the site to expected performance, and the demonstration that the CO_2 plume is behaving in a safe and predictable way within the reservoir. The wells uncemented to caprock risk scenario was added as a risk after review of the well integrity.

Containment/Assurance: the ability of the reservoir/caprock system to contain the injected quantity of CO_2 and assurance that the CO_2 injection will not endanger health, safety, and/or the environment.

Risk Scenario #	Risk Category	Risk Scenario	Risk Discussion
17	Conformance	Unable to Confirm CO_2 in Reservoir	If the location and quantity of CO_2 stored in the Weyburn unit cannot be confirmed by monitoring, there are implications on the effectiveness of the WMF to generate carbon credits for the storage of CO_2.
14		Change to Project Economics	This risk relates to a change in the project economics resulting in the target volume of CO_2 not being stored in the Weyburn Project.
15		Lateral Migration out of the Weyburn Unit	This risk is based on lateral flow occurring outside of the Weyburn Unit. It is assumed that the CO_2 is maintained within the geosphere, but that it leaves the designated Weyburn storage area.
16		Premature Closure	Premature closure of the site may be driven by a number of factors
13		Inadequate Source	This risk is related to there being an inadequate source of CO_2 to fill the Weyburn Storage Project to its target capacity.
12		Reduced Injectivity	This risk relates to the inability to input the target volume of CO_2 into the reservoir as a result of reduced injectivity in the wells.
10	Containment/Assurance	Well Casing Corrosion	Corrosion of well casing and retainer leads to migration of CO_2 to the biosphere
11		Well Cement Channeling	Cement channeling leads to migration of CO_2 to the biosphere
9		Well Micros Fracs, Micro Annuli	Micro-fractures and micro-annuli in the well cement lead to migration of CO_2 to the Biosphere.
18		Wells Uncemented to Caprock	Certain wells were found to not have cement up into the caprock, creating a potential migration pathway for CO2 to the Biosphere. This risk was added after the review of well integrity.
3		Nat Seismicity-Fault Reactivation	Naturally occurring event. Reactivation of existing faults through naturally occurring seismicity.
5		Nat Seismicity-Wells	Naturally occurring event. Loss of well Integrity may occur through naturally occurring seismicity.
1		EOR Minor Faults Network	Event resulting from EOR. CO_2 leakage through a network of minor faults or fractures.
4		Nat Seismicity-New Fractures	Naturally occurring event. Creation of new fractures through naturally occurring seismicity.
7		EOR Induced P/T-Reactivation	EOR - Induced temperature / pressure variation - reactivation of fractures Event resulting from EOR. EOR induced temperature and pressure variations lead to reactivation of fractures and migration of CO_2 to the biosphere.
8		EOR Induced P/T-New Fractures	EOR - Induced temperature / pressure variation - new fractures Event resulting from EOR. EOR induced temperature / pressure variations lead to new fractures and migration of CO_2 to the biosphere.
6		EOR Induced Chemical Fractures	EOR - Induced chemical variation - existing fractures Event resulting from EOR. EOR induced chemical variations leading to CO_2 migration through existing fractures.
2		EOR Through Faults	Event resulting from EOR. CO_2 leakage via through faults that extend from the reservoir to the biosphere.

Table 10 – Risk scenarios at Weyburn-Midale field

The URS (URS, 2010b) calculated risk quotient, levels of confidence were presented at CL50%, CL80%, and CL90%. CL90% is a conservative estimate where only 5% of simulated risk cases would exceed this value. CL50% is optimistic, meaning 50% of cases would exceed this value. CL80% is typically used for project planning. The difference between CL50% and CL90%

represents the degree of risk uncertainty between estimates. To compare the two categories (conformance and containment/assurance) the scales were normalized to a risk rating scale of 1-10 (1=low risk, 10=high risk).

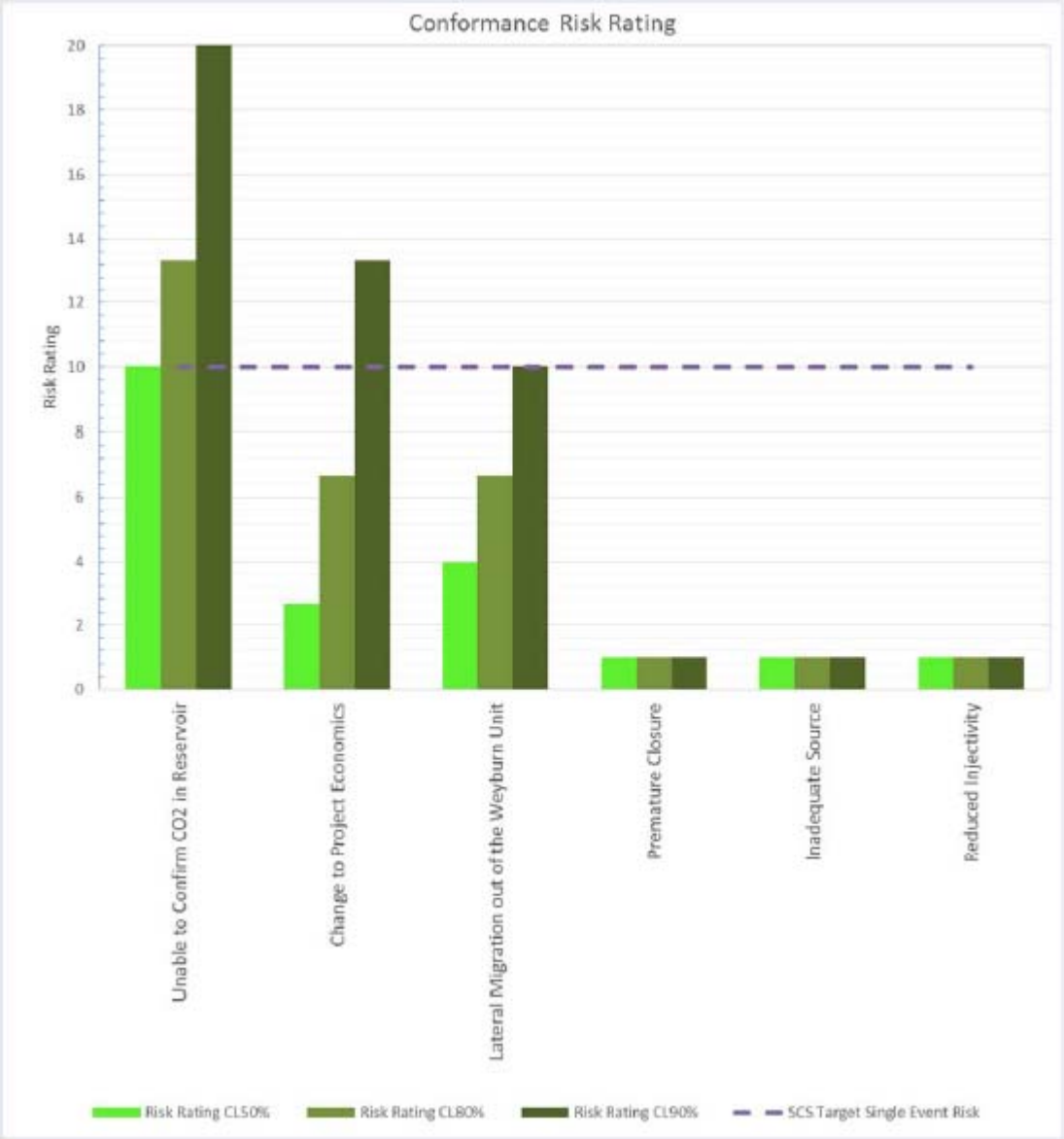

Figure 18 – Conformance risk rating

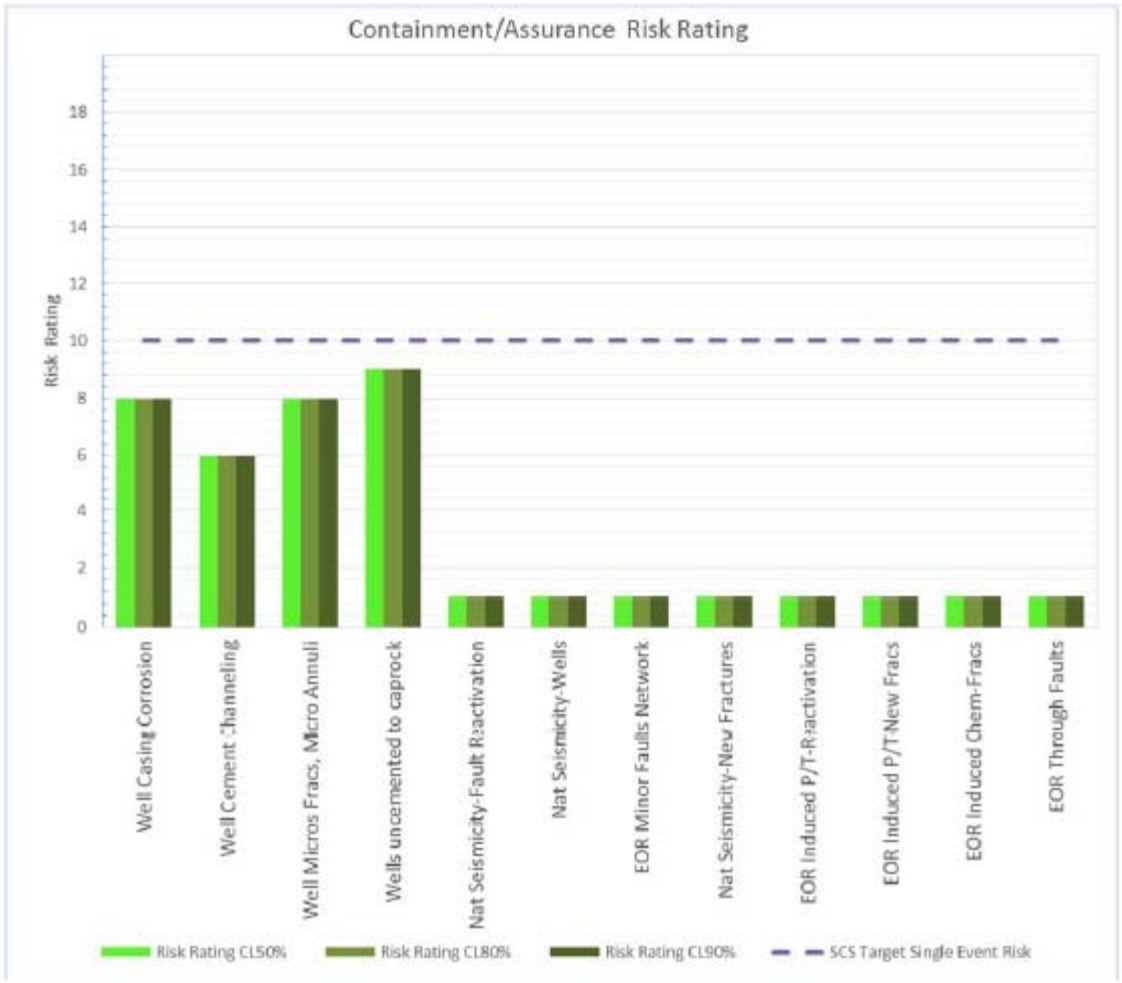

Figure 19 – Containment/assurance risk rating

For conformance, three risk scenarios were considered:

1. Inability to confirm CO_2 in the reservoir
2. Change to project economics
3. Lateral migration out of the unit

These were used to identify the most risk to the project. For the containment/assurance risk category, the individual risk scenario risk quotients were rated low compared to the threshold target, therefore posing acceptable risk to the project. Each risk scenario requires the monitoring of specific monitoring targets to reduce risk of each scenario. In Table 11, '1' indicates which targets require the application of monitoring technologies to reduce risk.

			Monitoring Target												
			Containment						Conformance				Assurance		
Risk Scenario #	Risk Category	Risk Scenario	Well Integrity	Caprock Integrity	Natural Seismicity And Injection Induced	Migration up into the Jurassic Fm.	Migration up into the Lower Watrous	Migration up into the Poplar & Ratcliff	Plume Location and	Quantification for	Storage Efficiency and Fine	Calibration of Predictive	Surface Leaks: Soil	Surface Leaks:	Public Assurance
17	Conformance	Unable to Confirm CO_2 in Reservoir							1	1	1	1			1
14		Change to Project Economics													
15		Lateral Migration out of the Weyburn Unit			1				1	1	1	1			1
16		Premature Closure													
13		Inadequate Source									1				
12		Reduced Injectivity		1						1	1	1			1
10	Containment/Assurance	Well Casing Corrosion	1			1	1	1					1	1	1
11		Well Cement Channeling	1			1	1	1					1	1	1
9		Well Micros Fractures, Micro Annuli	1		1	1	1	1					1	1	1
18		Wells Uncemented to Caprock	1			1	1	1					1	1	1
3		Natural Seismicity-Fault Reactivation		1	1	1	1	1					1	1	1
5		Natural Seismicity-Wells	1	1	1	1	1	1					1	1	1
1		EOR Minor Faults Network		1	1	1	1	1					1	1	1
4		Nat Seismicity-New Fractures		1	1	1	1	1					1	1	1
7		EOR Induced P/T-Reactivation		1	1	1	1	1					1	1	1
8		EOR Induced P/T-New Fractures		1	1	1	1	1					1	1	1
6		EOR Induced Chemical-Fractures		1	1	1	1	1					1	1	1
2		EOR Through Faults		1	1	1	1	1					1	1	1

Table 11 – Risk scenarios and monitoring target matrix

As noted, wellbores were identified as a high risk area for CCS/CO_2-EOR projects. A well risk assessment methodology was devised to rank risks to identify monitoring technologies for high risks. This methodology can be implemented at other similar EOR operations.

A method to calculate the risk of the individual wells in the field was adopted generally following previous work (Duguid et al., 2010). This method calculates a Total Likelihood score as the summation of the scores of judged to be proxies for likelihood and calculates a tTotal Impact score as the summation of the scores of FEPs judged to be proxies for Impact. The total well risk is then calculated as the product of Total Likelihood and Total Impact. Scoring criteria between 1 and 5 was adopted. Categories used were similar to those in the previous assessment with the addition of three new categories (identified in **bold** below).

- Well deviation
- History of gas migration and surface casing vent flow

- Suspension status
- Cement topo
- Casing failure history
- Well age
- Well depth
- **Well type**
- **Long-string casing set in the Midale Evaporite**
- **Plugging regulation in effect during abandonment**
- **CO_2 plume zone**

Tables 12 and 13 show the values used to quantify the likelihood and relevant factor categories.

Likelihood Category	Criteria	Old Score	New Score
Deviation	Slant wells	C	5
	Horizontal	B	3
	Unknown	B	5
	Vertical	A	1
	Deviated	--	3
	Pressure Observation	--	1
History Of GM_SCVF	Serious	E	5
	Non-serious only	D	4
	Not Tested	C	3
	None	A	1
Suspension Status	Inactive Not Suspended	E	5
	RISKY - not downhole compliant	D	4
	CAUTION > 10 y Non-Compliant Suspension	C	3
	LOW > 10 yrs	B	2
	LOW < 10 yrs	A	1
	CAUTION < 10 yrs	A	1
Cement Top	Very Low	E	5
	Unknown	D	5
	Low	C	4
	Moderate	B	3
	Above Surface Casing Shoe	A	1
	Missing Data	--	5
Casing Failure History	Unrepaired	E	5
	Yes	E	5
	Unknown	C	5
	Repaired	C	2
	Probable	B	4
	None	A	1
	Not likely	A	2
	No	A	1
Age	Unknown	E	5
	Spud between 1975 and 1985	E	3
	Spud Pre-1975	D	4
	Spud between 1986 and 1997	C	2
	Spud after 1997	A	1
Depth	Unknown	D	5
	>=2000 mKB	C	5
	>1000 <2000 mKB	B	3
	<=1000 mKB	A	1
Well Type	H_2O Injection	5	5
	CO_2 Injection	5	5
	CO_2 Injection	5	5
	H_2O Disposal	5	5
	Flowing Oil	4	4
	Med. Risk Gas	3	3
	Non-Flowing Oil	3	3
	Low Risk	2	2
	Low Risk Oil H2S < 50 m/mkm	1	1
	Low Risk Gas	1	1
	pressure obs.	1	1

Table 12 – Categories, criteria, old score and new score value for likelihood

Other Relevant Factors	Criteria	Old Score	New Score
Cement Quality	Excellent + Very Good meters of Cement 0 - 100 meters (Trouble)	E	5
	Excellent + Very Good meters of Cement > 100 meters (above Midale)	D	4
	Excellent + Very Good meters of Cement > 150 meters (above Watrous)	C	3
	Excellent + Very Good meters of Cement > 500 meters (above Manville)	B	2
	Excellent + Very Good meters of Cement > 800 meters (about Upper Colorado)	A	1
Casing Quality	Any penetrations	E	5
	Casing Anomaly, Poor Casing (leak) from SPINNER	E	5
	Any Class 4 (1,2,3&4) 60 - 80% wall loss	D	4
	Poor or Poor Casing or Poor Casing (possible leak) from SPINNER	D	4
	Any Class 3 (1,2&3) 40 - 60% wall loss	C	3
	Okay from SPINNER	C	2
	Any Class 2 (1&2) 20 - 40% wall loss	B	2
	All Class 1 joints or 0 to 20% internal wall loss	A	1
Plug Regulatory Regime	Pre-March 15, 1985	–	5
	Between March 15, 1985 and April 1, 2012	–	3
	After April 1, 2012	–	1
	Not Plugged	–	1
Long-String Set In The Midale Evaporite	Vertical Well	–	1
	Horizontal, Long-string set above the Midale Evaporite	–	5
	Horizontal, Long-string set in or below the Midale Evaporite	–	1
	Unknown	–	5
Co_2 Plume Zone	0 to 25,000 tonnes injected	–	1
	25,000 to 100,000 tonnes injected	–	2
	100,000 to 300,000 tonnes injected	–	3
	300,000 to 500,000 tonnes injected	–	4
	> 500,000 tonnes injected	–	5

Table 13 – Categories, criteria, old score value and new score value for other relevant factors

Impact categories (see Table 14) were identified as:

- Distance to neighbours
- Distance to water source
- Distance to environmentally sensitive areas
- Aquifer protection

Impact Category	Criteria	Old Score	New Score
Neighbors	<= 500 km	5	5
	> 500 m < 1 KM	3	3
	> 1 KM	1	1
Water Source	<= 1 km	5	5
	> 1 km < 2 km	3	3
	> 2 km	1	1
Environmentally Sensitive Area	<= 100 m	5	5
	> 100 m < 1 km	3	3
	> 1 km	1	1
Aquifer Protection	Non-saline water aquifer	5	5
	Not protected	5	5
	Unknown	4	5
	Base of Groundwater Protected	2	2
	Aquifer protected	1	1

Table 14 – Categories, criteria, old score value and new score value for impact

Scores for likelihood and impact were calculated for each individual well. The overall likelihood score was calculated by summing the individual likelihood and other relevant factors scores for each well. The overall impact score for each well was calculated summing the individual impact category scores. Likelihood and impact categories were considered high if the ratio of wells scoring 4 or 5 was above 0.6, medium if the ratio was between 0.3 to 0.6, and low if the ratio was less than or equal to 0.3.

The assessment evaluated 1,425 wells in the Weyburn-Midale field. The results of the assessment show total likelihood scores between 24 and 50, total impact scores between 8 and 20, and total risk scores between 192 and 900 (see Table 15).

	Total Risk	Total Likelihood	Total Impact
Mean	431.88	36.85	11.71
Median	410	37	12
Mode	370	37	10
Standard Deviation	115.91	4.63	2.70
Range	708	26	12
Minimum	192	24	8
Maximum	900	50	20

Table 15 – Statistics for total risk, total likelihood, and total impact.

The scores for the top 10 wells are shown in Table 16. Tables 17 to 24 summarize the likelihood of issues and impacts with the top-at-risk and lower-at-risk wells.

Rank	Likelihood													Impact				Totals		
	Well Deviation	Cement Top	Cement Quality	Depth	Well Age	SCVF	Casing Integrity	Casing Quality	Suspension	Well Type	Abandonment Regulation	Midale Evaporite	CO_2 Zone	Aquifer Protection	Proximity to People	Proximity to water source	Proximity to an environmentally sensitive area	Total Likelihood	Total Impact Score	Total Risk Score
1	3	5	3	3	1	5	5	4	3	4	1	5	3	5	5	5	5	45	20	900
2	3	5	3	3	1	1	5	4	3	4	1	5	5	5	5	5	5	43	20	860
3	3	5	3	3	1	5	5	4	3	4	1	5	3	5	5	5	3	45	18	810
4	3	5	3	3	1	1	5	4	5	4	1	5	5	5	5	5	3	45	18	810
5	3	5	3	3	1	1	5	4	5	4	1	5	4	5	3	5	5	44	18	792
6	3	5	3	3	1	1	5	4	3	4	1	5	5	5	5	5	3	43	18	774
7	3	5	3	3	1	5	5	4	3	4	1	1	5	5	5	5	3	43	18	774
8	3	5	3	3	1	1	5	4	3	4	1	5	5	5	3	5	5	43	18	774
9	3	5	3	3	1	3	5	4	3	4	1	5	3	5	5	5	3	43	18	774
10	3	5	3	3	1	1	5	4	3	4	1	5	4	5	3	5	5	42	18	756

Table 16 -- Ten highest total risk rated wells

	Well Deviation	Cement Top	Cement Quality	Depth	Well Age	SCVF/GM	Casing Integrity	Casing Quality	Suspension	Well Type	Abandonment Regulation	Midale Evaporite	CO2 Zone
Score:5	0	56	0	1	0	28	68	0	17	2	0	50	21
Score:4	0	7	0	0	8	3	0	70	0	58	0	0	10
Sum of 4s and 5s	0	63	0	1	8	31	68	70	17	60	0	50	31
Number of Wells Scored	71	71	71	71	71	71	71	71	71	71	71	71	71
Ratio of high risk wells	0.00	0.89	0.00	0.01	0.11	0.44	0.96	0.99	0.24	0.85	0.00	0.70	0.44

Table 17 – Likelihood category scores identified in the top 5% of wells

	Well Deviation	Cement Top	Cement Quality	Depth	Well Age	SCVF/GM	Casing Integrity	Casing Quality	Suspension	Well Type	Abandonment Regulation	Midale Evaporite	CO2 Zone
Score:5	0	51	0	1	0	28	45	2	0	21	0	29	9
Score:4	0	6	0	0	18	9	1	68	1	38	0	0	4
Sum of 4s and 5s	0	57	0	1	18	37	46	70	1	59	0	29	13
Number of Wells Scored	71	71	71	71	71	71	71	71	71	71	71	71	71
Ratio of high risk wells	0.00	0.80	0.00	0.01	0.25	0.52	0.65	0.99	0.01	0.83	0.00	0.41	0.18

Table 18 – Likelihood category scores identified in the 5% of wells around average risk value

	Well Deviation	Cement Top	Cement Quality	Depth	Well Age	SCVF/GM	Casing Integrity	Casing Quality	Suspension	Well Type	Abandonment Regulation	Midale Evaporite	CO2 Zone
Score:5	0	45	0	2	0	7	9	0	0	44	0	1	0
Score:4	0	2	0	0	18	8	0	65	3	5	0	0	0
Sum of 4s and 5s	0	47	0	2	18	15	9	65	3	49	0	1	0
Number of Wells Scored	71	71	71	71	71	71	71	71	71	71	71	71	71
Ratio of high risk wells	0.00	0.66	0.00	0.03	0.25	0.21	0.13	0.92	0.04	0.69	0.00	0.01	0.00

Table 19 – Likelihood category scores identified in the bottom 5% of wells.

Likelihood Category	Top 5%	Middle 5%	Bottom 5%
Well Deviation	Low	Low	Low
Cement Top	High	High	High
Cement Quality	Low	Low	Low
Depth	Low	Low	Low
Well Age	Low	Low	Low
SCVF	Medium	Medium	Low
Casing Integrity	High	High	Low
Casing Quality	High	High	High
Suspension	Low	Low	Low
Well Type	High	High	High
Abandonment Regulation	Low	Low	Low
Midale Evaporite	High	Medium	Low
CO_2 Zone	Medium	Low	Low

Table 20 – High, medium, and low likelihood category scores for the top, middle, and bottom 5% of wells

	Aquifer Protection	Proximity to People	Proximity to water source	Proximity to an environmentally sensitive area
Score:5	71	28	70	20
Score:4	0	0	0	0
Sum of 4s and 5s	71	28	70	20
Number of Wells Scored	71	71	71	71
Ratio of high risk wells	1.00	0.39	0.99	0.28

Table 21 – Impact categories identified in the top 5% of wells

	Aquifer Protection	Proximity to People	Proximity to water source	Proximity to an environmentally sensitive area
Score:5	71	4	7	12
Score:4	0	0	0	0
Sum of 4s and 5s	71	4	7	12
Number of Wells Scored	71	71	71	71
Ratio of high risk wells	1.00	0.06	0.10	0.17

Table 22 – Impact categories identified in the 5% of wells around average total well risk

	Aquifer Protection	Proximity to People	Proximity to water source	Proximity to an environmentally sensitive area
Score:5	71	4	7	12
Score:4	0	0	0	0
Sum of 4s and 5s	71	4	7	12
Number of Wells Scored	71	71	71	71
Ratio of high risk wells	1.00	0.06	0.10	0.17

Table 23 – Impact categories identified in the bottom 5% of wells

Impact Category	Top 5%	Middle 5%	Bottom 5%
Aquifer Protection	High	High	High
Proximity to People	Medium	Low	Low
Proximity to water source	High	Low	Low
Proximity to an environmentally sensitive area	Low	Low	Low

Table 24 – High, medium, and low impact category ratings for the top, middle, and bottom 5% of wells

This task was the primary deliverable of this study. It used the Weyburn-Midale field as a case study to evaluate risk and rank relevant monitoring strategies that can be used to shift the Weyburn-Midale field from CO_2-EOR to CCUS and, therefore ,able to claim CO_2 storage credits. This incorporated the risks identified above, the potential leakage pathways, various regulatory requirements, and the existing monitoring techniques. All recommended monitoring techniques were evaluated with respect to addressing project risks, cost-benefit, and technical applicability and ranked within a matrix for comparison. The general approach to ranking monitoring technology effectiveness was adapted from the IEAGHG Monitoring Selection Tool (IEAAGHG, 2015). Each monitoring technique was evaluated on a scale of 0-10 for how effective it is at monitoring each target (o for no effectiveness, 10 for high effectiveness). The results are displayed in Table 25.

Monitoring Technology	Monitoring Tech Total Effectiveness Rating (0-100)	Monitoring Target Effectiveness 0-10 Scale)												
		Containment						Conformance				Assurance		
		Well Integrity	Caprock Integrity	Natural Seismicity And Injection Induced Microseismicity	Migration up into the Jurassic Fm.	Migration up into the Lower Watrus	Migration up into the Poplar & Redcliff	Plume Location and Migration in Reservoir	Quantification for Regulatory Authorities	Storage Efficiency and Fine Scale Processes	Calibration of Predictive Models	Surface Leaks: Soil	Surface Leaks: Groundwater	Public Assurance
3D Seismic	52.3		8		7	3	9	9	9	8	9			6
Pulsed Neutron Log (Injection Well)	47.7	9	9		5	5	5	5	5	8	8			3
Pulsed Neutron Log (Prod Wells)	44.6	9	9		4	4	4	4	5	8	8			3
Full Time Monitoring Staff	42.3	4	4	4	4	4	4	4	4	4	4	4	4	7
Soil Gas and Soil Gas Flux Sampling and Analysis	36.9	7	7		3	3	3		5			7	6	7
Shallow Groundwater Fluid Sampling and Analysis	36.9	7	7		3	3	3		5			6	7	7
Downhole Pressure and Temperature Sensors (Injection Well)	32.3	5	5		5	3	5	3	3	3	7			3
Formation Pressure and Temperature Sensors (in and above zone)	31.5	5	5		5	3	5	3	3	3	6			3
Microseismic Monitoring Array: Surface or Borehole	30.8		7	7				6		6	7			7
Monitoring and Data Management System	29.2	2	3	3	3	3	3	3	3	3	3	3	3	3
Formation Fluid Sampling and Geochemical Analysis (Obs/Prod Wells)	26.2		3		3	3	5	5	3	3	6			3
Pressure and Temperature Sensors and Flow Rate (Wellhead)	25.4	3			2	2	2		9	6	6			3
Pressure Fall-off Test	24.6							6	6	9	8			3
Ultrasonic Imaging Tool	21.5	9			5	5	5	1						3
Geo-Mechanical Modeling	20.0		6	6				4		4	3			3
Offset Well Integrity Investigation	19.2	5			3	3	3					3	3	5
Forward Seismic Modeling	18.5							5	8	3	5			3
3D Vertical Seismic Profile	15.4		2		2	1	3	2	2	3	3			2
Distributed Temperature Sensors	13.1	3	3		3	3	3							2
Long-Electrode Electrical Resistance Tomography	13.1	2	4		1	1	1						5	3
Cement Bond Log	10.0	8	2											3
Mechanical Integrity Pressure Test (Tubing and Casing)	9.2	9												3
Packer Isolation Test, In-situ Stress Test	9.2	9												3
Gas Chromatograph at Injectate Source/transport Pipeline	9.2								6	3				3
Multi-Finger Caliper	6.2	5												3
Interferometric Synthetic Aperture Radar	5.4							2	2		2			1
Surface Gravity	5.4		1		1	1	1	1						2
Ariel Light Detection and Ranging	3.1							1	1		1			1

Table 25 – Monitoring technology effectiveness ranking

A methodology was then developed to quantify the benefit of each technology based on its ability to provide monitoring for each risk scenario. The following steps are evaluated for each risk scenario:

1. Technology selection
2. Monitoring Target (effectiveness 0-10 scale)

3. Total Effectiveness
4. Risk Percent Effectiveness
5. Monitoring Benefit.

After these steps are completed for each risk scenario a total monitoring benefit ranking is achieved. This ranking was calculated to provide a total monitoring benefit that honours all risk scenarios (Table 26).

Summary of Monitoring Technologies, Monitoring Targets and the Addressed Risk Scenarios

Benefit Rank	Monitoring Technology	Monitoring Tech Short Name	Risk Ranking (right) Monitoring Benefit per risk (matrix) Total Monitoring Benefit (below)	Risk Scenarios Addressed: Conformance: Unable to Confirm CO2 in Reservoir	Conformance: Change to Project Economics	Conformance: Lateral Migration out of the Heyburn Unit	Conformance: Premature Closure	Conformance: Inadequate Source	Conformance: Reduced Injectivity	Containment/Assurance: Well Casing Corrosion	Containment/Assurance: Well Cement Channeling	Containment/Assurance: Well Micro Frac, Micro Annuli	Containment/Assurance: Wells Unintended to Coprod.	Containment/Assurance: Nat. Seismicity-Fault Reactivation	Containment/Assurance: Nat. Seismicity-Wells	Containment/Assurance: EOR Minor Fault Network	Containment/Assurance: Nat. Seismicity-New Fractures	Containment/Assurance: EOR Induced PPT-Reactivation	Containment/Assurance: EOR Induced PPT-New Frac	Containment/Assurance: EOR Induced Chem-Frac	Containment/Assurance: EOR Through Faults
	Risk Ranking: The range is between 1 (low) and 10 (high). Taken directly from the risk assessment		Scenario #	17	14	15	16	13	12	10	11	9	18	3	5	1	4	7	8	6	2
			Number of Technologies applied to each risk	20	13	19	1	1	1	8	6	8	5	1	1	1	1	1	1	1	1
1	3D Seismic	3DSEIS	36.4	16.4		6.8				2.9	2.1	2.5	3.2			0.4	0.4	0.4	0.4	0.4	0.4
2	Full Time Monitoring Staff	STAFF	31.3	9.2		4.5			0.5	3.5	2.7	3.5	4.0	0.4	0.4	0.4	0.4	0.4	0.4	0.4	0.4
3	Pulsed Neutron Log (Injection Well)	PNL-INJ	30.1	11.6		4.8				3.1	2.3	2.7	3.5		0.4		0.3	0.3	0.3	0.3	0.3
4	Pulsed Neutron Log (Prod Wells)	PNL-PROD	28.0	11.2		4.7				2.7	2.1	2.4	3.1		0.4		0.3	0.3	0.3	0.3	0.3
5	Monitoring and Data Management System	DATA-MGMT	20.6	6.0		3.0			0.3	2.3	1.7	2.3	2.6	0.3	0.3	0.3	0.3	0.3	0.3	0.3	0.3
6	Pressure Fall-off Test	PFO	18.7	12.8		5.3			0.5												
7	Soil Gas and Soil Gas Flux Sampling and Analysis	Soil	18.1							4.1	3.1	3.6	4.6			0.5	0.5	0.5	0.5	0.5	0.5
8	Shallow Groundwater Fluid Sampling and Analysis	Gwater	18.1							4.1	3.1	3.6	4.6			0.5	0.5	0.5	0.5	0.5	0.5
9	Microseismic Monitoring Array: Surface or Borehole	MSEIS	18.0	10.4		5.5								0.3	0.2	0.3	0.3	0.3	0.3	0.3	0.3
10	Formation Pressure and Temperature Sensors (in and above zone)	DHPT	16.1	7.2		3.0			0.4	2.4	1.8				0.3	0.3		0.3	0.3		0.3
11	Forward Seismic Modeling	SEIS_MOD	13.6	9.6		4.0								0.0							
12	Formation Fluid Sampling and Geochemical Analysis (Obs/Prod Wells)	FFS-PROD	13.0	8.0		3.3								0.2	0.2	0.2	0.2	0.2	0.2	0.2	0.2
13	Downhole Pressure and Temperature Sensors (Injection Well)	DHP-INJ	12.3	7.6		3.2										0.3	0.3	0.3	0.3	0.3	0.3
14	Ultrasonic Imaging Tool	UIT	11.9							3.1	2.3	2.7	3.5		0.3						
15	Offset Well Integrity Investigation	WELL_INVST	11.0							2.9	2.1	2.5	3.2		0.3						
16	Geo-Mechanical Modeling	GEOMECH-Mod	10.7	5.6		3.3			0.3					0.2	0.2	0.2	0.2	0.2	0.2	0.2	0.2
17	Crosswell Seismic	CROS-SEIS	8.2	5.2		2.2										0.1	0.1	0.1	0.1	0.1	0.1
18	3D Vertical Seismic Profile	C-3DVSP	6.8	4.8		2.0															
19	Mechanical Integrity Pressure Test (Tubing and Casing)	MIT	5.3							1.4	1.0	1.2	1.5		0.1						
20	Packer Isolation Test, In-situ Stress Test	PIT	5.3							1.4	1.0	1.2	1.5		0.1						
21	Distributed Temperature Sensors	DTS	4.8								1.2	1.4	1.8		0.2	0.2					
22	Interferometric Synthetic Aperture Radar	InSAR	4.0	2.8		1.2															
23	Cement Bond Log	CBL	3.6								0.9	1.1	1.4		0.1						
24	Arial Light Detection and Ranging	LIDAR	1.6	1.6																	
25	Surface Gravity	GRAV	1.2	1.2																	
26	Pressure and Temperature Sensors and Flow Rate (Wellhead)	WHPT	1.0						0.5							0.1	0.1	0.1	0.1	0.1	
27	Multi-Finger Caliper	MFC	0.9							0.9											
28	Gas Chromatograph at Injectate Source/transport Pipeline	GAS-CHROM	0.5					0.3	0.2												
29	Long-Electrode Electrical Resistance Tomography	LEERT	0.0																		

Table 26 – Monitoring benefit ranking and summary of the addressed risk scenarios

These techniques were also evaluated in regards to a cost-benefit technology ranking. Table 26 presents the results in rank order with the monitoring objectives each technology presents. The benefit ratings were plotted (Figure 19) against corresponding estimated cost and a cost benefit ratio was used to rank the monitoring technologies (Table 27).

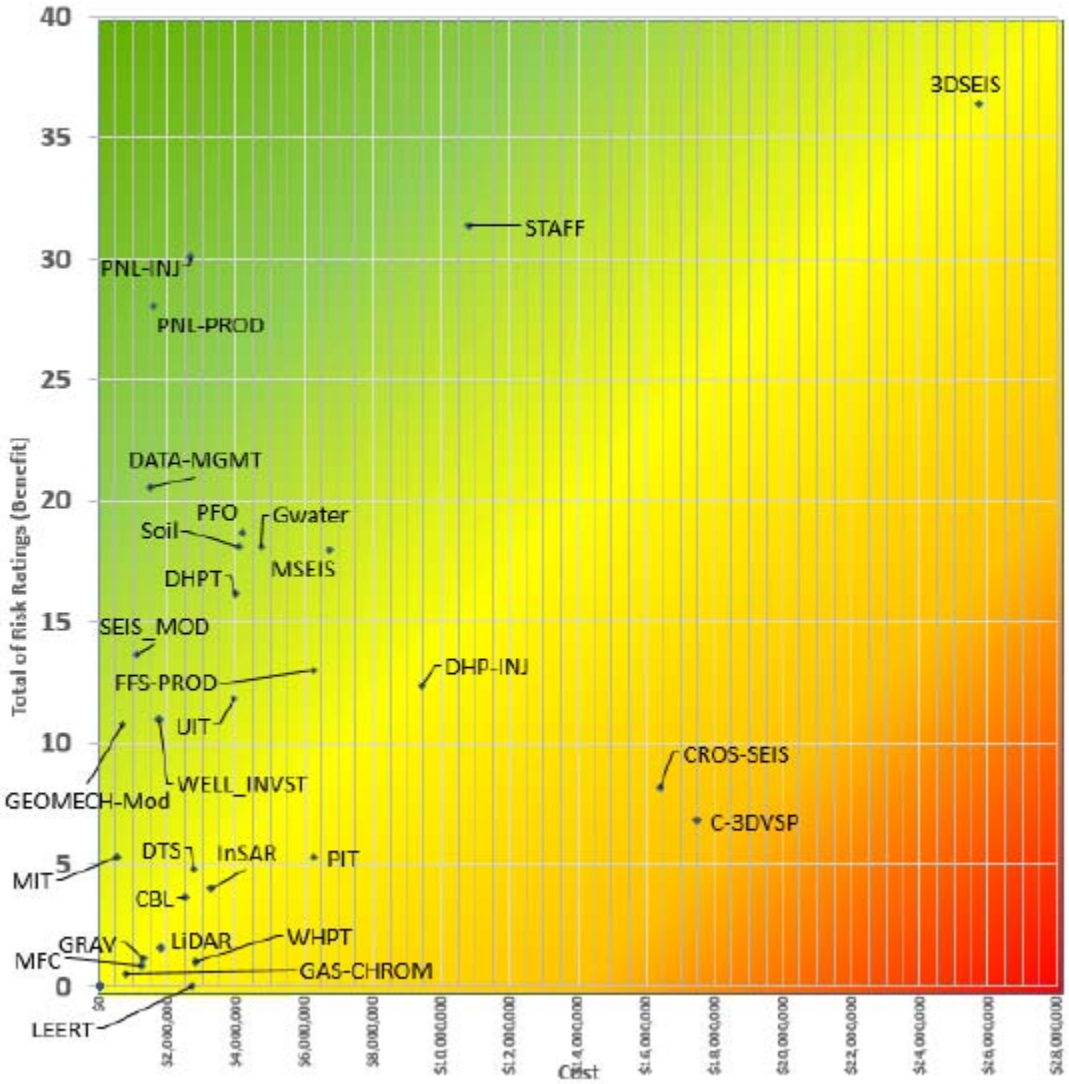

Figure 19 – Monitoring technology cost versus benefit rating.

Cost/Benefit Rank	Cost/Benefit Ratio	Life of Project Cost (21 Years)	Benefit Rating	Tech Short Name	Monitoring Technology and Solutions	Containment	Conformance	Assurance	Required (R) Recommend (RC) Optional (O) Not Feasible (NF)
1	1.78	$1,575,000	28	PNL-PROD	Pulsed Neutron Log (Prod Wells)	Y	Y		RC
2	1.53	$700,000	11	GEOMECH-Mod	Geo-Mechanical Modeling	Y	Y		RC
3	1.36	$1,512,000	21	DATA-MGMT	Monitoring and Data Management System	Y	Y		RC
4	1.24	$1,100,000	14	SEIS_MOD	Forward Seismic Modeling	Y	Y		RC
5	1.14	$2,646,000	30	PNL-INJ	Pulsed Neutron Log (Injection Well)	Y	Y		RC
6	1.05	$504,000	5	MIT	Mechanical Integrity Pressure Test (Tubing and Casing)	Y			RC
7	0.63	$1,750,000	11	WELL_INVST	Offset Well Integrity Investigation	Y			RC
8	0.44	$4,080,000	18	Soil	Soil Gas and Soil Gas Flux Sampling and Analysis			Y	R
9	0.44	$4,200,000	19	PFO	Pressure Fall-off Test		Y		RC
10	0.40	$3,998,000	16	DHPT	Formation Pressure and Temperature Sensors (in and above zone)	Y	Y		O
11	0.38	$4,770,000	18	Gwater	Shallow Groundwater Fluid Sampling and Analysis			Y	R
12	0.30	$3,927,000	12	UIT	Ultrasonic Imaging Tool	Y			RC
13	0.29	$10,800,000	31	STAFF	Full Time Monitoring Staff	Y	Y		O
14	0.27	$6,731,000	18	MSEIS	Microseismic Monitoring Array: Surface or Borehole	Y			O
15	0.21	$6,300,000	13	FFS-PROD	Formation Fluid Sampling and Geochemical Analysis (Obs/Prod Wells	Y	Y		O
16	0.17	$2,760,000	5	DTS	Distributed Temperature Sensors	Y			O
17	0.14	$2,520,000	4	CBL	Cement Bond Log	Y			RC
18	0.14	$25,740,000	36	3DSEIS	3D Seismic	Y	Y		RC
19	0.13	$9,425,000	12	DHP-INJ	Downhole Pressure and Temperature Sensors (Injection Well)	Y			RC
20	0.12	$3,300,000	4	InSAR	Interferometric Synthetic Aperture Radar	Y	Y		NF
21	0.09	$1,300,000	1	GRAV	Surface Gravity	Y	Y		NF
22	0.09	$1,800,000	2	LiDAR	Arial Light Detection and Ranging	Y	Y		O
23	0.08	$6,300,000	5	PIT	Packer Isolation Test, In-situ Stress Test	Y			O
24	0.07	$1,260,000	1	MFC	Multi-Finger Caliper	Y			O
25	0.07	$780,000	1	GAS-CHROM	Gas Chromatograph at Injectate Source/transport Pipeline		Y		O
26	0.05	$16,430,000	8	CROS-SEIS	Crosswell Seismic	Y	Y		NF
27	0.04	$17,500,000	7	C-3DVSP	3D Vertical Seismic Profile	Y	Y		NF
28	0.04	$2,808,000	1	WHPT	Pressure and Temperature Sensors and Flow Rate (Wellhead)	Y	Y		RC
29	0.00	$2,730,000	0	LEERT	Long-Electrode Electrical Resistance Tomography	Y	Y		NF

Table 27 – Cost benefit ranking of monitoring technology

Task 5 - Converting a CO_2 -EOR project to CCUS guidance notes

It is important to give weight to the cost effectiveness of technologies when examining them in respect to recommendations. It is apparent from this study that the majority of the highest ranked technologies are recommended. Pulsed neutron logging is important to ensure there is no leakage above zone formations as well as providing history matched model data. Furthermore, several regulatory regimes recommend pulsed neutron logging to be run in both injection and production wells.

As well, the wells are the highest points of leakage risk. Well integrity is an important consideration when making recommendations. It may be useful, if economically feasible, that each well should have a cement bond log and ultra-sonic imager log performed as a baseline to identify any potential issues with cement that could lead to a loss of containment later in the life of the well.

Due to CCS projects being relatively new, details and technologies are not well understood by all stakeholders. Because of this, there is the requirement of implementing a CCUS monitoring plan that contains a level of assurance that demonstrates the CCUS project will have no adverse effects on health, safety, or the environment. To accomplish this, soil gas and soil gas flux

sampling should be conducted, as well as shallow groundwater fluid sampling with associated analysis.

Currently, 3D seismic is the most effective technology available to image the subsurface. In the interest of containment and conformance it is recommended that a series of 3D surface seismic surveys be conducted to monitor plume progression.

A geomechanical model can be built and used to predict the development of the CO_2 plume for the purpose of guiding monitoring methods. A geomechanical model is not perfect in the prediction of the CO_2 plume development, however, when history matched to downhole pressure and temperature data, the ability to predict plume development can be improved. The placement of downhole pressure and temperature gauges in the injection well as well as pressure and temperature sensors on the wellhead with a flow meter to track the amount of CO_2 injected and produced are recommended.

Conclusions

The monitoring technology ranking demonstrated by the study can aid in the creation of a monitoring plan. It affords an operator a method of objectively comparing monitoring technologies to address specific needs related to site-specific risks, regulatory regimes, and economics, this ranking was tailored to the Weyburn-Midale field, however, it is adaptable to other CO_2-EOR fields interested in converting to CCS. CO_2-EOR operators adapting to this approach will have to adjust their approach based on site-specific and operation-specific factors.

If this ranking is used to develop a comprehensive monitoring plan it should be subjected to regular (preferably annual) performance reviews. It is unlikely that any monitoring plan will perform exactly as expected and significant deviations from expected results will require Weyburn-Midale field to adapt the monitoring plan in response to new information acquired. It is important to note that such deviations would not necessarily imply any failure of the storage facility to meet performance criteria. It may become clear that some technologies are working better than expected, not as expected, or that the plume is behaving in a way that is not expected.

The ranked monitoring technologies will aid operators in meeting the regulatory requirements by allowing selection of technologies that meet operation and regulatory requirements. This may allow an operator to select a minimum number of technologies deployed on a minimum schedule that will provide a reliable monitoring derived conclusion on containment, conformance, and assurance.

Final conclusions can be summarized as such:

- Every CO_2-EOR field requires a site specific approach

- This methodology can be tailored to other CO_2-EOR fields
- Regulations will vary depending on country, state and province.

7.0 SaskCO_2USER (WMP Optional Phase) – Casing Corrosion

Aging wellbores are a challenge for operators, and casing corrosion both during operations and post-abandonment remains a challenge. According to NACE International (2014), the total annual cost of corrosion in the oil and gas production industry is estimated to be US$1.372 billion, broken down into US$589 million in surface pipeline and facility costs, US$463 million annually in downhole tubing expenses, and another US$320 million in capital expenditures related to corrosion. Despite these realities, only limited work has been done in identifying specific mitigation strategies for CO_2-EOR operations.

The impacts of casing corrosion are multifold. The remediation and repair of failed wellbores can be costly; as well as hazard and environmental safety, financial and regulatory impacts exist. By reducing unnecessary monitoring, and identifying the wellbores and factors with the highest probability for failure, wellbore failure – and associated costs – will be reduced. Laboratory research has explored casing corrosion rates, and other jurisdictions have explored casing corrosion using publicly available data. This project focused on improving operational economics by comparing case studies and in-situ results.

Objectives for this casing corrosion project were to build a better understanding of corrosion mechanisms and identification strategies, and aid development of a relevant analytical strategy to aid in the identification and mitigation of potential corrosion issues during CO_2-EOR and/or CO_2 sequestration. The Energy and Environmental Research Center was selected as a subcontractor for this project by the PTRC.

7.1 Casing Corrosion – Approach and Methodology

The goal of this project was to conduct a corrosion and failure assessment for well casing in an area undergoing active CO_2 injection for enhanced oil recovery purposes and to determine corrosion rates, location of corrosion, and factors influencing corrosion. The Weyburn-Midale field was chosen as the site for this study. Oil and gas reservoirs are a primary target for CO_2 storage because of the CO_2's ability to increase oil production, with an additional benefit being the long-term storage of CO_2. For EOR and CO_2 storage to be successful, the targeted formation needs to be able to contain the injected CO_2. The large number of legacy wellbores in EOR fields has the potential to provide a leakage pathway for the injected CO_2 if a wellbore integrity is affected by corrosion. Corrosion can occur anywhere along the wellbore through the cement, casing, tubing, or plugs and is an important issue facing the oil and gas industry, with large capital expenditures being directed at the problem.

Three case study wells in the Weyburn Field near the area where CO_2 injection has actively been occurring and two where CO_2 injection has not occurred were chosen for this study. Wells from multiple areas were targeted because of vast difference in exposure to CO_2. The wells were identified from over 3100 in the field based on available logs and proximity to CO_2 injection activities. Logs of specific interest were those that evaluate casing or cement. All five of the wells chosen for this case study were producers, water injectors and, eventually, CO_2 injectors. The volume of CO_2 injected for the wells widely varied and provided a means to determine the impact that varying volumes of injected CO_2 may have on the casing.

The five cases all exhibited signs of internal corrosion, with most present in the lower sections of the casing, near existing production perforations. Corrosion ranged from small pits to complete penetration through the casing. Contributing factors to corrosion in these wells ranges from exposure to CO_2, packer placements, number of completions, formation fluid exposure, and stray current. In general, wells that were exposed to CO_2 exhibited more severe corrosion, but that may not be the only contributing factor. External corrosion was present in wells where appropriate logs were available to examine the outer surface of the casing. External corrosion was most prevalent in the section of free pipe from the top of cement to the surface.

Corrosion is a complex, naturally occurring phenomenon involving the deterioration of materials because of reaction with the environment. Corrosion affects all industries that use metallic materials; the oil and gas production industry is one of those industries (Brondel et al., 1994; Ossai, 2012; Popoola et al., 2013). According to NACE International (2014), the total annual cost of corrosion in downhole tubing and associated capital expenditures is about US$783 million. Thus corrosion can consume large resources for management and control.

Because of carbon constraints and EOR opportunities, CCS technologies are aggressively being pursued, especially storage in underground geologic formations. Given that CO_2, like H_2S and other chemicals, is corrosive when it dissolves in water or formation fluids, it is critical to identify and resolve CO_2-related corrosion issues to prevent failures in equipment that could lead to out-of-zone migration of CO_2 as well as save large financial resources involved in the management and control of corrosion problems. To effectively manage and/or prevent failures of well casings due to corrosion, it is critical to assess the risk factors associated with these failures in order to develop guidelines for proper monitoring, routine inspections, and adequate control options, particularly considering the nature of CO_2 storage in depleted oil and gas fields and in association with enhanced recovery schemes where vintage wells and well construction are prominent and where the ability to predict, monitor, and remediate corrosion plays a critical role in terms of site security, operations planning, and financial management and planning of those operations.

Work performed by Hawkes et al. (2012) assessed the construction details and factors affecting wellbore integrity in the Weyburn–Midale field. Data from approximately 183 wells were collected from public and private sources. The study indicates that a good cement job is an important step in protecting a wellbore from failure. The authors also stress follow-up monitoring (surface casing vent flow [SCVF] and annular pressure) to further monitor the well.

Positioning of plugs and packers and plugging procedures are also important factors that aid in isolating the subsurface environment. Field studies with the use of advanced logging tools were also demonstrated to show effectiveness in determining potential leakage pathways in unplugged wells and ensuring integrity in CO_2 injection wells.

The project was divided into five tasks:

1. Select wells with enough data to provide meaningful evaluation.
2. Collect public and nonpublic data in Saskatchewan and other appropriate fields relating to casing and cement evaluations of wellbores.
3. Maintain a database of pertinent data collected and identified.
4. Identify five case studies from collected data for further evaluations.
5. Determine corrosion rates and locations, as well as any contributing factors.

In regards to actual project deliverables, they can be understood as a chronological sequence focused on the five well case studies – each of those cases examined in detail under Results and Recommendations below – with the majority of the work focused on analyzing the five selected wells:

1. Background – mechanism and rates of corrosion.
2. Identification of five wells for evaluation and case study.
3. Well Work and Comparison
4. Conclusions and recommendations for future work

7.2 Casing Corrosion – Results and Recommendations

Task 1 – Background – mechanisms and rates of corrosion

Background factors were established through the provision of an overview of wellbore integrity, corrosion mechanisms, and the determination of corrosion rates. It was deemed necessary to study all related facets of corrosion to build a complete understanding of the challenges associated with corrosion in a subsurface environment.

Wellbore integrity. For CCS to be successful, a CO_2 storage formation needs to meet three fundamental conditions: 1) capacity, 2) injectivity, and 3) confinement (Bachu, 2003, 2010; Intergovernmental Panel on Climate Change, 2005; Zhang and Bachu, 2011). The targeted CO_2 storage formations have demonstrated the capacity and ability to hold materials such as oil,

natural gas, or saline water. Wellbore integrity is the ability of a well to maintain isolation of geologic formations and prevent the vertical migration of fluids (Crow et al., 2010; Zhang and Bachu, 2011). Wellbore integrity is crucial because any leakage of CO_2 poses a potential risk to surrounding groundwater, vegetation, and wildlife. In addition, it diminishes the quantity of CO_2 for which storage credits can be claimed as part of either monetary agreements or regulatory compliance. In the case of EOR, the loss of CO_2 also represents a tangible loss of economic resources and decreases the recovery efficiency of an EOR operation. For the purposes of this study, leakage was defined as a loss of CO_2 or other fluid from its intended storage formation and not necessarily losses to the atmosphere.

For a CO_2 leak to occur, three elements must exist: 1) a leak source, 2) a driving force such as buoyancy or head differential, and 3) a leakage pathway (Watson and Bachu, 2007). When the potential of CO_2 leakage at a carbon storage site is evaluated, the first two elements are presumed to already exist. The injected CO_2 is the leak source, and the driving force is CO_2 buoyancy and, potentially, the increased subsurface pressure caused by the CO_2 injection (Watson and Bachu, 2007). The leakage pathway is the third element for a leak to occur.

Wells are one possible pathway for CO_2 to escape the storage formation (Celia et al, 2004) as displayed by Figure 20. CO_2 could potentially leak along interfaces between different materials, such as the steel casing and cement interface (a), the cement plug and steel casing interface (b), within the cement (c), or a perforation in the casing (d), or fractures in the cement (e) and the rock and cement interface (f). Finally, leakage may also occur because of casing corrosion and subsequent failure leading to leakage pathways, with the wellbore as a conduit.

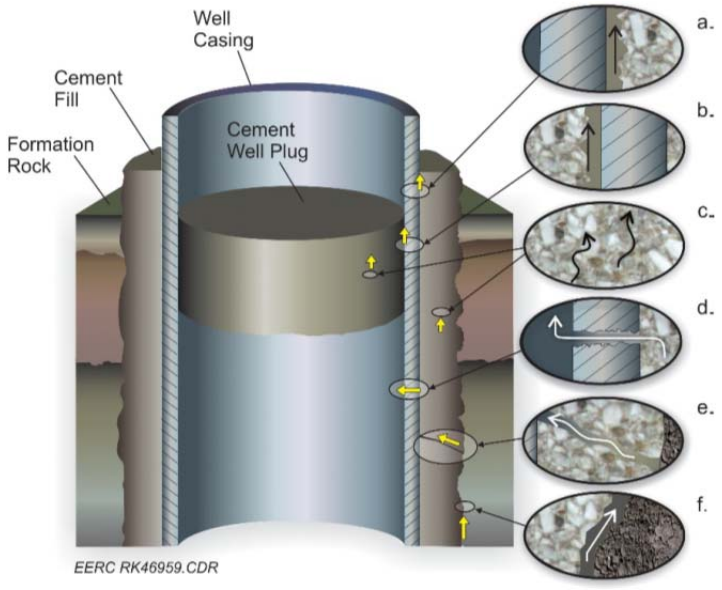

Figure 20 – Conceptual illustration of the potential leakage pathways for CO_2 in a well along the casing–cement interface (a and b), within the cement (c), through the casing (d), through fractures (e), and along the cement–formation interface (f) (Celia et al, 2004).

Corrosion mechanisms. Major forms of corrosion have been reviewed extensively. These reviews have indicated that corrosion problems during the deployment of CCS and CO_2-EOR technologies can become more complicated and fairly widespread throughout many facets of the process from surface storage and transportation equipment to downhole pipes/casings and associated accessories. A summary of these corrosion mechanisms includes sweet corrosion (CO_2-related corrosion), sour corrosion (H_2S-related corrosion), oxygen corrosion, galvanic or electrochemical corrosion, crevice corrosion, pitting corrosion, erosion corrosion, microbiologically induced corrosion (MIC), stress corrosion cracking, stray current corrosion, strong acid corrosion, and dense brine corrosion.

Sweet Corrosion. Sweet corrosion is the common name for CO_2 -induced corrosion, which occurs when CO_2 dissolves in an aqueous environment (water or formation fluids) to form mostly carbonic acid (H_2CO_3). The produced carbonic acid then promotes electrochemical reactions between steel and the aqueous phase. CO_2 -related corrosion can lead to a localized pitting attack on the metal due to rapid flow conditions (Canadian Association of Petroleum Producers, 2009a; Popoola et al, 2013). Sweet corrosion can be influenced by factors such as temperature, increase in pH, composition of the aqueous medium, nonaqueous phases, flow condition, and metal characteristics. The mechanism for sweet corrosion involves oxidation of iron in the steel to Fe^2+ and reduction of carbonic acid to bicarbonate and hydrogen atoms, which combine to form molecular hydrogen and iron carbonate by reaction with bicarbonate as shown in the following overall reaction (Popoola et al, 2013):

$$CO_2 + H_2O + Fe \rightarrow FeCO_3 + H_2$$

Sour Corrosion. H_2S, just like CO_2, dissolves in water to form a weakly acidic solution that is corrosive to steel, with iron sulfide (FeSx) as the major scale product. The formation of FeSx scale can help slow the corrosion at low temperatures (<300°F [150°C]) if Cl- and/or oxygen are not present in the environment. This type of corrosion can occur deeper in the well and generally takes the form of uniform pitting and stepwise cracking. At higher temperatures (e.g., around 300°F [150°C or higher]), the scale is cathodic and can initiate galvanic corrosion (Brondel et al, 1994, Canadian Association of Petroleum Producers, 2009b). Hydrogen atoms produced in the process can eventually lead to embrittlement of the pipe or casing. The major chemical mechanism involved can be represented by the following reaction:

$$H_2S(g) + H_2O(l) + Fe(s) \rightarrow FeS_x(s) + 2H + H_2O(l)$$

Pitting/Crevice Corrosion. Pitting and crevice corrosion are a localized corrosion event that can be caused by similar mechanisms, initiated by a scratch or crevice (joints, tubing collars or casing collars). This corrosion can also be a result of other factors that preferentially accelerate other types of corrosion (e.g., sweet, sour, or oxygen corrosion) at a localized spot on the casing

surface. This corrosion mechanism is influenced primarily by oxygen and chloride concentrations in and external to the scratch or crevice (Brondel et al, 1994).

Microbiologically Induced Corrosion. MIC is caused by bacterial activity in the environment of the casing pipe (Cord-Ruwisch et al., 1987; Lane, 2005; Enning et al., 2012; Popoola et al., 2013; Enning and Garrelfs, 2014). Because of the rapid growth of bacteria to form large colonies, MIC can be enhanced in a short time, leading to pitting in the areas with a mass of the colony. Many types of bacteria are known (Lane, 2005; Popoola et al., 2013), including species of *Bacillus*, *Pseudomonas*, *Micrococcus*, *Mycobacterium*, *Clostridium*, and *Escherichia*. Perhaps the most important of these bacteria species are sulfate-reducing bacteria (SRB), which reduce sulfate ions in an organic carbon source and anaerobic conditions to H_2S.

However, Enning and Garrelfs (2014) report that certain types of SRBs can also attack iron via withdrawal of electrons directly by metabolic coupling, a process known as electrical microbially influenced corrosion (EMIC). With the production of H_2S, chemical corrosion mechanisms are initiated. MIC can often lead to crevices or pitting, particularly in low-flow-rate environments where hard rust nodules with differing O_2 amounts form. MIC can be recognized by the appearance of a black, slimy waste material or nodules on the pipe surface, as well as pitting of the pipe wall underneath these deposits.

Iron bacteria have also been found to be involved as a key mechanism of biofouling and encrustation of casing material in wells (Walter, 1997). Iron–bacteria biofilms alter the chemistry of well water by removing iron, manganese, and sulfate from solution and by increasing the pH. Because legacy well casings are typically made of steel, with iron as the major component, iron–bacteria corrosion mechanisms can be a “hidden” threat to these types of materials that are commonly used in CO_2 sequestration/EOR projects.

Stray Current Corrosion. Potentially leaked AC and/or DC currents in the ground that come into contact with the conductive pipe or casing wall will turn the point of contact into a cathode, while the point where the current departs will become an anode. By creating a cathode and an anode connected by flowing current, electrochemical corrosion begins with loss of metal at the anodic point. Stray DC currents are known to be about 100 times more destructive than stray AC currents, and only 1 amp/year of stray DC current can corrode up to 20 lb-m (9 kg) of steel (Brondel et al, 1994). This type of corrosion event is often mitigated with cathodic protection systems.

Strong Acid Corrosion. Strong acid corrosion is a form of direct chemical attack on metals by acids such as HCl, HF, and formic acid, all of which are used for different well stimulation scenarios. Corrosion inhibitors and reduced exposure time can be used to reduce these types of chemical corrosion. The effectiveness of HCl corrosion inhibitors can be influenced by well depth and souring of the well (Brondel et al, 1994).

Concentrated Brine Corrosion. Dense brines containing metal ions such as Ca and Zn are typically used to balance formation pressures during production operations. These can be corrosive because of dissolved O_2 or entrained air or because of metal ion hydrolysis reactions such as Zn from $ZnCl_2$ brines. Because of the acidity created by the hydrolysis of Zn^{2+} ions, the more expensive $CaBr_2$ brines are most often used instead of zinc brines. It should be noted that these brines are not typically used in Canada.

Casing Corrosion Rate. Determining casing corrosion rates can be just as complex as the corrosion mechanisms themselves. Corrosion is a complex, naturally occurring phenomenon involving the deterioration of materials because of reactions with the environment. Typically, these reactions are electrochemical in nature and require electrons to be transferred to or from a reacting surface. The surface receiving the electrons is referred to as a galvanic cathode, and the surface that generates the electrons is the galvanic anode. The transfer of such electrons can be measured as current (I) in amperes according to Faraday's Law (Jensen, 2012; Orayith, 2012):

$$m = \frac{Ita}{nF}$$

where

m is the mass reacted (or equivalent weight for alloy composites)

I is the total anodic current

t is the time

a is the atomic mass (g/mol) of corroded metal)

F is the Faraday constant (96,500°C/mol electrons transferred)

n is the number of moles of electrons transferred during the reaction (i.e., mol electrons/mol of metal corroded)

The corrosion rate in terms of mass reacted per unit time per unit surface area of reaction can be easily obtained by dividing Equation 1 by time and total surface area of reaction. However, because corrosion rate calculations for casing steel alloys is not as straightforward as that for pure elements, ASTM International (ASTM, 2010) has developed a standard practice method for determining the corrosion rate for casing alloy materials. According to this method, the corrosion rates in terms of corrosion penetration rate (*CR*) or mass loss rate (*MR*) are given by:

$$CR = K_1 \frac{i_{corr}}{\rho} EW$$

$$MR = K_2 i_{corr} EW$$

where

CR is the corrosion penetration rate in mm/yr

i_{corr} is corrosion current density in μA/cm^2

K1 = 3.27 x 10^{-3} mm·g/μA/cm·yr

ρ is density in g/cm^3

MR is corrosion mass loss rate in g/m^2·d

K_2 = 8.954 x 10^{-3} g·cm2/μA/m·d

EW is equivalent weight of alloy considered to be dimensionless in these calculations.

In these calculations, the total anodic current (*I*) is assumed to be distributed uniformly over the total surface area (*A*) exposed to corrosion. For pure elements, the mass (m) is basically the atomic mass of the element, but for casing alloys, the calculation becomes a lot more complicated, and m is defined in terms of the equivalent weight (ASTM, 2010). Based on these equations, the corrosion rate can be estimated once the current density is known.

Task 2 - Identification of five wells for evaluation and case study

With over 3100 wells in the Weyburn Field, the first task was to select three wells with enough data to provide a meaningful evaluation. Location and the availability of corrosion evaluation logs were the primary drivers in selecting the case study wells. The preferred location was to be in proximity to where CO_2 had been injected. Logs that were sought included a combination of caliper logs, ultrasonic bond logs, sector bond logs, and casing imaging logs. The ideal case study wells were envisioned to have had an array of logs that had been run over the well's history, including pre- and post- CO_2 injection, to show how the cement and casing had changed over time.

Internal and/or external casing corrosion were deemed critical components of the evaluation, which was evaluated by a combination of caliper logs and casing imaging logs where available. The quality of the cement was evaluated by CBLs, sector bond logs, or ultrasonic bond logs. Some of the logs that were found covered the entire length of the wellbore, but in other cases, only targeted intervals of the well were logged. The case study wells were selected based on the best available log suites available in an area in proximity to CO_2 injection and in some cases were not as complete as ideally desired. Ideal case studies are difficult to obtain because well logging activities do not have scholarly research as a main objective.

The wells identified were selected based on historical well log data. Each well will be discussed and summarized in regards to history, location, corrosion evaluation, well log analysis, and conclude with a corrosion rate analysis.

7.2.1 Case Study Well One (1)

History

This well is a vertical water/CO_2 injector that was drilled in 1957 in the area that eventually became Phase 1a of the Weyburn CO_2 injection program. Production records indicate the well was in production from 1957 to 1964. Water injection in this well started in 1964, and it was converted to a water alternating gas (WAG) injector in 2000 as part of the Weyburn EOR project. This well was a WAG injector until late 2008, after which it injected only water until its abandonment in November 2010. Perforations created for production and/or injection purposes are in the interval from 1391.1 to 1400.3 mKB (meters below kelly bushing) and 1402.4 to 1403.9 mKB in the Marly and Vuggy Formations within the Midale Beds. An abandonment program was initiated in 2009 and completed in 2010 because the wellbore casing integrity was deemed unsuitable for WAG injection. As part of the abandonment process, a cement squeeze was performed in 2010 over the interval from 1210 to 1403.9 m to plug off the production perforations.

The casing record indicates that Steel Grade J-55 was used for the surface and production casing strings. Cement records indicate that the surface casing was cemented with 180 sacks of Saskatchewan construction cement with 2% $CaCl_2$. The production casing was cemented with 180 sacks of Dowell bulk cement with 3% gel to 365 meters above the shoe. Well data sheets also indicate that 25.5 tonnes of Class G cement with calcium chloride additive was used for the cement squeeze program in 2010.

String	Weight, kg/m	Grade	OD,[1] mm	ID,[2] mm	Depth m
Surface	35.72	J-55	219.1	205.7	90.74
Production	20.83	J-55	139.7	127.7	1420.37

[1] Outer diameter.
[2] Inner diameter.

Table 28 -- Casing record and characteristics for Case Study 1

This well was selected as a case study for two key reasons: 1) activity in the well spans the period before CO_2 injection (1957–2000), active CO_2 injection (2000–2009), and post-CO_2 injection (2009–present) and 2) logs are available in each of the three periods, although the log types vary as well as the interval that was logged. Such information provides a good assessment of the casing and cement integrity pre-, during, and post- CO_2 injection for this well.

Location

As noted, this well is located in the Phase 1a area of Weyburn oil field in the province of Saskatchewan, Canada.

Corrosion

An evaluation of corrosion for any production or injection well involves an assessment of at least the casing and cement integrity. For the subject well, Vertilog™ and acoustic CBLs are available from 1987; a casing inspection, Vertilog, and another CBL from 2002; an X–Y MIT (multifinger imaging tool) survey in 2008; and an SBT (sector bond tool) logged in 2014. Although, the intervals logged vary for different log types, these logs do provide an overview of the casing integrity for this well that covers the three periods of activities indicated above. Results from the examination of these logs are presented below for the casing integrity status and the cement integrity status. The results are presented in chronological order beginning in 1987 (Vertilog, CBL), 2002 (Micro-Vertilog^{TM}, CBL) 2008, 2014.

Well Log Analysis

1987

Corrosion was evident in the bottom of the casing from about 1375 to 1408 m, with multiple penetrations (nonproduction) observed. Two of the three penetrations were in the immediate zone above the existing production perforations at 1372.5–1383.5 m and 1383.5–1389.5 m. The third penetration at 1389.5–1402 m is likely an existing production perforation in this well. The lower half of the production casing from about 360 to 1375 m was in good condition at the time this log was run in 1987, while the upper half from 360 m to the surface casing shoe at 90 m displayed multiple single isolated pitting (SIP) instances of Class 2 type. The interval above 90 m showed only two Class 2 SIP defects at about 54.6 and 90.5 m. Generally uppermost casing interval was in good condition in 1987.

Code Symbol	Classification
U	Unclassified (< 20% wall loss)
2	21% to 40% wall loss
3	41% to 60% wall loss
4	61% to 80% wall loss
P	Penetration

Table 29 – Corrosion evaluation classification scheme

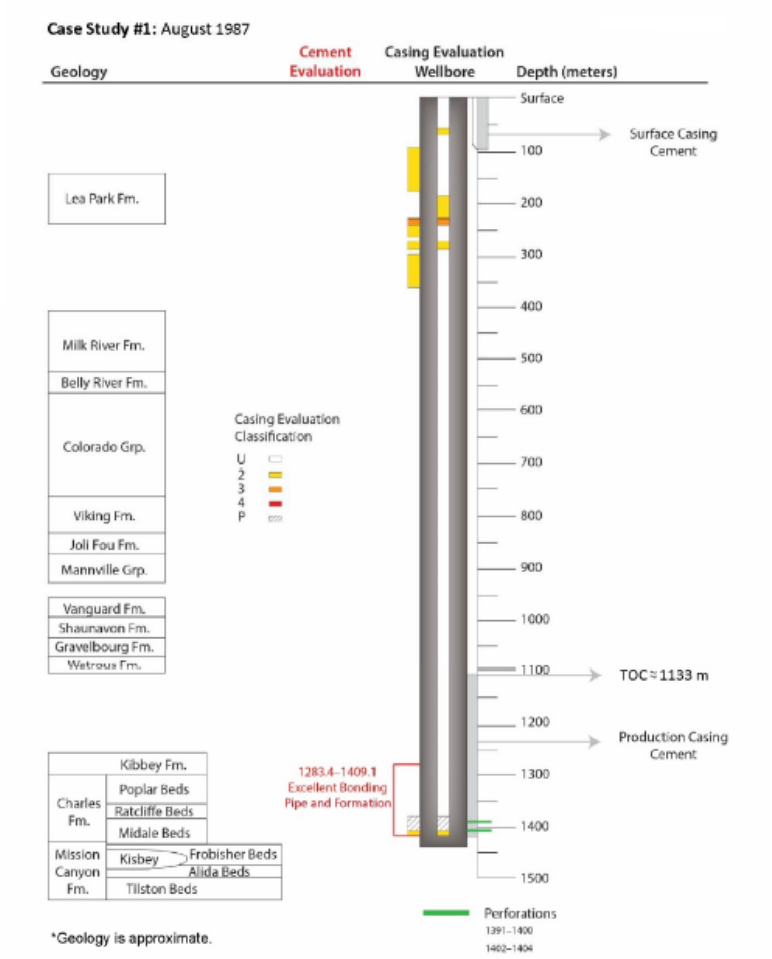

Figure 21 – Schematic representation of 1987 Vertilog results

An acoustic CBL was surveyed in 1987 over the interval from 1283.4 to 1409.1 m. The log results show excellent bonding to both pipe and formation over this interval. The VDL (variable-density log) shows strong formation arrivals and low-amplitude early arrivals, which are consistent with good bonding conditions. There was no cement map available, and it is not possible to deduce the presence of channeling or microvoids from this log.

2002

The Micro Vertilog surveyed in 2002 evaluated the interval from surface to 1353 m, with the bottom log interval about 55 m above the bottom log interval from the 1987 log (surface – 1408 m). Also, the 2002 interval does not include the zone with existing production perforations at 1372.5–1383.5 m and 1383.5–1389.5 m. The results indicate that production casing string had suffered increased corrosion since the 1987 survey. The top 100 m of casing was in very good condition in 1987 but had a Class 3 pit with 60% wall loss at 44.28 m. Additionally, 24 Class 3 pits were identified below 100 m in depth, of which 13 were located between 100 and 335 m. Also noted from the results is the fact that all of the Class 3 pits from

100 to 335 m are on the external casing surface, while most from 335 m and lower are on the internal surface, quite possibly due to additional isolation from geologic formations provided by the surface casing. A detailed list of the corrosion defects with more than 20% wall loss is schematically represented in Figure 21. Note that this well may show more external corrosion because of the specific tool that was used. Not every log studied in this report provides detail of external corrosion.

In 2002, a pressurized CBL survey at 7 MPa was conducted to check the cement integrity. The interval logged was from 1100 to 1351 m with the TOC (top of cement) being 1133 m. Based on the log results of the pressurized pass, there is poor cement bond to the casing pipe between 1133 and 1175 m, but there appears to be a weak bond to the formation. The VDL shows high-amplitude early arrivals and weak formation arrivals. However, the interval from 1175 to 1351 m has excellent bonding to both pipe and formation. The VDL shows strong formation arrivals and low-amplitude early arrivals, indicating good bond to pipe and formation. A high-speed overview pass (no pressure) was also run from the surface to 1349.97 m. The log results show the top of the fluid at about 180 m. The last section from 1175 to 1350 m shows excellent bonding to both pipe and formation. The VDL indicates both strong formation arrivals and low-amplitude early arrivals, which indicates good bond to pipe and formation. Figure 22 contains a schematic representation of the 2002 CBL.

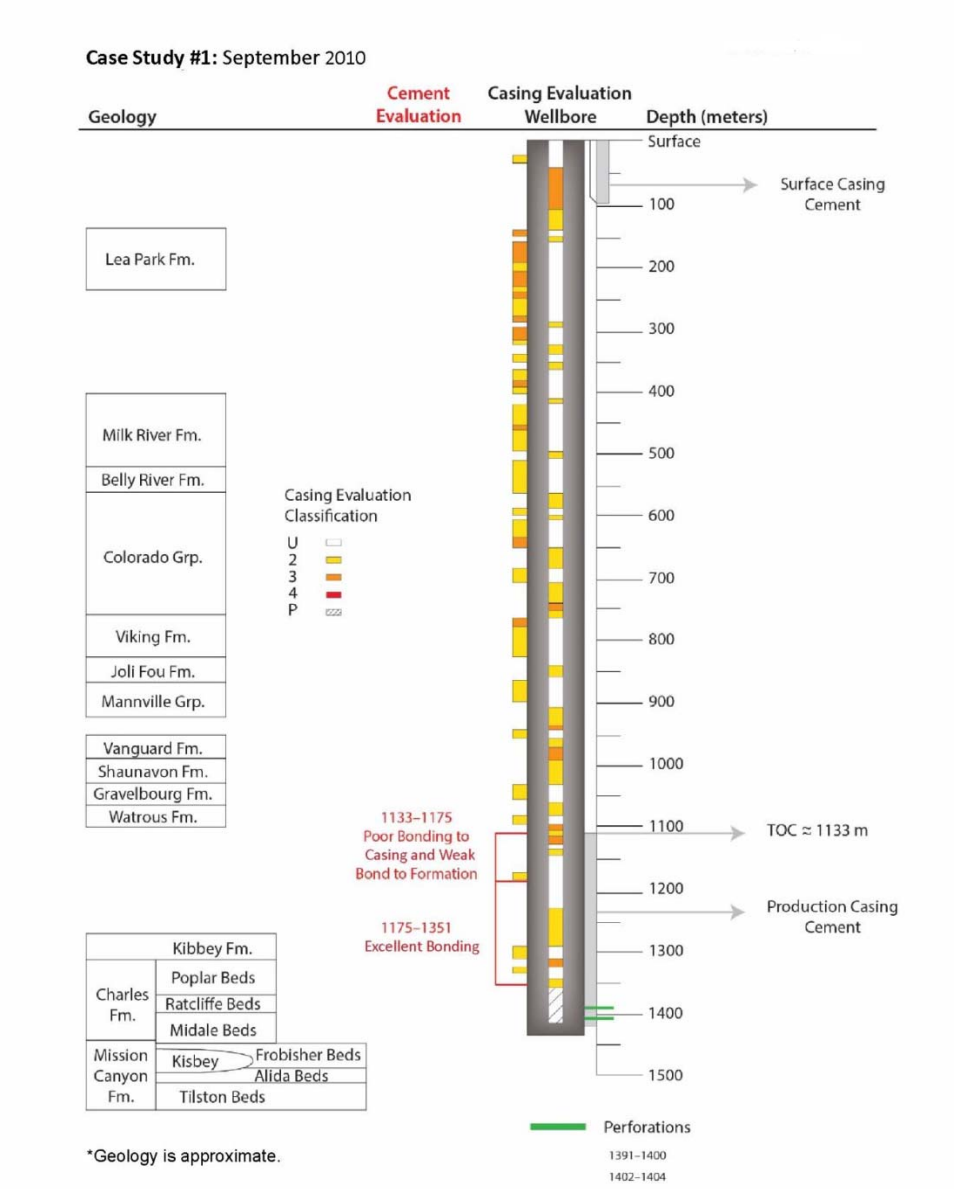

Figure 22 – Schematic representation of 2002 Micro Vertilog and CBL results

The 2002 log did not survey the bottom 55 m of the casing relative to the 1987 log and, therefore, did not include the zone with the three production perforations identified in the 1987 log. The 2002 log shows multiple Class 3 pits emerging on the production casing string. Given that most of these defects are on the external surface of the casing, cement quality will play a critical role in ensuring isolation between formation fluids and overlying zones via the wellbore should casing corrosion continue to intensify and not be remediated. Figure 23 shows a summary of the number of corrosion-affected joints by their classification for the 1987 Vertilog and 2002 Micro Vertilog. It should be noted that the resolution of the Vertilog is not as high as that of the Micro Vertilog and the Vertilog also did not have the accompanying

quantitative wall loss summaries and position of defects from the caliper arms as was the case in the 2002 Micro Vertilog. However, detailed inspection of the logs indicated that there was the presence of corrosion in some joints where the Vertilog simply reported one instance per joint.

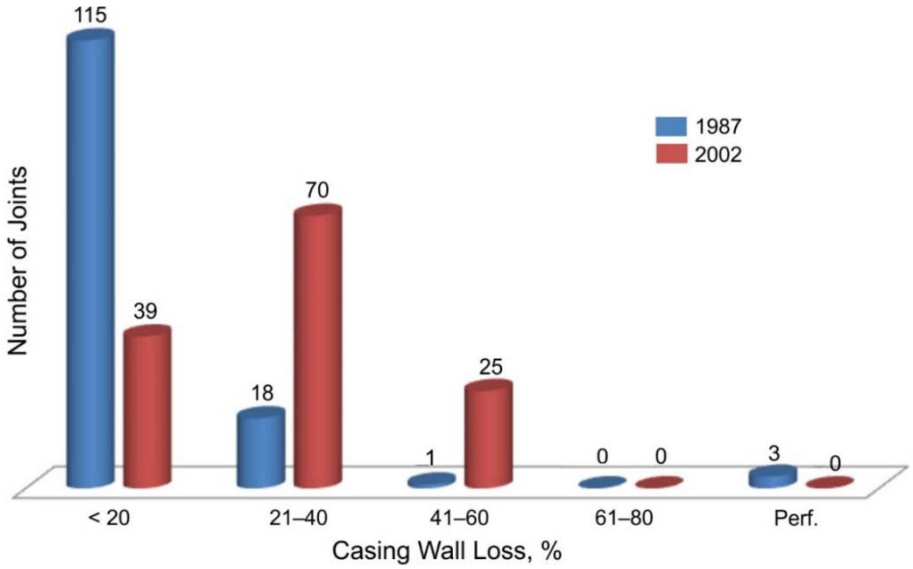

Figure 23 – Summary number of defective joints by classification, obtained in 1987 and 2002 for Case Study 1

2008

An X–Y caliper tool was logged in 2008 over the interval from 1336.65 to 1376.24 m. Based on observations from the log, corrosion was found in the interval from 1362 to 1368 m, with at least 70%–80% casing wall loss. It was also found from the log that the casing section from 1368 m was not present, as shown in Figure 24. The well files do not indicate that the casing was intentionally removed; rather they suggest corrosion is the reason for the missing casing. A schematic representation of the MIT results is found in Figure 25.

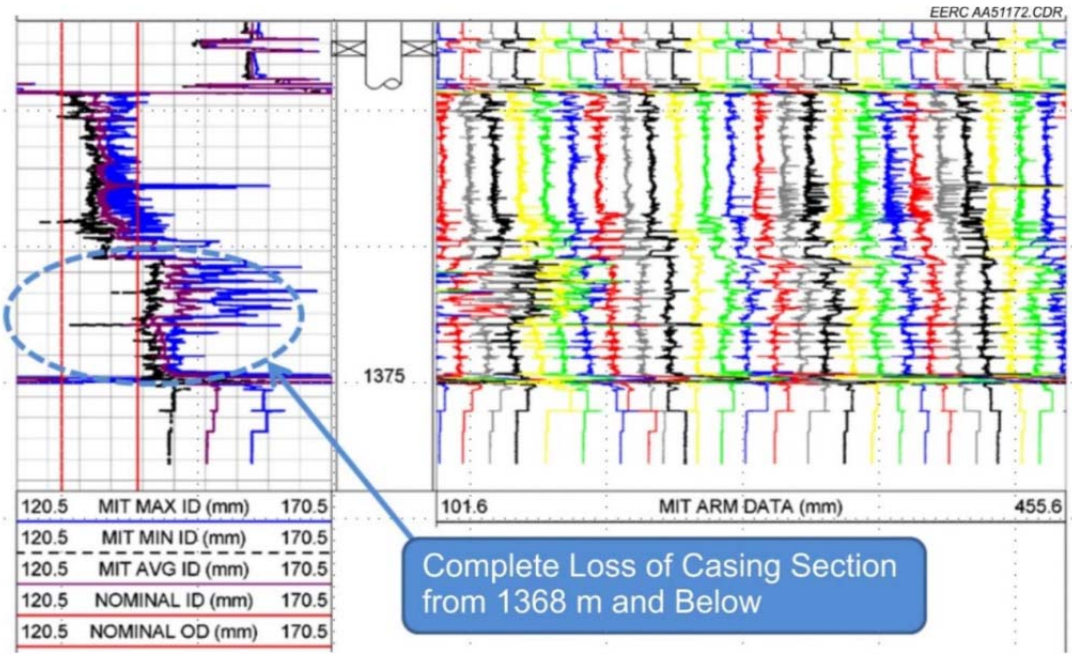

Figure 24 – X-Y caliper log indicates missing casing section in Case Study 1

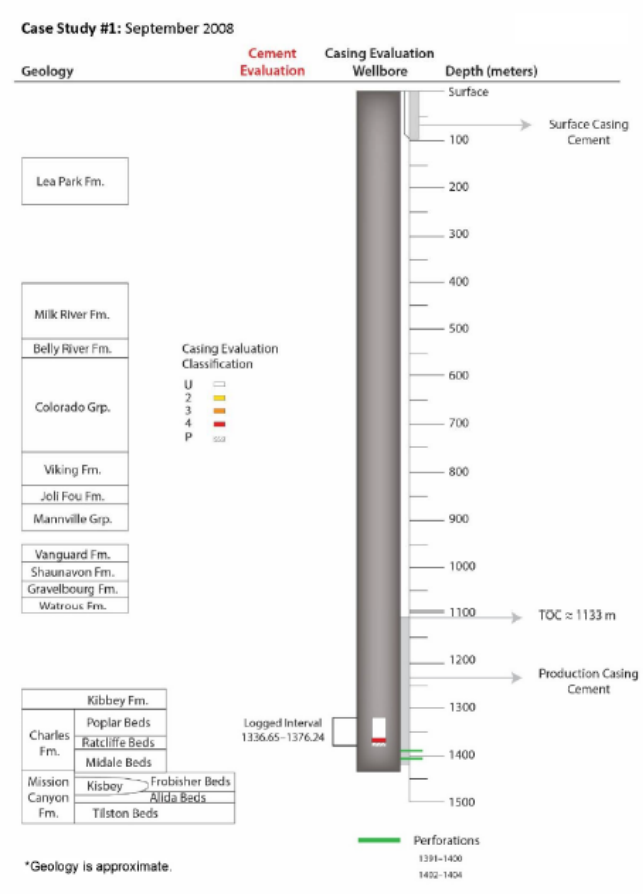

Figure 25 – Schematic representation of MIT

2014

An SBT was logged to evaluate the quality of the cement behind the casing in 2014. During this survey, the log was conducted without any pressure applied to the casing because the connection between the wellhead and the flange did not hold pressure. Based on available well information, there is no indication of the presence or absence of fluids in the wellbore during the SBT logging survey. The cement top was identified in this log as ~1147 m, previously near 1133 m. It is not expected that cement from 1133–1147 has deteriorated; rather, this can be explained by tool sensitivities or anomalies in the cement job not detected by previous tools.

Observations from the log show excellent cement bond from 1145 to 1256 m, with the 3-ft amplitude ranging from 0 to 5 and 0 to 12 mV, respectively. The VDL in the top interval (1145 to 1256 m) shows strong formation arrivals and low-amplitude early arrivals, indicative of good bond to both casing and formation. However, the bottom of the same interval from 1145 to 1256 m has good cement bond to pipe but poor bond to the formation. Also, the cement map shows no microvoids or channels in the top interval, but the bottom interval has a few circumferential microvoids. Extended zonal isolation is expected in the top interval, and some isolation and pipe protection can be achieved in the bottom interval.

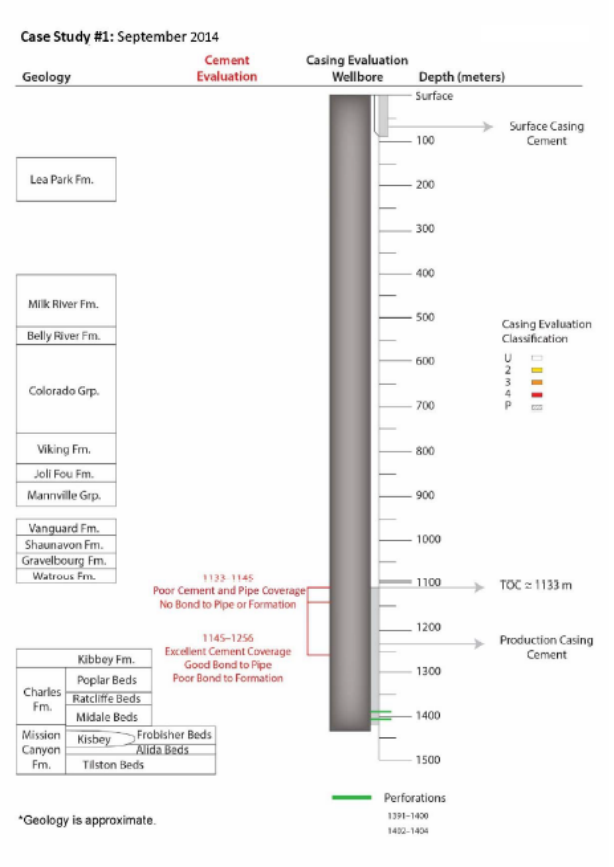

Figure 26 – Schematic representation of the 2014 SBT log

Corrosion rate analysis

A determination of corrosion rates required some estimate of the corrosion current density, surface area exposed to corrosion, and equivalent weight of the casing composite as discussed in the background section of this report. Although surface area and density of casing strings could be estimated from available casing record data, the current density data were not available for downhole well casings. Consequently, the only qualitative interpretation provided is based on first-principle estimations of rates using casing wall loss data obtained from caliper or other logs such as a casing imaging tool (CIT) log, Vertilog, and Micro Vertilog.

For this well, the rate data for all joints with corrosion evident based on the available 2002 Micro Vertilog were divided into internal and external corrosion and correlated with depth to obtain a general sense of the rate trend up or down the wellbore. It was observed that the internal rate of corrosion slightly increases from top to bottom of the wellbore casing, as shown by the slight positive slope of the trend curve. On the contrary, the external rate of corrosion increases from top to bottom as shown by the slight negative slope in the trend curve in Figure 28.

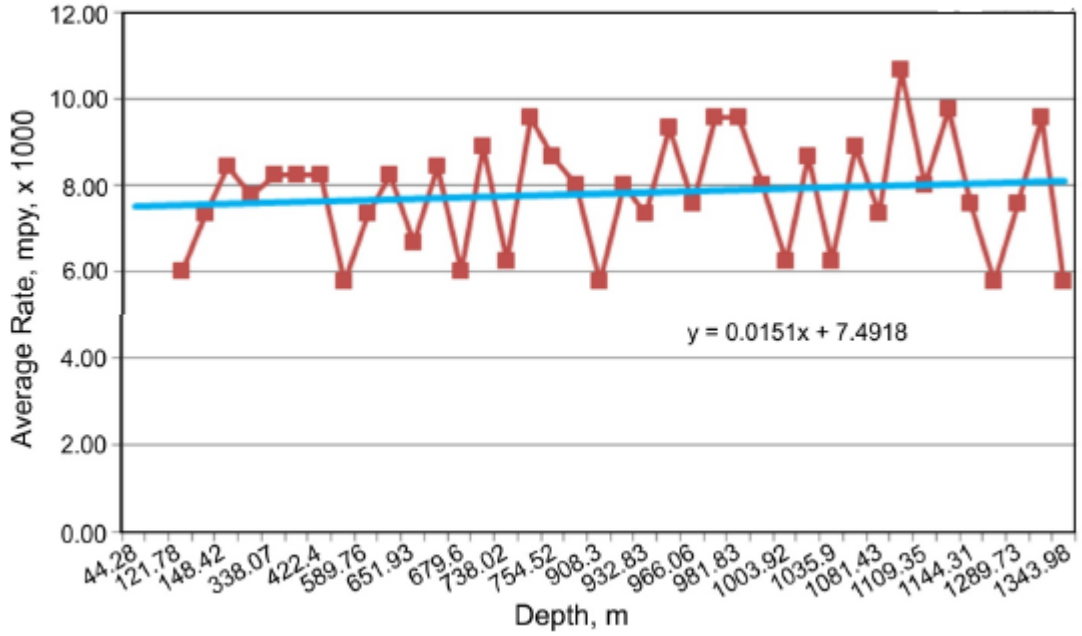

Figure 27 – Average internal corrosion rates with depth for Case Study 1

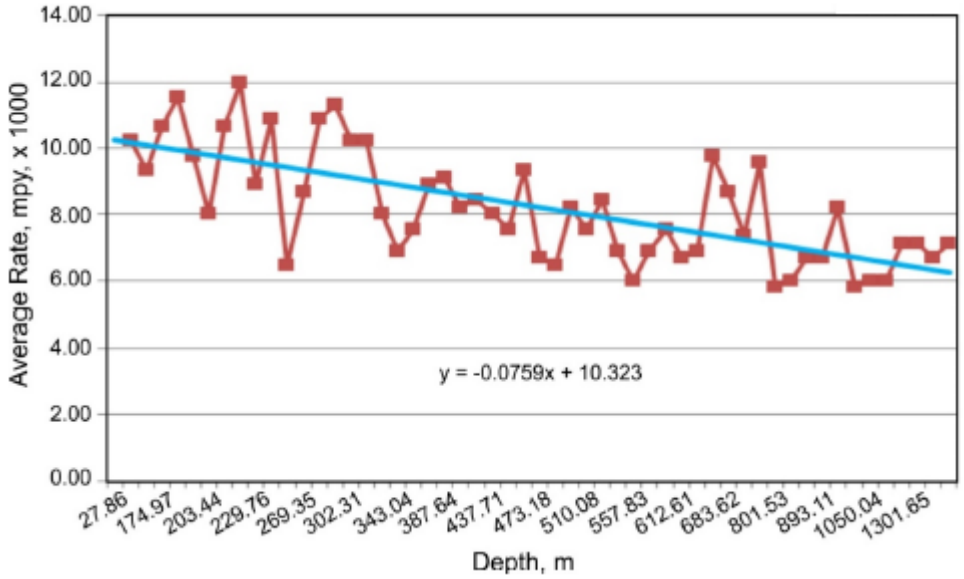

Figure 28 – Average external corrosion rates with depth for Case Study 1.

These results are consistent with expectations of the wellbore being protected externally at the bottom of the wellbore by well-bonded cement.

Case Study 1 Summary

Casing evaluation in 1987 showed two penetrations in the lower wellbore at (1372.5– 1383.5 m and 1383.5–1389.5 m), which is the zone just above the existing production perforation interval. However, the casing was generally in good condition in 1987. In 2002, the Micro Vertilog results indicate increased corrosion tendencies, with one Class 3 pit found in the upper interval and several in the lower interval. These pits exist on both the internal and external surfaces of the casing.

A 2002 cement bond log shows good cement from 1175 to 1351 m, with good bond to both formation and casing. A 2014 SBT log indicates good cement in the interval from 1145 to 1256 m; the bond to pipe is good but bond to formation is weak. Overall, the log indicates extended zonal isolation is possible in the lower wellbore based on current cement evaluation.

Corrosion rate analysis shows that the rate of internal corrosion slightly increases from top to bottom or wellbore, while external rates decrease from top to bottom. This is consistent with good external cement protection at the bottom of the wellbore and less in the section of free pipe from below the surface casing cement and above the TOC for the production casing.

It should be noted that this well was scheduled for abandonment in 2010 because of corrosion issues. Several packers/seals became distorted from exposure to CO_2 and were pulled and replaced throughout the well history. Potential contributing factors for corrosion in this well includes exposure to CO_2, and pulling and replacing packers.

7.2.2 Case Study Well Two (2)

History

The subject well has a spud date of 1957 and is located in the Phase 1c area of Weyburn Field. It was originally drilled vertically and was in production from 1957 to 1972. The well was converted to a water injector in 1989, and after 15 years of injecting water, it was converted to a WAG injector in 2003 as part of the Weyburn EOR project. The injection of CO_2 was stopped in September of 2008, but water injection continued until April 2012. Existing production perforations were initially created in the interval from 1438.7 to 1447.3 m and 1453.0 to 1458.8 m in 1957, and it was re-perforated in 1989 in the interval from 1438.7 to 1447.3 m and 1451.3 to 1457.2 m. These perforations are in the Marly and Vuggy Formations within the Midale Beds. Well data sheets indicate corrosion issues were found on the lowermost 13 joints of production casing in 1995, with a penetration on Joint 3 from the bottom. Consequently, all 13 joints from the bottom were replaced. In 2010, a casing leak was again suspected because of a failed pressure test, and the casing was repaired shortly after that discovery by installing a liner from 1435.8 to 1311.7 m. Activities involving this well were suspended in 2010; it is currently not active. However, according to well data sheets, a cathodic casing protection plan was implemented in 2012.

The casing record indicates that Steel Grade H-40 was used for the surface casing and Grade J-55 was used for the production casing string and a liner. The surface casing was cemented with 240 sacks of Saskatchewan cement with 2% $CaCl_2$. The production casing is cemented with 200 sacks of Howco bulk cement with 3% gel. This well was selected as one of the case studies for this project based on the logs available and the fact that it is situated in an active CO_2 injection area in the Weyburn Field.

String	Weight, kg/m	Grade	OD, mm	ID, mm	Depth, m
Surface	48.7	H-40	273	254.9	94.27
Liner 1	17.263	J-55	114.3	101.6	1438.30
Production	29.76	J-55	177.8	157.5	1468.52

Table 30 – Casing record and characteristics for Case Study 2

Location

This well is located in the Phase 1c area of Weyburn oil field in the province of Saskatchewan, Canada.

Corrosion

An evaluation of corrosion status in this well was made based on available logs that have been used to assess the casing and cement integrity over the history of the well. The logs that were found include SBT logs run in 2010 and 2012; MSC (multisensor caliper) logs run in 2003, 2010, and 2012; and an X–Y MIT log run in 2008. The MSC and MIT logs were used to evaluate the

internal casing integrity, and the SBT logs were used to evaluate the cement integrity. No logs were available that could be used to evaluate the external casing condition. Results from an examination of the available logs are discussed below in regards to casing integrity status and cement integrity status.

Well Log Analysis

Log Type	Log Date	Application	Log Top Interval, m	Log Bottom Interval, m
Caliper Log	10/2/2003	Internal corrosion	1240	1456
X–Y Caliper	9/22/2008	Internal corrosion	1360	1450
Caliper Log	7/25/2010	Internal corrosion	Surface	1457
SBL	7/26/2010	Cement integrity	800	1454
Caliper Log*	8/10/2012	Internal corrosion	Surface	1431
SBL*	8/10/2012	Cement integrity	Surface	1431

Table 31 – Well log analysis – case study 2.
**casing liner installed August 6, 2010 from 1312 to 1435 m.*

2003

An MSC log run in 2003 over the interval from 1240.50 to 1456.30 m evaluated a total of 18 joints in the interval. The results indicated three penetrations at depths of 1422.3, 1435.4, and 1448.2 m; one Class 4 pit at 1397 m; three Class 3 pits at 1361.5, 1383.7, and 1409.1 m. The remainder are Class U and 2 with a maximum wall loss of 40% or less. Of the Class 2 joints, there are two Class 2 defects of 36.7% wall loss at 1296.3 m and 35% at 1370.6 m. Because of the limited interval logged, these results do not offer an assessment of the entire casing string. However, the interval covers the existing production perforations and the zone immediately above the existing production perforations where corrosion is expected to be most prominent. One of the penetrations noted in the log is likely part of the existing production perforations, and the two at 1422.3 and 1435.4 m are in the zone immediately above the existing production perforations.

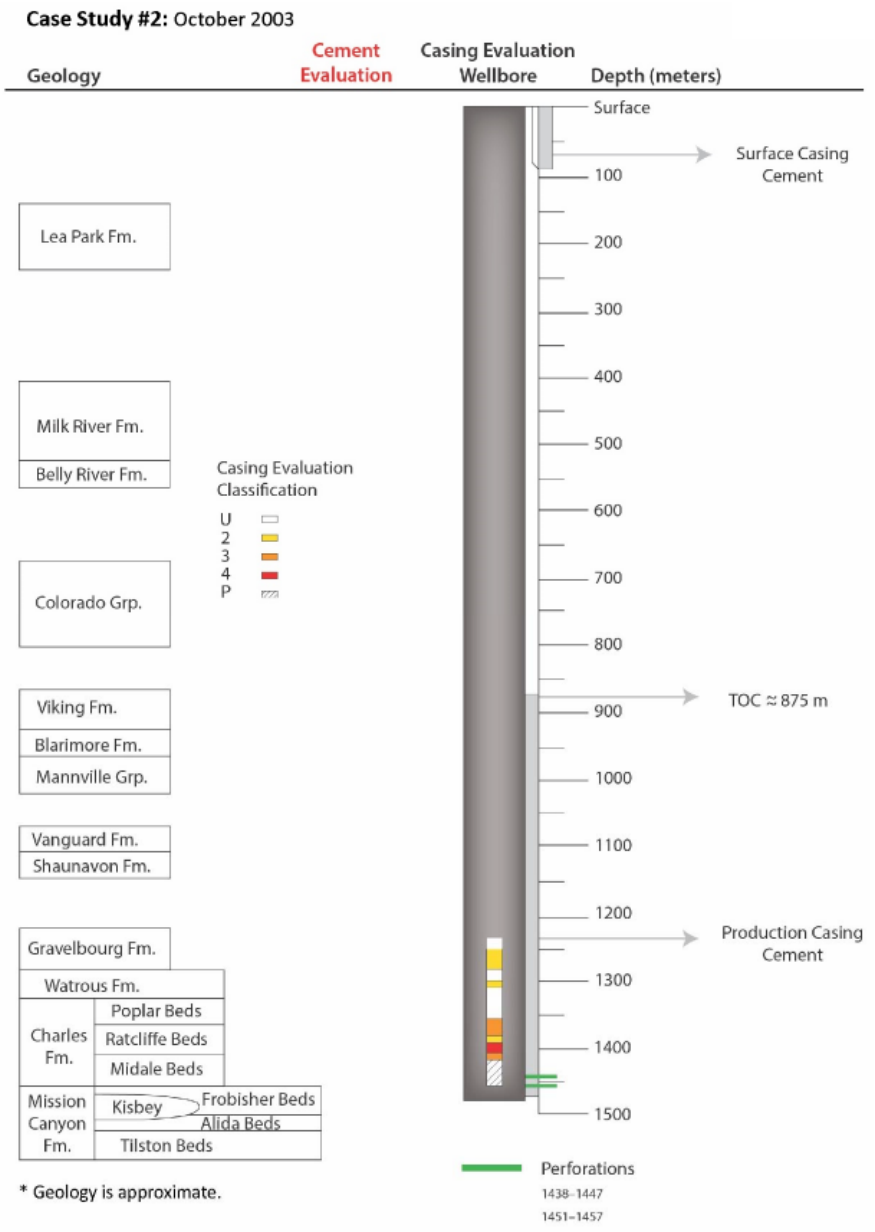

Figure 29 – Schematic representation of 2003 MSC log, Case Study 2

2008

A 24-finger MIT survey carried out in 2008 over the interval from 1360.15 to 1449.90 m indicated corrosion near the bottom of the well in the region just above the first existing production perforation interval. Because numerical data were not available from the X–Y MIT log, estimations of these corrosion defects indicate likely Class 3–4 pits and some potential penetrations. These corroded areas are indicated in the X–Y MIT log in Figure 30.

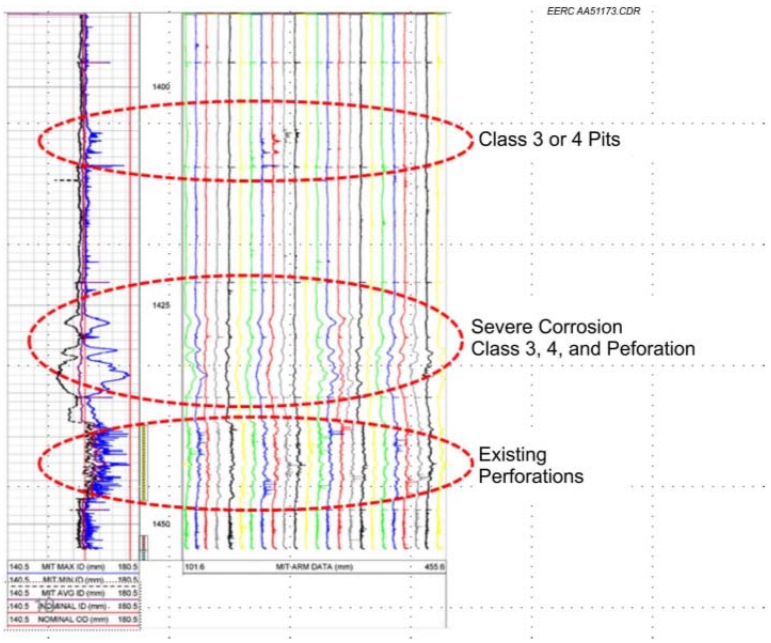

Figure 30 – Corrosion detected by X-Y MIT survey in Cast Study 2

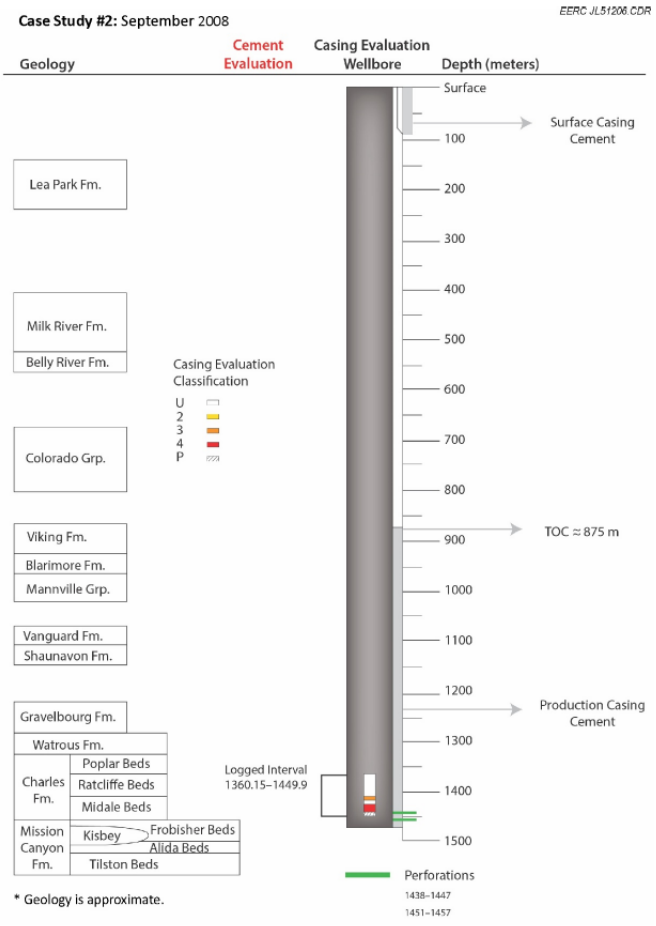

Figure 31 – Schematic representation of MIT log (2008) for Case Study 2

2010

In 2010, the MSC tool was used to survey a total of 114 joints from the surface to 1457.0 m. The corrosion evaluation classification scheme used for this caliper log is the same as that presented in Case Study 1, and a summary of the number of joints by classification is presented in Figure 32. The results indicate that 33 joints exhibited Class U corrosion (i.e., 20% wall loss or less), 74 joints displayed Class 2 pits, three joints with Class 3 pits, one joint with Class 4 pit; and three joints with penetrations. The Class 3 pits and the corresponding wall loss percentages, in parentheses, are located at the following depths: 1357.0 m (57.8%), 1383.8 m (46.6%), and 1408.9 m (43.7%), and the Class 4 pit is located at 1396.9 m (73.6%). The three observed penetrations are at the depths of 1422.1, 1435.1, and 1448.0 m. Of these, the penetration at 1448.0 m is within the first existing production perforation interval (1438.7–1447.3 m), and the other two penetrations are in the casing segment immediately above the first existing production perforation interval. These results suggest corrosion issues in the bottom portion of the well borehole, which is in agreement with the X–Y MIT survey conducted in 2008.

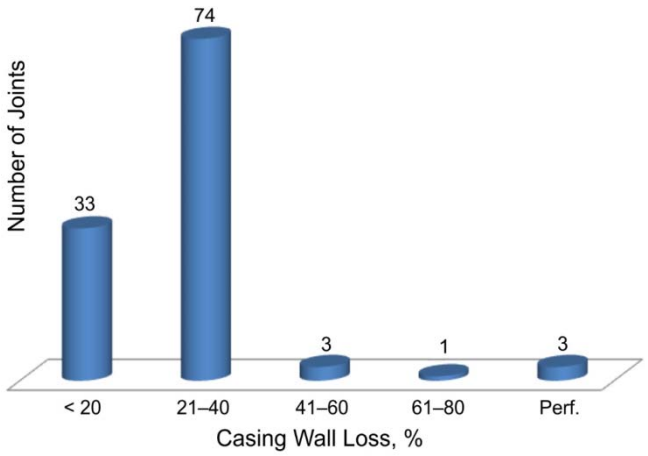

Figure 32 – Summary representation of the defective joints, by classification for 2010

The remaining casing strings from the surface to about 1240 m appear to be in relatively good condition, with mostly generalized corrosion and/or pitting with less than 30% wall loss. It should be noted that a casing liner was installed after completion of this log from 1312 to 1435 m.

In addition, the cement integrity was evaluated by surveying the wellbore with SBT over the interval from 800.3 to 1461.3 m. The logging was performed without any pressure on the casing. Based on the SBT log run in 2010, the cement top was found to be at ~877 m. General observations from the log indicate that the cement at the bottom segment of the wellbore is in

excellent condition, with only a few microvoids found, and extended zonal isolation can be expected as well as bonding to both casing and formation.

From 877 to 1215 m, the cement has poor bond to pipe with potential bond to formation. The cement map shows poor circumferential coverage in some areas and multiple large voids and channels. Several areas have weak and fast formation arrivals, which suggest some bond to pipe and formation in those areas. Zonal isolation in this interval is questionable given the channels and voids present. From 1215 to 1461.3 m, there is very good to excellent cement condition, with good bond to both pipe and formation expected. The VDL shows strong formation arrivals and low-amplitude early arrivals. The cement map shows very good circumferential coverage, although there are isolated microvoids and isolated spots with poor circumferential coverage.

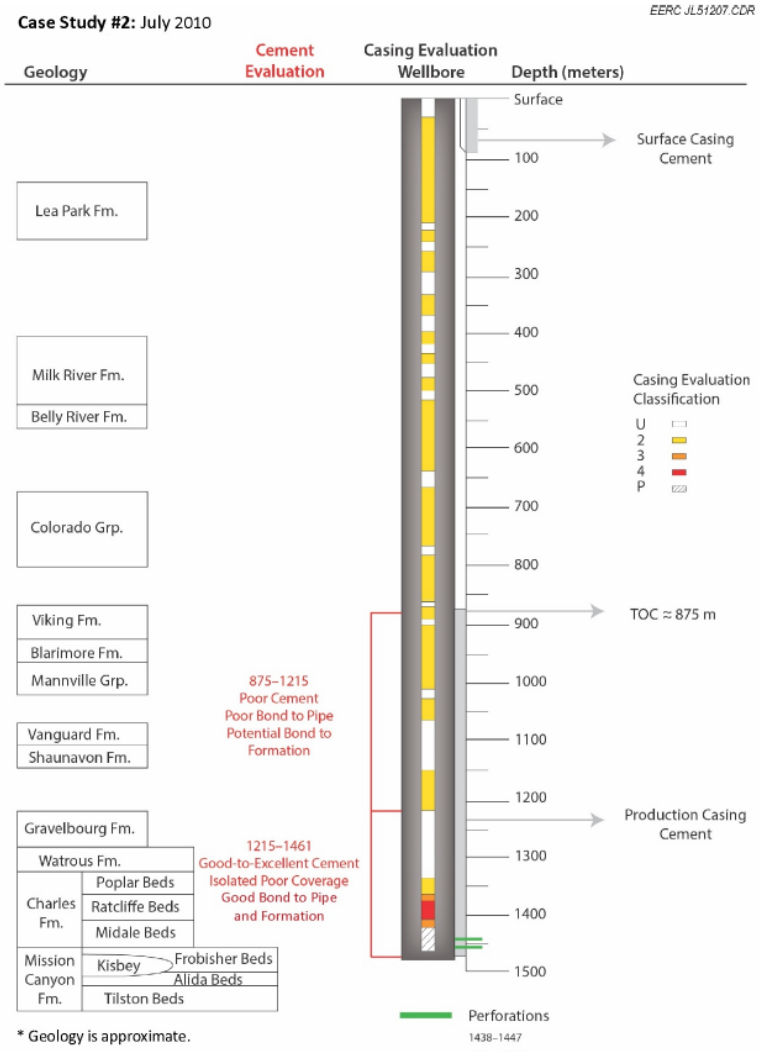

Figure 33 – Schematic representation of MSC (2010) and SBT log for Case Study 2

In 2012, a MSC tool was used to survey a total of 113 joints from the surface to 1431.8 m. The results indicate that 82 joints exhibited Class U corrosion (i.e., 20% wall loss or less), 30 joints displayed Class 2 pits, and only one joint showed Class 3 pit corrosion at 1310.6 m. Based on the classification scheme and the fact that a majority of the joints are of Class 2 and U, it can be concluded that the casing is in relatively good condition and has suffered mainly generalized corrosion and/or pitting with less than or equal to 40% wall loss. Most of these are located toward the bottom of the borehole.

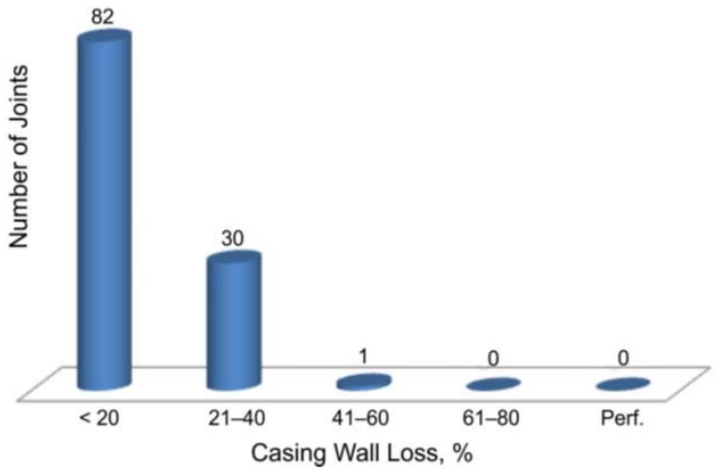

Figure 34 – Summary representation of the defective joints, by classification for 2012

By comparing the MSC results from 2003, 2010, and 2012 differences were observed.

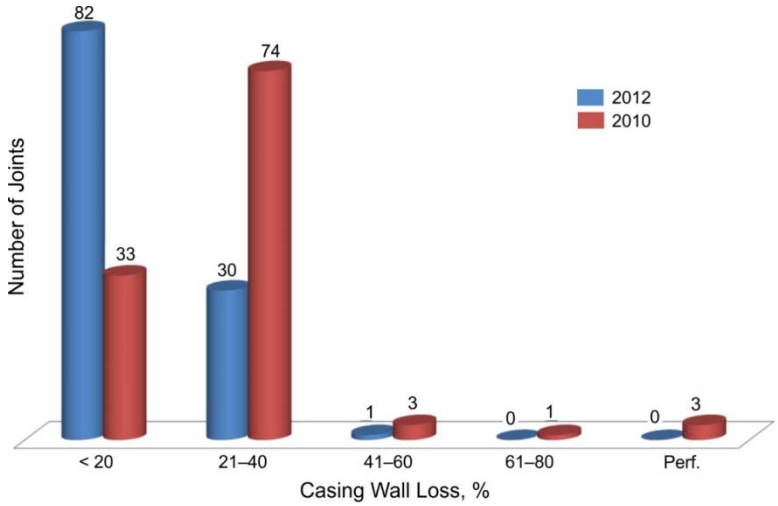

Figure 35 – Comparative summary of defective joints by classification (2010 and 2012) for Case Study 2.

In 2012, another SBT survey was conducted to evaluate the cement condition in the wellbore from the surface to 1431.1 m. The interval from 76 to 877 m is the section of free pipe between the surface casing and the TOC. The TOC is approximately 877 m. From 877 to 1210 m, the cement coverage is good, but there are some channels and microvoids in the cement map. The VDL shows some weak formation arrivals in some areas, with bond to formation and pipe. In the interval from 1210 to 1312 m, the cement quality is good with bond to pipe and formation. The coverage around the pipe is good with a few microvoids and potential microchannels. The VDL shows strong formation arrivals and low amplitudes (2– 10 mV), thus suggesting good bond to pipe and formation. The lower casing interval from 1312 to 1429 m received a liner in July to August of 2010; therefore, the SBT for this region of casing is not accurate. Figure 36 shows the difference between the 2010 SBT and the 2012 SBT with the casing liner in place.

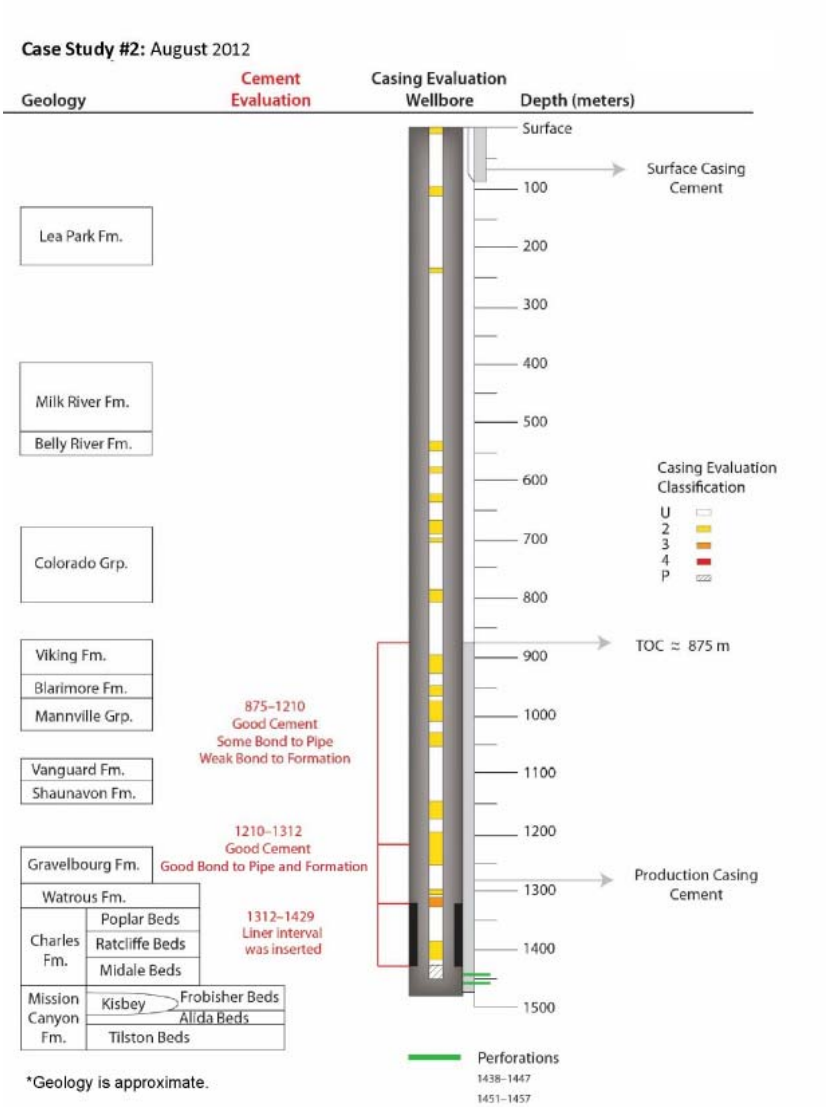

Figure 36 – Representation of 2012 MSC and SBT log for Case Study 2

Corrosion rate analysis

For this well, only caliper logs were available with quantitative estimates of internal rate casing wall loss that were used to derive corrosion rate estimates. As a result, external corrosion rate estimates could not be determined for this well. The rate data for all affected joints with greater than 20% wall loss are presented in the following figures. Based on these curves, the rate of internal corrosion appears to increase toward the bottom of the wellbore. This is consistent with the observed progression in pitting corrosion toward the bottom of the casing, with complete penetration in the zone just above the existing production perforations.

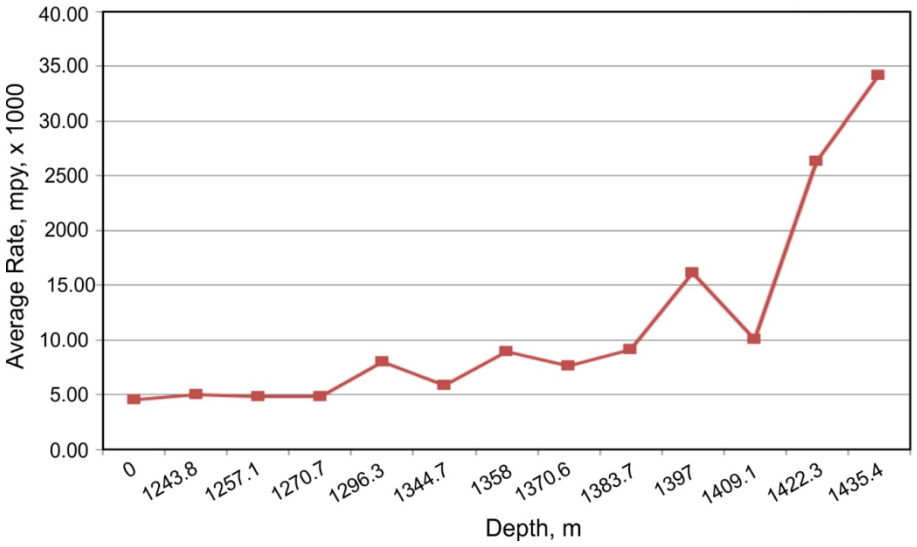

Figure 37 – Average internal corrosion rates with depth for Case Study 2 based on 2003 caliper log

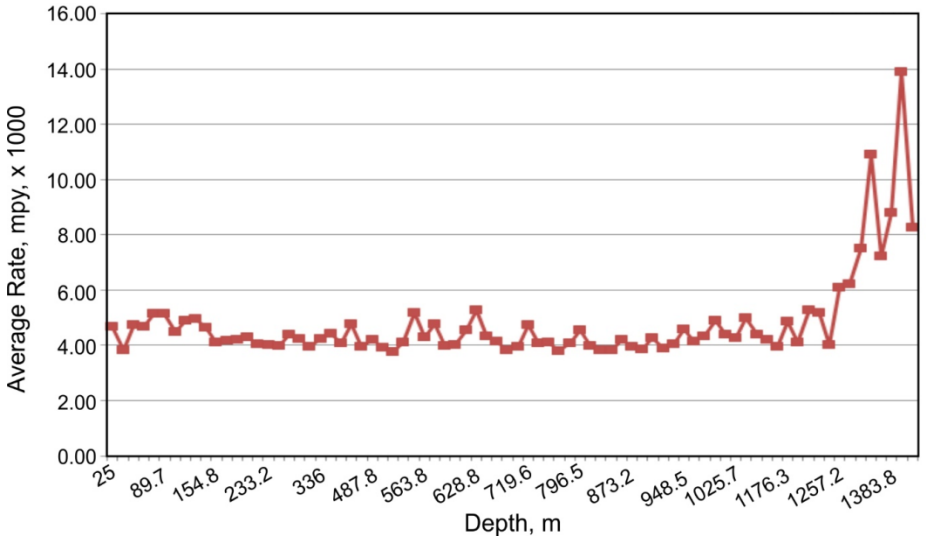

Figure 38 – Average internal corrosion rates with depth for Case Study 2 based on the 2010 caliper log, prior to installation of the casing liner

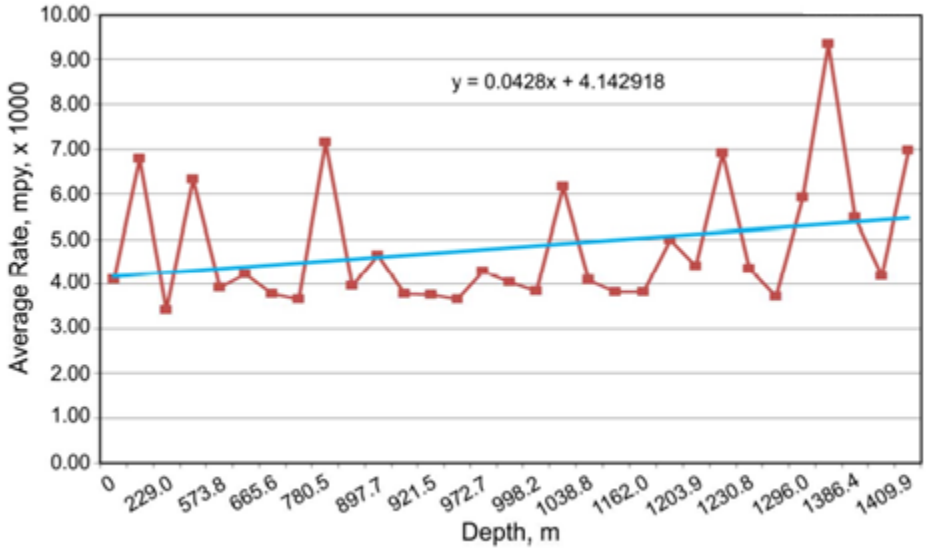

Figure 39 – Average internal corrosion rates with depth for Case Study 2 based on 2012 caliper log, after installation of casing liner (1312 to 1435m)

Case Study 2 Status Summary

The caliper logs examined from 2003, 2008, 2010, and 2012 indicate various corrosion problems on the internal surface of the casing, especially toward the lower wellbore. However, the challenge in the interpretation of these results lies in the differences in the intervals logged during each survey. A proper progression of corrosion was made by using all logs in a complementary manner. Overall, the internal corrosion increases toward the bottom of the well casing, including two penetrations at 1422.1 and 1435.1 m; multiple Class 3 pits at 1357.0, 1383.8, and 1408.9 m; and a Class 4 pit located at 1396.9 m. All of these pits are found in the immediate zone above these penetrations, and the rest of the casing toward the surface has varying degrees of Class 2 and uncoded corrosion occurrences.

The cement top was found at ~877 m, and the lower wellbore from 1215 to 1461 m showed very good to excellent cement, with good bond to both pipe and formation. The zone from 1435.8 to 1311.7 m was protected with a casing liner following logging activities in 2010. Contributing factors for corrosion present in this well may include the injection of CO_2, stray current corrosion (note that cathodic protection was added) and exposure to formation fluids. It is interesting to note that CO_2 injection volumes for this well are less than those for Case Study 1.

7.2.3 Case Study Well Three (3)

History

This well is a vertical oil production well drilled in 1958 in the development area that eventually became Phase 2e of the Weyburn CO_2 injection program. The well was perforated in the Marly Formation between 1441 and 1443.5 and 1445 and 1447 m MD. Production records indicate that the well was in production from 1958 to 2000. In December 2003, the well was transitioned to a WAG injector. Injection records indicate that 963,400 m3 of CO_2 was injected over a 2-month period in early 2006, with water injection comprising the remainder of post-2004 injection activity. This well is actively injecting as of July 2014.

Completion records available from well files indicate that J-55 steel casing was used for the surface and production casing strings, with L-80 steel used for a casing liner installed in April of 2011 (Table 32). The surface casing was cemented with 250 sacks of Canadian Portland cement and five sacks of $CaCl_2$, while the production casing was cemented with 200 sacks of Pozmix. The liner was cemented with lightweight cement. This well was selected as a case study for two key reasons: 1) activity in the well spans the period before CO_2 injection (1958–2006), active CO_2 injection (2006), and post-CO_2 injection (2006–present) and 2) logs are available in the pre- and post-CO_2 injection period, although the log types vary as well as the interval that was logged. The limited CO_2 injection duration and volumes experienced by this well provide contrast to Case Study 1. Such information provides a good assessment of the casing and cement integrity pre- and post-CO_2 injection for this well.

String	Weight, kg/m	Grade	Wall Thickness, mm	OD, mm	ID, mm	Depth, m
Surface	35.72	J-55	6.7	219.1	205.7	124.2
Liner	16.37	L-80	6.7	101.6	88.3	1439.61
Production	20.83	J-55	6	139.7	127.7	1473.7

* Liner installed April 7, 2011.

Table 32 – Casing record and characteristics for Case Study 3

Location

This well is located in the Phase 2e area of the Weyburn field, in the province of Saskatchewan.

Corrosion

An evaluation of corrosion for any production or injection well involves an assessment of at least the casing and cement integrity. A list of available logs that were used to perform the corrosion evaluation for Case Study 3 is presented in Table 33.

Log Type	Log Date	Application	Top Log Interval, m	Bottom Log Interval, m
MSC	1/13/2004	Internal corrosion	1227	1428
X–Y CAL	6/14/2007	Internal corrosion	1361	1462
CIT	8/11/2010	Internal/external corrosion	0	1465
SBT	8/11/2010	Cement integrity	835	1460
SBT	4/12/2011	Cement integrity	1270	1441

Table 33 – Well log analysis for Case Study 3

Well Log Analysis

2004

A maximum and average casing wall loss, 7.4% and 3.2%, respectively, was observed over the logged interval consisting of 21 casing joints. All corrosion was classified as Class U. Class U corrosion is defined as less than 20% casing wall loss. Only minimal internal corrosion appears evident in the logged interval during the pre-CO_2 injection period spanning from 1958 and 2004 (46 years). This result implies a well-isolated and inhibited tubing annulus which provided an effective barrier between formation fluids and the production casing. It should be noted that the bottom log interval is approximately 45 m above TD (total depth) and overlies the production/injection horizon. Therefore, interpretations regarding the presence of corrosion and corresponding corrosion rates of casing intervals exposed to formation fluids were not possible for the pre-CO_2 injection period because of the lack of adequate log data.

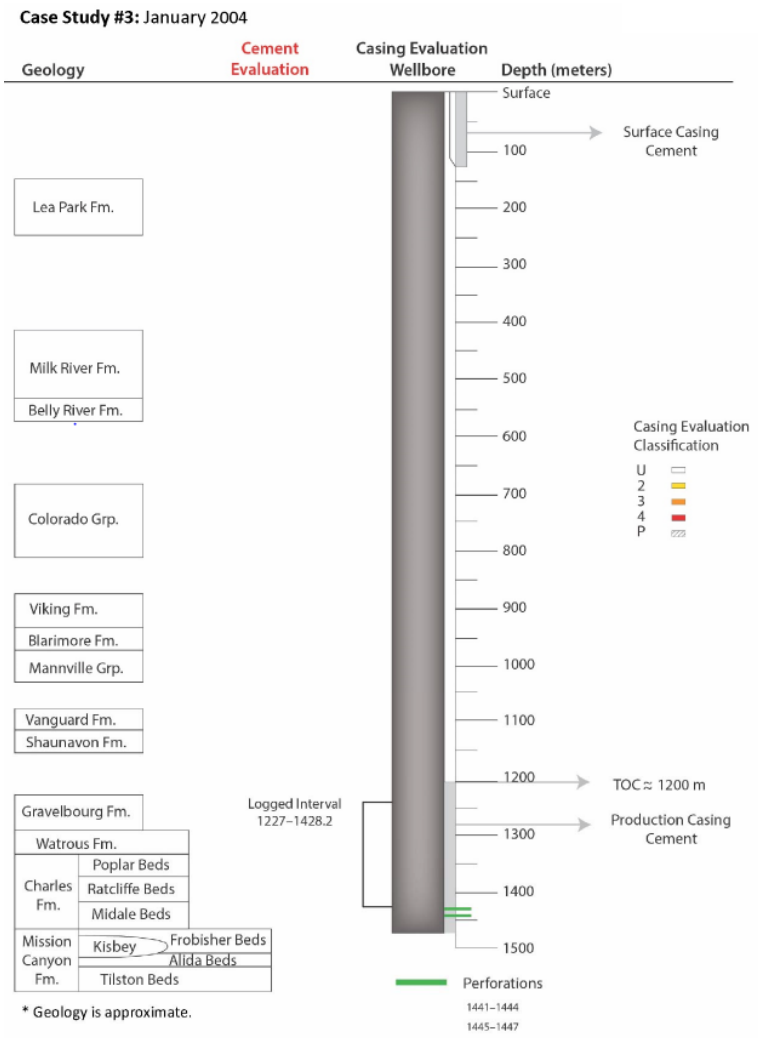

Figure 40 – representation of 2004 MSC log for Case 3

2007

This log was run with tubing present in the wellbore. Because of the lack of data regarding tubing specifications or service duration, only the interval below the tubing shoe was analyzed. The tubing bottom was located at 1413.3 m. The log interval from 1413.3 to 1462.0 m was analyzed to examine casing corrosion through an interval exposed to formation fluids post-CO_2 injection. However, because of a lack of pre-CO_2 injection data, corrosion rates or attribution of corrosion due to the presence of CO_2 or carbonic acid is not possible.

A maximum and average casing wall loss, 56% and 13%, respectively, was observed over the logged interval, which contained Class U, Class 2, and Class 3 corrosion. Generally, the highest concentration of observed casing wall loss (Class 2 and Class 3 corrosion) was associated with depths greater than 1440 m, which correspond to the perforated interval. This suggests that contact with injected or produced fluids at higher flow velocities in areas where the casing is pre-damaged or perforated, impacts the rate of corrosion. Smaller intermittent areas (less than 2-m intervals) of Class 2 and Class 3 corrosion were observed outside of the perforated interval but were generally bounded by larger intervals of casing with Class U corrosion. Figure 41 represents this log.

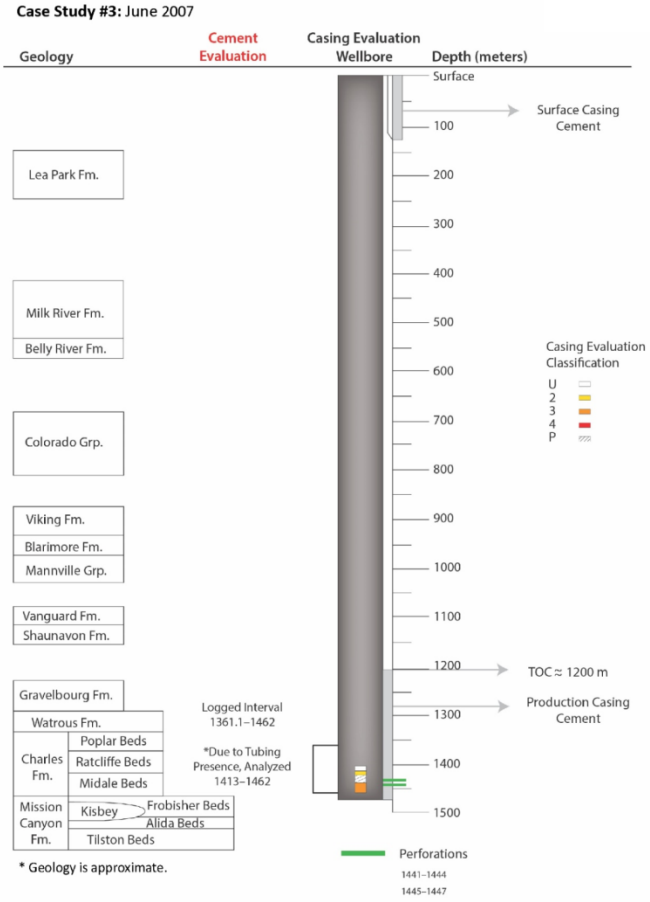

Figure 41 – 2007 X-Y caliper log

2010

A sector bond log was acquired in 2010 with casing pressurized to approximately 4.5 MPa. Pressurized passes are often performed if the presence of a microannulus is suspected. However, it is unknown if the pressurized pass was run because a microannulus was suspected or because of an operational decision not to kill the injection well.

TOC was identified at approximately 1195 m. In general, the SBT indicates good cement bond to both pipe and formation for the interval between 1195 and 1410 m which implies an effective barrier to vertical fluid migration and effective isolation of the casing from formation fluids. The lack of external corrosion though this zone is likewise evidenced by the 2010 CIT log.

The interval between 1410 m and 1460 m shows indications of channeling and generally intermittent poor or partial cement bond (see Figure 42) which implies the potential for ineffective isolation of the casing from formation fluids. Likewise, corrosion is evidenced through this interval by the 2010 CIT log, indicating that lack of isolation from formation fluids may be impacting casing corrosion rates. Because of the lack of consistent time-lapse casing integrity and cement integrity log data, the effect that operations and changing formation fluid chemistries have on cement integrity cannot be adequately quantified.

A CIT log was acquired from surface to 1465 m which provides information regarding both internal and external casing corrosion. The data available for this log did not include interpretation tables that normally contain measured casing wall loss percentages and the corresponding classification of the defects. As a result, interpretations made from this log are based on visual inspection of the log curves and a qualitative determination of defect types and/or their classification. The results suggest that the casing condition is generally consistent, with little indication of severe defects or corrosion in the interval above 1413 m, with mostly generalized corrosion tendencies and some external SIPs of about Class U or 2, with maximum wall loss of about 40%. However, the external SIPs in the 1190–1413-m interval are higher (probably 30%–38% maximum wall loss) than in the 125–1190-m interval (probably 20%–30% maximum wall loss). More localized internal pitting of about Class 3 (40%–60% wall loss) or Class 4 (60%–80% wall loss) was found in the interval from about 1413 to 1438 m, which is the region just above the first existing set of production perforations. There is a potential for penetrations to have occurred in this interval because the Class 3 or Class 4 pitting in this case is a conservative, qualitative estimation and not based on quantitative caliper data.

The interpretations from the 2010 CIT log agree generally with the MSC results from 2004 for the interval from 1227 to 1428 m. This implies that the casing interval from surface to about 1428 m is in good condition both internally and externally. However, the bottom of the casing has developed Class 3 or 4 pits and/or potential penetrations in the zone from 1413 to1438 m,

which is just above existing production perforations. This generally agrees with trends observed in the X–Y caliper log acquired in 2007.

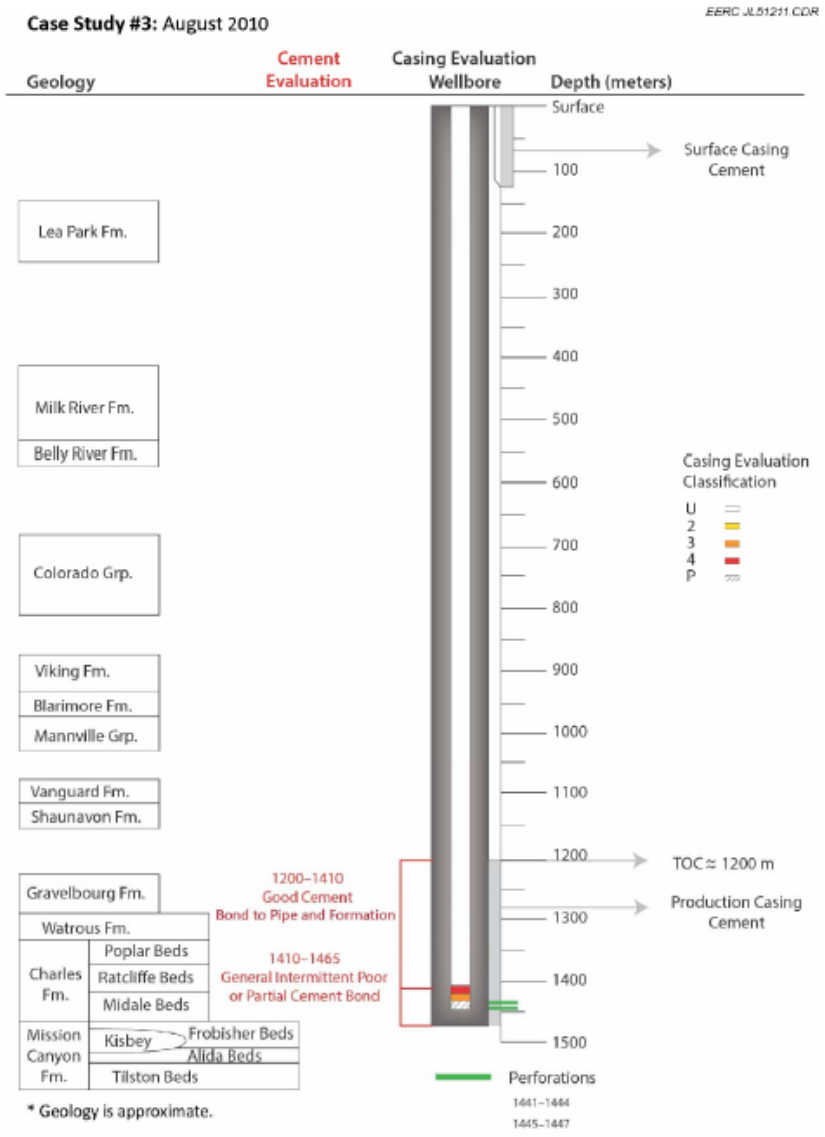

Figure 42 – representation of 2010 SBT and CIT log for Case 3

2011

A subsequent SBT log was acquired in 2011 covering the interval from 1270 to 1441 m; it is not noted whether this pass was logged under pressure. However, on April 7, 2011, a casing liner was installed through the depth interval of 1295 to 1439 m, changing the completion of the majority of the log interval. The liner was likely a result of depleted cement integrity and corrosion observed in logs acquired in 2010. Therefore, analysis of cement integrity is challenging because the previous log acquisition is not possible over the majority of the log

interval. For the unchanged portion of the completion (1270 to 1290 m), cement bond quality is good and comparable to the 2010 SBT. The indication of partial and intermittent cement bond over the liner interval is likely the result of the changing completion and multiple pipe strings and cement within the well. The small interval below the liner installation appears to be unchanged or improved compared to the 2010 SBT log.

A comparison of the 2010 and 2011 SBT logs reveals that no degradation was evident above and below the liner installation. The interval from 1290 to 1440 m, which shows poor cement quality in the 2011 log, is likely influenced by the changing well completions between the two log acquisitions and is likely affected by multiple pipe strings cemented in the well.

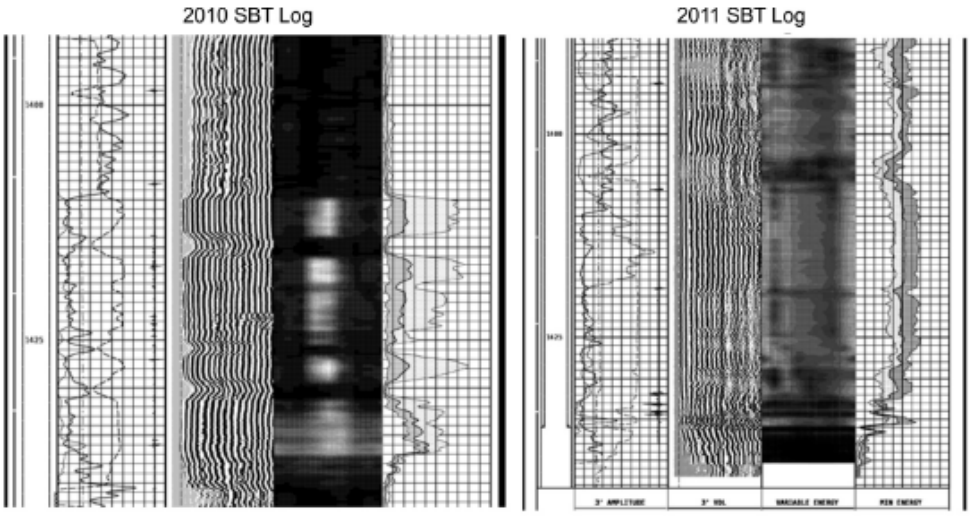

Figure 43 – Comparison of two SBT log segments surveyed in 2010 (left) and 2011 (right) for Case 3. The log segments are cropped so that approximately the same intervals are displayed.

Corrosion rate analysis

For this well, no available data could be used to perform a similar analysis of the rates as was done in Case Studies 1 and 2. The CIT log that was found did not contain quantitative values of metal loss, so only a qualitative interpretation was possible for this well. Based on the qualitative analysis, an increased corrosion rate is observed immediately below the base of tubing that was in place circa 2007 and corresponds to an area of poor cement bond within the injection interval.

The corrosion rate on the external casing surface appears to correlate with the quality of the cement behind the casing as determined from Case Study 1. Because of a lack of available well log data, it is unknown if the cement quality in the injection horizon has historically been poor since the initial well completion or if the cement quality is deteriorating over time. Additional

cement evaluation logs over time would be required to assess if cement degradation is occurring over time.

Case Study 3 Summary

Case Study 3 was first logged in 2004 with a MSC log, possibly in conjunction with the transition to a WAG injector during that same year. The logged interval of 1227–1428 m exhibited less than 20% casing wall loss throughout. In 2007, an X–Y caliper survey evaluated the casing from 1361 to 1462 m, which exhibited Class 2 and Class 3 wall loss through the perforated interval as did, to a lesser extent, casing exposed to injected and produced fluids below the tubing shoe. In 2010, a casing imaging tool was run for the entire wellbore (surface to 1465 m) that evaluated the internal and external casing. From the surface to 1413 m, the casing was in good condition with general corrosion and some external pitting, and the corrosion was generally classified as U or 2 (below 20% wall loss and 20%–40% wall loss, respectively) based solely on visual inspection of the log. However, from 1190 to 1413 m, the corrosion does seem to increase slightly. Class 3 and 4 corrosion was found in the 1413–1438-m interval, which is just above the production perforations.

Cement was evaluated by SBT logging runs in August 2010 and April 2011. Both logs focused on cement in the lower part of the wellbore (i.e., 835–1465 m in 2010, 1263–1443 m in 2011). There was a noticeable difference between the two logging sessions because of the installation of a casing liner. In 2010, generally good cement bond to pipe and formation was observed below the TOC other than the interval from 1410 to 1460 m, which showed evidence of channeling and evidence of ineffective isolation between cement and casing. In 2011, the quality of cement over the limited log interval not impacted by the change in well completion did not appear to change.

Potential contributors to corrosion for this well are more difficult to ascertain because of the lack of logging data early on in the well history. The contributing factors are most likely operational (running tubing), formation fluid exposure, or possible stray current corrosion. However, no cathodic protection system was installed on this well.

7.2.4 Case Study Well Four (4)

History

Phase 1c area of the Weyburn CO_2 injection program. The well was selected to evaluate the differences in corrosion, if any, for a well that had a similar history to Case Studies 1–3 but did not experience CO_2 injection. Case 4 was initially an oil producer and then later converted to a primarily water injection well. In addition, the well is located outside of the main CO_2 injection area and, therefore, should have little exposure to CO_2. Because of the initial spud date of this well, it should have similar completion practices as the first three case studies.

The well was perforated in the Midale Bed in the intervals from 1457.8–1462.4 m, 1466.5–1472.5 m, and 1475.5–1478.5 m. Production records indicate that oil production in this well was from 1957 to 2003, when it was converted to a water injector on August 11, 2003. Injection records indicate water was injected from 2003 to 2014. This well is actively injecting as of July 2014, the last month of records available for this study. The casing records indicate that Steel Grade H-40 was used for the surface casing string and Steel Grade J-55 was used for the production casing string. Cement records were not available at the time of this report; however, the TOC is at about 1158 m.

String	Weight, kg/m	Grade	OD, mm	ID, mm	Depth, m
Surface	48.7	H-40	273	254.9	95.51
Production	34.2	J-55	177.8	158.5	1486.8

Table 34 – Casing record for Case Study 4

Location

This well is located in the Weyburn oil field to the southwest of the three previous case study wells, in the province of Saskatchewan, Canada

Corrosion

An evaluation of corrosion status in this well was made based on available logs that have been used to assess the casing and cement integrity. The logs that were found include SBT, MSC, and CIT, all run in 2010 and 2011. While a good selection of logs is available on this well, the time period of when these logs were run falls within a short time span. Therefore, it is difficult to evaluate the corrosion over time, but the available data have been analyzed and used to compare with the other case study wells.

Log Type	Log Date	Application	Top Log Depth, m	Bottom Log Depth, m
CIT	5/28/2010	Internal/external corrosion	10	1473
SBT	5/28/2010	Cement integrity	5	1473
SBT	5/30/2010	Cement integrity	20	475
X–Y Caliper	10/15/2011	Internal corrosion	1425	1475

Table 35 – Well logs for Case Study 4

Well Log Analysis

2010

The results from a CIT log indicated multiple external SIPs from surface to 1440 m ranging from Class 1 to Class 2 defects, with maximum casing wall loss of 40%. This indicates that the casing

is in very good condition from surface to 1440 m. However, the interval just above the existing perforations shows multiple internal and external Class 3 pits; the worst of which showed an internal casing wall loss of about 51% at 1444.1 m. The next segment of the casing below 1444.1 m showed several casing penetrations in the log, which correspond to the expected existing perforations.

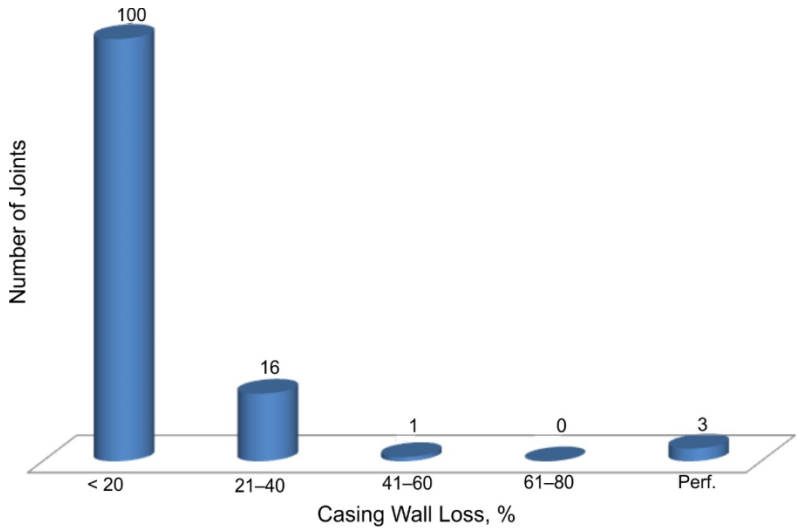

Figure 44 – Number of defective joints by classification in 2010 for Case Study 4.

An SBT was logged to evaluate the quality of the cement behind the casing. The logs were found to be generally poor in quality, especially the VDL waveforms and cement energy maps due to the presence of gasified fluids in the wellbore during logging as indicated in work reports.

Nonetheless, the VDL and amplitude readings indicate full circumferential coverage of low impedance material around the casing from surface to 545 m. Because there are no observed formation arrivals on VDL, there appears to be no cement bonding to formation in this zone and the bond to casing is reasonable in some areas and lacking in others.

From 1160–1290 m, the cement quality is poor, with patchy cement, but with a few zones of full circumferential coverage and zonal isolation capabilities. The interval from 1290– 1476.5 m has excellent cement bond. Low-amplitude (high-attenuation) early arrivals and strong formation arrivals indicate that the cement is bonded to both casing and formation. The cement map shows excellent coverage around the pipe. Hence, the complete interval is capable of zonal isolation with a few isolated channels above the perforated zone.

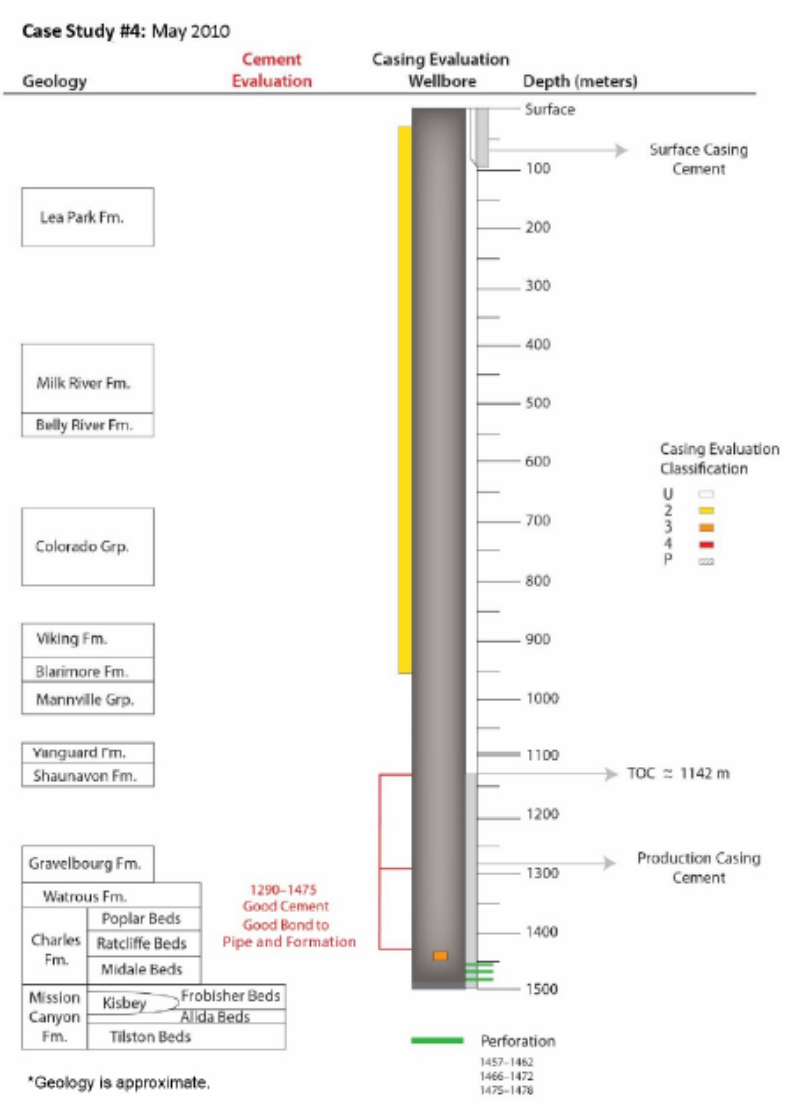

Figure 45 – Representation of 2010 CIT and 2010 SBT for Case 4

2011

A 24-arm Sondex multifinger caliper tool was also run in 2011 to assess the casing condition below the tubing string. The interval covered during logging was from 1425.9– 1475.0 m. The log shows penetrations in the interval from 1454–1474 m, and there is also an increase in ID of the casing from about 63 mm to about 165 mm, indicating penetration through the casing. These penetrations are consistent with expected existing production perforations created when the well was completed. According to the logging company report, the increase in ID was consistent with the presence of existing perforations.

Corrosion rate analysis

The CIT log data available for this well showed good casing condition from surface to about 1444.1 m but with more pitting toward the bottom. Quantitative data from this log regarding

internal and external corrosion showed that most of the defects were external, with one internal Class 3 pit at 1444.1 m.

Only one data point was available for the internal corrosion status, with more than 20% wall loss; therefore, no rate analysis was possible for internal corrosion. The external surface with multiple data points with more than 20% corrosion have been analyzed in detail.

Internally, the lower section of the wellbore below 1440 m showed more severe corrosion with multiple Class 3 pits (i.e., wall loss of 40%–60%), which represents an overall increase in internal corrosion tendency toward the bottom of the well. It should be noted that the cement at the bottom of the well had a few voids, and overall bond to the casing and formation was good.

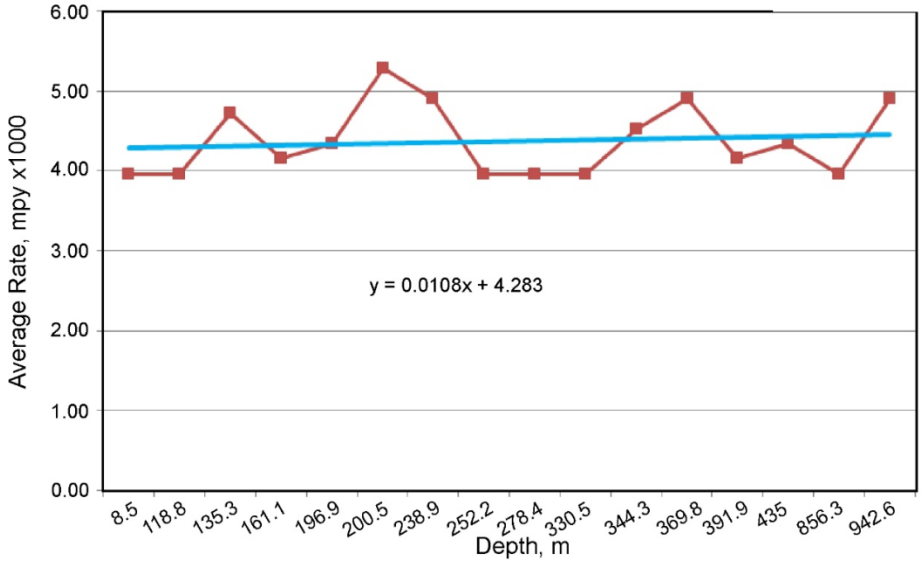

Figure 46 – Average external corrosion rates with depth for Case Study 4

Case Study Four Summary

The casing integrity was evaluated using a CIT log and an X–Y caliper log. The CIT log showed that the external and internal casing surfaces were in good condition from surface to about 1438 m, but an internal Class 3 pit with 51% wall loss was observed at 1444 m. The interval from 1440 m to the bottom logged depth of 1458 m showed some penetrations that correspond to expected existing perforations. The X–Y caliper survey of the zone with existing perforations showed an increase in the internal diameter (likely a penetration) of the casing, which was consistent with expected log tool behavior in the zone with existing perforations.

The integrity of the cement in this well is excellent in the interval from 1290–1476.5 m, where strong bonding to both pipe and formation are expected. In addition, full zonal isolation is also expected in this interval, although a few isolated channels are observed above the existing perforation zone.

Overall, the most serious corrosion spot in this well is the internal Class 3 pit at 1444 m, which can potentially soon become a penetration. When fully penetrated, the pit may grow in size as seen in previous case studies. This well was evaluated to compare corrosion rates and mechanisms in a well that has not been exposed to CO_2. Contributing factors to corrosion in this case study likely do not involve CO_2. This well has seen no CO_2 and also has very little internal or external corrosion for a well that has been in production since 1957. The small amount of internal corrosion present in the lower section of the well can be explained by multiple completions and perforations to allow water injection.

7.2.5 Case Study Well Five (5)

History

The Case Study 5 well was drilled in 1962 as a vertical oil production well, with existing perforations in the interval from 1470.1–1471 m in the Midale Bed. Production records indicate that oil production in this well was from 1962 to 1995, with production activities suspended on January 31, 1995. The well data files do not indicate the reason for the suspension, but a cement retainer was placed at 1459.24 m and the annulus was inhibited. Records indicate this well is still suspended as of July 2014, the last month of records available for this study. Based on casing integrity surveys conducted in 2011, it is possible the suspension had to do with deteriorating casing integrity evidenced by the multiple penetrations observed on a CIT log run in 2011. Steel grade J-55 was used for the surface and production casing string. Cement records were not available at the time of this report. The well has a TOC at 1142 m.

This well was selected as a case study in part because of its location outside of the main CO_2 injection area and because it is a vertical oil producer. Although it was completed in 1962, it was expected that the completion practices were largely similar to those of the other case study wells to allow for a comparative analysis of the corrosion status. Furthermore, this well is the only case study well that was only used as a production well; thus, it has not had direct contact with injected fluids.

String	Weight, kg/m	Grade	OD, mm	ID, mm	Depth, m
Surface	35.72	J-55	219.1	205.7	127.9
Production	14.14	J-55	114.3	103.9	1488.9

Table 36 – Casing record for Case Study 5

Location

This well is located in the Weyburn oil field to the southwest corner of the Phase 1c injection area, in the province of Saskatchewan, Canada.

Corrosion

An evaluation of corrosion status in this well was made based on available logs that have been used to assess the casing and cement integrity. The logs that were found include SBT, MSC, CIT, and URS (ultrasonic radial scanner). Although the logs represent a desired set of logs that can be used to evaluate both the internal and external casing surfaces as well as the cement around it, all the logs were run in 2011; thus, long-term evaluation of the corrosion status over time is made difficult. Nonetheless, the current assessment can be used as a basis for future evaluations and to compare with data from the other case studies in this report.

Log Type	Log Date	Application	Top Log Interval, m	Bottom Log Interval, m
SBT	10/09/2011	Cement integrity	7.9	1452.8
MSC	10/10/2011	Internal corrosion	3.1	1454.6
CIT	10/11/2011	Internal/external corrosion	0	1454.3
URS*	10/21/2011	Cement integrity and casing evaluation	3.1	1447.2

* URS data were found not to be reliable because of problems during logging and were thus not included in evaluation of this well.

Table 37 – Well log analysis for Case Study 5

Well Log Analysis

2011

An SBT was logged to evaluate the cement quality. The SBT was logged with both pressured and unpressured passes to investigate the presence of a microannulus and/or its severity. A detailed analysis has been performed using the SBT log from the unpressurized pass to be consistent with the analysis done for other wells in this report. Based on the SBT log, the cement top was found to be at ~1142 m.

The interval from 1142–1455 m has excellent bonding to both casing and formation as indicated by the strong formation arrivals and low-amplitude early arrivals in the VDL. The cement map also shows very good cement coverage around the pipe in this interval and effective zonal isolation can be expected. However, there are a few microvoids and a few isolated channels present in the cement map towards the top of this zone from 1142 to 1160 m.

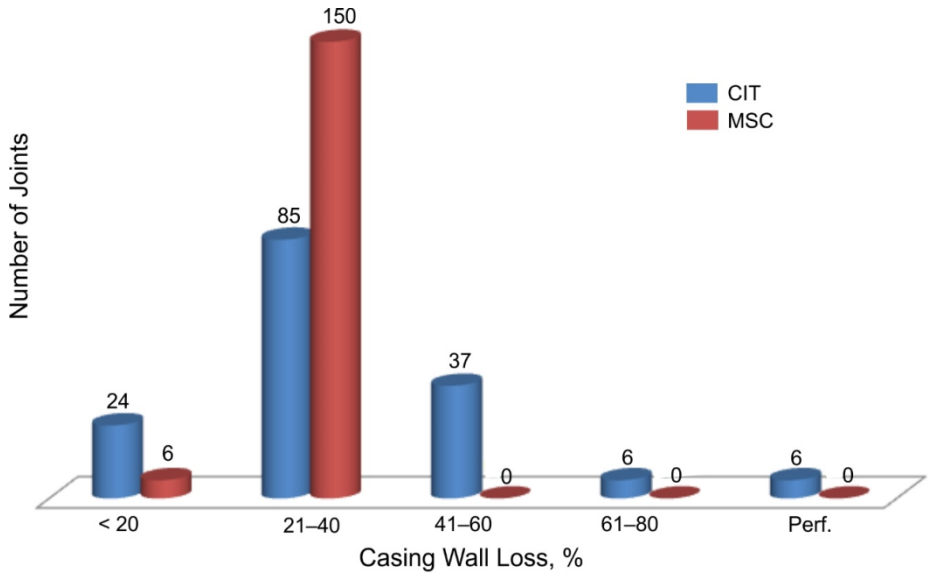

Figure 47 – Comparison of defective joints by classification, from CIT and MSC for Case Study 5.

The MSC log indicates that 150 or 156 joints are Class 2 pits and 6 are unclassified (Code U), which would suggest mainly generalized corrosion with 20%–40% casing wall loss. However, the CIT results show a much different condition that shows multiple severe pits and penetrations. Figure 47 shows a comparison of CIT and MSC defective joint summaries by classification. According to the logging company documentation, this difference is due to the 8-mm spacing of the MSC feeler arms that possibly miss some of the SIPs identified by the CIT tool. As noted by the logging company personnel, the MSC caliper results also indicated a nonsymmetrical ID throughout the complete interval logged (i.e., from surface to 1458.2 m), as well as a small ovality and helical buckling as a result of a lack of cement support and a 10-mm casing offset at approximately 1062 m.

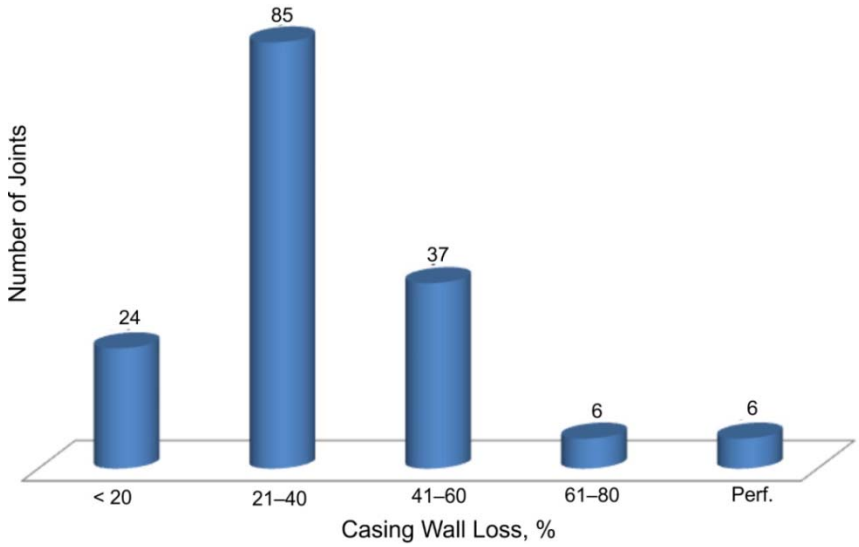

Figure 48 – Number of defective joints by classification, CIT, Case Study 5

The CIT log surveyed in 2011 shows several SIP defects from surface to 950 m ranging from Class U to 4 and several penetrations. Penetrations (Class P defects) are at logged depths of 485.6, 820.2, 835.7, 850.2, 875.2, and 878.7 m. Reports from the logging company show that the casing was tested under pressure at 7 MPa and Joint Number 95 was found to have no penetration as had been observed in the CIT tool classification. The casing below 878.7 m to 1458.2 m appears to be in relatively good shape with defect codes ranging from Class U to Class 3. Most of these defects appear to be on the internal surface of the casing.

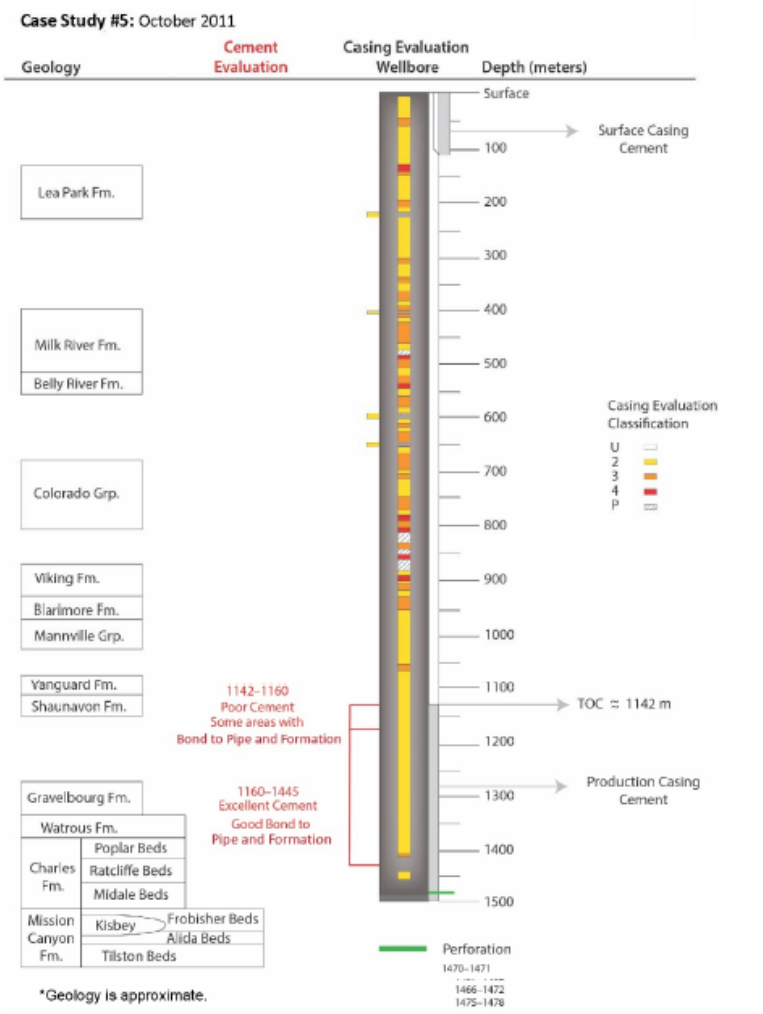

Figure 49 – Representation of 2011 SBT and CIT for Case 5.

The URS tool was also run in this well and, in general, URS results can provide useful information about the ID of the casing and a detailed evaluation of the cement. However, the results obtained in this well were not used for any evaluation purposes because some

challenges were encountered during the survey process, so the results were deemed unreliable by the logging company personnel.

Corrosion rate analysis

The rates calculated based on available data from the CIT log show a slight increasing trend in external corrosion rate from surface to a depth of about 700 m as shown in Figure 50, but no definitive trend can be inferred for internal corrosion rates based on the plot in Figure 50. The plot in Figure 51 shows several peaks corresponding to several penetrations in the interval from the surface to about 900 m, after which the casing status appears to be reasonably good and only Class U and 2 pits are observed. The SBT log showed the cement top to be at ~1142 m, with excellent cement quality observed in the interval from 1142 to 1455 m. The cement quality in this interval explains the lack of external corrosion in the lower wellbore, since the casing would have been adequately protected.

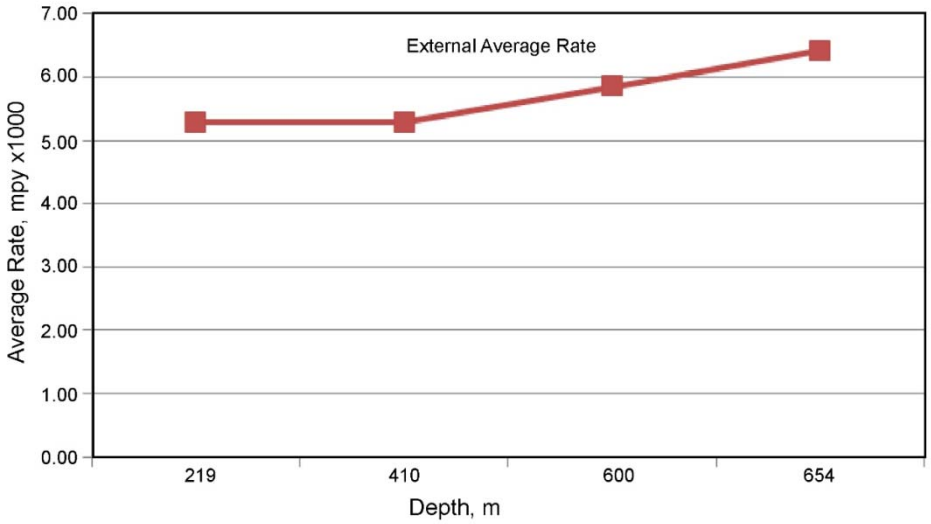

Figure 50 – average external corrosion rates, with depth case

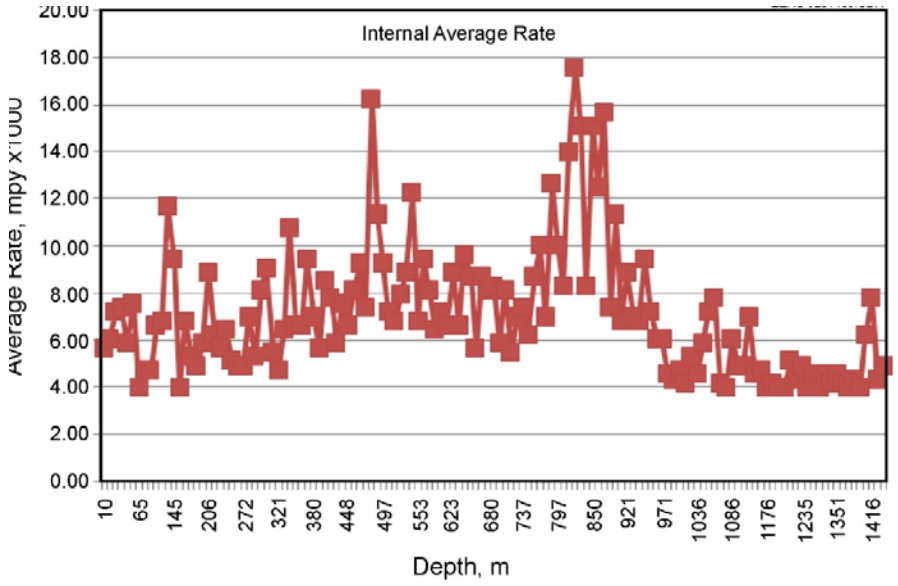

Figure 51 – Average internal corrosion rates with depth for Case Study 5.

Internal corrosion rates are lower in the interval from about 1000 m to 1458 m; i.e., average rate is 4.87×10^{-3} mpy, compared to 7.87×10^{-3} mpy average rate from surface to 1000 m. This finding is contrary to what has been observed in a water-only injector Case Study 4 and WAG injectors in Case Studies 1 to 3, where the internal corrosion rate showed an increasing trend toward the lower wellbore and was often highest in the region that is just above the existing perforation zone.

Case Study Five Summary

The casing integrity status of this well was evaluated by a CIT log and an MSC log in 2011. The results from the CIT log indicate several locations in the interval from around 400 m to about 900 m with severe pitting corrosion involving wall metal loss of 80% to 93%; specifically at depths of 485.6 (86%), 820.2 (93%), 835.7 (80%), 850.2 (80%), and 875.2 m (83%). Although a pressure test conducted at the time this log was surveyed did not indicate the presence of a leak. The MSC log run just 2 days before the CIT log showed no serious corrosion problems, with 150 of 156 joints displaying only Class 2 pits corresponding to wall loss of 20%– 40%. The large difference between MSC and CIT results appears to be due to the 8-mm feeler arm spacing in the MSC that potentially miss some of the pits that were evident in the CIT log. Thus, the choice of logging tool in the investigation of casing integrity is very important.

The quality of the cement is excellent from the cement top at 1142 m to the bottom logged depth at 1455 m, although there are a few voids and microchannels from 1142–1230 m. Despite the observed small microvoids and microchannels, this interval is expected to be capable of full zonal isolation.

Task 3- Well Work and Comparison

Well Operations

The first three case study wells selected for this study each had a similar operational history in that they were each drilled as production wells where they produced for a period of time, used as water injectors, transitioned to WAG injection, and then continued as water injection.

Well	Production	Water Injection	WAG Injection	Water Injection	Current Status
Case Study 1	1957–1964	1964–2000	2000–2008	2008–2010	Abandoned (Nov. 2010)
Case Study 2	1957–1972	1989–2003	2003–2008	2008–2012	Nonactive
Case Study 3	1958–2000	N/A	2004–2014*	N/A	Active
Case Study 4	1957–2003	2003–2014	N/A	N/A	Active
Case Study 5	1962–1995	N/A	N/A	N/A	Suspended

* Case Study 3 was defined as WAG injection but primarily injected water with the exception of 2 months in 2006 where CO_2 was injected.

Table 38 -- operational overview of case study wells

The wells were spread out spatially among different phases in the Weyburn Field but were all in or near Phases 1a, 1b, and 1c.

Case Study Well 4 has undergone a single transition from oil production to water injection that occurred in 2003 and has since been an active water injection well in the field until 2014 when this study was conducted, while Case Study Well 5 is an oil producing well drilled in 1962 that has suspended activities since January 31, 1995. Case Study Wells 3 and 4 were on oil production for 42 and 46 years, respectively, prior to making a switch to water injection; Case Studies 1 and 2 wells produced for only 7 and 15 years, respectively, and Case Study Well 5 has not experienced water or CO_2 injection. From the start of CO_2 injection in the Weyburn Field, CO_2 has been injected into Case Study Wells 1 and 2 for a period of 8 years and 5 years, respectively, while Case Study Well 3 had approximately 2 months of CO_2 injection.

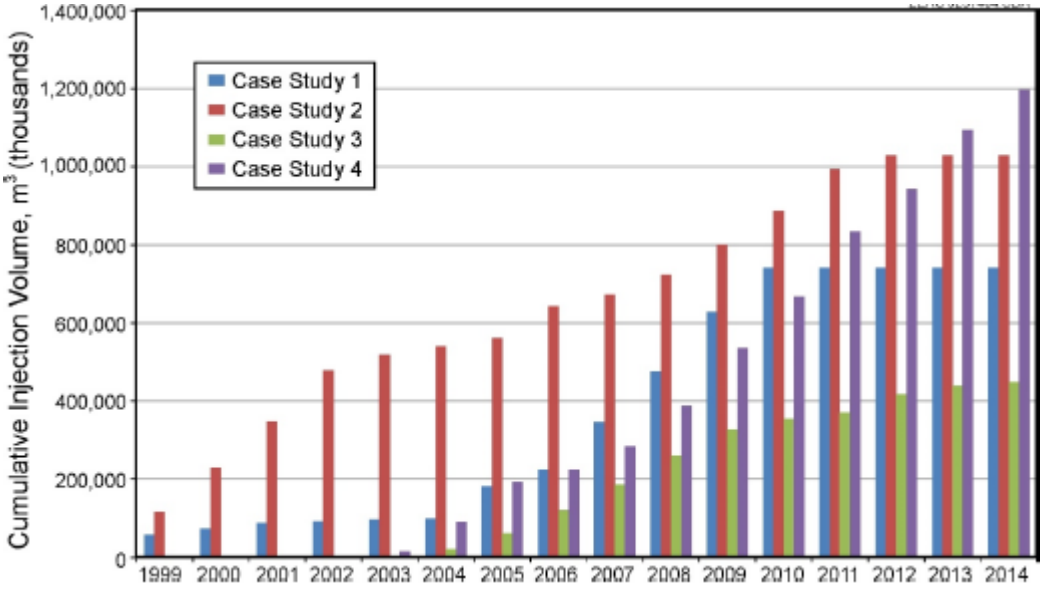

Figure 52 – Cumulative volume of water injected

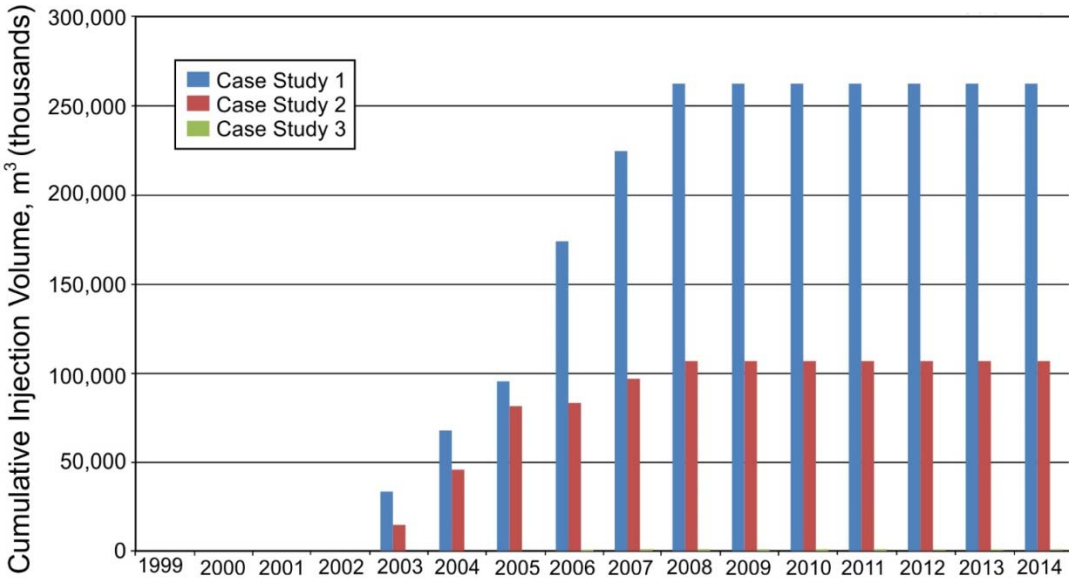

Figure 53 – Cumulative volume of CO_2 injected

Well Logging

The various types of casing corrosion and cement logs are a valuable tool to assess the state of the wellbore and cemented intervals. If logs are run multiple times in the same interval over the course of a well's life, valuable information can be gleaned. However, it is not economical to

run a suite of logs simply for scholarly purposes. Logs are typically run when there are indications of a problem within a wellbore that may need to be addressed. Mechanical integrity tests, pressure tests, and the presence of SCVF may be indicators of a problem within a wellbore that needs evaluation. Operators can often target the location of a problem to a specific interval for evaluation, thus eliminating the need to run a log over an entire wellbore.

For the purpose of well casing integrity and corrosion evaluation, the choice of logging tools deployed is important. The casing can suffer corrosion damage on both internal and external casing surfaces, thus requiring tools that have the capability to assess both internal and external surfaces. However, because of the high cost of running some of these tools, a choice can be made to use only internal casing surface survey tools such as calipers or imaging devices. Experience gathered in the course of this study indicates that caliper devices can have large limitations in the number of feeler arms and therefore lead to a less accurate evaluation. Hence, it is recommended using higher-resolution imaging devices as much as possible for detailed assessment of casing internal surfaces; such devices typically also have the capability to evaluate the external casing surface as well.

In the case of cement quality evaluation, sonic or ultrasonic devices are common for such surveys. With advancing technological knowhow, multiple devices are now combined into a single tool to provide the capability to measure not only the traditional sound wavefronts and the associated variable density logs for discriminating signal types but also possess the ability to produce higher-resolution cement maps and attenuation energy maps for a more detailed evaluation of microfeatures in the cement sheath. It would, therefore, be desirable to deploy one of the latest technologies that are capable of a high-resolution assessment of the cement, especially in CO_2 injection study programs where micro-openings in the cement could serve as potential leakage pathways by allowing gas migration and/or diffusion.

Well Corrosion Details

Each of the case study wells has experienced various degrees of corrosion as indicated by operator notes and the well logs.

Case Study 1

Case Study 1 appeared to be in good shape in 1987 as logs indicated some Class 2 and 3 casing corrosion between 50 and 400 m, and the cement had excellent bonding in the 1283–1409-m interval. Within 2 years of WAG injection, a second log was run in 2002. This log indicated Class 2 and 3 casing corrosion throughout the wellbore, and cement had poor bonding in the 1100–1175-m interval. Operator notes for the Case Study 1 well indicated seals in the tubing were distorted from the CO_2 in 2003. In 2006, large chunks of scale were reported, and injection appeared to be entering old cemented perforations at 1375 m. In 2008, injection was again noted to be entering the old perforations at 1375 m, and the losses were greater than a 2007

RA (radioactive)/spinner survey. A caliper survey and operator notes in 2008 indicated corroded/missing casing from the tubing end to 1375 m. In this period of time, greater than 250,000,000 m3 of CO_2 were injected in the well. In 2010, pitting was found on several joints, and the tubing was sent off to be inspected shortly before abandonment began. The well was abandoned in November 2010 because the wellbore casing integrity was not suitable for CO_2/WAG injection. Casing corrosion for the upper part of the wellbore (i.e., above 1100 m) was not known after the 2002 log because the 2008 casing survey focused on the bottom of the well (i.e.,1336–1376 m) and no other casing evaluation logs were conducted.

Case Study 2

Case Study Well 2 was first evaluated in 2003 when the first log was run, although it was a limited MSC log survey over the interval from 1240–1456 m. This log revealed Class 2, 3, 4, and P corrosion throughout the logged interval. In 2008, another caliper logged similar corrosion in the 1360–1449-m interval. In July 2010, operator notes described a pressure test that indicated a suspected casing leak. A 3-D caliper log revealed a warped segment of casing at 1432–1433 m, and there was Class 2 corrosion present throughout the wellbore and Class 2, 3, and 4 corrosion and penetrations below 1300 m. In August 2010, the casing was repaired at 1311–1435 m with a casing liner. In 2012, a casing leak was discovered at 1411 m and confirmed with MSC/CBL logs. The well was subsequently suspended with a bridge plug set at 1305 mKB.

Case Study 3

Case Study Well 3 was first logged with an MSC in January 2004 over a limited interval of 1227 to 1428 m, and it was again logged with an X–Y caliper in 2007 from 1361 to 1462 m. The initial log from 2004 revealed that very little corrosion was present. The first signs of casing corrosion were observed in the X–Y caliper log from 2007, with maximum and average casing wall loss of 56% and 13%, respectively, observed over the logged interval which contained Class U, 2, and 3 pitting corrosion. A CIT log showed Class 3 and 4 pitting corrosion just above the production perforations; however, the rest of the casing had limited general corrosion. In 2010, generally good cement bond to pipe and formation were observed below the TOC other than the interval from 1410 to 1460 m, which showed evidence of channeling and evidence of ineffective isolation between cement and casing. In 2011, the quality of cement over the limited log interval not impacted by the change in well completion did not appear to change. In December 2013, x-ray diffraction analysis identified gypsum as the primary crystalline material recovered from drilling returns (1346–1390 m).

Case Study 4

Case Study Well 4 was in operation for 46 years as an oil producer, then switched to water injection in 2003, and has been injecting water for 11 years to the date of this study. During this time, several corrosion events have occurred, including a tubing leak of the pump seating

nipples (PSN) and another leak on Joint 147 that were found in 2000 and 2001, respectively. Because of corrosion problems, a corrosion inhibitor program was initiated in late 2000 with Corgard 700 and was switched to Corgard 900 in 2001 after discovering the leak on Joint 147. Upon conversion to water injection in 2003, a pressure test conducted 2 years later (2005) did not appear to indicate any concerns. However, in 2010, additional repairs were necessary to replace and lower the packer, and corrosion evaluation logs were also conducted.

The results from the casing inspections showed very good casing condition from surface to about 1440 m, with minor (maximum wall loss of 40%) multiple Class 1 and 2 external SIPs. However, the interval just above the existing perforations shows greater corrosion problems internally and externally, with an internal Class 3 pit with wall loss of about 51% at 1444.1 m. Such a trend of increasing corrosion tendency towards the lower wellbore is similar to what has been observed in the other case studies, especially in the zone just above the existing perforations. The logs also showed that the integrity of the cement is generally good, especially in the interval from 1290–1476.5 m where strong bonding to pipe and formation as well as full zonal isolation are expected. Nonetheless, a few isolated channels were observed above the existing perforation zone. The most serious corrosion spot in this well is the internal Class 3 pit at 1444 m, which can enlarge over time and become a penetration.

Case Study 5

The Case Study 5 well was evaluated in 2011 using multiple log types that allow full assessment of both the internal and external surfaces of the casing and the quality of the cement. Prior to the recent extensive survey campaign, there had been no logging to evaluate the corrosion status in the well, but there was a corrosion-related tubing leak above the PSN in 1992 reported in the well data files. The CIT log was used to assess the internal and external surfaces of the casing, the MSC caliper log surveyed only the internal surface of the casing, thus providing two data sets for the internal casing surface. The MSC log results indicated no serious corrosion problems, with 150 of 156 joints displaying only Class 2 pits corresponding to wall loss of 20%–40%. On the contrary, the CIT log indicated several locations in the interval from around 400 m to about 900 m with severe pitting corrosion involving wall metal loss ranging from 80% to 93%; specifically at depths of 485.6 (86%), 820.2 (93%), 835.7 (80%), 850.2 (80%), and 875.2 m (83%). However, a pressure test conducted at the time this log was surveyed did not indicate a leak. The large difference between MSC and CIT results appears to be due to the 8-mm feeler arm spacing in the MSC tool that potentially miss some of the pits that were evident in the CIT log, thus underscoring the importance of a careful choice of logging tool in the investigation of casing integrity.

The quality of the cement was found to be generally in good condition, with good bonding to casing and formation in the lower wellbore from TOC at 1142 m to the bottom logged depth at

1455 m. Despite the observed small microvoids and microchannels, this interval is expected to be capable of full zonal isolation.

Well Comparison

All five case study wells are in or near Phases 1a, 1b, and 1c, and considering their close proximity, the geology is similar, although the formation properties such as formation fluids may vary. The case study wells are also similar in their spud date (i.e., within a narrow window of time from 1957 to 1962), and thus their drilling and completion procedures are likely to be similar.

Case Study Well	Casing Integrity	Cement Quality	Corrosion Rates	Cum. CO_2 Injected, m^3	Cum. Water Injected, m^3
Case Study 1	Severe corrosion internally and externally throughout wellbore; bottom 55 m of casing plugged off	Good cement bond below TOC (1133 m), zonal isolation possible in lower wellbore	Internal rates increase slightly from top to bottom of wellbore, but external rates decrease	>263,000,000	>741,000,000
Case Study 2	Corrosion in the lower wellbore near existing perforations	Cement quality below TOC appears reasonable but has a few microvoids; zonal isolation possible	No data to calculate external rates; internal rates increase slightly with depth	>106,000,000	>1,029,000,000
Case Study 3	Corrosion in lower wellbore near existing perforations	Generally good cement bond to pipe and formation below TOC (1195 m); effective zonal isolation expected	Internal and external rates higher near the existing perforation interval	>963,000	>450,000,000
Case Study 4	Corrosion near existing perforation interval	Good cement bond below TOC at 1158 m; full zonal isolation possible	Internal and external rates higher near the existing perforation interval	N/A	>119,000,000
Case Study 5	Severe internal and external corrosion throughout most of the wellbore	Good cement bond below TOC (1142 m) with possible effective zonal isolation	External rates increase with depth; internal rates oscillate with depth	N/A	N/A

Table 39 – Comparison of case study wells

In all five case studies, casing corrosion appears to be more serious in the lower wellbore just above the production/injection perforations interval. In Case Studies 1 and 5, casing corrosion was more widespread. These trends are similar to the trends observed in internal corrosion rates, but external corrosion rates tend to decrease, in general, with depth. The external corrosion rate trends are consistent with observed better cement quality in the lower wellbore that offers better protection to the external casing surface. It should be noted that external corrosion could not be determined for all wells because not all logs can detect external defects.

Case Study 5 status of more widespread corrosion was a bit anomalous because the well has neither been used for water injection nor CO_2. It does suggest that produced fluids may have accelerated corrosion or other contributing factors such as galvanic corrosion or simply multiple completion/packer settings. Sulfur-reducing bacteria, which typically feed on organic matter such as crude oil; iron bacteria; and stray current corrosion are known corrosion mechanisms that may be potentially involved. Because multiple large pits with 80%–93% wall loss occur relatively close to the surface casing, i.e., within the 400–900-m interval, it is plausible that stray current corrosion mechanisms could be a contributing factor to what is observed in Case Study Wells 1 and 5. However, laboratory analysis or the casing would be needed to fully substantiate these suggestions and to pinpoint specific mechanisms.

Task 4 - Conclusions and Recommendations for Future Work

The wells chosen as case studies for this project provided some insight into casing corrosion in well environments that have experienced CO_2 injection, as well as two wells that have been exclusively water injection and oil-producing wells, respectively. In all cases, the rate of casing corrosion increased near the lower sections of the well near the existing production perforations. This increase in corrosion can easily be explained by injected CO_2, produced fluids, 63 and the highly corrosive environment that is present in the perforated area of a well.

In Case Study 1, the entire lower section of casing was completely corroded during the 6-year time period when CO_2 was injected. The loss of casing in this area eventually led to the abandonment of the well because it could no longer be used for injection activities.

The well for Case Study 2 underwent casing repair with a liner in the lower sections of the well to repair corroded joints. In all five case studies, the overall conditions of the cemented intervals were of sufficient quality to provide zonal isolation and protect the well environment.

In general, zones with effective barriers (e.g., isolated annular space coupled with good cement bond and zonal isolation) experience little degradation, whereas areas exposed to reservoir and injected fluids at high-flow velocities experience accelerated corrosion and cement degradation. The greatest safeguard against corrosion remains a good cement job and effective isolation from reservoir and injected fluids. The presence of microvoids and microchannels in

cement poses an even greater threat in CO_2 injection scenarios because gas migration and/or diffusion can be accelerated by the presence of such microfeatures.

Generally, two characteristic corrosion scenarios were observed for the five case study wells. One scenario is where corrosion is more prevalent in the lower wellbore near production perforations and another involves more widespread corrosion closer to the surface. It is possible that different corrosion mechanisms other than water- and/or CO_2-initiated pathways are involved. For instance, sulfur-reducing bacteria, iron bacteria, and stray current corrosion are some of the potential mechanisms that might be playing a role in the corrosion process. Laboratory analysis would be required to elucidate these potential mechanisms.

Additional research studies monitoring time-lapse casing corrosion and cement integrity under varying operating conditions are critical to understanding not only the factors that influence corrosion and cement degradation under field conditions but to quantify the rates and probability at which they occur. The rate calculations conducted in this study are based on two to three logging runs which do not lead to the ability to provide a statistical analysis. While several factors influencing wellbore integrity have been discovered, completion methods play a critical role in mitigating their impact. Furthermore, laboratory analyses are required to fully investigate and pinpoint the key corrosion mechanisms involved.

8.0 SaskCO_2 USER (WMP Optional Phase) – Passive Seismic Monitoring

Induced seismicity related to underground injection of fluids (including CO_2, waste fluids, and brine) has become a topic of heightened interest as CO_2 storage projects progress to industrial-scale. Of particular concern are the ramifications of seismic activity for the long-term security of the geologically stored CO_2. Southeastern Saskatchewan is host to a number of hydrocarbon production fields that have been subject to water injection and/or CO_2 injection dating as far back as 1965, many of which are ongoing today. This historical and continued injection provides an opportunity to assess the level of induced seismicity associated with these activities.

The University of Bristol and Outer Limits Geophysics LLP was selected as a subcontractor for this research project. This research compiled and reviewed the natural seismicity of southern Saskatchewan. This data set was cross-referenced with a historical record of the regional fluid injection. A thorough examination of existing and new seismic and microseismic data was undertaken to establish whether any temporal-spatial correlations of microseismic activity and injection/production activities existed. Results were integrated with general geomechanical models with an objective of providing insight into microseismic activity in Southern Saskatchewan, with a goal of informing future exploration of induced seismicity by both regulators and operators.

8.1 Passive Seismic Monitoring – Approach and Methodology

The project was divided into seven tasks:

1. Review of existing event catalogues
2. Saskatchewan injection/production data
3. Weyburn microseismic data
4. Monitoring events using the Estevan array
5. Installation of Weyburn network
6. Geomechanical assessment

A review of existing events was necessary to establish a baseline prior to any further exploration. Task one used both USGS and GSC catalogues and re-evaluated existing USArray data. Task two focused on reviewing industrial activity. Injection data held by the Saskatchewan Ministry of Economy was reviewed, as was production data, as seismic events can be induced by both the injection and production of fluids. In Task three, the existing event catalogue was compiled and efforts were made to detect events post-2011, although limited data was available. Event magnitudes and population statistics relevant to induced seismicity were considered. Task four involved the monitoring of a microseismic network deployed in South Eastern Saskatchewan. Events were monitored using automated triggering.

In 2015, Task five was undertaken which involved the installation of an additional network in the Weyburn area. Three (3) broadband 3-component seismic stations were installed in the area, and data was harvested and analyzed in conjunction with that of the Estevan network. Any correlation of events and industrial activity was explored in Task six. Detected events were investigated, and the Davis Frohlich criteria employed to assess whether events were induced or natural. The possibility of remote triggering via large, distant seismic events was also investigated. Finally, the world stress map data was incorporated with anisotropy and other relevant data from the WMP to determine stress conditions. Evaluations were undertaken to determine the pore pressure increases necessary to initiate seismic activity.

8.2 Passive Seismic Monitoring – Results and Recommendations

Task 1 – Review of existing event catalogues

Relatively speaking, seismicity in Saskatchewan is rare, and generally of low to moderate magnitude.

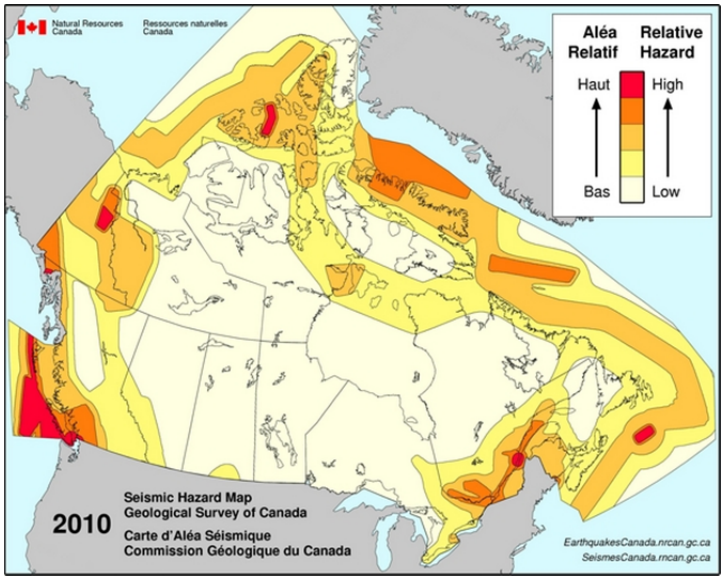

Figure 54 – Seismic hazard map of Canada

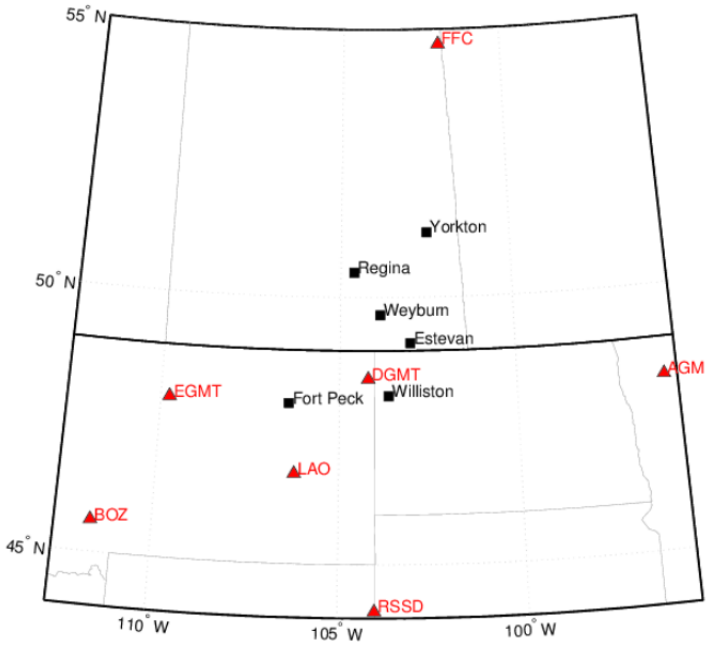

Figure 55 – The USGS and GSN stations utilized

Several Global Seismographic Network (GSN) and USGS Advanced National Seismic System (ANSS) monitoring stations were used in this project, with the nearest located in Dagmar, Montana (DGMT), which is 130 km from the project site. The lack of seismic activity in the area means that there has been a limited coverage of the area.

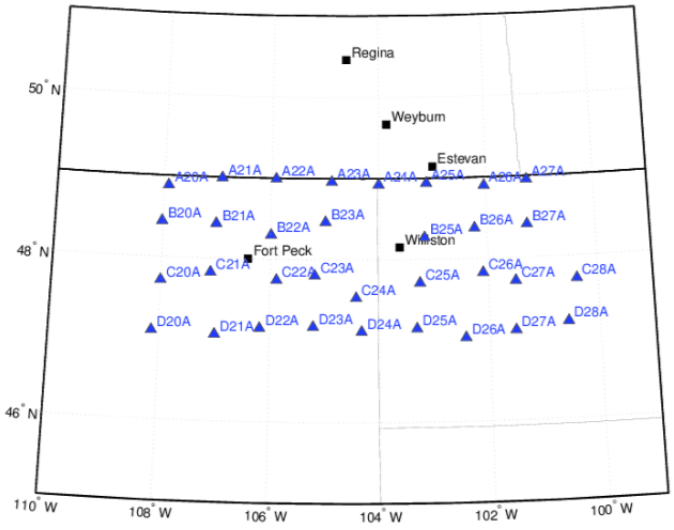

Figure 56 – USArray Transportable Array stations

From 2008 to 2011 the Earthscope USArray Transportable Array was moved from west to east across the USA which represented a significant improvement of coverage for a limited period of time.

The largest earthquake known in the region occurred in 1909. The magnitude of this event is estimated to be 5.3 (Bakun et al., 2011). This event was felt across southern Saskatchewan, North Dakota and Montana. However, the lack of instrumentation at the time means that the location of this event is not well constrained. A total of 93 events have been recorded since 1960. The majority of events recorded have magnitudes of 2.5 or greater, with the largest being magnitude 4.0.

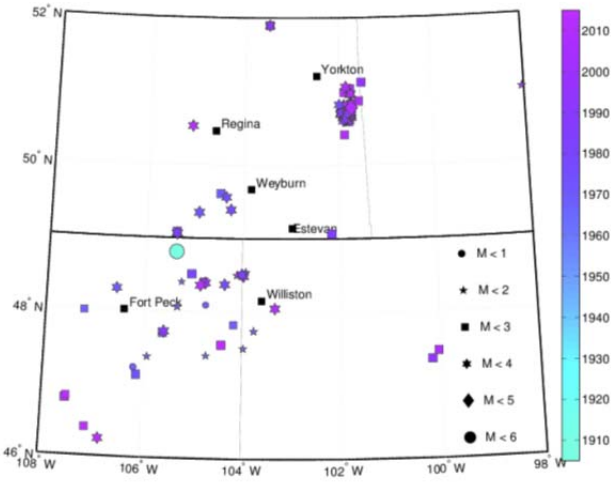

Figure 57 – Map of recorded seismicity as catalogued in data sources

A series of smaller events were detected in 1966-67. These were detected by Reinbold and Gillispe (1974) using the Large Aperture Seismic Array (LASA), which was based in Montana.

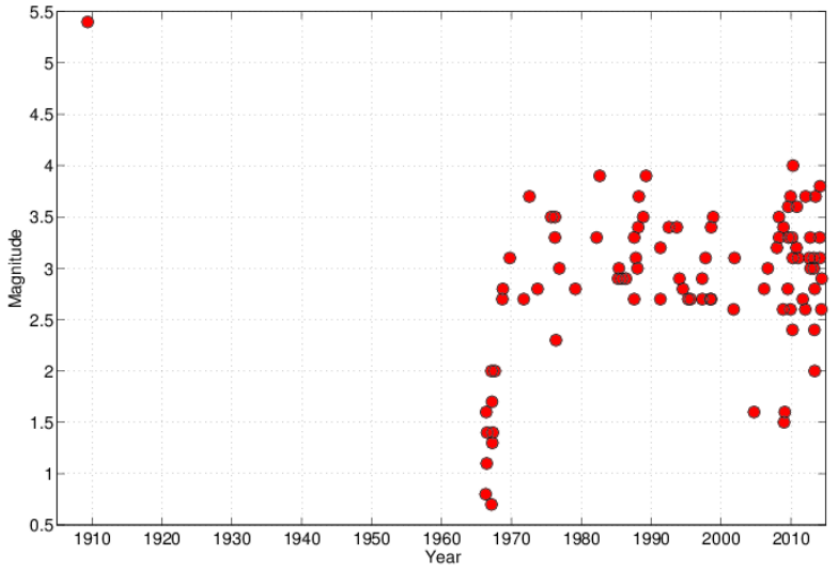

Figure 58 – Event magnitude by year of occurrence for all events recorded in the project area of interest

LASA was designed to record teleseismic events, and as such does not provide accurate locations for regional events. Bakun et al. (2011) attribute these events to strip-mining operations near to the Montana –North Dakota border. The lack of seismic monitoring networks means that location errors are generally large. Location errors are estimated to be at least 20km laterally, while event depths are generally unconstrained.

The naturally occurring seismicity in this region is linked to both basement structures and to the natural dissolution of the Paleozoic Prairie Evaporite deposits. Both Horner and Hasegawa (1978) and Bakun et al. (2011) identify a NE-SW trend to event locations in NE Montana, a trend which aligns with the mapped Hinsdale, Weldon and Brockton-Froid fault zones, interpreted as zones of weakness in basement rocks.

The Prairie Evaporite deposit, of Middle Devonian age, is found in the sedimentary sequence across much of the region. It is more than 200m thick in places, and lies at depths of between 400m – 3000m (Hasegawa et al., 1989). Wilson et al. (1963) suggest that basement lineaments lead to the localisation of upward fluid migration, which in turn results in the dissolution of the evaporites. Horner and Hasegawa (1978) argue that the salt dissolution produces stress changes that cause seismicity, pointing out that some of the recorded seismicity correlates with the edges of the Prairie Evaporite deposits, and with major salt dissolution structures. The Prairie Evaporite is mined for potash across Saskatchewan. A significant number (42) of recorded events are located near to the Mosaic Company (International Minerals and Chemical

Corp as was) potash mining operations near Esterhazy, SK. While there is some brine injection occurring in the area, Hasegawa et al. (1989) and Gendzwill and Unrau (1996) attribute the seismicity to subsidence in the rocks overlying the mined zone. As above, Bakun et al. (2011) have also attributed some seismicity to strip-mining operations in the region.

To identify induced seismicity, an automated picking algorithm was used to search for potential events, based on FilterPicker (Lomax et al, 2012). This ensures that individual noise spikes, which might occur on a single station, are not used. This automated algorithm produced a total of 4,345 potential triggers. These triggers were then examined manually to determine whether they could be classified as earthquakes.

A total of 60 triggers were identified by manual analysis as local or regional seismic events, and considered for further analysis. To locate the events, the previously identified stations were used to locate the hypocenters. Of the 60 events identified, 20 were already listed on existing USGS catalogues, while 40 represent newly identified events.

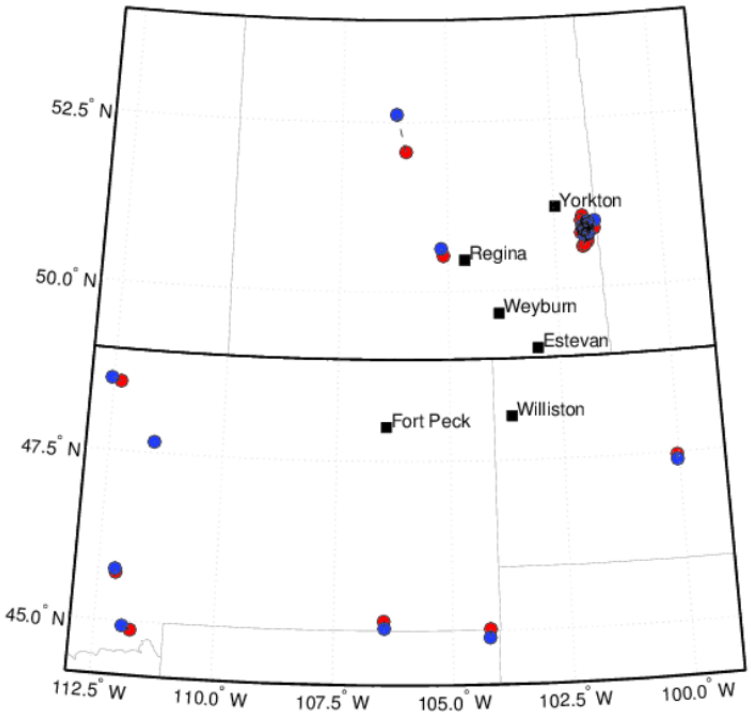

Figure 59 – Comparison of event locations from USGS catalogues (red) vs. relocations (blue) for all events

Locations were plotted, and the majority appears to have been located in Southern Montana. Investigations revealed the presence of a large strip mine in close proximity, which suggests these events were associated with mining activity as has been suggested (Bakun et al, 2011). The events located in Saskatchewan are also potentially linked to the presence of potash mines.

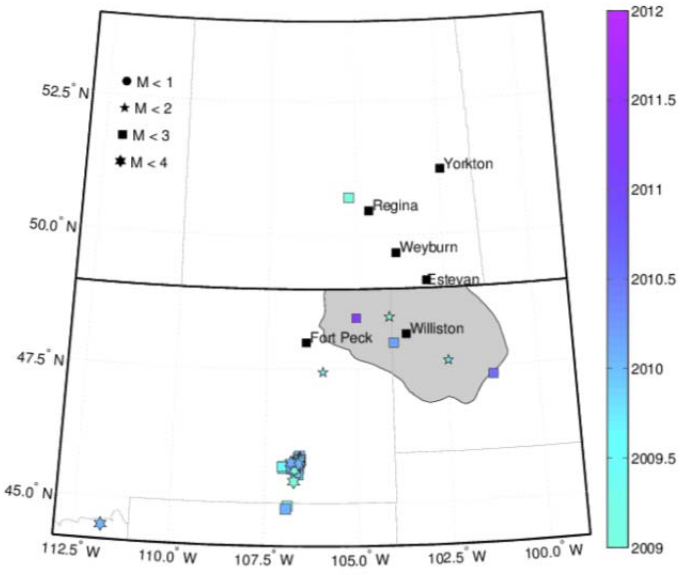

Figure 60 – Additional events identified using USArray data. Symbols are scaled by event magnitude, and coloured by occurrence time. The extent of the Bakken Shale in the USA is shaded in grey (no shapefile for the Bakken Shale in Canada was available).

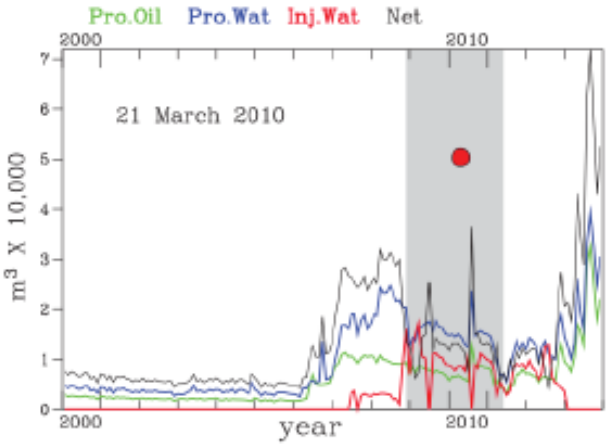

Figure 61 – Oil (green) and water (blue) production rates and water (red) injection rates, as well as net volume change (black), for wells in proximity to the 2010-03-21 event. These changes may have triggered the observed ML = 2.3 earthquake (Frohlich et al, 2015).

There are 5 events located across the Montana – North Dakota border. Apart from the south-westernmost event, these events fall within the area of Bakken Shale development, and so may potentially be linked to shale gas extraction. In a recent study Frohlich et al. (2015) used similar

methods to search for events associated with Bakken Shale extraction, and also identified 4 of these 5 events.

Frohlich et al. (2015) are only able to link one Bakken event to injection and/or production activities, namely the ML = 2.3 event on 2010-03-21, where increases in both production and injection had occurred in wells that were within 5km of the epicentre (Figure 61). The remaining events do not occur in close proximity to active wells. Indeed, the events of 2009-2-06 and 2011-04-06 occur in approximately the same vicinity as previous earthquakes that have been associated with the Brockton-Froid fault zone (Figure 60) that occurred prior to the current increases in Bakken Shale activity (for example events in 1975 and 1998) No additional events that might be related to oilfield activities in southeastern Saskatchewan were identified.

In sum, seismic events occur rarely, and are generally of low magnitude. However, the occurrence of a magnitude 5.3 event in 1909 indicates that there are faults of sufficient size in the area such that larger events can occur, albeit very rarely. Historically, seismometer coverage in the area has been poor, meaning that small-magnitude events may have gone undetected.

Naturally occurring seismicity that has been detected in southern Montana/North Dakota and extending into Saskatchewan tends to follow a NE-SW trend associated with the Hinsdale, Weldon and Brockton-Froid fault zones. In terms of induced seismicity, a number of events have been linked to two potash mines in Saskatchewan. In addition, one seismic event in North Dakota has been tentatively linked to production and/or injection activities in the Bakken Shale. However, no seismicity has been recorded in Saskatchewan that is obviously linked to conventional oilfield production, water re-injection or CO_2 injection.

Task 2 – Saskatchewan injection/production data

South-eastern Saskatchewan has a long history of oilfield activities, including oil and gas production and reinjection of produced water. More recently, CO_2 has been injected to enhance oil recovery. Injection and production data provided by Saskatchewan Ministry of Economy was used to investigate any correlation between oilfield activities and seismicity in the area. Data was provided for a period covering 01-2000 to 12-2014. A total of over 25,000 wells were included in this dataset.

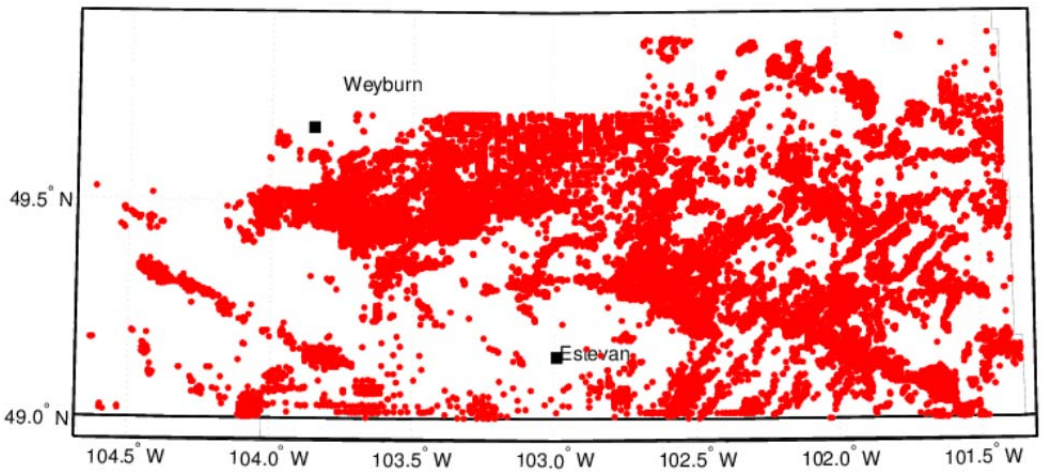

Figure 62 –Locations of wells for which injection and production data was provided by Saskatchewan Ministry of Economy

The overall volumes of fluids produced and injected in the region were examined. Overall, more fluid has been produced than injected, resulting in a net volume decrease.

Fluid	*Volume*
Oil Produced	$1.39x10^8$
Water Produced	$1.95x10^9$
Fluid Produced	$2.09x10^9$
Water Injected	$1.96x10^9$
Net Fluid Prod – Inj	$1.33x10^8$

Table 40 – Total volumes of fluids produced and injected in south-eastern Saskatchewan (in m^3)

Although the net volume change is negative (i.e. more fluid is produced than injected), there may be areas where injection volumes exceed production, and which would therefore potentially be more prone to seismicity. Therefore, the study area was divided and considered 'block' by 'block'. In the majority of blocks fluid production exceeds injection, however, some individual blocks present a situation in which the amount of fluid injected exceeds the volume produced.

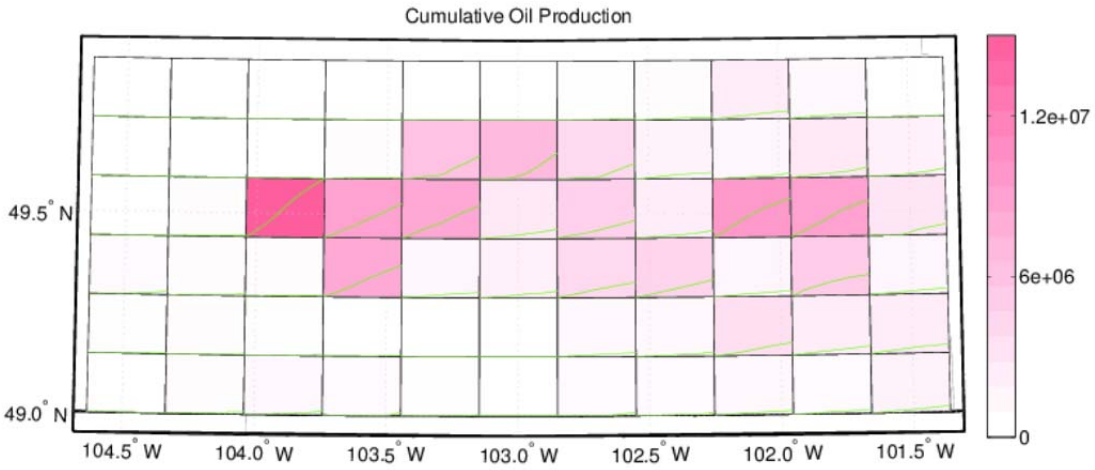

Figure 63 -- Spatial variations in oil production. Block colours represent total production, while green lines represent cumulative production from 2000 to 2014

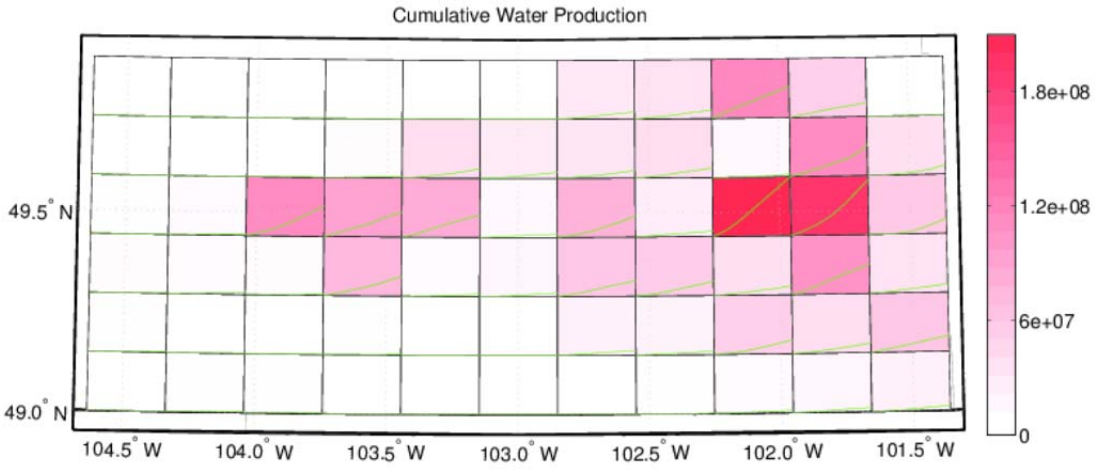

Figure 64 – Spatial variations in water production

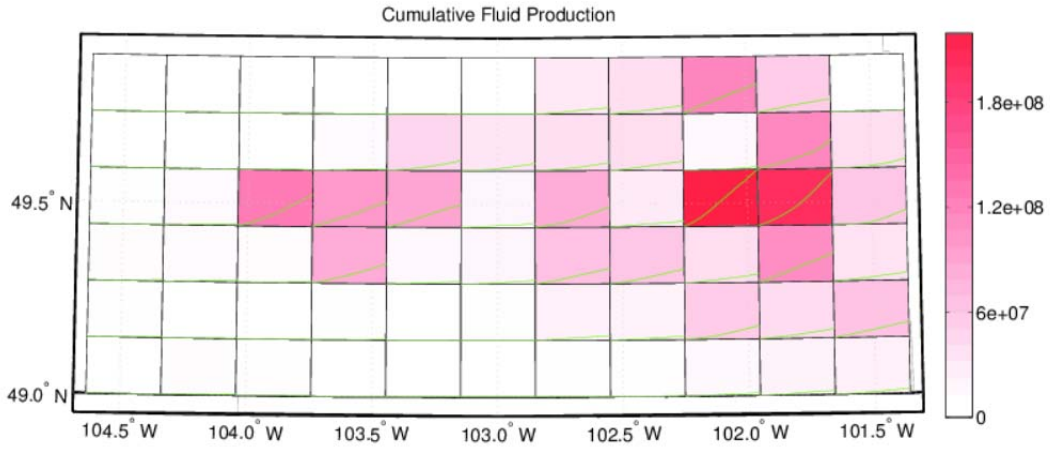

Figure 65 – Spatial variations in total fluid production

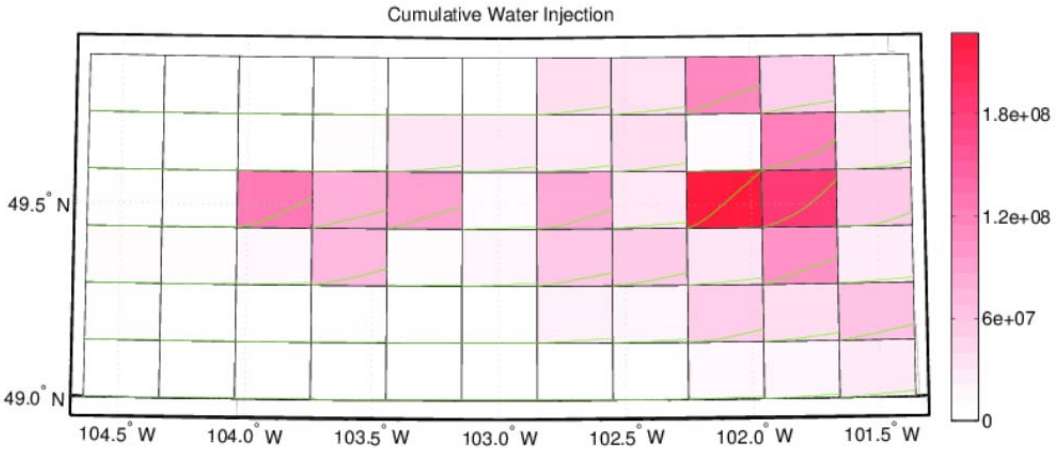

Figure 66 – Spatial variations in water injection

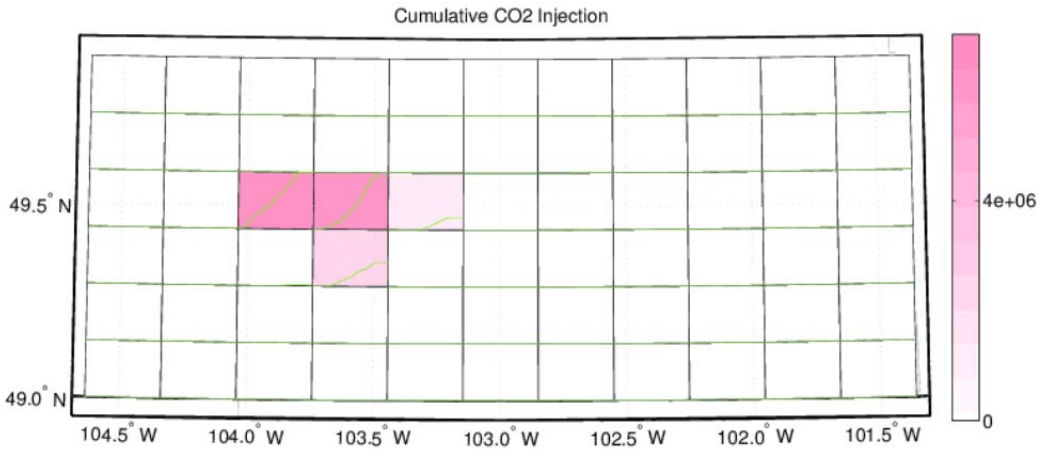

Figure 67 – Spatial variation in CO_2 injection

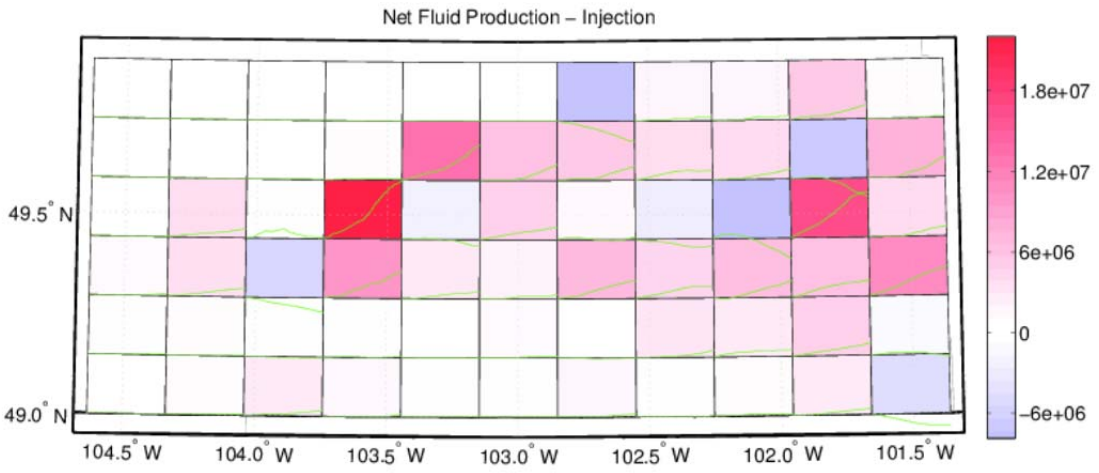

Figure 68 – Spatial variation in net fluid production-injection

Injection and production in the region occurs in different geological units. In the data files provided the target zones of each well were specified. A total of 47 units were specified. The majority of injection and production occurs in Mississippian units.

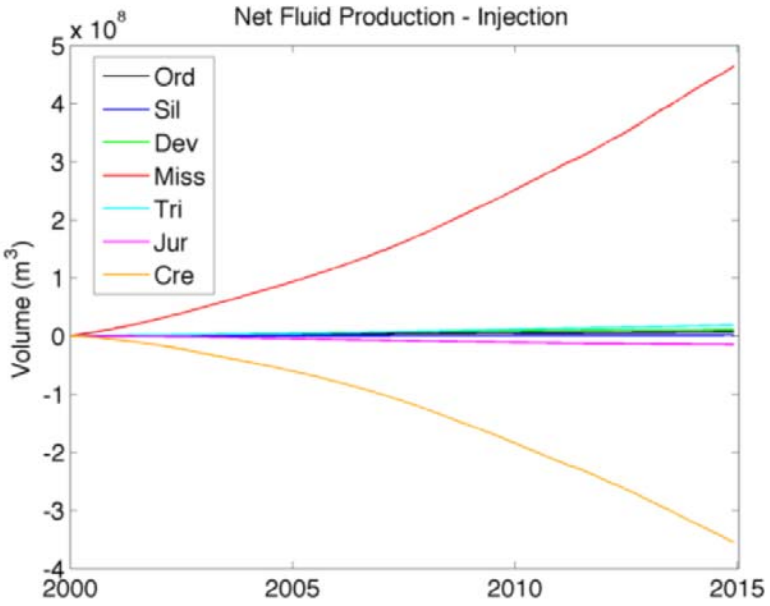

Figure 69 -- Net fluid production-injection volumes by geologic period

In the Mississippian unit, net fluid production exceeds injection, implying a net volume decrease. However, in the Cretaceous units, fluid injection volumes are substantially larger than production volumes, implying a net volume increase.

Seismicity associated with oilfield activities can be induced by both fluid injection and production (e.g. Frohlich and Brunt, 2013). However, it is generally accepted that increases in pore fluid volumes (and therefore pore pressures) associated with fluid injection are the more common cause of induced seismicity. Therefore areas and/or units experiencing a net volume increase will be most prone to induced seismicity.

Overall, fluid production volumes in the study area exceed injection volumes. However, within the region there are blocks where injection volumes do exceed production. Most oilfield activity in the region occurs in Mississippian units, in which production volumes exceed injection. However, there are Cretaceous units where injection volumes exceed production volumes. Injection-induced seismicity is often associated by activity near to the crystalline basement (e.g. Verdon, 2014). This being the case, volume increases in basal layers may be of greater concern that shallower layers.

For this area volume changes in lower layers are small, with most activity focused in Mississippian and Mesozoic layers. Moreover, the only units experiencing a substantial increase in injection volume are of Cretaceous age, and so are unlikely to be connected to the basement.

Task 3 – Weyburn microseismic data analyses

In 2003 a microseismic array was installed to monitor a portion of the CO_2 flood in the Weyburn oilfield. Oil has been produced from this field since the 1950s, and CO_2 injection began in 2000. However, the microseismic monitoring array was installed in the Phase 1B area, approximately 5 months before the start of CO_2 injection in the nearest well to the microseismic monitoring well.

This monitoring array recorded data from August 2003 until the end of 2010, and the detected microseismic events have been the subject of many studies (e.g. Verdon et al., 2010; Verdon and Kendall, 2011; Angus et al., 2011; Verdon et al., 2011; Verdon et al., 2013).

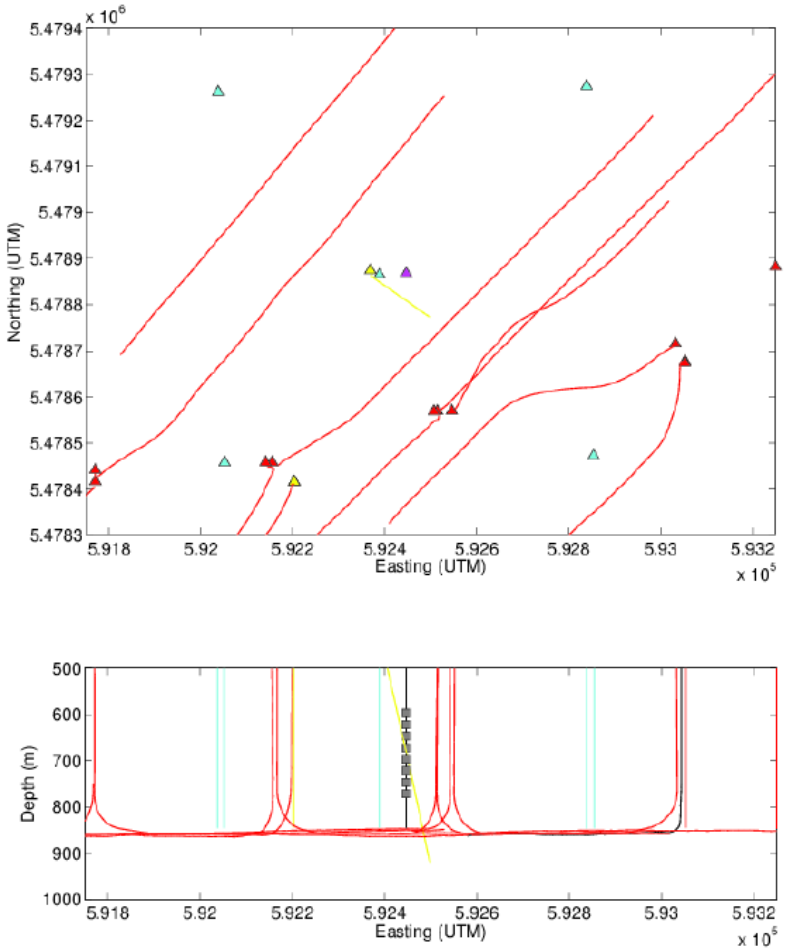

Figure 70 – Map (upper panel) and cross section (lower panel) of the microseismic monitoring setup installed at Weyburn. Red lines and triangles show oil producers, blue lines and triangles show WAG injection wells. The microseismic monitoring well is indicated by the magenta triangle in the upper panel, while the monitoring geophone depths are shown by the grey squares in the lower panel.

8 three-component geophones were installed in a disused vertical well in the Phase 1B area. Apart from occasional pauses due to technical issues, these geophones recorded continuously from August 2003. From January 2004, CO_2 and water were injected into a vertical well approximately 50m to the east of the microseismic monitoring well. Meanwhile, oil was produced from several horizontal production wells surrounding the injection well. A number of additional WAG injection wells are also located within the nearby area, although the main focus has been on the nearest injection well.

The initial, raw data was processed on a monthly basis by a contractor, ESG. The initial processing consisted of a triggering algorithm to search the data for possible events. Where triggers were detected, P- and S-wave phases were picked, and travel times inverted for the best fit location, using a velocity model derived from a sonic log. The frequency spectra of the arriving phases were used to determine event magnitudes.

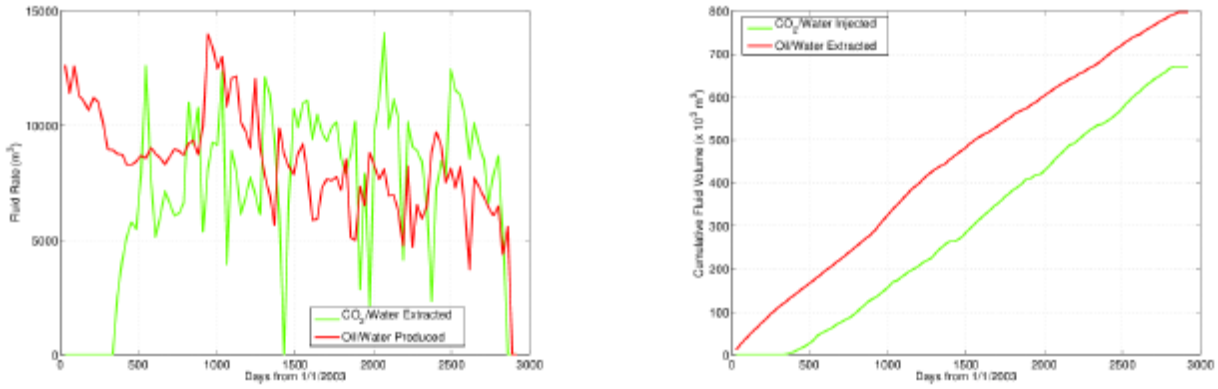

Figure 71 – Monthly injection and production rates (a) and cumulative injected and produced volumes (b) for wells around the microseismic monitoring array.

With only a single downhole well, the array aperture does not have sufficient width to allow event source mechanisms to be determined.

Recorded Events

Over the full monitoring period, a total of 207 microseismic events were identified. The largest event had magnitude of -0.5, while the smallest event had a magnitude of -3.5.

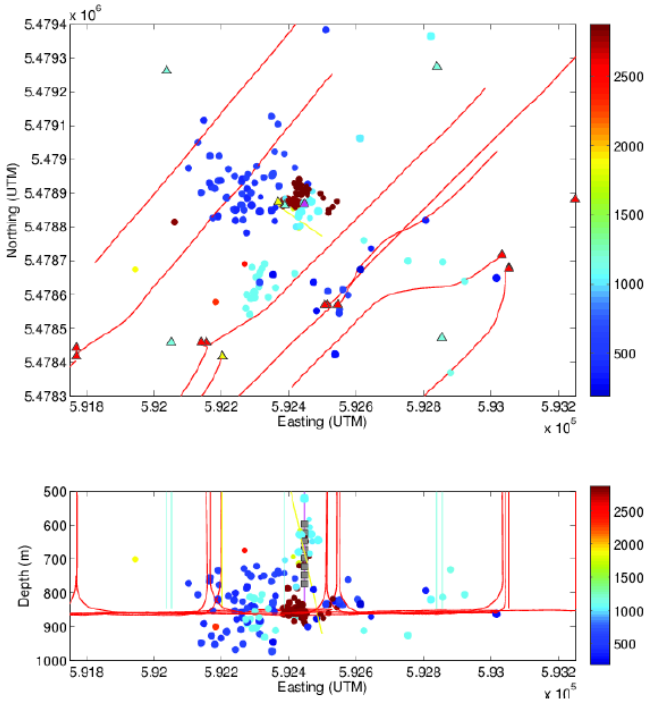

Figure 72 – *Locations of microseismic events recorded at Weyburn*

It should be noted that 200 events of magnitude -3.5 < M < -0.5 over a 7 year period is a very low level of seismicity. For comparison, at the In Salah CCS project, over 9,000 events were recorded in one year, with a maximum magnitude of M = 1.7 (Stork et al., 2015).

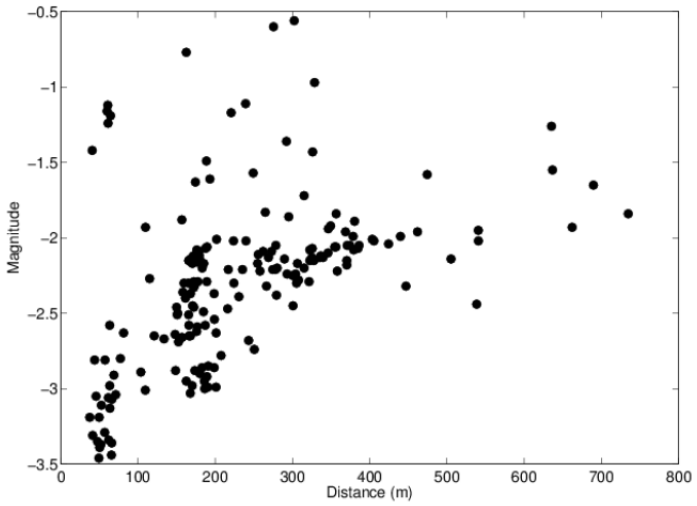

Figure 73 – As distance increases, the detectable magnitude reduces

For events of such small magnitude, the range of detection is extremely limited. While events with magnitudes of -3.5 can be detected within 100m of the array, at distances of 500m the detection threshold reduces by an order of magnitude to 2.5.

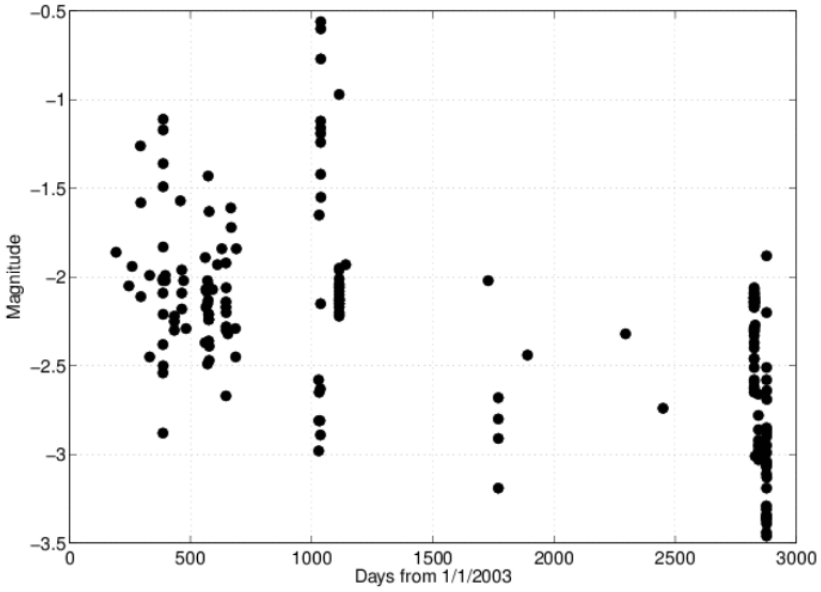

Figure 74 – Occurrence time and magnitude of microseismic events recorded at Weyburn

In the time between array installation in August 2003 and the start of injection in well 121/06-08, 8 events were recorded by the array. These events were all located to the SE of the injection well, near to production well 191/09-08. This indicates that oil production from the field was able to trigger microseismicity even prior to CO_2 injection.

At the onset of injection in well 121/06-08, 15 events were detected within 2 days of the start of injection. These events were primarily located around the production well to the NW of the injection well, well 191/11-08, and in between this well and the injector. A further 45 microseismic events were recorded over the spring and summer of 2004, the majority of which were located to the NW of the injection well, with a few events recorded to the SE, in the same area as the events detected prior to injection.

The monitoring well was disabled from November 2004 until October 2005. A further 18 events were recorded in October 2005. These events were located at a range of depths (900 – 1500m below surface) in close proximity to the monitoring well. The mechanism for these events remains unclear. A further 21 events were recorded in January 2006, and were mainly located to the SE of the monitoring well, near to production well 191/10-08.

From 2006 until 2010 only a further 8 events were recorded. In 2010 however, the injection well was shut in and abandoned. During the month following shut-in, a further 92 events were recorded. All of these events were located in close proximity to the injection well.

Event Depth and Leakage Potential

The majority of events occur in the reservoir interval. However, it is clear that a substantial number of events occur in the overburden and under burden.

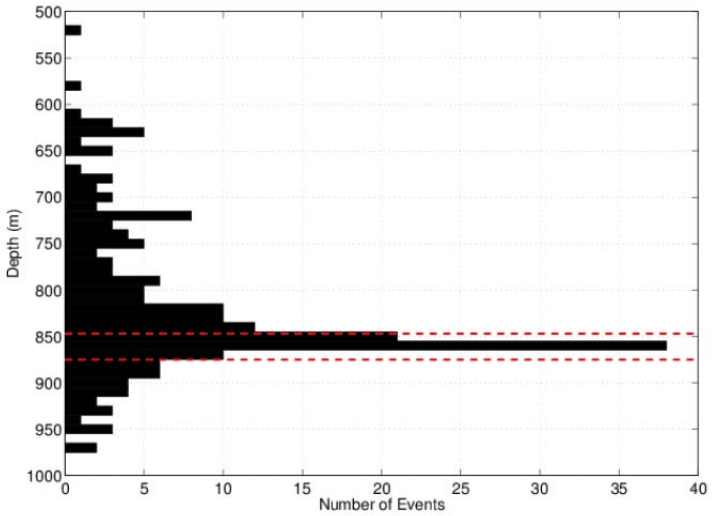

Figure 75 – Histogram of event depths. Red lines indicate the approximate depth of the reservoir in the microseismic monitoring area

At face value, such an observation might pose a concern with respect to fluid migration through the caprock. However, overburden seismicity could also be triggered by stress arching transferring stress through the rock frame into the overburden. In order to address this issue, geomechanical modelling was conducted to improve the interpretation of these events.

Interpretation of Event Locations

Conventional theory pertaining to injection-induced seismicity is that pore pressure increases that accompany injection act to reduce the normal stress, promoting the possibility of failure on optimally oriented planes of weakness. As such, we would expect seismicity to correlate with areas of elevated pore pressure, and moreover the presence of microseismic activity would imply a hydraulic connection between injection wells and the loci of microseismic events. In terms of CO_2 storage integrity, such a connection into the overburden would be of concern, particularly if overburden events were located directly above injection wells.

However, at Weyburn we observed many microseismic events around the production wells, where pore pressures should be lower. Events in the overburden were observed, but principally above the horizontal production wells. When injection is shut in, and it would be expected that reducing pore pressure would reduce seismicity, when contrarily, seismicity occurs. This implies that to understand microseismicity at Weyburn more than the most conventional theory about injection-induced seismicity is needed. A commercial reservoir flow model was used to simulate pore pressure changes cause by production and injection. These pore pressure changes are passed to a geomechanical model to simulate how the changes in pore pressure lead to stress changes in and around the reservoir.

The model was a simplified representation of the setup at Weyburn, with three vertical CO_2 injection wells situated in between 4 horizontal oil production wells. Initially, the production wells were switched on without injection, to simulate the initial stages of unsupported production at Weyburn. At a later stage, the injection wells were switched on. The geomechanical model provides a map of stress as a function of time. In order to simulate induced microseismicity, Verdon et al. (2011) computed changes in the fracture potential, *fp*, which describes how close the stress state is to the Mohr-Coulomb failure criteria. The higher the fracture potential, the more likely it is that a microseismic event will occur.

In their model, Verdon et al. (2011) found that a softer-than-expected reservoir unit promoted stress transfer into the surrounding under- and overburden rocks. The result of this stress change was to increase *fp* in the rocks around the production wells, and especially in the overburden above the production wells, while *fp* in the rocks around the injection wells, where pore pressures were highest, was actually reduced slightly. The areas of elevated *fp* modelled by Verdon et al. (2011) correspond to the areas where most microseismicity was observed at Weyburn, i.e. near to and in the overburden above the horizontal production wells. This also explains why microseismicity might occur after shut-in of the injection well. The model produced by Verdon et al. (2011) is informative with respect to storage integrity. There is no evidence from other geophysical measurements that substantial amounts of CO_2 have leaked

from the reservoir into the overburden. However, a number of microseismic events are located in the overburden.

The Verdon et al. (2011) model has no hydraulic communication between reservoir and overburden – all of the injected CO_2 remains in the reservoir. Instead, stress is transferred through the rock frame, which is capable of producing the observed patterns of microseismicity. The fact that a model that explicitly has no leakage is able to re-create the observed microseismic features is encouraging vis-à-vis storage integrity.

Summary

Microseismic monitoring has revealed that operations in the Weyburn oilfield have triggered microseismicity with magnitudes ranging from $-3.5 < M < -0.5$. Approximately 200 events have been recorded over a 7 year period, representing a low level of seismicity, relatively speaking.

Events are generally located near to production wells, both in the reservoir and overburden. Geomechanical models have shown that this activity is consistent with stress transfer through the rock frame in response to small amounts of reservoir deformation, and is not directly triggered by CO_2 injection as per the mechanism often used to account for injection-induced seismicity (where pore pressure increases lead directly to failure through a reduction in effective normal stress).

Task 4 – Monitoring events using the Estevan array

Estevan Array

In 2012, an array of 3 broadband seismometers was installed at the proposed Aquistore site near to Estevan (Worth et al., 2014). For the purposes of this study, the broadband stations were used only to search for additional earthquakes in the region. Data was used from the entirety of 2014, using the *FilterPicker* algorithm to detect potential events. The auto-picker detected a total of 1281 potential triggers, which were then manually examined to determine whether any represented local earthquakes.

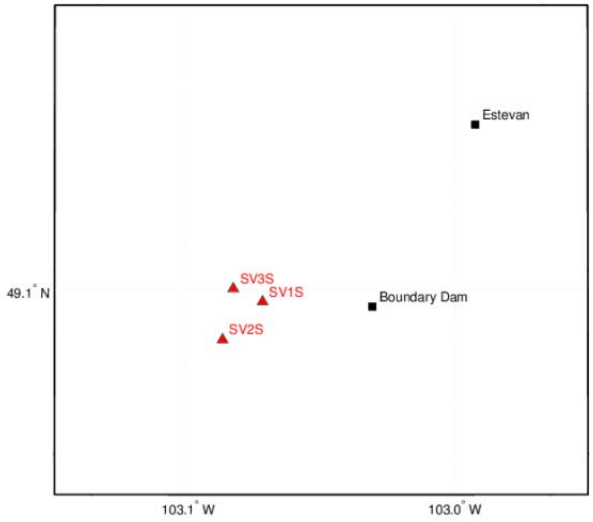

Figure 76 – Map showing the locations of the Aquistore broadband seismometers used in this analysis

Noise Spikes

Manual examination of the triggers revealed a substantial number what appear to be noise spikes. While these spikes resemble earthquakes in some respects, it is apparent from their occurrence times that they are not.

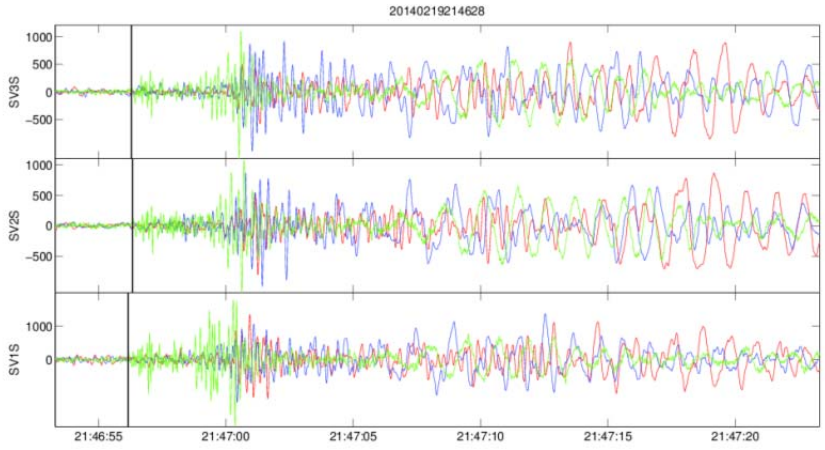

Figure 77 – Example waveforms from the most common noise source. These events are putatively located near to a power station

An impulsive P-wave arrival is recorded on the vertical components, followed by an emergent, higher amplitude arrival on all 3 components, followed by lower frequency waves on the

horizontal components. A total of 95 of these events were identified by manual analysis. These events all occur at a similar time of day.

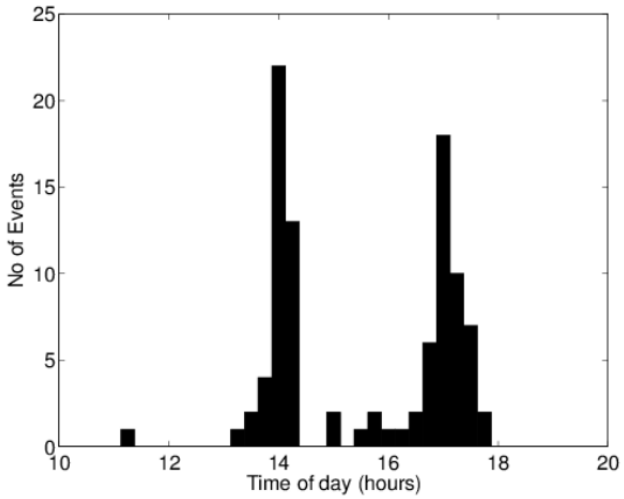

Figure 78 – Histogram showing the time of day (local time) when the most common type of noise spike occurs (this noise source always occurs in the mid- to late-afternoon)

Regional Events

A total of 4 triggers that were identified on the Aquistore network were characteristic of regional seismic events.

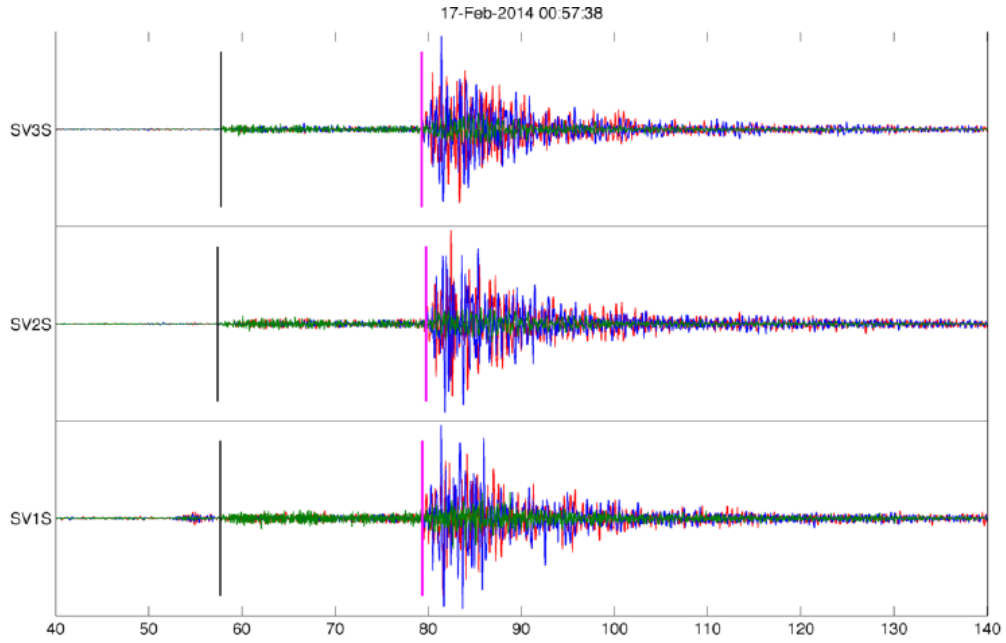

Figure 79 – Waveforms from a regional seismic event recorded on the Aquistore array

Arrivals from these events were also visible on data from the ANSS and GSN stations.

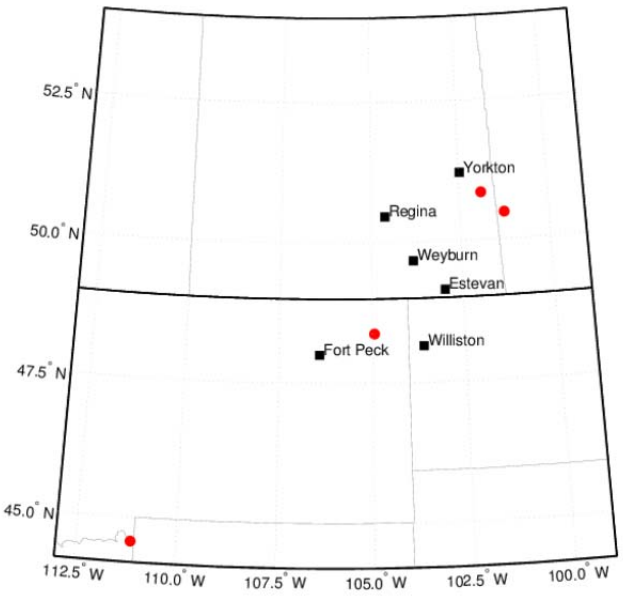

Figure 80 -- *Locations of regional events identified using the Aquistore broadband stations.*

In addition to the noise spikes described above, numerous other spikes were identified. However, none had the clear P- and S-wave arrivals that would be indicative of a local seismic earthquake. It was determined that these events are noise spikes from nearby industrial activity. As such no local earthquakes were detected during the monitoring period.

Summary

One year of monitoring data from Aquistore was analyzed. Numerous noise spikes were detected, the most likely source of which is industrial activity most notably associated with the Boundary Dam Power Station. Four distinct regional earthquakes were already present in catalogues held by the CNSN and SGS. No local seismic activity was detected in the area.

Task 5 – Installation of the Weyburn network

In order to directly investigate whether CO_2 injection was triggering low-magnitude seismicity at Weyburn, Outer Limits deployed 3 broadband seismometers over the field for the duration of approximately one year. The stations were deployed in August 2014, and retrieved in late July 2015.

Deployment

Gurlap 6TD instruments were used, which have a flat response between 30s (0.03Hz) to 100Hz. Each instrument was buried in a vault at a depth of approximately 50 – 80cm, which was then

back-filled with earth. The instruments were each powered with a 128Ahr battery, connected to a 50W solar PV panel, placed on an elevated stand (with the top at approximately 150cm) to ensure that snow did not cover it.

Figure 81 – Vault dug to 80 cm.

Figure 82 – Solar panel in deep snow in February 2015

The 3 sites for the seismometers were chosen with the assistance and agreement of local landowners. The deployment is focused on the Phase 1A area, which has seen CO_2 injection for the longest duration (since 2000).

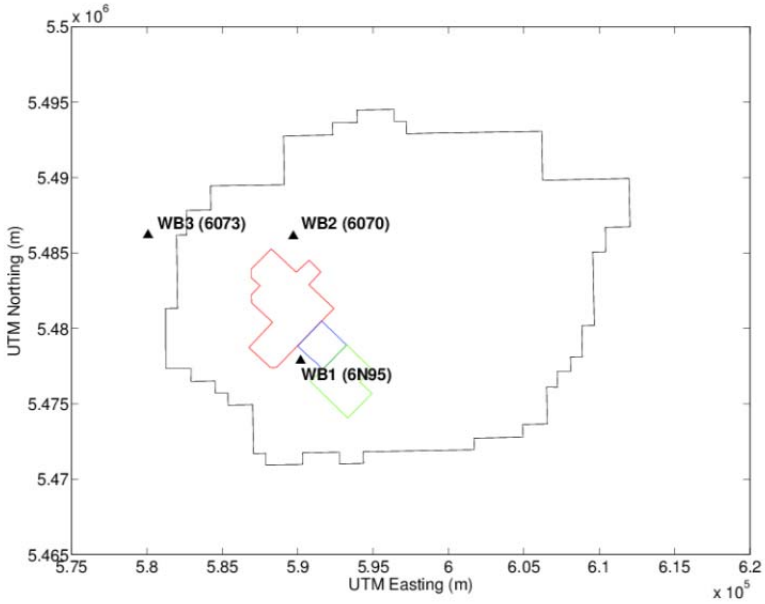

Figure 83 – *Seismometer locations relative to the Weyburn oilfield.*

Owing to a technical fault, station WB3 did not record data before 16/10/2014. The GPS signal for this station also failed on 29/04/2015. The GPS signal is used to ensure the internal digitizer clocks are accurate. Without GPS signals, the digitizer timings can drift. No obvious time drifts were observed, nevertheless the data from this station was treated with caution due to its earlier failure.

Data Processing

A total of 157 potential triggers were generated by the auto-picking algorithm. However, manual analysis showed that none had waveforms that would be indicative of a local earthquake.

This lack of events is expected, for a number of reasons:

- During the monitoring period neither the USGS NEIC nor the CNSN identify any earthquakes in the study region.
- Frohlich et al. (2015) have examined USArray data from the Williston Basin in North Dakota and Montana, finding very low rates of seismicity in the area, despite extensive hydraulic fracturing activity and waste-water injection. Geology does not respect the 49th Parallel, so low rates of seismicity should be expected at Weyburn.
- Statistical analyses of microseismicity recorded during CO_2 injection at Weyburn (see WP3) indicate a low seismogenic index and seismic efficiency, and therefore events with magnitudes larger than 0.0 are unlikely.

Figures 84 – All earthquakes occurring within 750km of the study area as catalogued by (a) the USGS NEIC and (b) the CNSN. No events are seen within any proximity to the study area.

Teleseismic Events

Several large teleseismic earthquakes occurred during the monitoring period, most notably the magnitude 7.8 Gorkha earthquake on 25th April 2015, Nepal, which caused a large amount of damage and received extensive publicity around the world. This was recorded on the monitoring array.

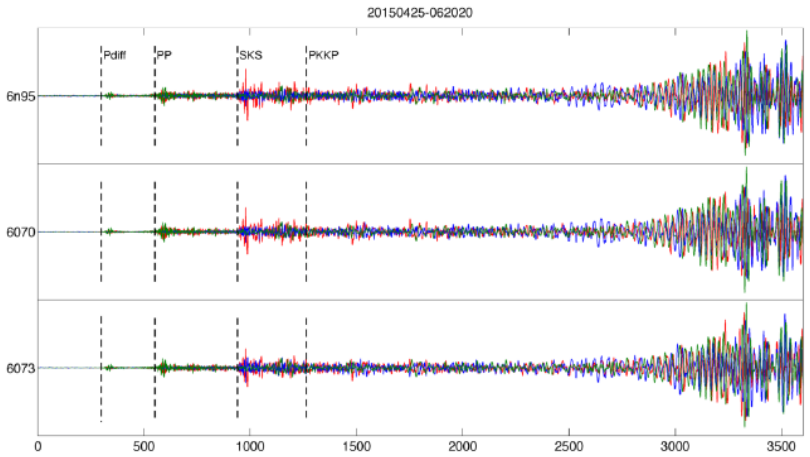

Figure 85 –Teleseismic phases recorded from the April 25th magnitude 7.8 Nepal earthquake.

Correlation: Seismic and Industrial Activity

Davis and Frohlich (1993) established how natural and induced events can be distinguished:

1. Events are first known earthquakes of this character?

2. Clear temporal correlation between injection and seismicity?
3. Earthquakes occur near injection wells?
4. Earthquakes occur at injection depths, or …
5. There are known geologic structures to channel flow?
6. Change in fluid pressure at the well and/or hypocentre is sufficient to induce an event?

In regards to the Weyburn-Midale Field, previous tasks have underscored the efforts made in compiling fluid injection/production and cataloguing seismic data from a variety of sources. However, only 4 events have been identified within the project area. These events occurred in 1968, 1976, 1976 and 1985, respectively. In the figure below, they are shown overlain on the cumulative fluid production-injection plot. This should not be used as a direct comparison, as injection data is from 2000 onwards, well after these events.

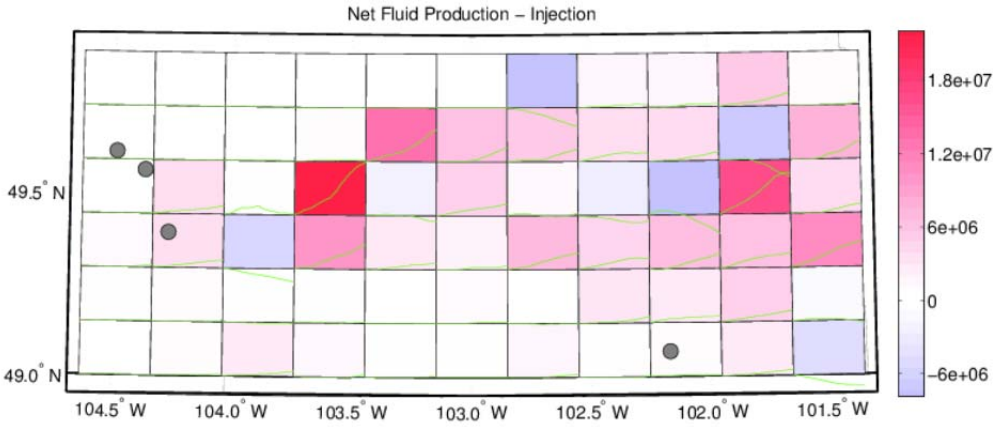

Figure 86 – Dots represent the only 4 events to have been detected at any time within the area of interest, overlain on the plot of spatial variation in net production – injection developed in Task 2. Injection volumes are from 2000 onwards, while these events occurred in 1968, 1976 and 1985.

However, given the large amount of oilfield activity in southeastern Saskatchewan since the 1950s and the very small number of events detected, it is reasonable to conclude that oilfield activities have not generated induced seismicity in this area.

Summary

One year of data from the three broadband stations deployed at the Weyburn Midale field was analyzed. The area is seismically quiet, with few noise spikes. No local seismic events were detected during the monitoring period. Indeed, the USGS and CNSN catalogues do not detect any events within 300km of the site during the monitoring period, and no regional events were

detected on the array. The only earthquakes picked up by the array were teleseismic arrivals from large, global events.

The microseismic analysis performed in Task 3 indicated that no events larger than magnitude 0.0 should be expected. Despite the large volumes of fluid injected and produced this area remains seismically inactive. Only 4 events have been detected in total, all occurring between 1960 to 1980. There is no correlation between oilfield activities and seismicity.

Task 6 – Geomechanical Assessment and Conclusions

Tasks 1 – 5 established that oilfield activities did not appear to have induced any seismicity in the project area, or southeastern Saskatchewan as a whole. Task 6 investigated the geomechanical conditions of the area and whether fluid injection could be expected to induce seismicity.

In-situ Stress Conditions

For industrial activities to trigger seismicity, pre-existing natural faults must be present in the subsurface, and the stresses on these faults must be sufficiently close to the critical stress such that a small increase induced by fluid production and/or injection is sufficient to trigger an event. Therefore knowledge of the present day stress conditions – both the orientation of the principal stress axes and their magnitudes – is very important. Stress data can be obtained via the World Stress Map (WSM) database (Heidbach et al., 2008). However, WSM data for the study region are sparse, with a single data point from a borehole breakout available.

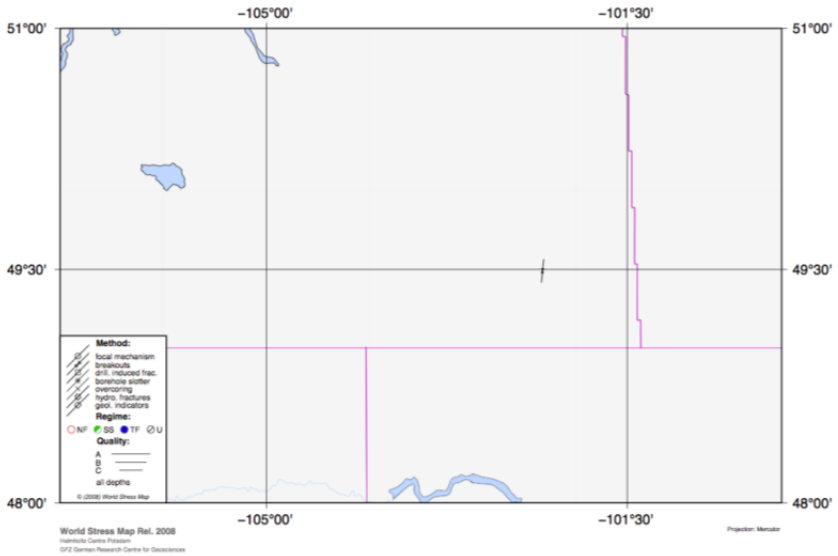

Figure 87 – World Stress Map data for South-Eastern Saskatchewan. A single data point from a borehole breakout is available

The globally-smoothed WSM (Heidbach et al., 2010) provides additional coverage for the area (Figure 88). These data indicate a principal horizontal stress orientation ranging from NNE to NE moving westwards across the region, with a mean of 29.

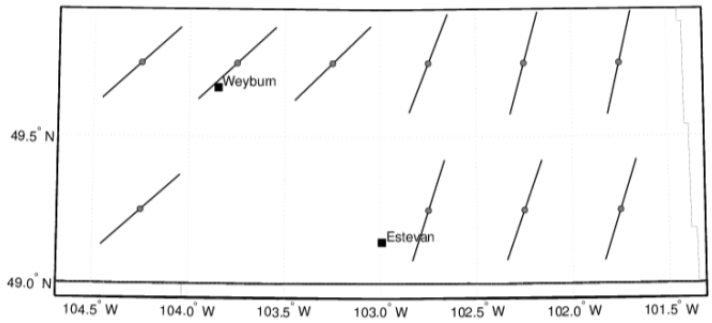

Figure 88 – Smoothed World Stress Map orientations for South-Eastern Saskatchewan (mapped on a 0.5° grid)

More detailed measurements of stress conditions are available from studies of the Weyburn oilfield (Jimenez Gomez, 2006). Based on prior studies of borehole breakouts, natural fractures and inelastic strain recovery tests (McLennan et al., 1986; McLellan et al., 1992) Jimenez Gomez (2006) reports a maximum horizontal stress azimuth of 40-50, a vertical stress gradient of 24kPa/m and a minimum horizontal stress gradient of 18kPa/m. Jimenez Gomez reports a maximum horizontal stress gradient of 28kPa/m, although this is not well constrained, and he suggests a more realistic value to be 26kPa/m.

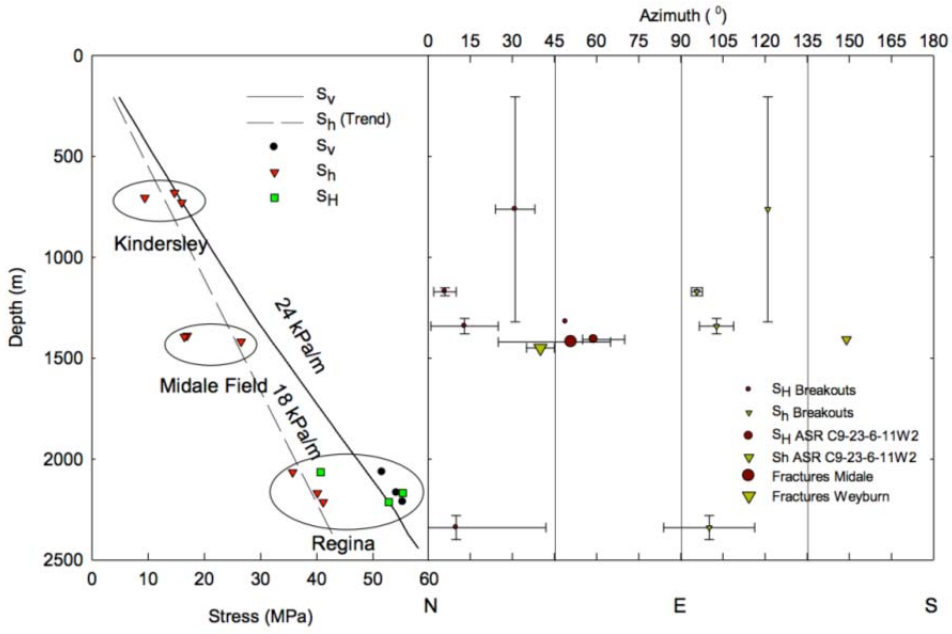

Figure 89 – In situ stress conditions at Weyburn, taken from Jimenez Gomez (2006). The left hand panel shows data used to constrain the vertical and minimum horizontal stress gradients, while the right hand panel shows the data used to constrain the orientation of the maximum horizontal stress.

Stress orientations can also be determined from measurements of seismic anisotropy, where the fast shear wave polarization is found to be parallel to the SH direction (Boness and Zoback, 2006). Using both shear wave splitting measurements made on microseismic data (Verdon et al., 2011) and controlled source AVOA observations (Duxbury et al., 2012), the anisotropic fast axis at Weyburn appears to be oriented at an azimuth of 45°, which is in agreement with the orientation reported by Jimenez Gomez (2006).

Potential for Fault Reactivation

Based on the above, we take the initial stress conditions at Weyburn to be: SH = 37MPa, Sh = 26MPa, SV =35MPa, with a principal stress azimuth of 45°. Hydrostatic pore pressure at these depths is 14.5MPa. We can resolve this stress tensor onto fault planes of arbitrary angle, computing normal stress, σn, and shear stress, τ, for all possible fault planes. Mohr-Coulomb theory states that a fault plane will reactivate if

$$\tau - \varphi\sigma n - C > 0,$$

where φ is the friction coefficient, and C is the cohesion. Faults are therefore most likely to be reactivated if they have strike and dip such that $\tau - \varphi\sigma n$ is maximized. In Figure 90 we plot $\tau - \varphi\sigma n$ as a function of fault-normal azimuth and inclination, noting that this analysis suggests that faults striking ENE-WSW and NNESSW are most likely to be re-activated.

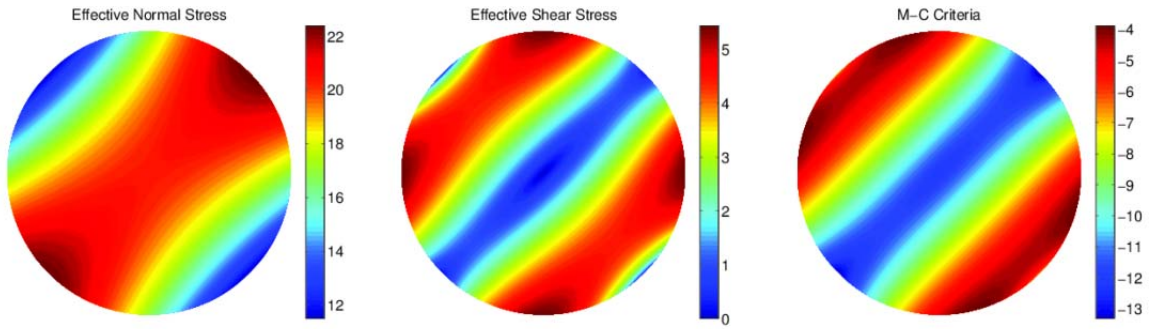

Figure 90 – Stereoplots showing (a) effective normal stresses, (b) shear stresses and (c) τ – ϕσn as a function of fault-normal (i.e. the line drawn perpendicular to the fault plane) azimuth and inclination. Faults will be prone to failure when τ – ϕσn is maximized. In this case, faults striking NNE and ENE will be most prone to failure.

No felt seismicity associated with fluid injection has been observed at Weyburn. It is worth examining whether pressure changes over the field's history are sufficient to exceed these Mohr-Coulomb criteria. In terms of the field history, the pore pressure has been maintained at close to hydrostatic by water injection. Even during the CO_2 injection period, while pore pressures have increased in some parts of the field, pressures have not exceeded the estimated 10MPa above hydrostatic that we estimate is required to re-activate faults, which is only

slightly below the pore pressure increase required to exceed the minimum horizontal effective stress and begin to hydraulically fracture the rock.

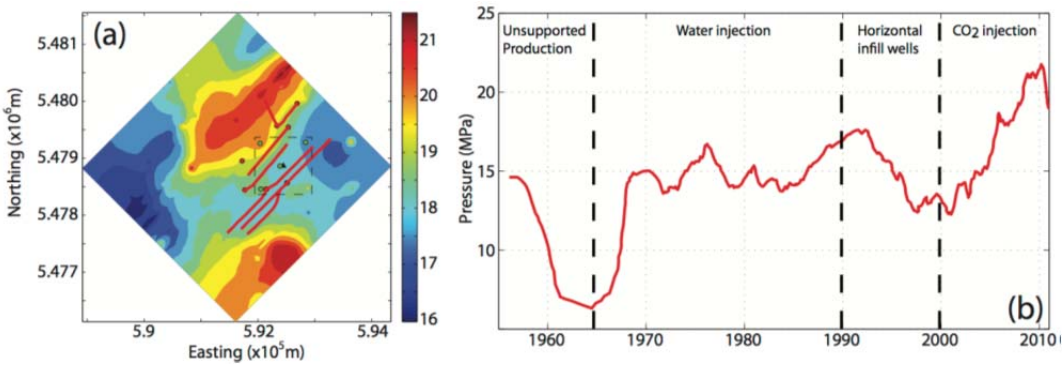

Figure 91 – A map of Weyburn reservoir pore pressures during CO_2 injection into the Phase IB area, and a history of pore pressures through the life of the field.

Summary Conclusions

In-situ conditions at the Weyburn-Midale Field were examined in relation to preexisting literature. These stress conditions were used to estimate the optimum orientation of a fault for it to be reactivated by injection. Faults that strike ENE-WSW and NNE-SSW will be most prone to failure, and that a pore pressure increase of 10MPa above hydrostatic would be required to re-activate such a fault. Pore pressures at Weyburn have not exceeded such values, which may account for the fact that no large, felt induced events have occurred in this area.

9.0 SaskCO_2USER (WMP Optional Phase) – Well Design

As CO_2-EOR advances, unique challenges face wellbores post-closure. SaskCO_2USER's wellbore design project focused on addressing challenges facing the full life-cycle of a CO_2-EOR well – whether vertical or horizontal – including well abandonment. Well design is critical to regulatory bodies, and this project looked beyond the constraints of existing regulations to develop optimal well design for CO_2-EOR.

Wells must be designed for optimal performance – from completion to production to abandonment. Managed by Bissett Consulting, the objectives of this wellbore project included: analyzing methods which provide an effective and reliable seal for CO_2 and other injected fluids; a basic drilling program which could be used as a model for future operators; cost estimates; options for future horizontal well designs; and completion and abandonment procedures, tools and materials. Operational and abandonment techniques focused on the challenges associated with CO_2 flooded reservoirs will reduce migration risks, along with re-entry and repair related-costs. This project aimed at helping future operators and regulators limit liability, mitigate risk, and constrain costs.

This project was unique among SaskCO_2USER in that it resulted in specific technical recommendations. While still a research project, this section of the project produced actual field recommendations, design, vendor and product options, and plans, as opposed to a lengthy technical research report.

9.1 Well Design – Approach and Methodology

The project provided results grounded in ten challenges-areas:

- Injection well design considerations and casing setting depth options;
- Surface and intermediate casing design;
- Completion design features (for increased injection and long-term abandonment reliability);
- Cementing operations (for improved displacement efficiency and annular seal reliability);
- Cement blends, intervals, volumes, and placement recommendations;
- Technical and directional well considerations (for improved long-term wellbore integrity);
- Well design (drilling and injection);
- Long-term abandonment (with or without mechanical plugs);
- Offset wells (surface and intermediate casing and completion type);
- Costing and estimates.

Results were summarized into four (4) high-level areas:

1. Well construction
2. Cementing
3. Well completion equipment
4. Abandonment

9.2 Well Design – Results and Recommendations

As this project was distinct and resulted in specific field recommendations, an overview of the project progress and overall plan is highlighted below. This summary provides insight into the efforts undertaken to produce clear, relevant, and field ready designs and recommendations for actual well design, drilling, and abandonment in a CO_2-EOR field.

The project began by gathering data and general design considerations. This involved locating and analyzing technical reference material, contacting drilling fluid companies to review current designs and initiating meetings with cementing companies to discuss alternatives for CO_2 compatible cements. Corrosion resistant alloys were investigated and evaluated vis-à-vis requirements, performance, and economic feasibility. Offset well data was gathered to ensure accurate and relevant information could be harvested to assist with well-designs. Well data was

gathered from sources such as GeoVista and AbaData with specific attention paid to CO_2 injector wells.

Barrier and element analysis was launched, and consideration of cementing methods was focused on reducing the risk of leakage pathways to surface. The investigation of drilling fluids then focused on minimizing formation damage to ensure proper protection, production, and maintaining gauge hole conditions for improved cement performance. Tubular suppliers were consulted and a review was launched to investigate optimum materials with respect to corrosion resistance and modified conventional low alloy materials for high-corrosion sections of the wellbore. This research and investigation was incorporated into well design and material changes on an ongoing basis with the final goal being a field ready, relevant, and costed design.

Cementing processes and issues became a central focus, in regards to both corrosion and for centralization options and suitability for in gauge, near gauge, and over-gauge wellbore sections. Cement was also considered vis-à-vis operational efficiencies with the goal of improving displacement efficiency and reducing channelling. As such, levels of excess cement requirements were reviewed with the objective of reducing risk of poor annular displacement within key lower sections of the well. Ongoing work continued to focus on barrier analysis. A risk assessment was performed on the highest risk elements, identified by severity and likelihood, with special regard to key leak path and corrosion concerns. An initial test protocol for CO_2 resistant cement was proposed to determine the suitability of fondue based formulations. Down-hole suppliers were identified and suitable and practical requirements for materials in tailpipe and packer assemblies were developed.

Throughout the process well design options were continually under investigation, as well as the quantity and placement of specialty equipment and materials. Casing size, weight, and connection requirements were continually investigated in both build sections of the well above and below the packer. Open hole well logs were reviewed with specific attention paid to evaluating caliper logs, to determine areas of hole enlargement, which would be critical to zonal isolation. Various surface casing setting depths in the Midale area were analyzed to establish a minimum depth for preventing contamination of potable water aquifers.

A directional drilling plan was developed which incorporated optimized downhole motor settings to match the expected build rate, in order to drill the smoothest curve possible prior to landing horizontal in the Midale zone. After the completion of the initial upgraded wellbore construction design Bissett prepared estimated additional costs involved with proposed design(s) compared to existing well design(s) and prepared a scoping cost estimate for recommend design. Final work focused on reviewing the range of injection pressures and estimated risk of fluid leakage with standard API connections and/or the use of semi-premium connections as a possible option for cost reduction. The project accomplished its objective and

produced recommended well designs and directional drilling plans, costed, and complete with vendor and material recommendations.

The summary findings of this project were divided into four key sections identified as critical to the construction and abandonment design for life-cycle wellbore integrity for CO_2-EOR:

1. Well construction
2. Cementing
3. Well Completion Equipment
4. Abandonment

These four areas are discussed below with recommendations and conclusions provided accordingly.

Task 1 – Well Construction

Although certain acceptable options exist in several well construction areas, general recommendations for the well configuration and downhole borehole and tubular sizing for the drilling phase include:

- setting 406.4 mm conductor to approximately 20 m
- drilling 311.2 mm surface hole and setting 244.5 mm surface casing to a minimum depth of 325 m
- setting deeper surface casing if high reservoir pressures are anticipated and/or if the potential of encountering the porous section of, or a connected fracture from, the injection zone is relatively high
- setting 59.53 kg/m 244.5 mm LTC surface casing, in either K55 or J55 grade
- drilling the 222.3 mm intermediate hole using a gel chemical or gel polymer mud system to the intermediate hole total depth, just above the permeable section of the Midale Beds
- setting 177.8 mm casing into the top of the Midale Formation at an inclination angle of slightly less than 90 degrees
- building angle at approximately 9.5°/30 m below the kickoff point (KOP)
- including a short tangent section (20 to 30 m in length), near the 50 degree inclination point of the build section
- setting approximately 20 m (two joints) of 38.69 kg/m corrosion-resistant alloy (CRA) intermediate casing in the tangent section of the build, using the same connections as selected for the L80 casing used in the remainder of the build section
- using higher collapse strength 177.8 mm intermediate casing (38.69 kg/m L80) with upgraded connections from the KOP near 1225 mKB to the intermediate casing point
- using 38.69 kg/m J55 or K55 LTC intermediate casing above the KOP to surface

- drilling 155.6 mm open hole to total horizontal well depth using a gel polymer mud system
- preparing for an open hole completion in the horizontal section

If necessary for cement seal integrity, it is recommended that an alternative (non-conventional) well configuration be considered, except in cases where the permeable section of the Midale zone is potentially highly over-pressured from nearby injection operations.

Where permissible, the alternative well configuration could include drilling below the target formation and then returning to a lower true vertical depth (TVD) in the Midale Beds before setting intermediate casing. If conditions are appropriate for a non-conventional horizontal well, a reverse section configuration to reduce horizontal displacement at the intermediate casing shoe may also be considered

Task 2 - Cementing

Cementing quality and displacement efficiency is of primary importance with respect to long-term wellbore integrity (Konogorov, 2012; Kutchko et al., 2012; McDonald et al., 2014; Zulqarnain, 2012). Cement job quality, particularly on the intermediate casing string involves a combination of number of considerations, including:

- cement volumes and types
- cementing operations
- casing string accessories and preparation

As previously highlighted, specific efforts were paid to cement, due to its critical relationship to wellbore integrity and risk mitigation for CO_2-EOR operators. The recommendations are summarized in the following sub-sections.

Cement Volumes and Types

Recommended cement volumes and types include:

- higher than normal excess volumes (in the range of 110% above open hole gauge annular volume) for the:
    - surface casing cement slurry
    - intermediate casing lead cement slurry, assuming a 222.3 mm intermediate hole size

CO_2-resistant cement should be a consideration (Choi et al., 2013; IEA Environmental Projects, 2008; Nygaard, 2010). Although not mandatory, using CO_2-resistant cement may provide additional resistance to long-term wellbore integrity:

- where cementing efficiency is not optimized

- when injected CO_2 is expected to flow past an exposed intermediate casing or abandonment cement sheath

A minimum of 60% excess cement for the intermediate casing tail cement slurry is also recommended. The replacement of a portion or all of the tail cement slurry with CO_2-resistant cement brings a higher degree of confidence to long-term wellbore integrity. Cement volumes for the tail slurry should not be reduced and effective cementing operations and casing centralization should be maintained.

Cement for open-hole abandonment operations should be of similar type and quality as that used for the intermediate casing tail cement slurry.

Open-hole abandonment cement is subject to similar environmental conditions as is the lower portion of the cement used for the intermediate casing. Corrosive mobile fluids may be present in the reservoir transverse to the direction of the horizontal hole and lower portion of the intermediate casing. Because of the potential for mobile fluids, both the intermediate tail cement and the horizontal abandonment cement may need to be upgraded in areas where injection fluids may reasonably be expected to pass across abandoned horizontal sections.

If CO_2-resistant cement is used in the lower portion of the intermediate casing, compatibility must be confirmed with conventional cement, and if not fully compatible, the entire intermediate casing string may require cement that is resistant to CO_2 attack. Incompatibility with conventional cement may result in dramatic changes in cement thickening times, therefore bringing unacceptable operational risks.

Cementing Operations

Effective cementing operations are dependent on a number of factors, including:

- proper conditioning of the wellbore and drilling fluids:
  - while conducting clean out trips
  - prior to running casing
  - prior to cementing casing
- use of an effective type and quantity of spacer fluid for surface
- and intermediate casing cementing
- casing movement, such as reciprocation and/or rotation, which is of primary importance to improve displacement efficiency
- cement rheology and fluid loss control, which affects the successful and efficient placement of cement
- mixing and particularly displacement rates, which should be optimized considering wellbore integrity as well as maximum practical annular velocities, for the intermediate casing string and for placement of open hole abandonment plugs

Because of the anticipated levels of uphole evaporitic formations (e.g., salt) the requirement for high displacement efficiency is more critical than normal in fields such as the Weyburn field. These types of formations may result in severe external corrosion that is not directly related to CO_2 injection operations. With respect to external salt corrosion attack, the importance of consistent and positive centralization is of particular importance. This is because exposure of the string to high levels of salt at any point may result in an external corrosion-based failure, which would limit the future usability of the well.

Casing String Accessories and Preparation

Centralizers are the main casing string accessories used to improve cementing quality, with specific recommendations as follows:

- Use stand-off bands or equivalent type of non-collapsing centralization tools to maintain stand-off under high side loads and to minimize risk of downhole centralization failure that could lead to annular packoffs, excessive drag or inability to run intermediate casing to bottom.
- Increase frequency (i.e., decrease spacing) of stand-off bands to two bands per casing joint over critical intervals below the KOP, such as:
  - over the lower portion of the intermediate casing that is below key seal formations above the injection zone
  - at least one per joint above key seal formations up to the KOP

In addition, specific cases of difficult standoff such as non-uniform wellbore geometry (which can result in high bending related side loads), may require more than two stand-off bands per joint.

- Use a relatively high frequency of high physical integrity centralizers immediately above the KOP and continuing to a depth of 800 m or shallower.
- Consider preparing the lower portion of casing with a surface treatment, such as sandblasting, to improve the cement bond to casing surface.

Task 3 – Well Completion Equipment

The recommended well completion equipment includes using CRA materials for tools in critical areas, particularly if the tools are difficult to replace on a periodic basis. Key well completion equipment and tools are summarized below.

Packer and Tailpipe Assembly

Recommendations for the packer and tailpipe assembly include a permanent packer:

- with, as a minimum, all surfaces that would be exposed to injected fluids made of full CRA material, such as Inconel 718, Incoloy, G3, or other similar alloys

- set in the lower portion of the +/- 20 m long, 177.8 mm CRA premium connection casing section, to allow stacking of a second packer if required
- with a sting in design, that includes two independent release points. This configuration would provide the ability to pull out the inside portion of the packer prior to abandonment to permit running at least 73.0 mm tubulars for abandonment cementing.

It is recommended that the tailpipe portion of the assembly have:

- 73.0 mm tailpipe pup joints, with full CRA material and premium connections
- two full CRA profile nipples
- a lower tailpipe nipple that includes a no-go profile with an integral re-entry sub to minimize tool costs and number of premium connections

Tubing String

It is recommended that the tubing string:

- have non-CRA materials for the entire tubing string assembly, with the exception of the on/off tool and a short CRA sacrificial pup joint to attach to the tubing hanger
- be 88.9 mm or 73.0 mm
- be internally coated and use modified couplings suitable for internal coating

Metal seal connections (often referred to as metal to metal seal connections) are recommended for the tubing string, because of a significantly lower chance of initiating a leak path as a result of differential injection pressures.

Metal to metal connections with flank (cone shaped) seals normally produce metal contact pressures several times higher than wellbore pressures and are typically resistant to leakage even when under conditions of bending and tension. However, EUE connections are acceptable if they are pressure tested periodically and if annular pressure monitoring is conducted.

Wellhead Equipment

As they are not directly exposed to the injection fluid stream, many of the components used in the wellhead do not need to be fabricated from corrosion-resistant alloys and may be built using API sour service Class DD, and in many cases EE materials in product specifications levels (PSL) 1 or 2 for specific components. However, materials that may be directly exposed to production and injection fluid streams should:

- provide a significant level of resistance to mixed acid gas corrosion
- retain integrity when exposed to H_2S

However, because the wellhead components are ultimately replaceable, materials with direct exposure to H_2S do not need to be made of, or clad with, CRA material, and other options, such as internal coating of H_2S resistant low alloy steel, can be considered.

Standard Material Major Wellhead Components

Major and miscellaneous wellhead components that are recommended to be of standard materials include the:

- casing head, casing slips and side outlet gate valves
- ring gaskets, studs, nuts, needle valve and pressure gauge tubing head and secondary pack-off
- flow cross, companion flanges and the wing valve above master valve

Components that May Require CRA Materials

Components for which CRA materials should be considered include:

- the tubing head adapter (bonnet) and master valve (CRA clad)
- the master valve, which should, as a minimum, use an Inconel 718 or equivalent valve stem
- the tubing hanger, which is recommended to have a full CRA body, although a non-CRA tubing hanger would be acceptable under certain conditions, such as when suitable non-coated injection tubing is used in conjunction with a plan to periodically pull and inspect the injection string. In this case, the tubing hanger body, seals and threads could also be periodically inspected before re-running the tubing hanger into the tubing spool.

Task 4 – Abandonment

Reliable long-term abandonment is of critical importance in the well design. For this reason, recommendations include:

- the entire open hole section be cemented, using a tubular reaching to the toe end of the well
- the open hole cement plug should extend well into the intermediate casing
- excess cement should be circulated out to just above the remaining packer element shell
- a mechanical barrier should be placed in the upper portion of the 177.8 mm CRA casing
- an extended cement plug is to be run above the mechanical barrier, at least up to the top of the Mannville Formation or higher, as required, to meet specific regulations
- casing cutoff caps are to be welded at surface

Summary Conclusions

The project successfully completed the design and costing of CO_2-EOR wells drilled or converted to injectors. This project highlighted key well design requirements, operational procedures and proper material selection, to construct wells in CO_2-EOR and storage reservoirs that have a high degree of wellbore integrity for all phases of the well's potential life cycle.

To achieve this goal, horizontal drilling techniques were reviewed and evaluated to establish procedures and bottom hole assembly configurations capable of drilling build sections with minimized dog leg severities to enable efficient placement of cement and to reduce risk of leakage in casing string connections.

Operational procedures to maximize fluid containment reliability within the injection zone, including tubular connection selection options were developed, and options for future horizontal well designs and investigate techniques of minimizing potential risk of losing seal against sour CO_2 laden fluids were built.

The basic drilling program built can be used as a model for incorporating the selected well design for production/CO_2 injection, and long term effective abandonment. Corrosion resistant performance properties were examined for several levels of CRA materials and material grade levels for key wellbore components including casing in vicinity of packer, packer, tailpipe, tubing and wellhead. IN addition, various alternatives for cement blend compositions, particularly those adjacent to and immediately above the potential injection zone were reviewed. A system failure tree was developed to identify potential areas of loss of fluid containment or long term corrosion based impacts, including a review of fluid containment barrier redundancy.

The completion design and procedure as well as a recommended tool configuration, including CRA material requirements, can be used for CO_2 injection and facilitates removal prior to final abandonment of the openhole and cased hole intervals of the well. Wellbore design features were incorporated which addressed the containment of high pressure CO_2 injected fluids for extended periods and which maintain wellbore integrity for long term abandonment. Estimated additional costs involved with the proposed design(s) were compared to existing well design(s) a scoping cost estimate for recommended design was prepared.

10.0 SaskCO_2USER (WMP Optional Phase) – Minimum Data-Sets

As not all information is relevant to all types of risk assessment, it is critical to identify data that are important to identification of post-EOR CO_2 migration pathways. The Minimum Dataset Requirements (MDR) attempted to define the level of detail at which data are sufficient to enable representative modeling of potential CO_2 migration/leakage, and yet are not excessively onerous in terms of compilation and analysis requirements.

During the course of this project, the existing WMP reservoir model was translated from Eclipse 300 CMG GEM.

Several strategies exist for data reduction. The first is based on geologic model simplification, which typically involves upscaling a fine-resolution geological model for flow modeling. Such an approach has been adopted in single-pattern simulations and 75-pattern simulations for

Weyburn Field, in which the goal was to reproduce important features of the fine-scale model (Hitchon, 2012). At Weyburn, Zhou et al. (2004) used a "unit cell" approach to assess potential leakage, in which a "unit cell" model consists of a single well and a portion of the reservoir and its size is equal to the average well spacing (240 m) derived from UTM coordinates of all the existing wells in the focused area. The second is based on dimension reduction or reduced-order modeling techniques, in which high-dimensional physical parameters are projected onto low-dimensional parameter spaces to alleviate computational demand of risk assessment. A third approach is based on decomposition, in which the original problem is divided into a set of sub-problems of smaller scale.

For this project, Texas BEG tackled the MDR requirements by adopting a facies clustering approach (Shenawi et al., 2007; Roy and Marfurt, 2011; Li and Geng, 2014; Chilès and Delfiner, 2012) during which the "data worth" of various static datasets available to us was assessed. A total of 8 then 17 facies, not necessarily continuous, were identified from petrophysical properties using pattern recognition and geostatistical techniques. Petrophysical properties (3D-anisotropic permeability, porosity, and rock density) that are most critical for reconstructing the facies patterns are retained in the minimum data sets. Conversely, data that are less important for reconstructing the facies patterns, such as matrix density, water and oil saturation, are removed. A pressure sensitivity study was then conducted to identify zones that are most influential to pressure perturbations, which are suitable for pressure-based monitoring.

10.1 Minimum Data Sets – Approach and Methodology

The project objective was to develop an applicable workflow for leakage detection of CO_2 geological storage during post CO_2-EOR storage with the objective of having the most economical data acquisition investment.

The methodology chosen deployed a systematic approach to determine the minimum data set is presented with an integrated reservoir modeling workflow for post CO_2-EOR stage, from the 3D seismic data, geologic data, well log and core data, and field flowing history data collected during CO_2-EOR period. The minimum data set considers the minimum petrophysical data types as well as maximum vertical and lateral separations of the monitoring wells and temporal sampling intervals. Reservoir pressure evolution patterns are simulated with numeric reservoir modeling so that CO_2 leakage areas are predicted.

To identify the most critical data from the entire reservoir data repository, one approach is to characterize formation property values into geologically and petrophysically distinguishable facies-based units at acceptable resolution compatible with risk-informing requirements. Another approach is to find the spatial areas most sensitive to fluid and pressure changes.

When CO_2 saturation reaches a level so that the local pressure exceeds the formation's fracture thresholds, CO_2 leakage might occur through generated fractures. To reduce data sampling rate, monitoring wells could be placed primarily at areas most sensitive to CO_2 composition changes or with low formation fracture pressures (that is, not accepting very high pressure).

The facies-based approach mainly uses static properties, while the latter (pressure sensitivity) utilizes both static and dynamic ones. The two approaches are complementary, both serving to reduce the data volume while maintaining the characteristics pertinent to CO_2 distribution and migration and were utilized by this project.

Facies-based unit supervised classification and parameter random field generation

There have been efforts from petroleum geologists and hydrogeologists to define petrophysical-geological rock units by the capacity of "storage containers" and "flowing conduits" (Langston and Chin, 1968; Ebanks, 1987; Rincones et al., 2000). The traditional practice of reservoir zonation uses geophysical measured data (Amaefule et al., 1993; Cao et al., 2005; Farzadi, 2006; Roy and Marfurt, 2011; Marroquín, 2014) and derived petrophysical properties (Carle and Fogg, 1997; Soto et al., 2001; Shenawi et al., 2007; Sun et al., 2008). The candidate geophysical measured data in facies classification include 3-D seismic data, gamma-ray log, density and neutron logs, sonic log, resistivity log, mud log, formation tester log pressure, fluid sampling data, etc. The candidate petrophysical properties include lithology, shale content, permeability, porosity, irreducible and total water saturation, movable hydrocarbon, relative permeability, anisotropic velocity, etc. from well log or core data. Geophysical measured data or petrophysical properties compose the parameter data space for facies identification. In the traditional way, facies identified from well log, core data, or derived petrophysical properties have high resolution on the vertical unit recognition thanks to the advanced logging techniques, but lacks in representing reservoir heterogeneity in the lateral direction due to an insufficient number of wells drilled laterally.

The facies-based units from supervised automatic pattern recognition proposed in our research have the properties: (1) they are divided based on storage capacity and flowing properties; (2) the "units" may contain one or more geological facies based on the similarities in petrophysical properties and geological continuity, and also may have multiple units within one geologic facies based on the internal difference in the parameter space; (3) the facies-based units are identified from well log or core data, so the dimension of the units are determined by the well spacings, i.e. if the well spacings are smaller, the units could become smaller, and vice versa. The "units" are different from the stratigraphic facies labeled by geologists. They are identified from similarity in parameter data space is a structured upscaling of geologic and petrophysical models, analog to the principal component analysis (PCA) in machine learning (Carle and Fogg, 1997; Roy and Marfurt, 2011; Ferraretti et al, 2011; Sartore, 2013). The "units" are spatially

clustered and might occur repeatedly over a spatial distance (Carle and Fogg, 1997; Li and Geng, 2014), calculated as categorical random variable in 3D space that satisfies Markov property. The classification accuracy turns out to be greatly improved if the geological facies information is available.

The facies-based approach was adopted for this data reduction project because:

- Only petrophysical properties that are from most routine well log measurements and most pertinent to CO_2 storage and migration are selected for facies definition. Other measurements are ignored in the calculation
- Transition probability matrix between the facies in the 3D geospace is calculated, so the facies classifications at un-sampled sites are assessed. The petrophysical properties at un-sampled sites are estimated from the properties of the facies the sites belong to.
- Monitoring wells are only set up in the facies most sensitive to CO_2 migration, and only the most sensitive petrophysical data are measured with well logging or coring.

The project started with the information available from well logs and core data, petrophysical properties, and 3D seismic data. The grid for the target volume for CO_2 leakage detection was then established. The rock types, water and oil composition and saturation, as well as initial reservoir pressure and temperature were established for the baseline of reservoir simulation. The workflow can be summarized as:

1. Selected petrophysical properties (anisotropic permeability, density, and porosity) most critical to CO_2 migration from available properties interpreted from well data and stratigraphic layer definition.
2. Implemented facies-based unit supervised classification from selected petrophysical properties, 3D seismic data and stratigraphic layer definition.
3. Calculated transiogram for facies-based units in the horizontal and vertical directions, and obtained unit definition in the target grid system.
4. Calculated anisotropic permeability and porosity in the target grid system, which is stochastic generated from values characteristic of each facies, and conditioned by the sampled well data.
5. Implemented CO_2-EOR and post-CO_2 injection with generated porosity and permeability in Step 4, and obtained pressure distribution. If at a certain simulation time, the pressure has exceeded CO_2 leakage threshold specified by requirements, CO_2 leakage is predicted at that time.
6. Reduced sampling data gradually, and iterate step 2 to 5 to obtain pressure changes.

To be successful - if the pressure change is less than 5%, the reduced dataset is accepted, and further sampling reduction continues, otherwise, the minimum data requirement is achieved.

10.2 Minimum Data Sets – Results and Recommendations

Task 1 - *Select parameter data types most critical to CO_2 storage and migration*

The available geophysical measured data and petrophysical data in the zones of interest in the WMP domain comprised the parameter data space for facies-based unit classification. The inter-dependence between the data types and their impacts to the capacity of CO_2 storage and leakage were analyzed and redundancies reduced.

Data parameters were reduced initially to well log and/or core porosity, anisotropic permeability, and density measurements. 3D seismic amplitude data was then incorporated. The pattern must honour the stratigraphic facies vertically, yet contain smaller areas laterally. The facies-based units were automatically identified using supervised classification toolboxes "caret" (Kuhn, 2015) and "NbClust" (Charrad et al., 2015) that are available in the R statistical computing platform.

The CMG-GEM simulated post-EOR CO_2 injection scenarios from the reservoir conditions at the end of CO_2-EOR in 2033 (Wilson and Monea, 2004), using the generated porosity and permeability from the advanced package spMC (Sartore, 2014) available in R platform. The risk itself is produced when the probability of CO_2 leakage is over a certain level where the simulated pressure exceeds the formation fracture pressure thresholds. Conditioned well log or core data are gradually reduced spatially until that the simulated pressure field differ over a certain margin, which defines the minimum data set.

Distributions of porosity, permeability, and water saturation for each of the 8 facies were plotted to assess the various differentiation capacities of each data type for dataset 1.

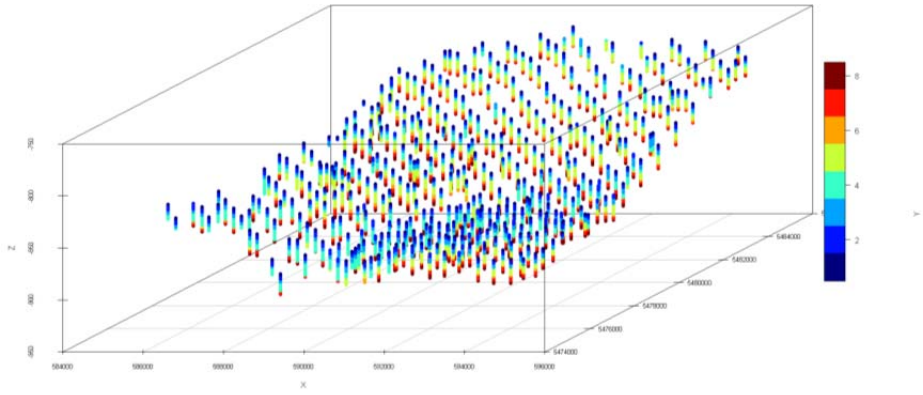

Figure 92 – Stratigraphic facies of each well in dataset 1

In these figures it is evident that that permeability has the richest variability over the facies among all parameters. Water saturation distributions overlap for most of the facies, they are only able to differentiate the Marly and Vuggy formations in WMP, and are not helpful in classifying the sub units. Oil saturation distributions vary among stratigraphic facies and are more effective in discriminating units.

The distributions of 8 data types (anisotropic permeability, porosity, water and oil saturation, bulk density, and matrix density) on 5 stratigraphic facies were considered and plotted.

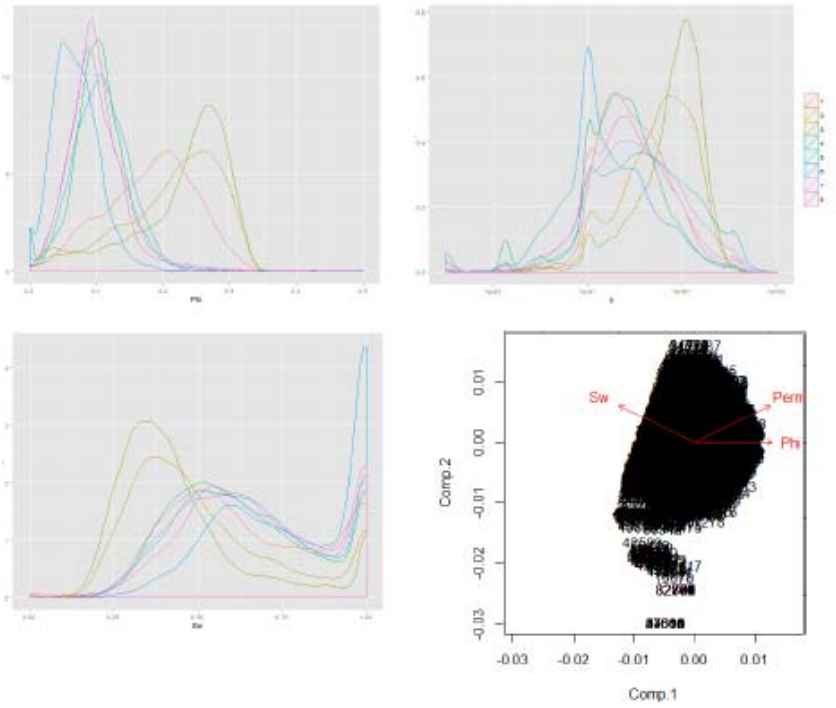

Figure 93 – Parameter separation and independence analysis for dataset 1

Note the upper-left, upper-right, and lower-left plots which give the distribution of porosity, permeability, and water saturation respectively for the 8 facies (From 1 to 8 are: M0, M1, M3, V1, V2, V3, V4, and V6). The lower-right plot is projecting the parameters to the PCA first 2 components (Comp.1 and Comp.2) space. The X and Y axis are the scores of the two first PCA components. The red arrows indicate the contributions of each data type to the PCA components. The black numbers represent the index of the data points.

For each parameter, the more variations there are between different facies, the easier to separate facies. Water saturation distributions overlap for most of the facies, they are only able to differentiate the Marly and Vuggy formations in WMP, and are not helpful in classifying the sub units.

Task 2 - *Implement facies-based unit supervised classification*

With the input data parameters determined in Step 1, NbClust (Charrad et al, 2015) was used to determine the optimal number of clusters and clustering scheme. All combinations of desired numbers of clusters, distance measures between clusters, and 30 indices were calculated for measuring the clustering performance and compared, so that the number of clusters proposed by the majority of indices is chosen.

For dataset 1, the classification was implemented in the Marly zone (M0, M1, M3), Upper Vuggy zone (V1), and Lower Vuggy zone (V2-V6) separately, each using permeability, porosity, and the stratigraphic facies indicator. The figure below shows the clustering results for the Marly zone. The number of clusters attempted varied from 3 to 7 for all the indices in NbClust. According to the majority rule, 4 is the preferred number of classes in the Marly. Similarly, the Marly zone, the Upper Vuggy zone, and the Lower Vuggy zone are divided into 4, 3, and 5 facies-based units respectively.

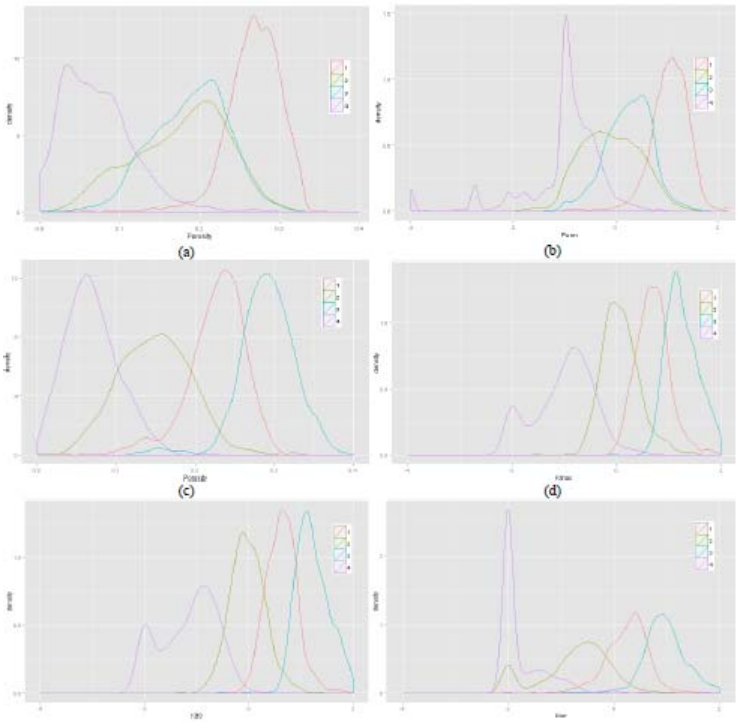

Figure 94 – Classification results on Marly zone – porosity and permeability distributions are shown, obtained from K-means clustering in dataset 1 and dataset 2 respectively

Pattern classification using additional 3D seismic data

The lateral distances between wells can be from tens to hundreds of meters, which constrain the lateral resolution of the facies-based unit. The vertical resolution of available seismic amplitude data is 1 meter higher than the decimeter scale of well log or core data. The lateral resolution of the seismic data varies from several meters to 40 meters. Incorporation of seismic data in the classification process benefits from lateral classification, but not in vertical direction.

Subsequently, the area was clustered into 15 facies-based units, as shown below in Figure 95. The lateral resolution has been reduced to 640 m, but averaged vertical resolution becomes 1.57 m.

Accordingly, the seismic data was preprocessed. While all parameters are normalized to be zero-centered and unity deviated, a multiplier of 0.2 is applied to the normalized seismic data before going into clustering. The results are 17 facies-based units from the parameter distributions of porosity, anisotropic permeability, bulk density, and seismic amplitude.

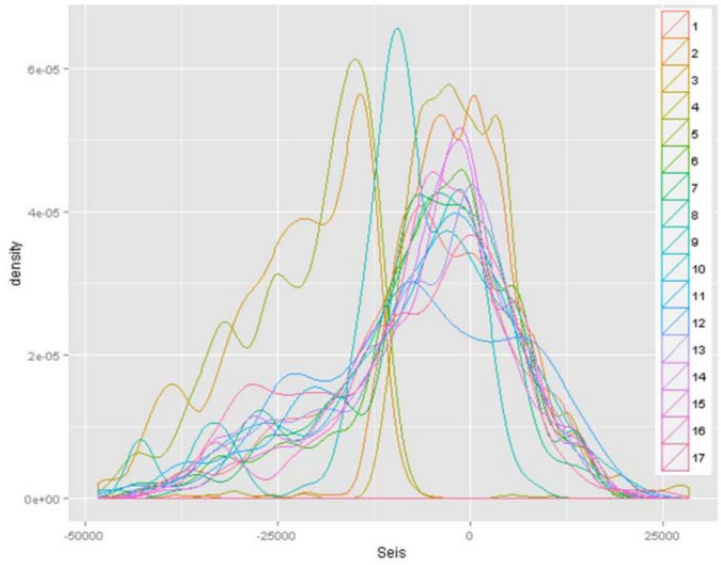

Figure 95 – Seismic amplitude data distribution for the 17 facies-based units

Task 3 - Calculate transition probability matrix

After the “units” were identified with the characteristic distributions of the data parameters (porosity, permeability, and bulk density) determined, the quantitative spatial transition patterns, i.e., the transition probability matrix of the facies-based units for all directions were calculated using the advanced package spMC (Sartore, 2014).

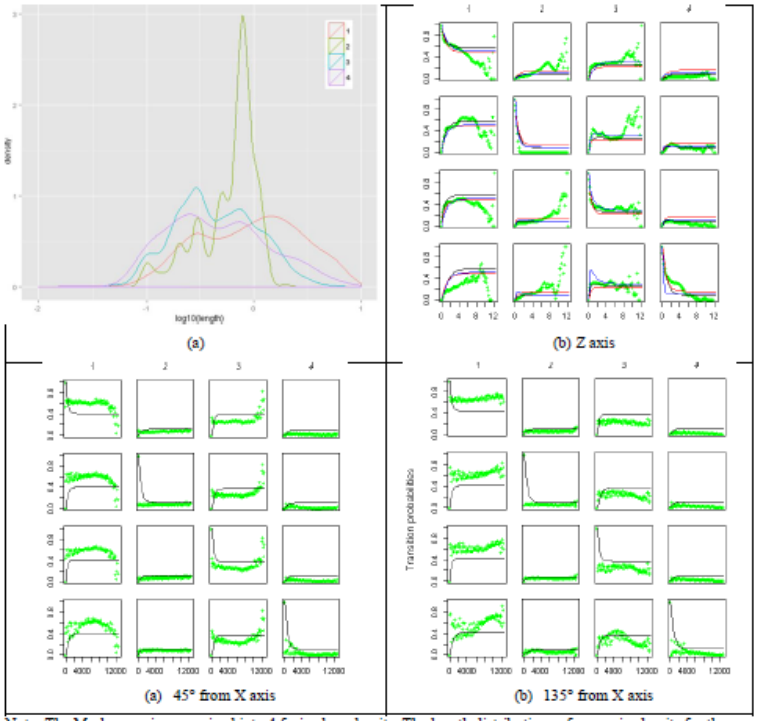

Figure 96 – Length distributions and transiograms for the Marly zone

The Marly zone was recognized into 4 facies-based units. The length distributions of recognized units for the units in vertical direction are shown in (a). Transition probabilities are plotted in vertical direction (b), 45 from X-axis (c) and 135 from X axis (d). X-axis is the lags in meter. Y-axis is the transition probabilities from one unit type to another. Empirical transiograms are in green points, and the calculated models are in lines. In (b), models from mean length method (black), maximum likelihood method (red), and iterated least square method (blue) were plotted in comparison to demonstrate that mean length method provides best matching with the empirical transiograms. In (c) and (d), only mean length method modeling results are shown (black).

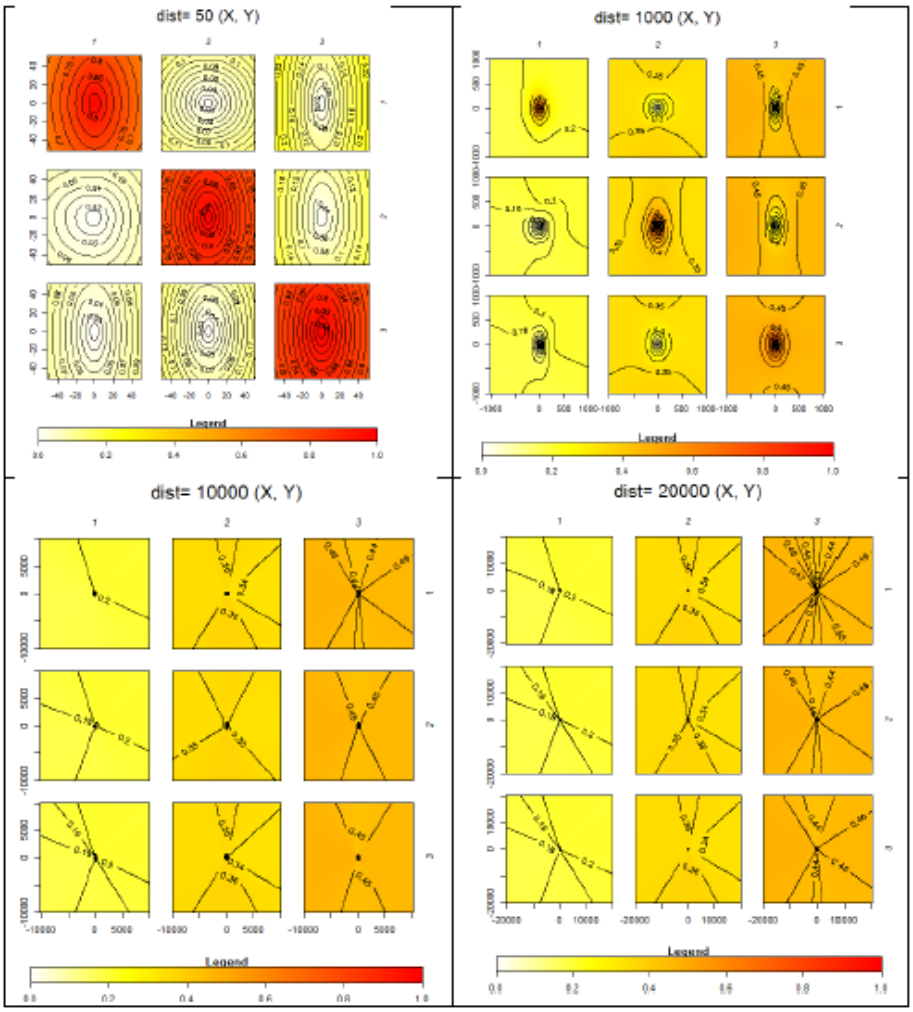

Figure 97 – Transition probability maps in the S-Y plane with varying smallest lag distance settings for the Upper Vuggy Zone

As shown above, the multidimensional theoretical transiograms in X-Y plane was calculated from interpolation via mean length method. The smallest lag distances are 50 m (upper left), 1000 m (upper right), 10,000 m (lower left), and 20,000 m (lower right). The color of each point in the graphic represents the probability level.

The 3D transition rate matrix were interpolated from 1D matrixes along vertical and 4 horizontal directions that are 45° separated. Transiogram models were attempted by deploying a mean length method, maximum entropy method (Bogaert, 2002), and iterated least square method for comparison. The simple mean length method gave the best match with the empirical transiograms and was used in this modeling. The smallest lag distance is an important parameter in the successful modeling. Different least lag distances are exercised to observe the best results (see previous figure). The smallest lag was set at 0.15 m in vertical direction and 70

m in the lateral directions, both a little bigger than the data point separation in respective directions. Similarly, a 3D transition probability matrix for a total 12 units in the phase 1A area were calculated for Task 4.

		Vol%	Mean length (V)	Mean length (H)	Perm	Kmax	K90	Kver	Rhob	Porosity
unit #			(m)	(m)	(md)	(md)	(md)	(md)	(kg/m^3)	
1	Marly	3.00	0.85	762.79	0.10	0.10	0.07	0.02	2357.78	0.07
2		2.81	0.79	719.27	0.82	1.24	0.95	0.19	2540.68	0.18
3		9.79	0.70	730.92	1.80	5.05	4.30	1.75	2153.88	0.19
4		16.52	1.58	751.91	11.49	21.22	18.49	9.64	1982.84	0.27
1	Upper Vuggy	1.10	0.55	714.55	1.01	5.56	2.59	1.04	2455.93	0.02
2		2.83	2.00	744.85	6.06	30.00	19.55	7.77	2307.72	0.17
3		15.06	0.76	698.95	0.47	0.31	0.17	0.05	2596.25	0.10
1	Lower Vuggy	8.95	1.36	867.27	11.12	11.45	8.73	4.76	2030.27	0.14
2		13.57	1.07	883.73	0.74	0.55	0.35	0.08	2540.75	0.09
3		7.16	1.31	888.27	0.07	0.05	0.05	0.01	2460.17	0.05
4		12.09	1.29	890.86	0.47	1.92	1.60	0.61	2263.78	0.09
5		7.13	0.99	857.66	5.41	1.81	1.42	0.73	2335.07	0.13

Table 41 – Spatial and numerical statistics of recognized facies-based units

After the transition rate matrixes were evaluated, the facies random field across the target phase 1A simulation grid area was simulated through indicator kriging, which approximates the conditional probabilities by considering the twelve nearest neighbors for all points in the simulation grid (Sartore, 2014).

The facies definition in the target area is plotted below. The resulting mean formation thicknesses of each facies-based unit varied from a fractional meter to 13.3 meters, averaged at 1.1m, and laterally spanned an averaged 820 m.

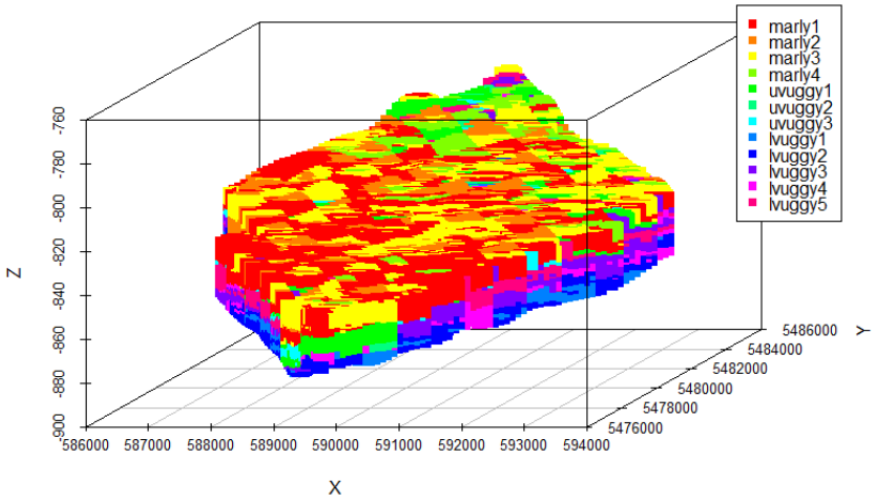

Figure 98 – Facies-based unit classification with porosity, permeability, and bulk density (17 facies)

In Figure 99 the upper plot illustrates simulation results with all normalized parameters while the lower illustrates simulation results with the seismic data reprocessed.

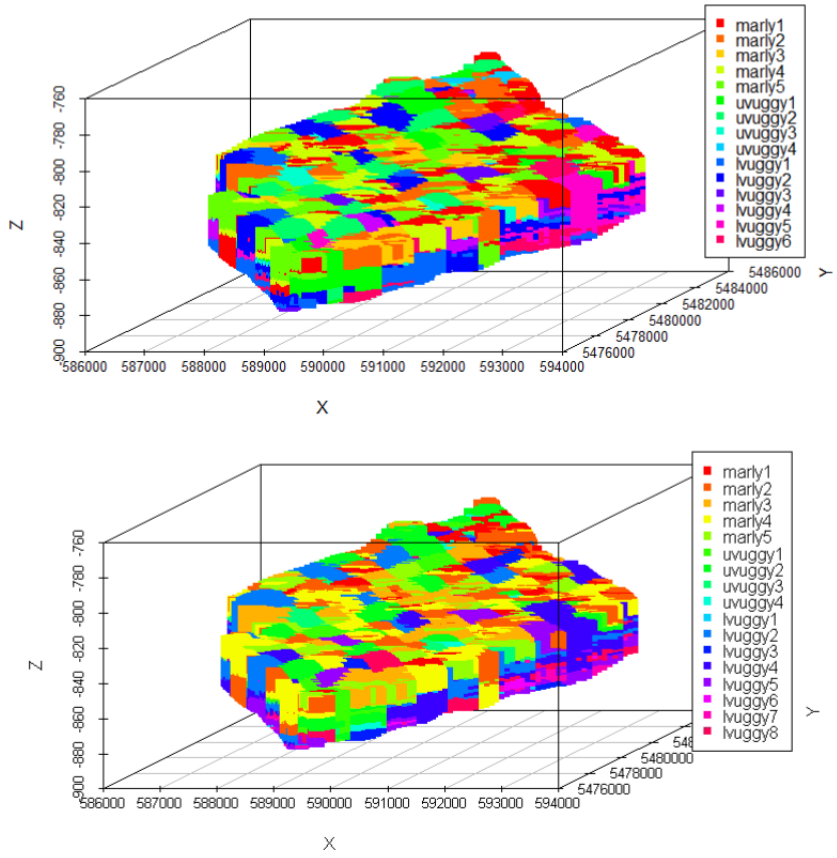

Figure 99 – Facies-based unit classification with porosity, permeability, bulk density, and seismic data

Task 4 - Generate porosity and permeability probability distribution from recognized facies and conditioning well log data

The porosity and permeability crossplots were drawn and relations derived for each recognized pattern. The probability distributions of porosity and permeability were generated using continuous lag Markov Chains with the spatial categorical random patterns (Weissmann and Fogg, 1999; Srinivasan and Sen, 2011) using spMC. The generated porosity and permeability probability distribution covered the phase 1A area, using the conditioning data provided by well log and/or core data. The figures below illustrate the porosity and permeability probability distribution for recognized facies.

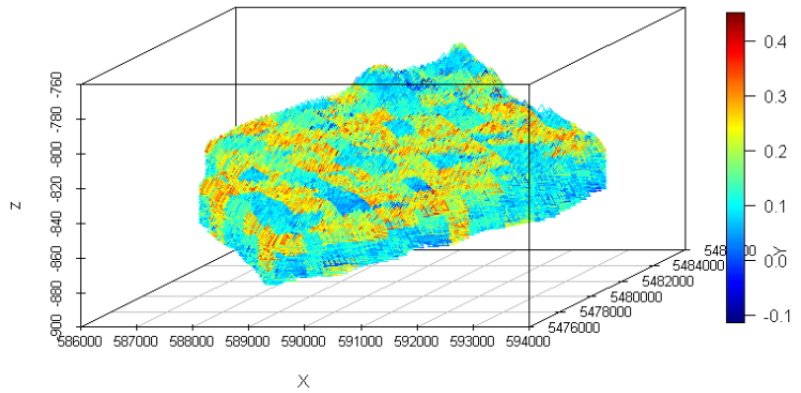

Figure 100 – Indicator simulated porosity with random field distribution

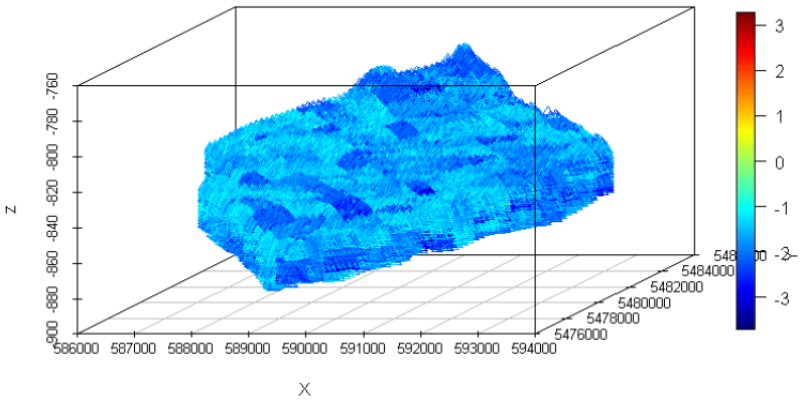

Figure 101 – Permeability value distribution for the identified facies-based units (md)

Task 5 - *Iterate and reduce conditioning data*

The reservoir conditions at the end of CO_2-EOR were obtained, with average of reservoir pressure established at 29.201 MPa, of oil saturation at 28.6%, and of gas saturation at 14.0%.

Pressure sensitivity analysis

Based on the GEM model inputs, the porosity values were increased by 0.1%, 0.2%, and 0.3%, and anisotropic permeability was increased by 1%, 5%, and 10%, and the numerical simulation was implemented for the CO_2 injection scenarios (2034 to 2055).

The resulting pressure fields were compared with the one from original porosity and permeability inputs, and the gradients of pressure versus porosity and permeability were calculated. The places with highest pressure gradients are areas the most sensitive to porosity and permeability changes, and coincide with the dense well log data areas suggested from the first approach with pattern recognition by 41%.

Based on the GEM model inputs, the porosities were increased by 0.1%, 0.2%, and 0.3%, and anisotropic permeability increased by 1%, 5%, and 10%, and the CMG-GEM simulation implemented for the CO_2 injection scenarios. The resulting pressure fields were then compared with the one from original porosity and permeability inputs, and the gradients of pressure versus porosity and permeability calculated.

The places with highest gradients are sensitive areas to porosity and permeability, and coincide with the dense well log data areas suggested from first approach with pattern recognition by 41%. There are 141*280*27 grids, among which 77768 cells were valid and analyzed.

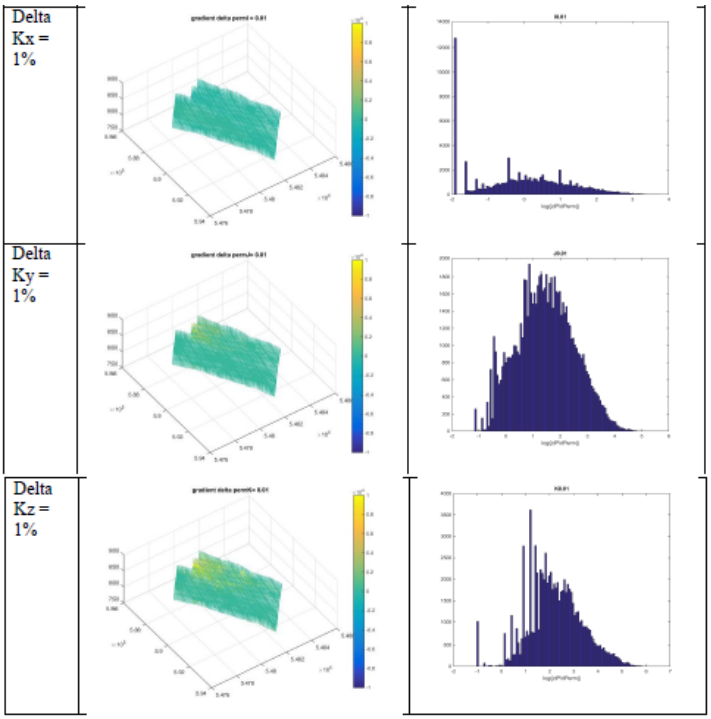

Figure 102 – Pressure sensitivity to permeability of 1%

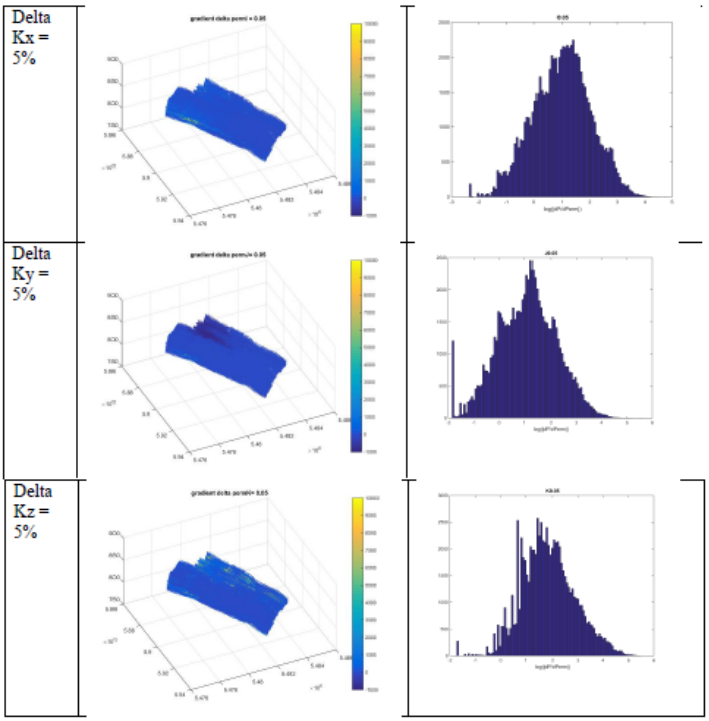

Figure 103 – Pressure sensitivity to permeability of 5%

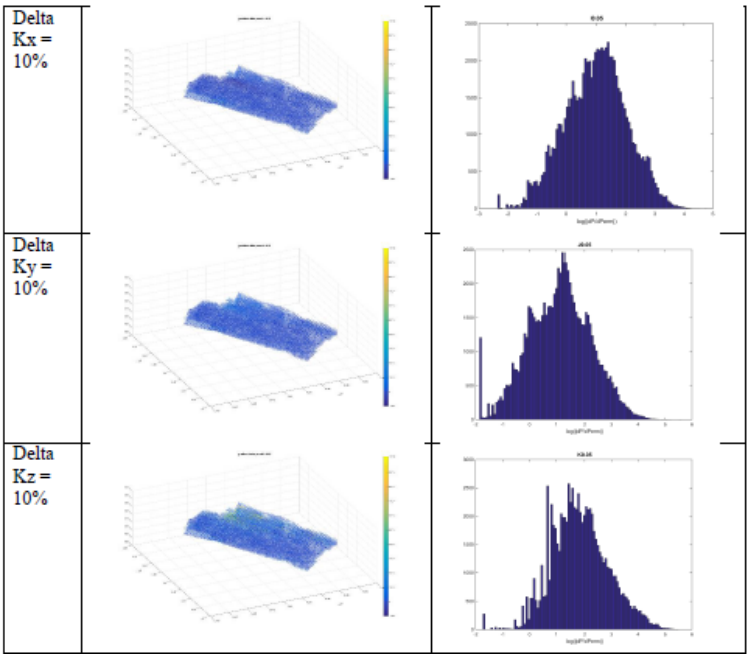

Figure 104 – Pressure sensitivity to permeability of 10%

Reservoir Sensitivity to porosity

The reservoir simulation for the phase 1A area is very sensitive to porosity. Under the same reservoir conditions and production constraints in the EOR process, an increment of 0.3% meant the simulation would fail, as compared to 10% in permeability sensitivity analysis.

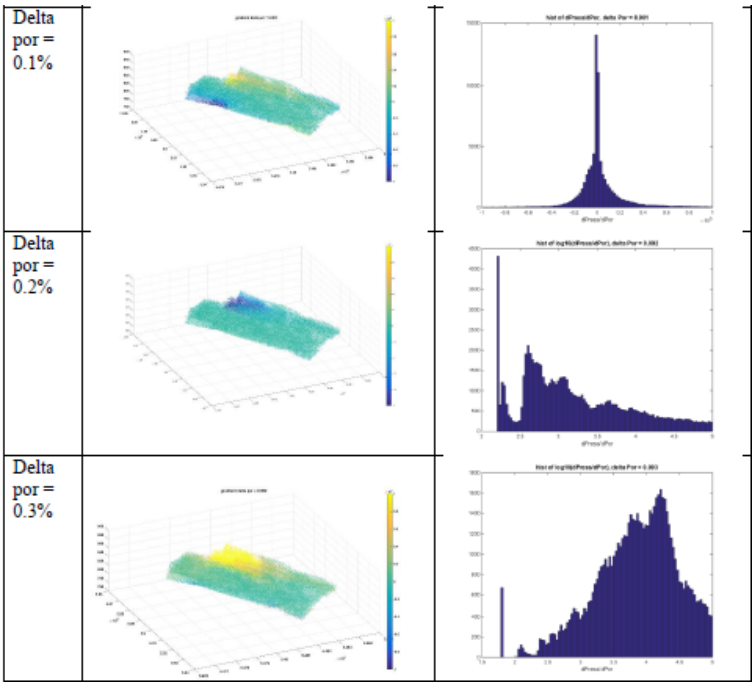

Figure 105 - Pressure sensitivity to porosity

Minimum Data Requirements Summary

Based on the research and demonstrations above, the minimum parameter set to model the reservoir flow system, predict storage capacity and monitor CO_2 migration that meets a certain level of risk assessment includes:

- The types of formation petrophysical properties that are most sensitive to the CO_2 geological storage prediction and migration monitoring,
- A large spatial range of data acquisition that captures the potential CO_2 migration range, which is normally larger than the storage complex,
- The smallest spatial resolution of sampling measurements, determined from local geologic and petrophysical heterogeneity and anisotropy,
- The smallest temporal span of data acquisition for the purpose of reservoir monitoring.

In this research, following the work steps in the automatic pattern recognition approach, were noted:

- The minimized petrophysical properties should be reduced to include porosity, anisotropic permeability, and bulk density.
- The data beyond the storage complex was not explored in this research. The research area focused on the Marly, Upper Vuggy, and Lower Vuggy formations, between the upper

boundary of Three Finger Zone and Midale Evaporite, and lower boundary of Frobisher Evaporite.

- The smallest lateral resolutions are at an order of 50 m for the Weyburn phase 1A area, and smallest vertical resolutions vary according to the formations, varying from centimeters to meters.
- The smallest temporal sampling rate is monthly commencing at the start of CO_2 injection.

Summary Conclusions

As a modeling workflow for predicting CO_2 migration path prediction during post-EOR storage is developed, and the minimum physical data parameters for CO_2 geologic storage recognition are recommended based on the results of the risk-informed objective-oriented systematic approach.

The workflow recommended by this project can be distilled into 6 key steps:

1. A predictive reservoir simulation should be completed towards the end of CO_2-EOR to provide the reservoir conditions for a CO_2-injection scenario.
2. Automatic facies pattern recognition should be conducted with available well log and/or core porosity, anisotropic permeability, bulk density, as well as geologist labeled stratigraphic facies, and 3D seismic attribute data.
3. Transition probability matrixes of the facies are calculated with indicator kriging or co-kriging.
4. Porosity and permeability probability distributions are generated from facies (as recognized from step 2) and by conditioning well log and/or core data in the area of interest.
5. Implement post-EOR CO_2 injection with generated porosity and permeability (see step 4), and obtain the pressure distribution.
6. Repeat step 4 and 5 to reduce conditioning data under specified risk informed threshold, which should be related to and informed by pressure changes.

Pattern recognition from well log and/or core data with the help of 3D seismic attribute data and stratigraphic facies picked by geologists is an effective way towards the reduction of conditioning data requirements for CO_2 migration risk prediction.

Porosity, anisotropic permeability, and bulk density are the main petrophysical properties for hydraulic flowing pattern recognition. Geochemical and geomechanical models should be involved in the workflow spatially and periodically to identify potential CO_2 breakthrough and development of new fractures as the CO_2 storage reservoir pressure evolves during CO_2 interaction with the surrounding rocks and fluids.

More advanced seismic interpretation techniques could be utilized to increase the pattern recognition accuracy, and monitoring and comparison of seismic interpreted properties along years of CO_2 injection provide directly monitoring of CO_2 migration.

11.0 SaskCO_2USER (WMP Optional Phase) – Stochastic Inversion

This research project focused on completing stochastic inversion of time-lapse seismic data coupled with flow simulations for permeability and porosity.

Achieving agreement between predictive modeling and observable subsurface CO_2 migration requires substantial effort and resources. Predictive modeling used to project flow simulations usually vary from the progress of monitored CO_2 throughout the reservoir. During the IEAGHG Weyburn-Midale Storage and Research Project an algorithm based on Bayesian stochastic inversion methods was developed and applied to a set of time-lapse seismic data. Building on this work, this project sought to optimize agreement between predicted and observed storage performance. By minimizing time and resources required in the traditional 'trial-and-error' model updating, this history matching project aimed to provide increased efficiency and efficacy for the long term containment and liability related monitoring of CO_2 during both CO_2-EOR operations and permanent storage.

In the SaskCO_2USER project, Dutch-based TNO is advancing this work by completing a stochastic inversion of time lapse seismic coupled with flow simulations for reservoir porosity and permeability. By adapting the existing algorithm, a history-matching method was developed with the goals of being flexible, efficient and effective. This algorithm was demonstrated on a synthetic data set before being applied to existing data from an operational CO_2-EOR field.

The outcome of this project was the development of a consistent methodology for seismic history matching in an oil reservoir undergoing CO_2-EOR. The experiments were conducted on a sector model for a single well pattern selected from a larger model containing 9 patterns. The sector model has closed boundaries and the initial state was taken from a full-model simulation. Simulation of the sector model produced results of comparable quality as the full model, as determined in terms of differences with historic well data. An updated reservoir model was developed as a final outcome

11.1 Stochastic Inversion – Approach and Methodology

This project was divided into seven tasks:

1. Review of data and/or relevant literature
2. History matching algorithm
3. Seismic data processing
4. Sector model evaluation ensemble creation

5. Synthetic data experiments
6. Experiments with historical data
7. Sensitivity experiments

A number of observations (signal amplitude, non-monotonic CO_2 spreading, different published interpretations, inconsistency with simulations) suggest that the quality of the seismic signal is rather low. Based on analysis of amplitude and time differences, as well as pressure fields from the full model suggest that the 2002 time-lapse maps may be most reliable.

An iterative version of the Ensemble Kalman Filter (EnKF) was selected for the inversion/history matching experiments. This approach requires the availability of a prior ensemble of model realizations that captures the uncertainty in the relevant model parameters. Geo-statistics of permeability and porosity were determined from the available 9-pattern model and were assumed to be applicable to the well pattern of the sector model. Four prior model ensembles were generated using different approaches to perturb permeability and porosity. Some features of both the time-lapse seismic and of the measured well data were not captured by any of the ensembles which suggests data or modelling errors other than can be directly associated with uncertainty in permeability or porosity.

Synthetic inversion experiments were conducted to verify the suitability of the ensemble-based inversion algorithm and data parameterization based on front positions. These synthetic experiments showed that the algorithm is able to produce multiple models that are consistent with observed front positions as can be interpreted from time-lapse seismic data. The match to synthetic production data also improved for models conditioned to synthetic time-lapse seismic data only. A combined match to time-lapse seismic and production data produced a compromise solution with improvements in the match to both seismic maps and to well data.

Application of the algorithm to inversion of the real data produced results of a more diverse nature. It was found that a subset of the data (the 2002 time-lapse seismic map) could be reproduced after history matching more accurately than before history matching and more accurately than by the reference model. The 2001 and 2004 maps could not be reproduced with the same accuracy. A combined match to the 2002 seismic and production data showed a 78% reduction of the data mismatch. These results were achieved at relatively low computational cost.

The success of the synthetic experiments as well as results from sensitivity experiments rules out shortcomings in the algorithm as an explanation for the difficulties in matching the measured data. It is concluded that the uncertainty in the measurements and in relevant model parameters may not have been adequately captured, and that possibly not all relevant parameters have been identified yet. A number of recommendations are provided that should help to improve results and to extend the application of the developed workflow to a larger

domain of the field. The main recommendation is to perform a sensitivity study that takes into account the expected uncertainty ranges in all potentially relevant parameters as well as the impact of alternative modelling approaches (resolution, fracture representation).

11.2 Stochastic Inversion – Results and Recommendations

Task 1 - Review of data and/or relevant literature

Available data was used and provided by PTRC to TNO.

Simulation model geometry and sector selection

Simulation model data was provided. Among the simulation data were an incomplete dual-porosity deck and documentation on earlier simulation work performed by Alberta Innovates (Uddin et al., 2011). It is a single porosity compositional Eclipse 300 (Schlumberger) model covering a 9-pattern area of the Phase 1A development. A single well pattern area was selected from the provided 9-pattern simulation model (referred to here also as the full or large model). The selected well pattern is the same as that used by Uddin et al. (2011) and Ramirez et al. (2013)

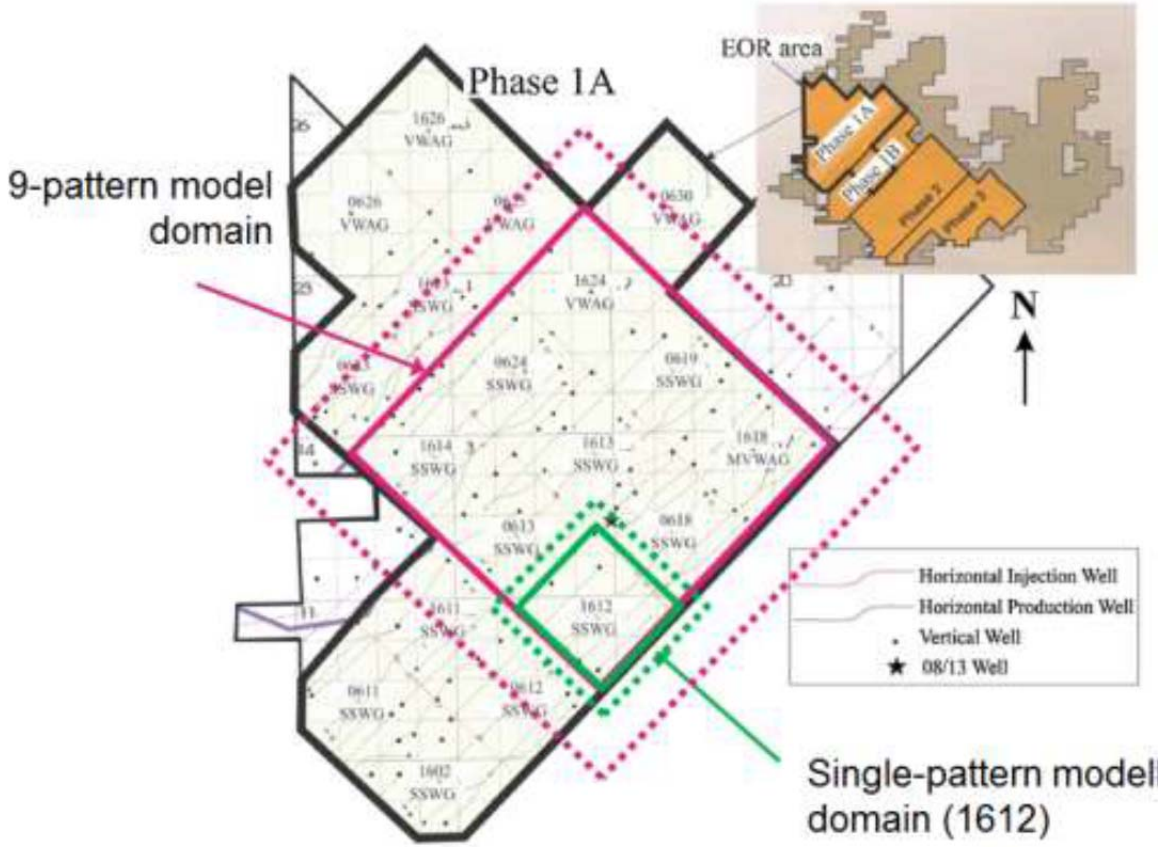

Figure 106 – The location of the 9-patter and selected single pattern model domains. The green area indicates the sector model whereas the pink is indicative of the 9-sector model

The recovery strategy in the selected pattern is Simultaneous but Separate injection of Water and Gas (SSWG). In the literature the reservoir temperature and pressure and the fluid properties are generally assumed to be consistent with miscible flooding conditions (i.e. the oil and CO_2 mix fully at all fractions). Grid cells have dimensions of 100 m by 50 m, which is coarser than was used in some previous studies which are reviewed later. The model contains 27 layers, 7 of which (layers 2 to 8) discretize the Marly zone , while the lower layers constitute various sub-units of the Vuggy zone.

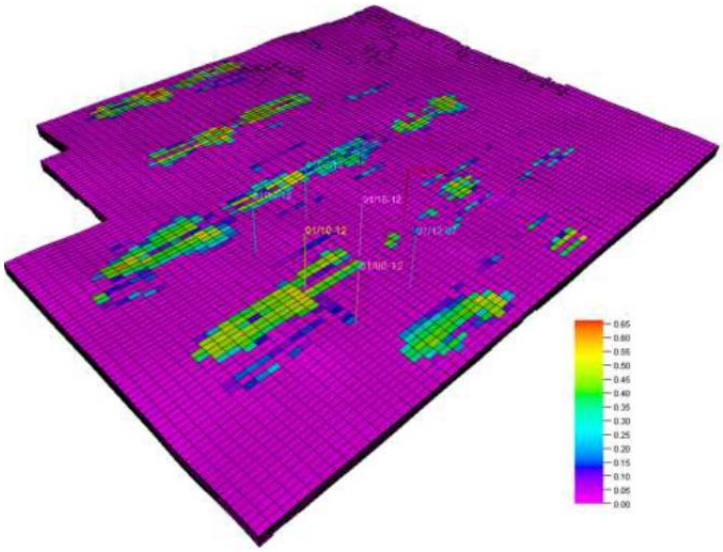

Figure 107 – Overview of the 9-pattern model configuration. Colors show the simulated gas (CO_2) saturation at the time of the 2004 seismic survey. The vertical wells indicate the location of the selected sector. Only the original inverted 9-spot well pattern development in the sector domain is shown.

Fluid and Flow Properties

Relative permeability and capillary pressure functions in the simulation deck are shown below.

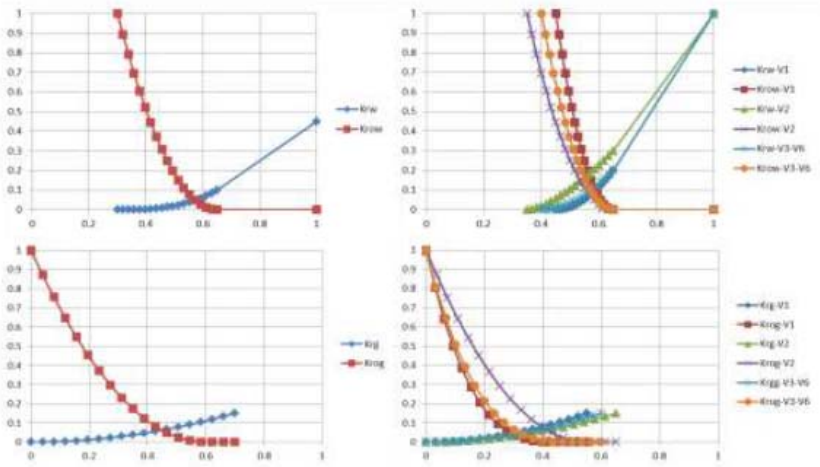

Figure 108 – Water, oil and gas relative permeability functions as used in the simulation deck. The panels on the left are for the Marly unit and the ones on the right are for the Vuggy unit

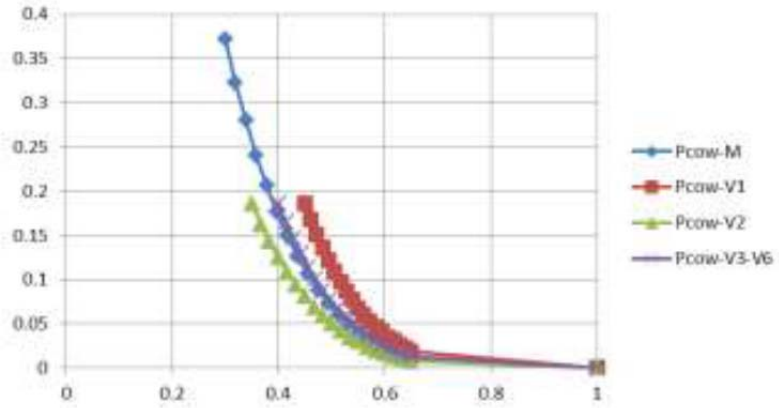

Figure 109 – Oil-water capillary pressure as used in the simulation deck. The oil-gas capillary pressure is zero everywhere.

The reservoir temperature is a constant 63°C.

Dynamic Data

The schedule section covers the period from 1 January 1956 to 31 December 2006 and includes measured historic well data: total liquid production rate (WLPR), water-cut (WWCT), gas production rate (WGPR), water injection rate (WWIR) and gas injection rate (WGIR). The BHP values included in the schedule are not actually measured values.

The data package also included a file containing shut-in pressures obtained using a range of techniques from wells across the Weyburn field. However, these shut-in pressures were not implemented in the model, and have therefore been excluded for history matching at this point. It is noted that previous history matching exercises have also ignored pressure (Brown, 2002) although Johnson and White (2012) mention the existence of injection pressure histories. No accompanying reservoir engineering report was available with the model.

Seismic Data

The inversion cubes were analyzed, the main part of the further analysis and processing though was done on the balanced post-stack data cubes.

Literature

Previous studies on history matching of (parts of) the Weyburn field have been presented in Jafari et al. (2011), Uddin et al. (2011), Johnson and White (2012), and Ramirez et al. (2013). Some simulation work was presented by Brown (2002).

Task 2 - History matching algorithm

Ensemble Kalman Filter and Smoother

The EnKF was proposed as an extension of the Kalman Filter to nonlinear situations. It was originally applied primarily to state estimation problems, such as e.g. weather forecasting, in which the main unknowns are the dynamic states at a particular time. It was soon realized, however, that the same logic could also be applied to parameter estimation or mixed state-parameter estimation problems.

Over the past decade a large number of studies have demonstrated the applicability of the method to reservoir model history matching, which is traditionally approached as a parameter estimation problem. That is, the main uncertainty is assumed to be contained in the values of time-independent model parameters, primarily the grid cell values of permeability and porosity, and the dynamic states (saturations, pressures) are assumed to be pre-dominantly determined by the initial state, these parameters and the physics as implemented in the simulator. Some studies have extended the uncertain parameters with relative permeability and capillary pressure function parameters, structural parameters, etc.

While in state estimation problems model updates are typically computed in a sequential fashion, in reservoir engineering applications a simulation over the full history period is normally desired based on a single, constant, set of parameters. Therefore, simulations are typically restarted from the initial time, and updates are often based on simultaneous incorporation of all available data within a large time window (possibly the entire history period) in an iterative manner. The resulting algorithm is often referred to as an Ensemble Kalman Smoother. A particular version known as Ensemble Smoother with Multiple Data-Assimilation (ES-MDA) has been used, as proposed by Emerick and Reynolds (2011). The workflow is described below. The evaluation of a simulation model (i.e. a forward run), can be written as follows:

$$\varphi(t_{k+1}) = M(\varphi(t_k), p).$$

The vector ( ) contains the dynamic variables at time tk. The state at a later time tk+1 depends on ( ), on the static properties (parameters) of the model p, and on the dynamic equations M. A measurement model may be used h to simulate a measurement set (tk+1) from the model state at the same time:

$$d(t_{k+1}) = h\big(\varphi(t_{k+1})\big),$$

where $d(tk$+1) are the simulated values, and $y(tk$+1) are the measured values. If it is assumed that the dynamic equations and initial state are perfectly known, the simulated state and measurements at any time uniquely depend on the parameters set p. The uncertainty of knowledge of the parameters can be expressed by an ensemble of different realizations

$$A = \begin{bmatrix} p_1^1 & \cdots & p_1^N \\ \vdots & \ddots & \vdots \\ p_n^1 & \cdots & p_n^N \end{bmatrix}.$$

where $pj\ i$ is element j of the parameter vector for realization i. That is, there are n uncertain parameters, and we use an ensemble of size N to represent the uncertainty therein.

$$D = \begin{bmatrix} d_1^1 & \cdots & d_1^N \\ \vdots & \ddots & \vdots \\ d_m^1 & \cdots & d_m^N \end{bmatrix}.$$

The traditional EnKF model update can be obtained as:

$$A^{new} = A + K(Y - D),$$

where the matrix Y consists of N randomly perturbed measurement vectors, that is,

$$Y = \begin{bmatrix} y_1 & \cdots & y_1 \\ \vdots & \ddots & \vdots \\ y_m & \cdots & y_m \end{bmatrix} + \begin{bmatrix} \epsilon_1^1 & \cdots & \epsilon_1^N \\ \vdots & \ddots & \vdots \\ \epsilon_m^1 & \cdots & \epsilon_m^N \end{bmatrix}.$$

The matrix K is the Kalman gain matrix which is defined as:

$$K = A'D'^T(D'(D')^T + R)^{-1},$$

where A' = (1 − IN)A and D' = (1 − IN)D, and R is the measurement error covariance matrix R = < ϵ, ϵ >. Emerick and Reynolds (2011) proposed an iterative update scheme as follows,

$$A^{i+1} = A^i + K^i(Y^i - D^i),$$

where $R \rightarrow Ri = \alpha iR$, that is, the measurement error variance is multiplied by a factor αi that depends on the iteration i, with the requirement that Σ 1 αi = 1.

Typically, decreasing values of αi are used, such that the measurements get relatively increasing weight with increasing iteration number. This iterative version of the EnKF is used here, in which simulations are re-started from the initial time after each update (iteration), with the additional modification of the original EnKF that measurements from multiple times are used simultaneously in a single update. The validity of this approach has also been discussed by Emerick and Reynolds (2011) and references therein. The matrix $A0$ contains the ensemble of model properties defined prior to any incorporation of measurements and is therefore referred to as the prior model ensemble. The ensemble obtained at the final iteration contains the solution of the history matching process and consists again of an ensemble of property values. EnKF theory suggests that the mean of this ensemble is the best estimate (minimum error variance solution).

Parameterization of seismic data

Experience has shown that incorporation of large numbers of measurements (i.e. m is very large), may lead to inferior performance of the EnKF algorithm (see e.g. Aanonsen et al., 2009; Leeuwenburgh et al., 2011). In particular, it has been observed that in extreme cases all ensemble members tend to be become identical, which means that both the spread and the rank of the ensemble are reduced beyond what may be assumed realistic (i.e., the model uncertainty will be underestimated).

A variety of methods have been proposed in the past to (partly) address this problem. For example, inflation aims to increase the ensemble spread, while localization aims to increase the ensemble rank. Both approaches address only part of the problem, and have undesirable disadvantages as well.

Leeuwenburgh and Arts (2014) proposed a parameterization of differences between model simulations and seismic data in terms of the oil-water front position. The method results in distances between observed and simulated front positions which can be used as innovations in the EnKF equations (i.e., the term ($Y - D$) in the equations above). The distances are computed using the Fast Marching Method (Sethian, 1996). This method solves an equation for the arrival times of a monotonically expanding front in a 3D grid domain. Under the assumption of uniform velocities, the time solution can be translated directly into a distance solution when the distances are evaluated between the observed and simulated front positions. This approach has a few favourable properties:

- The front can be represented by far fewer data than the full 3D seismic cube of seismic attributes (or its interpretation on the model grid), while still capturing the main information contained in the seismic data.
- The distances have a more linear relationship with the uncertain model properties (permeability and porosity).
- Determination of the front position from the seismic amplitude data does not require a full seismic inversion and may still be possible for poor quality data sets.
-

These properties result in a potentially better performance of inversion algorithms.

Task 3 - Seismic data processing

Petrophysical issues

No unambiguous petrophysical model for the Midale formation exists that incorporates pressure and saturation of a mixed fluid system. The line of thought presented by both White (2013) and Brown (2002) who concluded that for the Pwave response the CO_2 saturation

change is more important than the pressure change was followed. Also Johnson and White (2012) neglected any pressure contribution

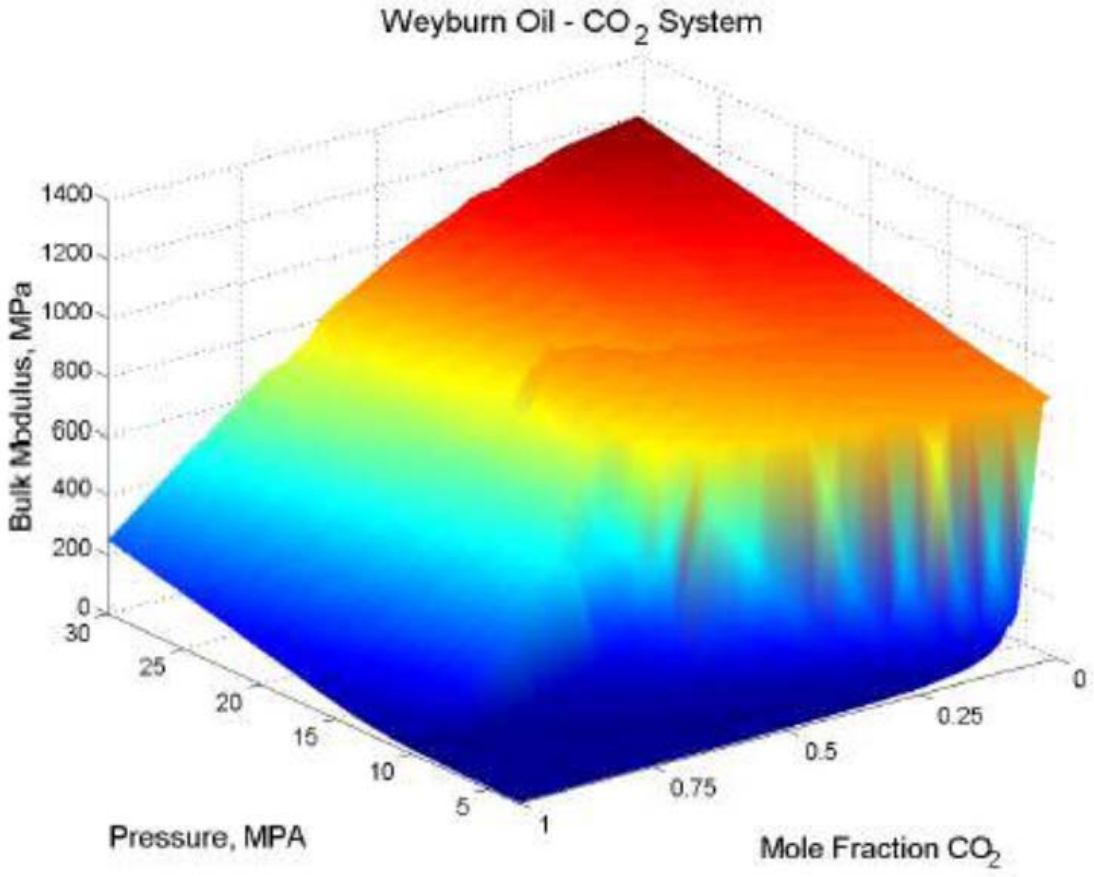

Figure 110 – Variation of effective bulk modulus with composition and pressure for the Weyburn oil- CO_2 system (63 deg. C); from Brown (2002).

It is seen that for pressures around 18 MPA (as prevails in the reservoir) and for a Mole fraction of CO_2 up to 25% there is a nearly linear relationship between Mole fraction CO_2 and effective bulk modulus. The density is nearly constant in this pressure and mole fraction region. This results in a nearly linear relation for both Vp and the reflection coefficient versus CO_2 fraction. It is noted that this is somewhat contradictory to what is shown in other references (e.g. Hitchon, 2012), in which results indicate that the largest change in reflection coefficient occurs for low CO_2 saturations and that for larger CO_2 concentrations the relative change decreases.

Thin layer response

It is relevant for the Weyburn seismic data to recall the response of thin layers (see Widess, 1973). For a thin layer, i.e. thinner than 1/8th of the wavelength, in a homogeneous formation, the response increases both with thickness and SI contrast. The dominant wavelength of the Weyburn seismic data is: $\lambda \approx 3300$ [m/s] / 50 [Hz] ≈ 67 [m]. One eighth of this is about 8 m: the

whole Marly unit. So for the Marly unit, and especially for the CO_2 in the Marly, the Widess thin layer response holds. This means that the seismic response of e.g. 2 m of a certain CO_2 saturation equals the seismic response of 4 m of half that CO_2 saturation (the SI changes somewhat linearly for saturations below 30%). For a constant porosity this means that the seismic response is approximately proportional to the total volume of CO_2 in the Marly. This implies that the difference of seismic amplitude (vintage minus baseline) is proportional to the change in the total CO_2 volume in the pillar below the measuring point for a constant porosity medium, or otherwise stated, to the mean saturation over that interval

Amplitude of the time-lapse signal

Various analyses on the seismic data were carried out. After careful examination of the seismic data available, it was concluded that the amplitude of the time-lapse signal is too low, and that in combination with the resolution of the seismic signal, the data do not allow a separate Marly and Vuggy time-lapse signal. Therefore, front positions were based on the figures in White (2013), as these are probably the best guide in defining the front positions.

Determining the CO_2 front position

Modelling of the seismic response of the Weyburn field (White, 2013) showed that a significant larger response in amplitude differences can be expected from CO_2 in the Marly and CO_2 in the Marly and Vuggy than from CO_2 only in the Vuggy.

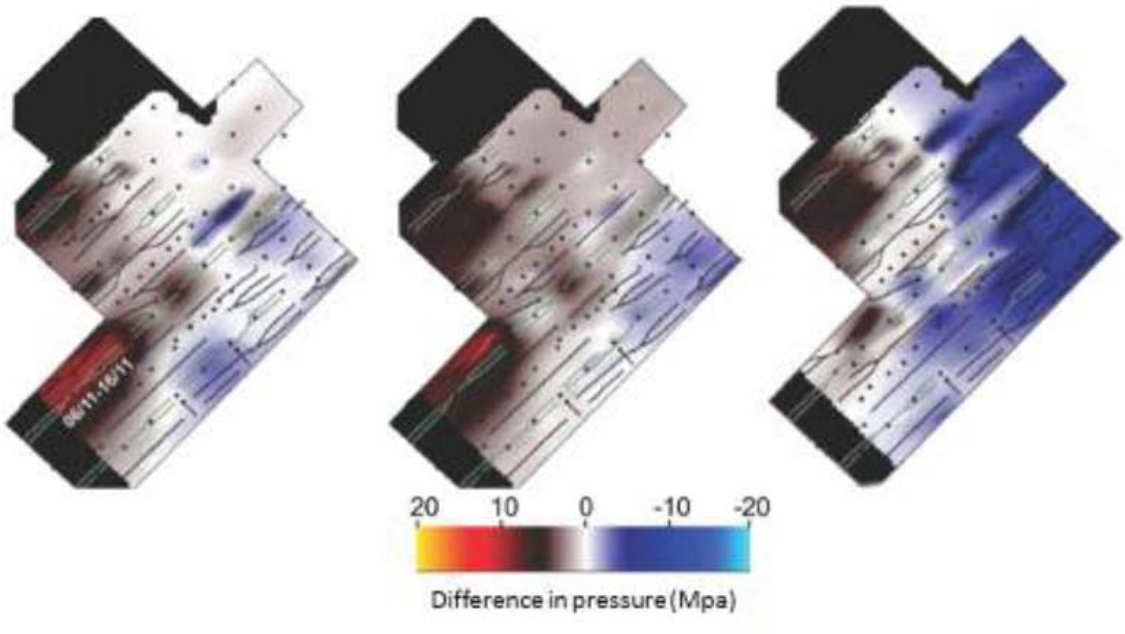

Figure 111 – Difference of pressure in the reservoir relative to 1999 from a CRM. From left to right: December 2001, December 2002, December 2004.

The pressure change between Dec 1999 and Dec 2002 is not significant. A minimal influence of pressure on the seismic difference results is already assumed, but the 2002 anomalies in the amplitude (SAD) and travel-time (TTD) difference maps can therefore be attributed only to variations in CO_2 saturation with even more certainty.

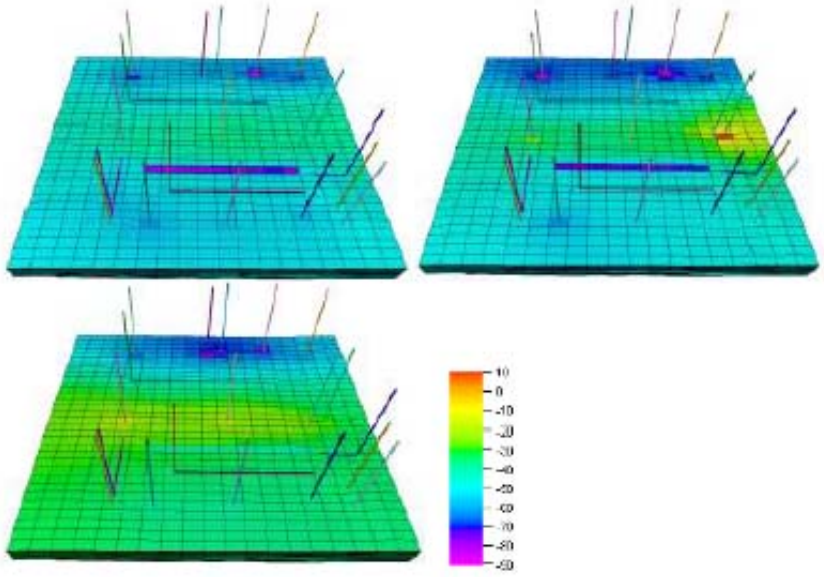

Figure 112 – Pressure differences with respect to the time of the initial seismic survey (1999) for (clockwise from top left) 2001, 2002 and 2004.

Pressure fields as simulated with the sector model (Figure 112) suggest significantly lowered pressures along the horizontal producers. The fact that these features are not observed in the time-lapse differences could also be interpreted as support for the idea that pressure effects do not significantly affect the seismic response.

The following sources of information were studied to map oil-CO_2 front positions:

- Figure 16 in White (2013): differences in seismic amplitude (SAD)
- Figure 18 in White (2013): differences in travel time (TTD).
- Figures 9.2 – 9.5 in Brown (2002): amplitude differences between 1999 and 2001.
- Our own maps of amplitude changes and travel time differences.
- Seismic modeling (1D) performed by TNO and from White (2013).
- Maps of changes in CO_2 saturation from the provided calibrated reservoir model (CRM).
- Maps of changes in reservoir pressure from the provided calibrated reservoir model.
- Geological characteristics of the reservoir from various publications.

To map the oil fronts in the Marly, the SAD-maps from White (2013) were used. To do so, the figures were positioned in such a way in the Petrel project of the reservoir simulation, that the

well bores indicated in the figures overlapped the position of the well-bores of the reservoir model. In such a way the position of the front is directly mapped in reservoir coordinates and there is no issue of coordinate transformation. Then the contour of a colour transition was manually picked and traced as the front position. The manual picking leads to somewhat smoother front positions. The advantage is that noisy parts of the data are suppressed by the interpretative mind.

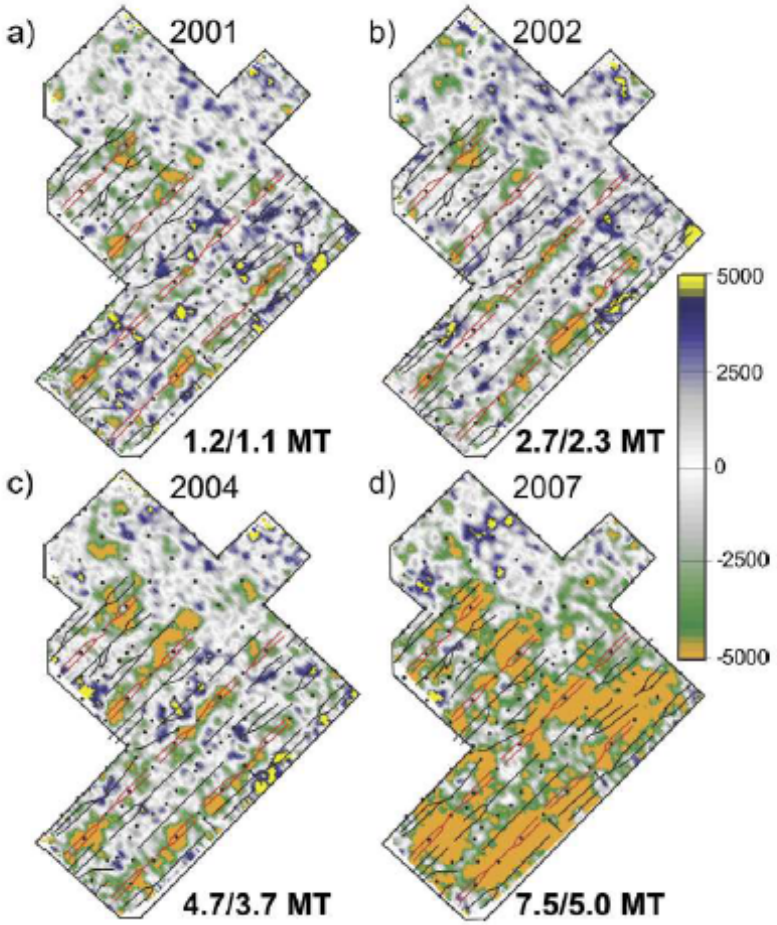

Figure 113 – Seismic amplitude of vintage minus amplitude of baseline from 1999 (White, 2013)

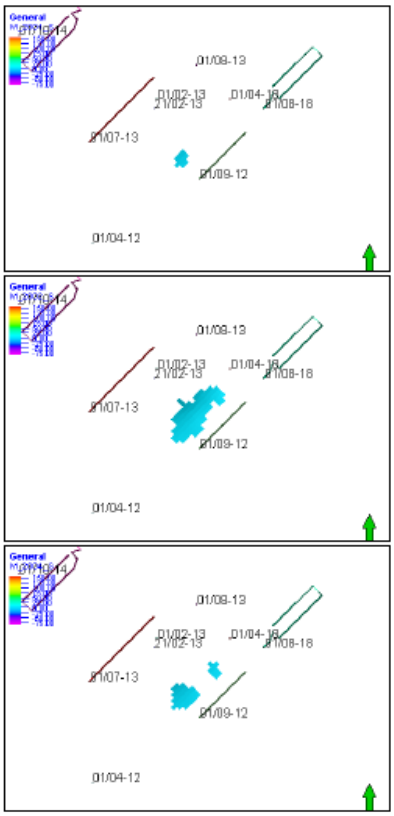

Figure 114 – Interpretation of >15 % mean saturation in Marly in the study sector.

An alternative identification of the CO_2 swept area was generated as well by picking and tracing another colour contour, presumably associated with a lower CO_2 saturation. The two sets of resulting seismic maps that are used in the history matching experiments are presented in the subsequent figure. Note that an interpolation from the reservoir grid to a regular 50m x 50 m grid was performed to facilitate all comparisons between measured and simulated maps.

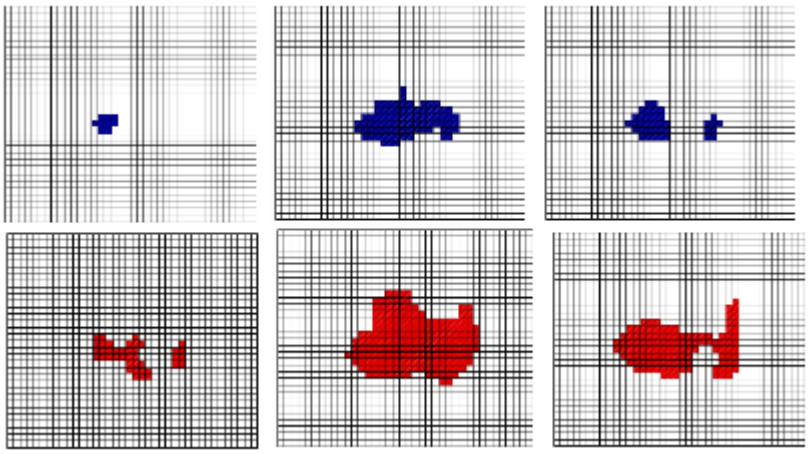

Figure 115 – CO_2 distribution maps 1 (top) and 2 (bottom) in the Marly in the study sector for (from left to right) 2001, 2002 and 2004, based on two different colour outlines in the White (2013) seismic interpretations.

The amplitude difference map of White (2013) and the resulting interpretations of the flooded area for 2002 are markedly different from the corresponding figure from Hitchon (2012) which is reproduced below:

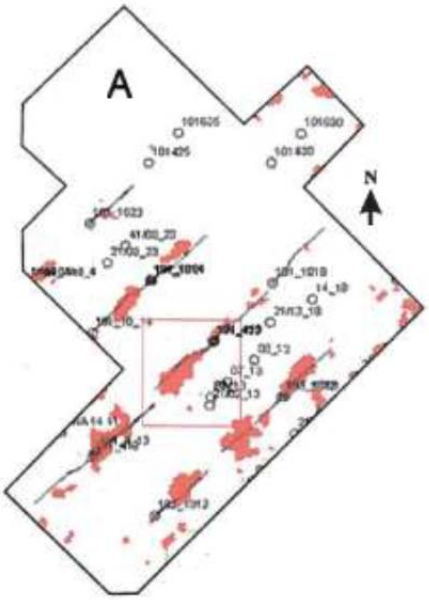

Figure 116 – Distribution of CO_2 at the time of the 2002 survey as interpreted from the P-wave amplitude difference map by Johnson and White, 2012.

Task 4 - Sector model evaluation ensemble creation

Sector Selection

As indicated above already, but repeated here for convenience, a single well pattern was selected from the provided 9-pattern simulation model (referred to here also as the full model). The selected well pattern is the same as that used by Ramirez et al. (2013) and is indicated below:

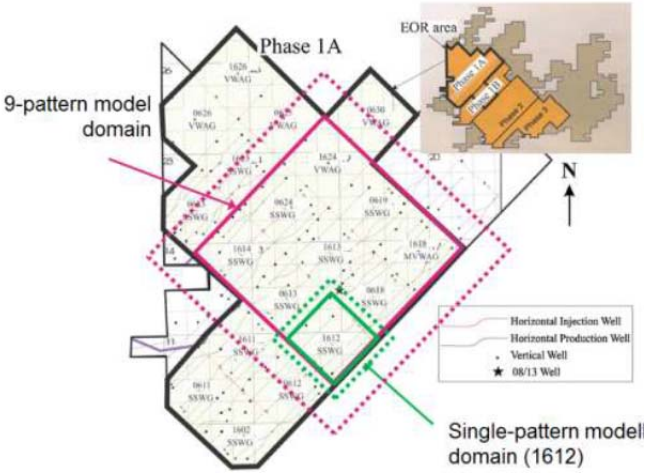

Figure 117 – Location of the 9-pattern and selected single pattern model domains and approximate indication of the boundary zones.

Model configuration

A sector model was created by making all cells and wells outside a 4-cell boundary zone around the selected pattern inactive. No communication is allowed through the outer boundaries of the sector. The dynamic state (consisting of pressure, saturations and component mass fractions) on 01/12/1999 from the full-field model simulation is used as the initial state for all simulations of the sector model. An overview of producing and injecting wells within the resulting sector model is provided in the table below. Wells drilled after 01/01/2005 (indicated in red) will not be considered since simulations are only performed until this date. In Eclipse the listed aliases are used as well names. Gas injection well 93/10-12 and producer 92/09-12 are positioned in the lower part (model layer 5) of the Marly formation, while the other horizontal wells are positioned in the upper part (model layer 2) of the Marly. The vertical wells generally extend through both formations and are completed in the layer range indicated in the table. Well 92/14-07 is drilled from the same vertical well as 91/14-07 but higher up in the formation.

	wells	*alias*	*type*	*layers*	*position*	*comments*
1	101021300614W200	01/02-13	P	5-19	B	boundary well
2,3	101041800613W200	01/04-18	P,W	5-19	B	Conversion to water injector from 01/02/2001
4	101081200614W200	01/08-12	P	4-25	C	not producing 1999-2005
5	101081300614W200	01/08-13	P	2-25	C	
6	101101200614W200	01/10-12	W	2-26	B	shut in between 01/04/1997 and 01/08/2000
7	101120700613W200	01/12-07	P	3-21	B	
8	101140700613W200	01/14-07	P	2-24	C	not producing 1999-2005
9	101141200614W200	01/14-12	P	2-24	C	
10	101161200614W200	01/16-12	W	5-26		
11	111071300614W200	11/07-13	P	2-24	B	
12	121021300614W200	21/02-13	P	2-16	B	
13	121140700613W200	21/14-07	P	4-6, 15	B	
14	141081200614W200	41/08-12	P	3,5,15-19	B	
15	191011300614W200	91/01-13	P	H	UM	
16	191041800613W200	91/04-18	P	H	B	shut in between 01/03/1997 and 01/05/2003
17	191091200614W200	91/09-12	P	H	UM	
18	191101200614W200	91/10-12	P	H	B, UM	
	191121200614W200	91/12-12	P	H	B	on stream from 01/09/2005
	191140700613W200	91/14-07	P	H	B	on stream from 01/04/2006
	191141200614W200	91/14-12	P	H	UM	on stream from 01/05/2005
19	192091200614W200	92/09-12	P	H	LM	
	192140700613W200	92/14-07	P	H	B	on stream from 01/04/2006
20	193101200614W200	93/10-12	G	H	LM	

Table 42 – Overview of wells in the selected sector domain. W indicates a water injector, G indicates a gas injector, P a producer, H a horizontal well, B a boundary well and C a corner well. UM indicates Upper Marly and LM Lower Marly. Wells indicated in red are not active during the simulations presented here.

Sector model evaluation

For the purpose of comparing the full-field and sector model performances, a full-field model simulation was run from 01/01/1956 until 31/12/2006, while the sector model was run from 01/12/1999 onward. Two sector model versions are compared; one from which all manual history matching changes to permeability and porosity were removed ('clean'), and from which only the permeability limits (minimum and maximum allowed values) were removed ('modified').

In the simulator, liquid rates (the sum of oil and water rates) are prescribed to all wells in the deck on a monthly basis. BHP limits are set at extreme values: 10 bar for producers, and 260 bar for injectors. Figure 118 shows simulation results for the full and sector models. In the plots, time will be indicated in number of days from 01/12/1999. Rates and pressures are reported in units of m3/day and bar respectively.

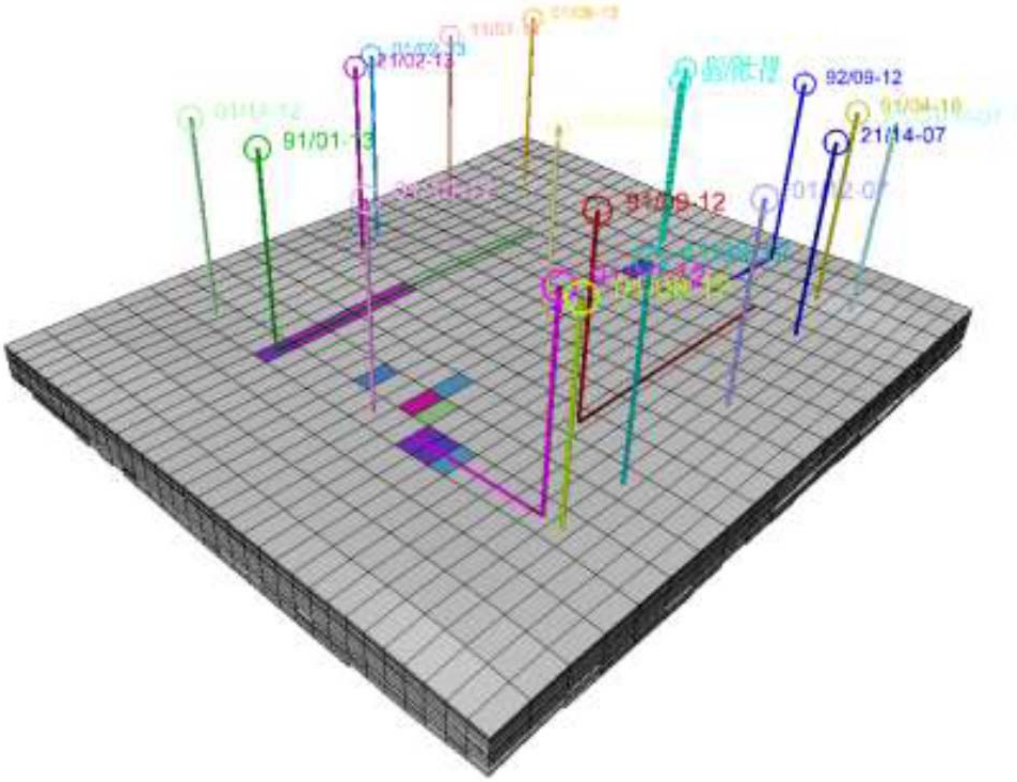

Figure 118 – sector model geometry layout, wells.

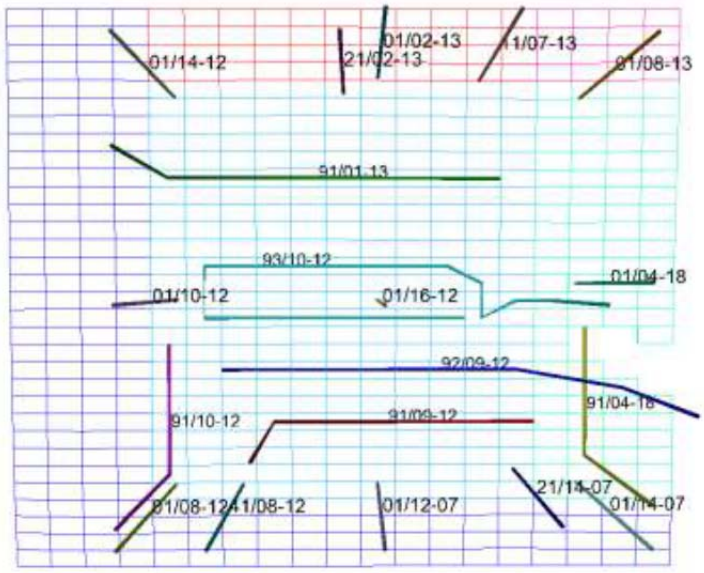

Figure 119 – top view of sector model and well trajectories.

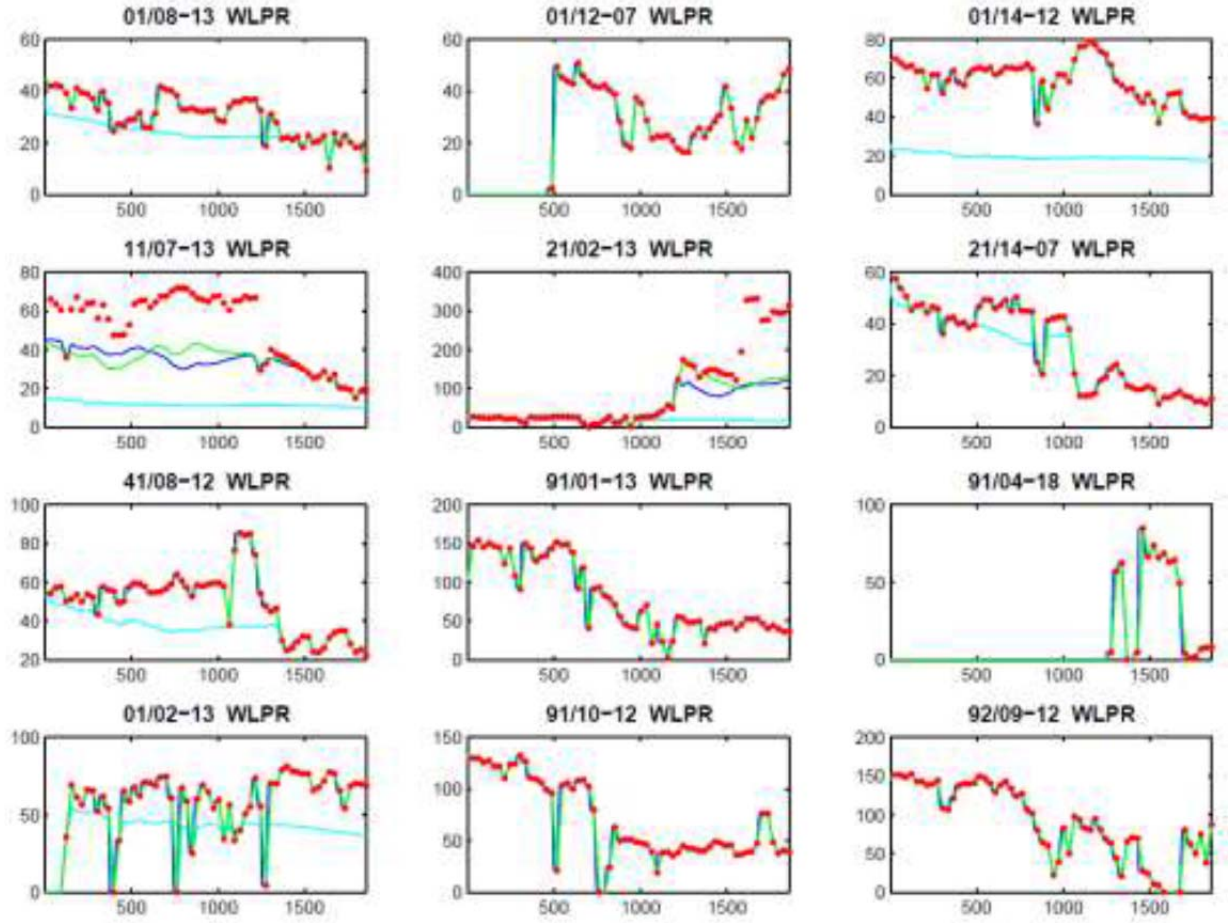

Figure 120 – Liquid production rate for producing wells in the sector domain. Simulation with the full field model (green), simulation with the clean sector model (cyan), simulation with the modified sector model (blue), and historic measured values (red). Results for well 91/09-12 (low production) and non-producing wells are not shown.

The imposed historic (measured) liquid production rates can generally be realized by the simulator in both the full field model and modified sector model, but not always in the clean sector model. This suggests that the clean reference model may not be ideally suited as the basis for history matching. On the other hand, appropriate perturbations of the permeability and porosity fields may result in models that are able to realize the historic liquid rates. Therefore, for the purpose of history matching, different ensembles were generated, based on both the modified and clean sector models.

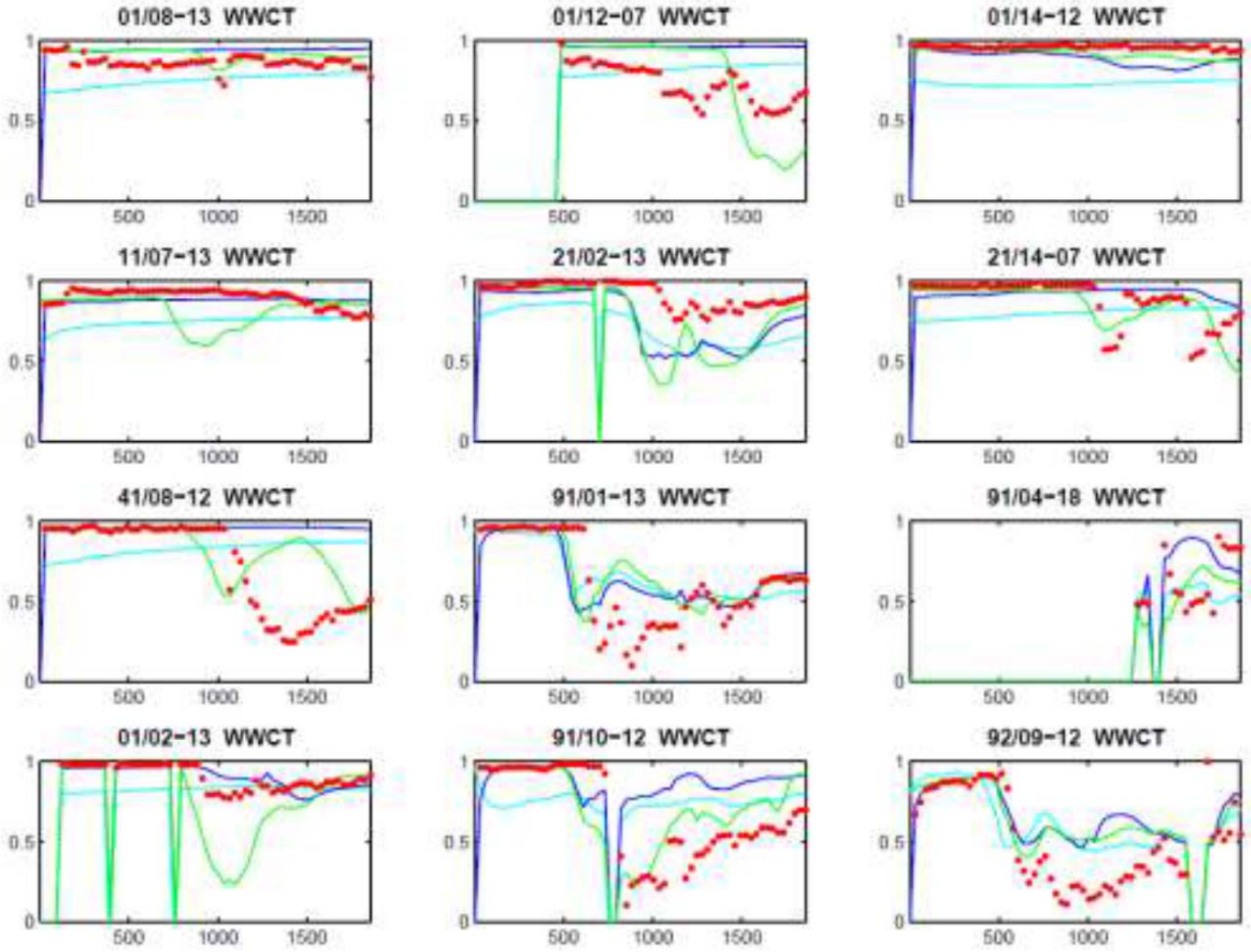

Figure 121 – Water cut for producing wells

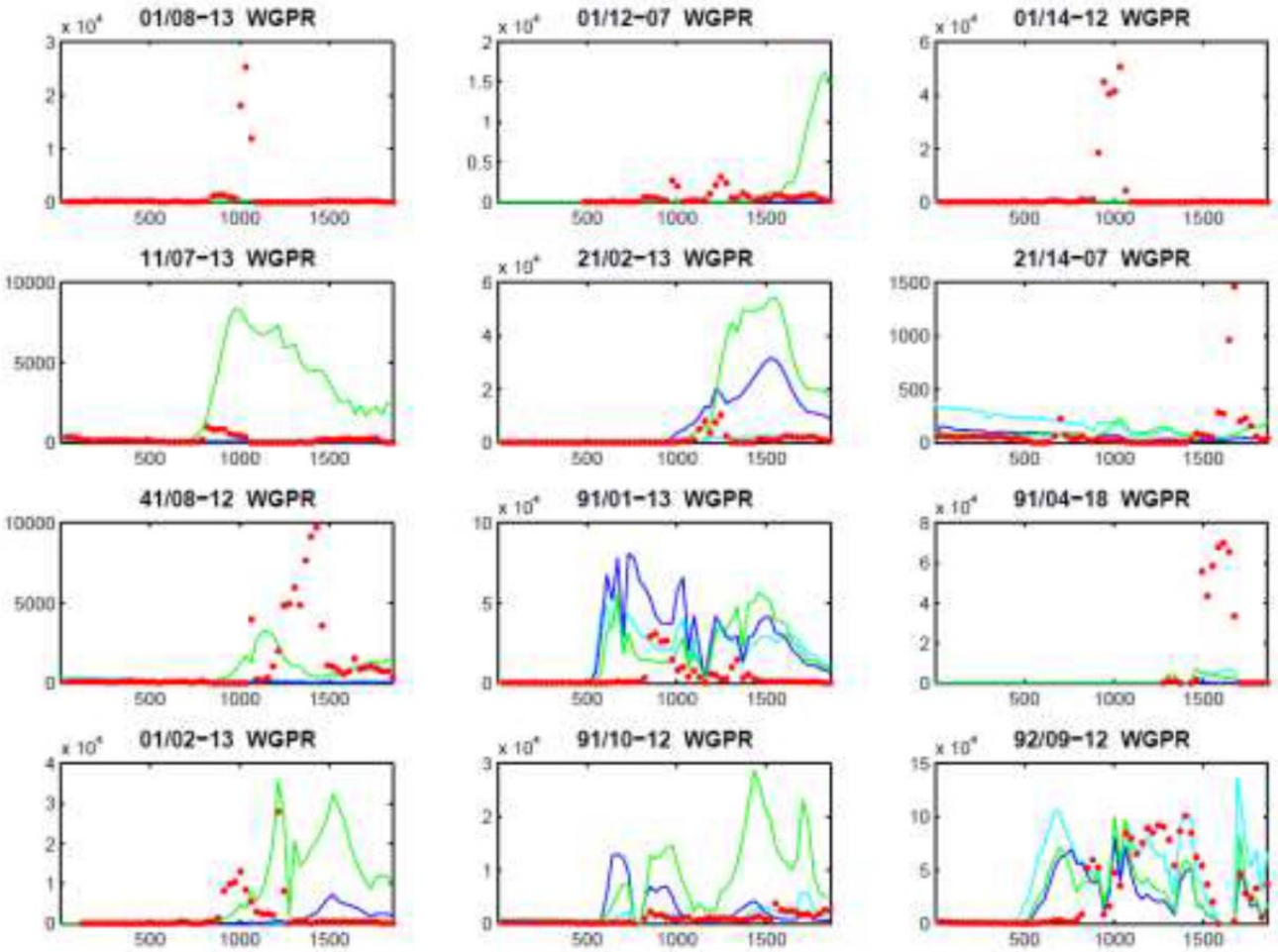

Figure 122 – Gas production rate for producing wells.

There are no clear indications that the sector models perform significantly worse overall than the full-field model in terms of reproducing the observed WCT. This supports the idea that at least the modified version of the sector model is suitable for use as the basis for history matching the sector model.

Ensemble creation

For the purpose of multi-model history matching, it is necessary to generate an ensemble of models, where all ensemble members are based on independent realizations of the uncertain properties. In this project only permeability and porosity are considered to be uncertain. Based on inspection of the full model property distributions, it was assumed that the distribution of these properties in the four identified geological zones in the model (Marly, Vuggy V1 Intershoal, Vuggy V2 Shoal, and Vuggy V3-V6 Shoal) can be characterized by different geo-statistical parameter sets. Random log-permeability and porosity perturbations fields with different length scales and orientation were therefore computed for each of the four zones using sequential Gaussian simulation (the package SGeMS was used for the synthetic

experiments, whereas an in-house developed spectral simulation-based tool was used for the real-data experiments). Minimum porosity bounds were imposed to ensure that no cells would become inactive as a result of a minimum pore volume requirement specified in the simulator deck.

Four ensembles of 100 permeability and porosity realizations each were generated (referred to as ensembles A to D in the following). The approach was slightly different for each. The basis for all four ensembles were the permeability and porosity fields of the provided 9-pattern model which are referred to as the reference fields.

Task 5 - Synthetic data experiments

A single model realization based on the clean sector model was selected as representing the 'truth' for the purpose of performing synthetic twin experiments. Production data (gas rates and water-cuts) and synthetic seismic maps were extracted from a simulation of this truth model.

Synthetic truth

The figures below show the permeability and porosity respectively in 2 layers of the synthetic truth model. It illustrates the correlation between the two properties and the differences between the Marly and Vuggy property distributions.

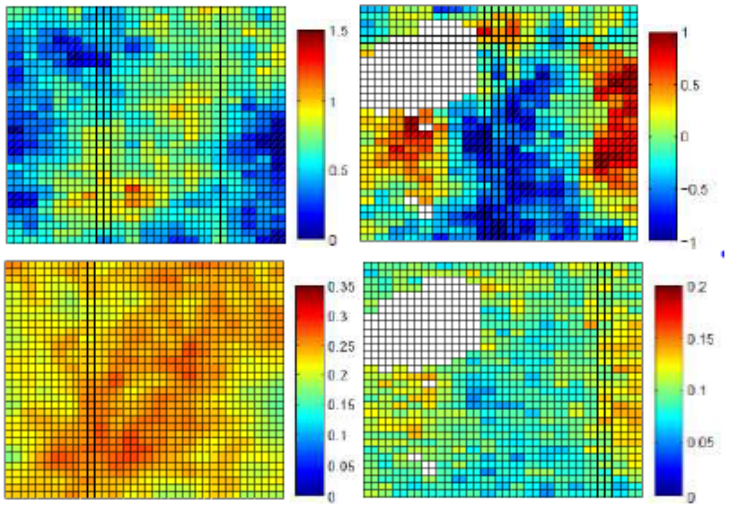

Figure 123 - permeability (top) and porosity of the truth in layer 2 (left) and 9 (right)

The synthetic truth model was simulated to generate synthetic measurements, including seismic maps on 1 December 2002. The seismic maps were generated by vertically averaging the saturation over the layers corresponding to the Marly (layers 1 to 8) and Vuggy (layers 9 to 27) separately, or over all layers (the combined case). In the experiments with separate seismic

maps for the Marly and Vuggy lateral smoothing was applied in order to mimic the processing typically applied to real data and the resulting data resolution. The positions of the front are determined from applying a threshold value of 0.001, and tracking the outline of the resulting area swept by CO_2.

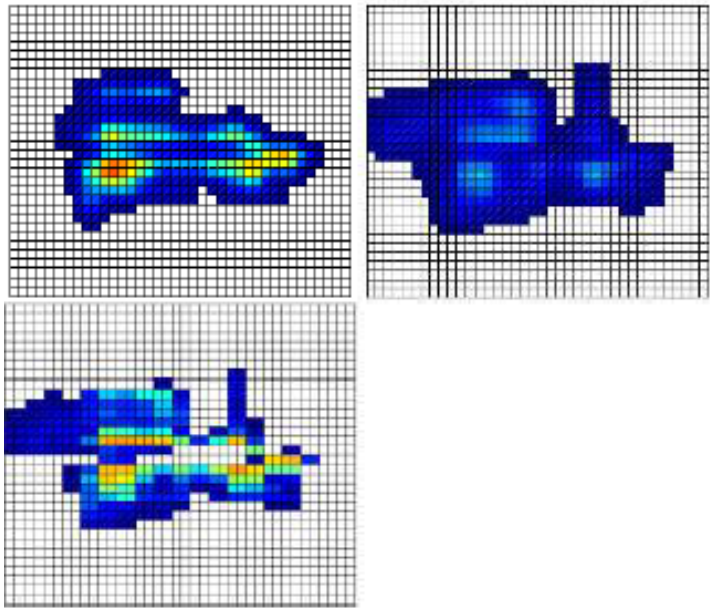

Figure 124 – Seismic maps at 1 December 2002 used as measurements in the synthetic data experiments. (a) map for the Marly only (top left), (b) map for the Vuggy only (top right), (c) map for the combined Marly and Vuggy (bottom left; no smoothing applied). Note that only the outlines of these maps are used as measurements.

Experiments and conclusions

Experiments were conducted on 4 cases (A-D). The experiment conclusions can be summarized as such:

- The TNO workflow for multi-model history matching to time-lapse seismic data was applied to a sector model of the Weyburn field. Synthetic data were generated from simulation of one model realization that was designated as the truth.
- Improved matches to seismic maps were obtained in all cases. The best match was obtained when only seismic data was used and separate maps for the Marly and Vuggy were used.
- A history match to both production and seismic data showed improvements in both data types. It produced the best match to production data of the cases considered, at the cost of some reduction in the quality of the seismic data match.

- The estimated permeability fields improved in all cases. The best match for the Marly was obtained when both production and seismic data were used. The best match for the Vuggy was obtained when only seismic data were used.

Further experimentation could be done to further explore some of the observed differences in performance between the various cases. However, it is clear already from these results that the applied history matching procedure is able to provide improved matches to seismic data, as characterized by maps outlining CO_2-flooded areas.

Task 6 - Experiments with historical data

Reference sector model

It was already established that the sector model setup and configuration are suitable for history matching, based primarily on the observations that the sector model did not perform significantly worse than the 9-pattern model in a comparison with historic well data. The sector model was extended to simulation of CO_2 saturation as the first step in matching to the time-lapse seismic data.

Experiments with seismic data

Appropriate corresponding saturation thresholds need to be determined for identification of the front in the simulated seismic maps. Based on visual inspection of maps resulting from different thresholds the values of 0.05 and 0.025 were chosen to facilitate comparison with the first and second interpretations respectively. The resulting seismic maps are constructed as simple indicator maps of swept and non-swept cells. It should be noted that the choice for the threshold values was based on visual comparison with model results, and that more appropriate values could perhaps be determined by some automated minimization procedure.

All experiments in this section were conducted with 50 ensemble members. The error in the interpretation of the front position was taken to be 25 m (corresponding to half a cell length). This error is very small, but was chosen to ensure that a significant change of the model properties would result. In other words, by choosing a small measurement error, relatively more weight is given to the data than to the prior models. For large measurement errors, model adjustments will be very small, and it would be difficult in that case to determine for example which ensemble performs best. Four iterations were conducted in each case. The results of the experiments are depicted in Figures 125 – 132 below. Experiments were conducted on 4 cases (A-D).

Ensemble A

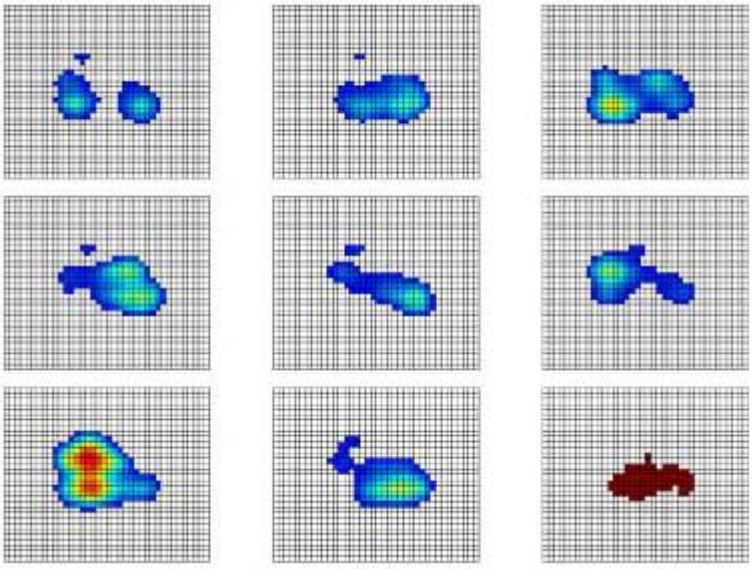

Figure 125 – Simulated saturation maps after vertically averaging over the Marly for the first 8 members of ensemble A before history matching to the observed map at 2002 (bottom right).

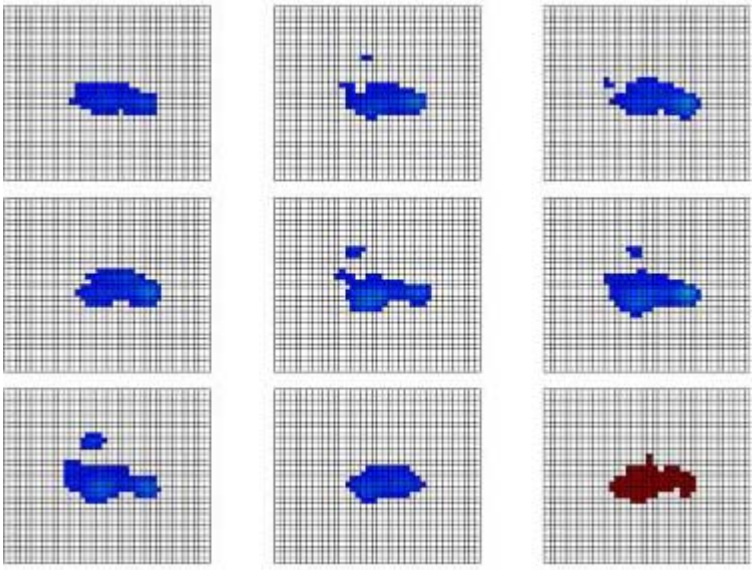

Figure 126 -- Simulated saturation maps after vertically averaging over the Marly for the first 8 members of ensemble A after history matching to the observed map at 2002 (bottom right).

Ensemble B

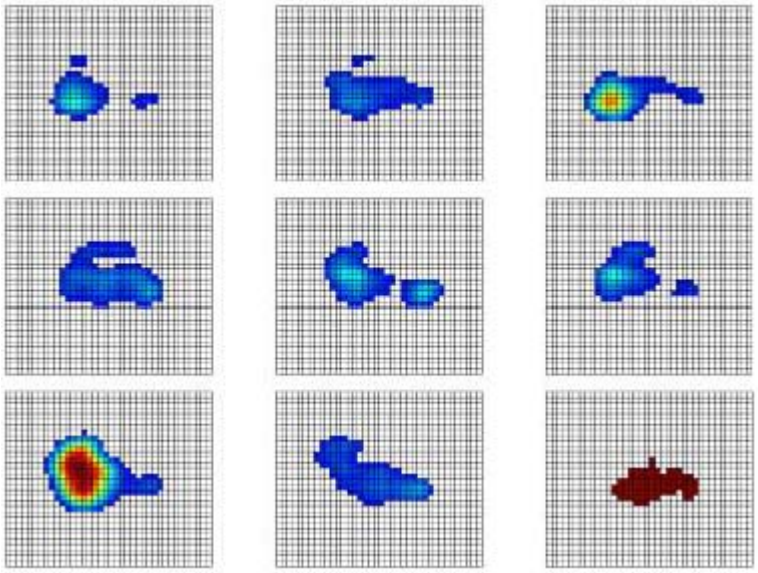

Figure 127 – Simulated saturation maps after vertically averaging over the Marly for the first 8 members of ensemble B before history matching to the observed map at 2002 (bottom right).

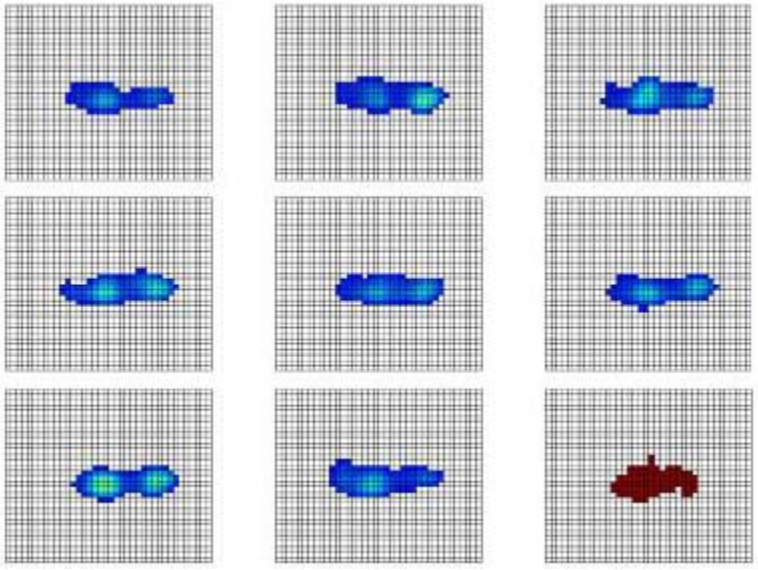

Figure 128 – Simulated saturation maps after vertically averaging over the Marly for the first 8 members of ensemble B after history matching to the observed map at 2002 (bottom right).

Ensemble C

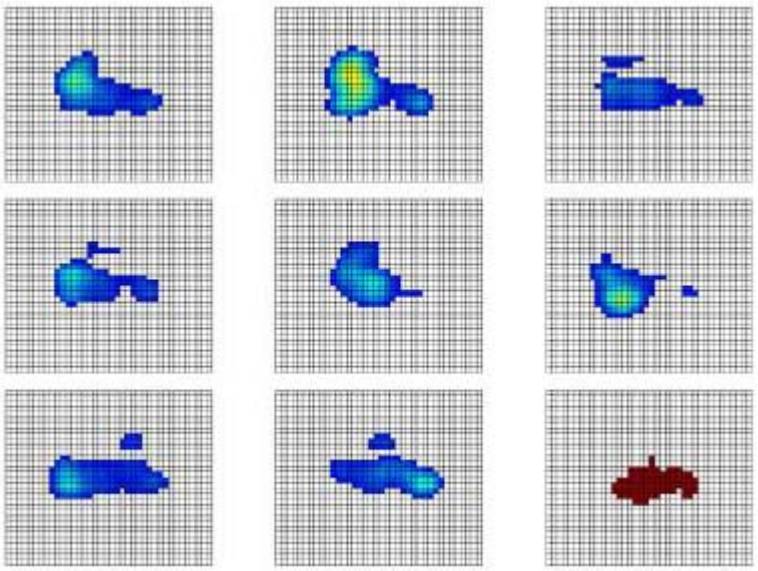

Figure 129 – Simulated saturation maps after vertically averaging over the Marly for the first 8 members of ensemble C before history matching to the observed map at 2002 (bottom right).

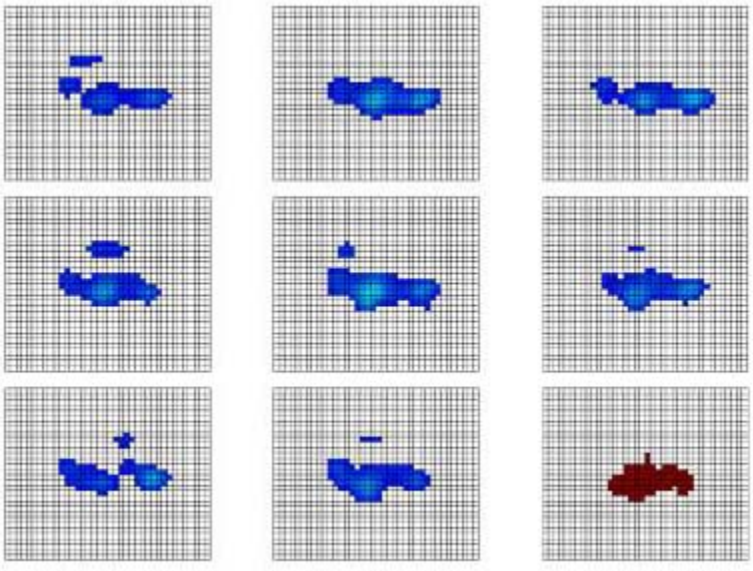

Figure 130 – Simulated saturation maps after vertically averaging over the Marly for the first 8 members of ensemble C after history matching to the observed map at 2002 (bottom right).

Ensemble D

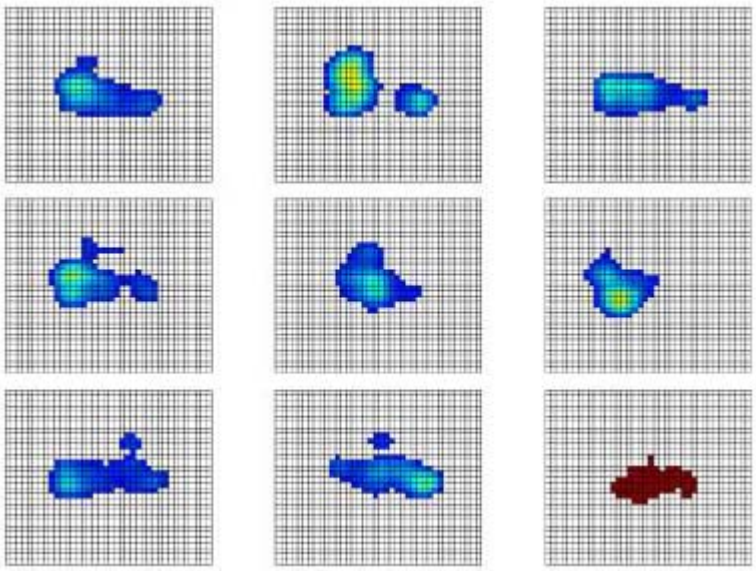

Figure 131 – Simulated saturation maps after vertically averaging over the Marly for the first 8 members of ensemble D before history matching to the observed map at 2002 (bottom right).

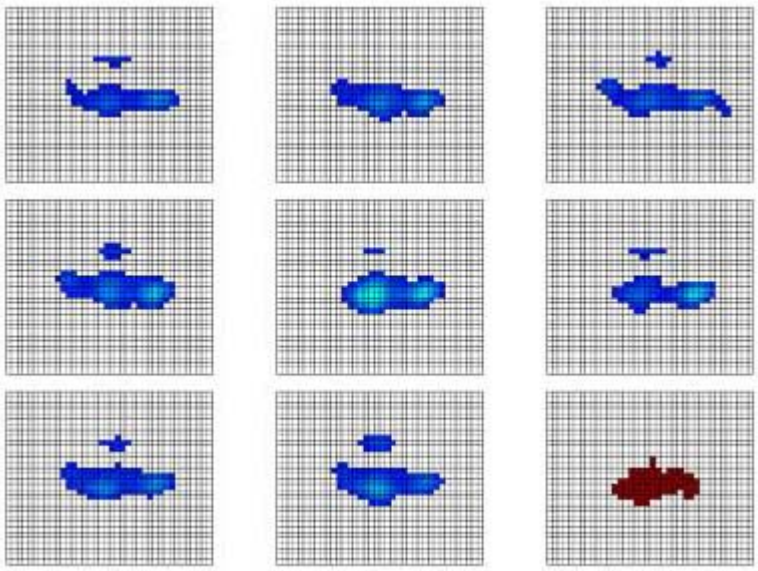

Figure 132 – Simulated saturation maps after vertically averaging over the Marly for the first 8 members of ensemble D after history matching to the observed map at 2002 (bottom right).

A number of observations can be made. First of all, in all cases, the initial predictions of the CO_2 saturation distributions are very variable. The large variability before history matching suggests that the porosity and permeability realizations are sufficiently different that they might be

combined in such a way that the observed map can be recovered. If the variability would be very small, such that all members simulated more or less the same response, there would be no hope of recovering the measured response through combination of the member inputs (i.e. the grid properties). However, a second observation is that none of the prior predictions are particularly similar to the interpreted map, which could mean that the ensembles are not sampling the correct uncertainty subspace. The saturation response before history matching does not always consist of a single continuous swept area, but two or three patches can be observed in some cases. This may complicate the update somewhat since a unique measure of distance between simulated and observed front can no longer be made. The history matching code was modified in order to ensure that single isolated front cells are not taken into account, i.e. the distance field is only based on fronts that consist of more than one connected cell. Ensemble B and C appear to perform best in terms of reproducing the area swept by the CO_2, and to a somewhat lesser extent, the shape of swept region. The area is best reproduced by ensemble B, while it performs slightly worse in reproducing characteristic features of the shape of the contour.

Further experiments indicated that the results of a history matching based on the alternative interpretation do not look very promising.

History matching to production data

The results do not indicate a major improvement in the fit. In fact, the fit seems worse than that resulting from the use of the seismic maps. This can most likely be ascribed to the fact that the starting ensemble did not adequately capture the measured production data.

History matching to production and seismic data

The simulated CO_2 saturation distribution (after vertical averaging and smoothing) is fairly similar for the different ensemble members. All members show a single connected area with the highest values on its left side. The similarity with the observed map is less good than for the case with seismic data only, which may be expected based on the synthetic data experiments which also showed the best results for the seismic-data-only scenario. This impression is confirmed by the statistics computed over all 80 members which further indicates a general 'flattening' of the shape of the CO_2 flooded area after history matching, but also an extension towards the left and right. This might be a general re-distribution of CO_2 that was positioned further towards the top of the domain before history matching but this has not been confirmed in detail. Figure 133 below shows the decrease in the combined root-mean-square data mismatch over all 8 iterations.

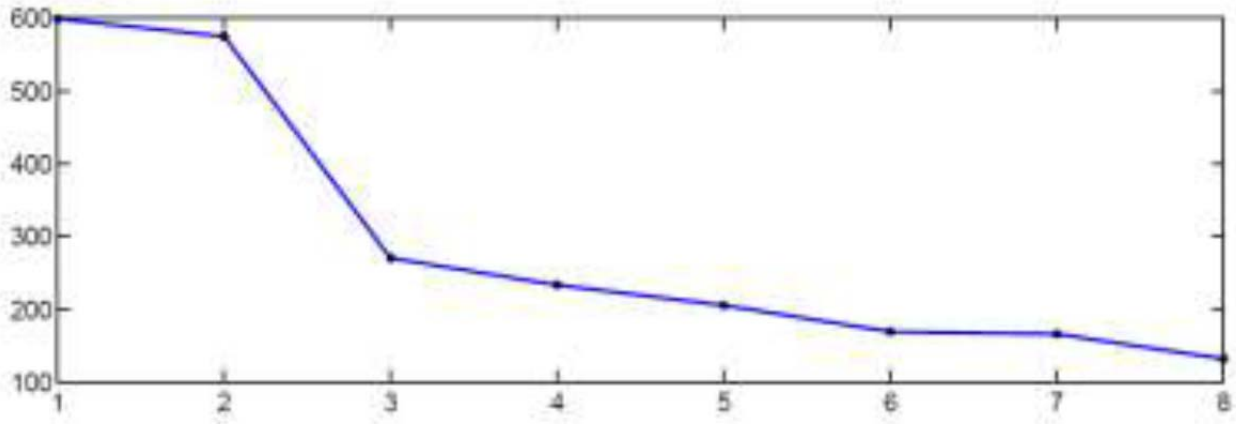

Figure 133 – RMS data mismatch (vertical axis) evolution over all iterations (horizontal axis) for the experiment with combined use of seismic and production data.

The mismatch for iteration k was computed as follows:

$$\mathrm{rms}_k = \frac{1}{n}\sqrt{\sum_{j=1}^{n}\frac{1}{N}\sum_{i=1}^{N}\frac{\left(d_j^i - y_j\right)^2}{\sigma_j{}^2}}$$

where the indices i and j loop over all ensemble members and measurements respectively, yj are the measurements, σj are the error standard deviations for those measurements, and dji denote the simulated measurements for each ensemble member. The normalization by the measurement error, allows the combination of the mismatches for different measurement types into one measure.

The results indicate a 78% reduction in the combined mismatch as evaluated over all ensemble members. The trend of the curve suggests that a further reduction should be possible if more iterations were performed. We also show below the mismatch reduction for the experiment based on seismic data at 2002 only. This experiment was run for 4 iterations and delivered a reduction of the RMS mismatch measure of 57%.

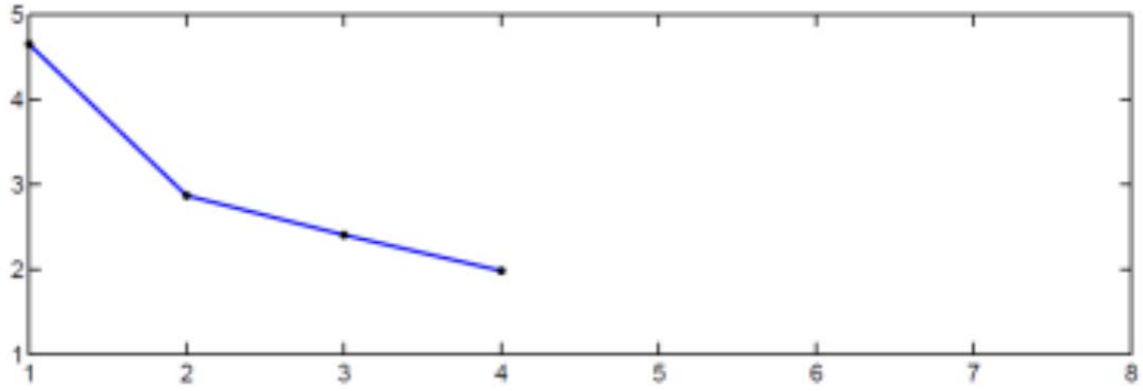

Figure 134 – RMS data mismatch evolution over all iterations for the experiment with use of seismic data only.

Task 7 - Sensitivity experiments

Initial state

It can be observed that some features of both the production and seismic data are not reproduced by any of the sector models. Therefore the main assumptions underlying the described approach were revisited. The model realizations were created by perturbing only the permeability and porosity of the grid cells. This implicitly suggests that uncertainties in other rock and fluid model parameters can be neglected. Furthermore, the initial state at 1 December 1999 and the boundary conditions were the same for all sector model runs. This can be interpreted as implicitly assuming that the initial state and conditions at the sector boundary are either exactly known, or that the errors in them do not have an impact on the dynamic state in the sector after 1999. The initial state assumption is perhaps the strongest and most likely to be wrong since it can be expected to be directly affected by the permeability and porosity, which are known to be uncertain.

Neglecting for the moment the possibility of incorrect data, it appears likely therefore that other aspects of the simulation model should be reassessed in order to improve the match to measured data.

Measurement error

All model ensembles have been run with the historic liquid production and injection rates imposed as targets. These rates have been measured in the field and therefore presumably contain measurement errors. In the following we have simulated the reference sector model ten times with 10% relative error imposed on the liquid rates. That is, different uncorrelated random errors sampled from a Gaussian distribution with standard deviation equal to 10% was added to the measured rate. The possibility of errors being correlated over time, which could have a larger impact, was not considered.

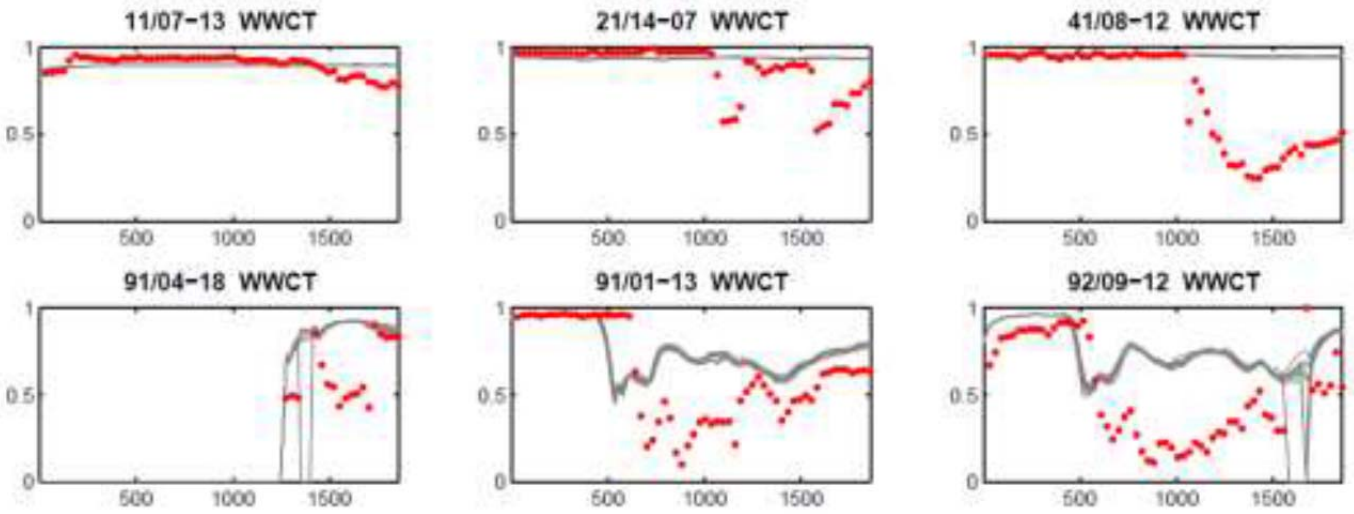

Figure 135 – Water-cut at selected producers for 10 runs with perturbed liquid rate targets

It was noted that the observed peaks in gas production in the measured historic data are generally followed by a strong reduction in the gas rate. This behaviour generally suggests interference by the operator. However, in the data this reduction in gas rate is not always accompanied by a reduction in water or oil rate. It could not be verified from the provided data if any well activities were actually performed.

Summary Conclusions

In this report the results are described of a set of history matching experiments conducted as part of the SaskCO_2User project on inversion of time-lapse seismic data from the Weyburn field for permeability and porosity. The experiments were conducted on a sector model for a single well pattern carved out of a larger coarse-grid model containing 9 patterns. The sector model has closed boundaries and the initial state is taken from a full-model simulation. Simulation of the sector model produced results of comparable quality as the full model, as determined in terms of qualitative differences with historic well data.

The seismic history matching approach applied in this report is based on identification of the CO_2-oil front position in both the data and in the model simulations and minimization of the distance between these front positions. This approach is innovative and has not been used before on a real field, nor in combination with real seismic data. The algorithm used to minimize the differences between models and data is a version of the Ensemble Kalman Filter, the Ensemble Smoother with Multiple Data Assimilation (ES-MDA).

Four different sets (ensembles) of realizations of permeability and porosity were generated. These realizations were all constructed by modification of a reference field which was taken to be the property field of the available 9-pattern model. The geo-statistics of these modifications

were estimated from this same model and resulted in random perturbations that were applied in slightly different ways in the four ensembles.

One of the four ensembles was used in a set of experiments with synthetic data. One model realization from the ensemble was designated as the synthetic truth and was used to generate synthetic measurements, while the remaining model realizations were used in the history matching workflow. Both seismic and production data were incorporated. We considered two situations with regard to the seismic data availability and quality:

1. time-lapse seismic maps are available for the Marly and Vuggy separately, or
2. only a single map is available that represents the combined response of the Marly and Vuggy.

The results show that in all cases the updated models were able to reproduce the synthetic measurements with much greater accuracy than before history matching, with reasonable values for the permeability and porosity updates. An experiment in which also production data were included produced a compromise result in terms of the fit to the seismic maps and to the well data. The history matching experiments used an ensemble of 50 realizations, each of which were simulated for 4 iterations over the history period, thus requiring a total of 200 simulations runs, which compares favourably with earlier reported approaches.

The real historic well data that were used in the final experiments were extracted from the schedule file of the provided simulator deck and included liquid rate, watercut, and gas-oil ratio. No dynamic pressure data were available. The time-lapse seismic information was extracted from published maps of amplitude changes. The travel-time changes were judged not to contain additional information. All four TNO ensembles of model realizations were considered in the final experiments based on the historic measured data. An initial series of experiments was conducted in which only the interpreted time-lapse seismic data for December 2002 were included.

These seismic data are considered to be more reliable than those for 2001 and 2004. These experiments suggested that it might be possible to constrain the models to some extent, since either the flooded area, or in some cases, specific features of the shape of this area, could be better reproduced after history matching. Based on these experiments, ensembles A and D did not appear to deliver much added value and were discarded during later experiments. Incorporation of the 2001 and 2004 seismic data maps did not produce useful results. Also the match to production data from the sector domain did not significantly improve. An experiment with seismic data from 2002 and production data up to 2002 showed significant improvements in the quality of the history match.

An overall data mismatch reduction of 78% relative to the prior model mismatch could be achieved. It was observed that all prior models (i.e. from all four ensembles) showed poor

consistency with the measured data. This raised the question if the prior uncertainty can be adequately captured by considering only permeability and porosity. A number of sensitivity runs was conducted to investigate possible limitations associated with the set-up of the sector model. However, neither the use of well fractions on boundary wells, nor the impact of permeability uncertainty on the initial state for the sector simulations appeared to be able to explain the large prior differences with (production) data. Since a full sensitivity study falls outside of the scope of this report, we provide recommendations for further work that address the identification of remaining uncertainties.

Final conclusions can be consolidated into four key categories.

Quality and interpretation of the seismic data

- We were able to confirm that amplitude and travel time differences as computed from the provided seismic data cubes are consistent with maps published by White (2013).
- The signal amplitude is low.
- The maps show large differences with other published interpretations, notably Johnson and White (2012), which suggests that the interpretations are subject to large uncertainty.
- The maps show indications of CO_2 spreading that is non-monotonic with time. No clear explanation or confirmation for such behaviour has been found in the models, and may therefore indicate limitations in either data quality or in the model suitability. Isolated accumulations of CO_2 may be an indication of increased local vertical transport and accumulation, with intermediate CO_2 saturations being too low to be picked up by the seismic. Accurate representation of this behaviour in models would require correct positioning of high-vertical-permeability transport pathways, use of fine enough resolution, and properly tuned seismic simulation models (smoothing parameters, threshold values for observable CO_2 saturation changes). Matching of models to isolated accumulations of CO_2 may require further improvement of the history matching approach, which is ideally suited for a single monotonically increasing front.

Quality of the simulation model

- The resolution of the simulation model is low in comparison to the inter-well spacing, and the large size of the grid cells may lead to significant numerical dispersion.
- The consistency between model and data prior to history matching was rather low.
- The production data suggest that a number of well workovers may have taken place during the period of investigation. We were not able to confirm that modifications of wells or connections were properly implemented in the simulation model.

Synthetic data experiments

- The synthetic experiments showed that the history matching algorithm is able to produce many models that are consistent with observed front positions as interpreted from time-lapse seismic data.
- The match to synthetic production data improved also for models conditioned to only synthetic time-lapse seismic data.
- A combined match to time-lapse seismic shows that the history matching workflow is able to produce a compromise solution with improvements in the match to both seismic maps and to well data.

Historic data experiments

- Some features of both the time-lapse seismic and of the measured well data were not captured by any of the ensembles. This could mean one or more of several things:
    - The data contains large (possibly systematic) errors.
    - The uncertainty in permeability and porosity is not captured correctly by the starting ensembles.
    - There are uncertain factors other than grid cell permeability and porosity which have a significant impact on the dynamic response and are incorrectly represented in the model.
- It was found that a subset of the data (the 2002 time-lapse seismic map) could be reproduced after history matching more accurately than before history matching and more accurately than by the reference model.
- Additional use of production data up to 2002 resulted in a 78% reduction of the mismatch relative to the initial mismatch for the prior models. The match to seismic data was less good than for the experiment with seismic data only, in agreement with the results from the synthetic experiments.
- In all experiments a rather small error has been assumed in the identification of the front position. This was done primarily to demonstrate the potential of the algorithm. Use of more realistic (i.e. much larger) measurement errors might have resulted on model matches that are actually consistent with the data given their uncertainty.
- Sensitivity experiments did not indicate major shortcomings of our approach. The use of closed sector boundaries and a single initial state were found to not significantly impact the results. It could also be confirmed that the influence of measurement errors on the well targets in the simulations could be neglected.
- Finally, the implementation of vertical transmissibility multipliers on the layers separating the Marly and Vuggy did not improve the similarity with measurements, indicating that vertical upscaling of permeability probably did not affect the model outcome very much.

A number of follow-up activities are recommended in order to improve results and to extend the application of the developed workflow to a larger domain of the field:

- Improve the characterization of the uncertainties (errors) in the available measurements. This could contribute to an improved balancing of production and seismic data during the history matching and a more proper measure of the quality of the match.
- Improve the characterization of the uncertainty in the property variograms (i.e. uncertainty in the properties). The impact would be the same as for measurement uncertainties.
- Investigate the impact of model resolution and the representation of the natural fracture network. The current model may be too coarse to properly simulate the dynamics of flow in a fractured medium.
- Account for parameters other than permeability and porosity that may be relevant for obtaining a good match to all data. Examples could be thin layer vertical transmissibilities, relative permeability descriptions, near-well fracture network properties (e.g. through a skin), etc. We cannot also exclude the possibility that permeabilities in the field may have changed over time as a result of the CO_2

12.0 SaskCO_2USER (WMP Optional Phase) – Core Assessment

The purpose of core assessment is to investigate the effect of injected CO_2 on rock framework and the pore space in the Weyburn Midale reservoir. Two pressure observation wells with extensive cores have recently been drilled in the Weyburn field. This provides a unique situation to observe the influence of 15 years of injected CO_2 on the mineralogy and rock properties of the reservoir. Comparing the recently drilled wells to wells that were drilled prior to CO_2 injection will reveal effects of injected CO_2 on the reservoir matrix.

This field scale "laboratory" provides a rare opportunity to investigate the results of injected CO_2 on the reservoir at an active injection site leading to a better understanding of the response of the reservoir to CO_2 injection. The analytical techniques that are being utilized to determine if the injected CO_2 has impacted the reservoir include QEMSCAN to determine the mineralogy and porosity, SEM images, and cathodoluminescent analysis.

12.1 Core Assessment – Approach and Methodology

QEMSCAN operation and QC verification

The Quanta 650F QEMSCAN of the SRC AMC laboratory was operated using the "Field Stitched Analysis (FSA)" mode to measure the quantitative mineral modal abundance. Mineral grains are identified using back-scattered electron imaging and qualitative energy dispersive X-ray (EDS)

spectra are collected from each analytical point with a spacing of 20 µm. The individual EDS spectra are compared to the localized mineral database determined to be best suited for these samples for mineral identification.

12.2 Core Assessment – Results and Recommendations

Analytical statistics

Statistics from the QEMSCAN analyses are presented in Table 43. A minimum of 7,272,295 data points were analyzed per core.

Sample ID	4-30-6-13W2_M	4-30-6-13W2_V	10-30-6-13W2_M	10-30-6-13W2_V	SGS-101_M
Pixel spacing (µm)	20	20	20	20	20
Measurement Mode	Field Image	Field Image	Field Image	Field Image	Field Image
X-ray data points	11,954,890	12,037,225	12,028,848	12,858,693	12,262,568

Sample ID	SGS-102_V	SGS-103_M	SGS-104_V	SGS-105_M	SGS-106_V
Pixel spacing (µm)	20	20	20	20	20
Measurement Mode	Field Image	Field Image	Field Image	Field Image	Field Image
X-ray data points	7,272,295	11,598,112	8,106,643	11,312,141	12,906,875

Table 43 – QEMSCAN operational statistics

Modal Analysis

The modal analyses of the samples are shown in Tables 44 and 45 below and graphically in Figures 136 and 137.

The modal abundance is typically given in weight percent, but for the purposes of reporting the internal pore space both weight and volume percent are shown. This is because the modal percent of internal pore space is zero when looking at the modal abundance in weight percent as they have no mass. As such the abundances differ between the two ways of reporting the data.

Sample	4-30-6-13W2_M	4-30-6-13W2_V	10-30-6-13W2_M	10-30-6-13W2_V	SGS-101_M	SGS-102_V	SGS-103_M	SGS-104_V	SGS-105_M	SGS-106_V
Calcite	0.89	92.86	1.21	96.31	1.40	96.54	1.67	99.24	5.77	98.47
Calcite with Cl	0.00	1.85	0.00	0.17	0.00	0.19	0.00	0.11	0.01	0.10
Calcite with Na Cl	0.00	2.95	0.00	0.08	0.00	0.21	0.00	0.12	0.00	0.06
Celestine	0.00	0.00	0.31	0.00	0.45	0.01	0.02	0.00	0.05	0.00
Dolomite	95.56	0.86	93.91	1.21	67.31	0.09	78.39	0.04	81.55	0.09
Gypsum/ Anhydrite	1.08	0.92	1.04	1.93	14.97	0.83	8.49	0.01	4.04	0.12
Halite	0.01	0.05	1.57	0.00	0.16	0.28	0.08	0.16	0.25	0.13
K-Feldspar	0.49	0.07	0.17	0.02	1.18	0.08	0.85	0.02	0.93	0.12
Pyrite	0.13	0.05	0.21	0.09	3.69	1.17	1.91	0.06	3.57	0.18
Quartz	1.84	0.39	1.57	0.18	10.83	0.61	8.59	0.25	3.83	0.73
Pores	0.00	0.00	0.00	0.00	0.00	0.00	0.00	0.00	0.00	0.00

Table 44 – Modal abundances of minerals in weight percent

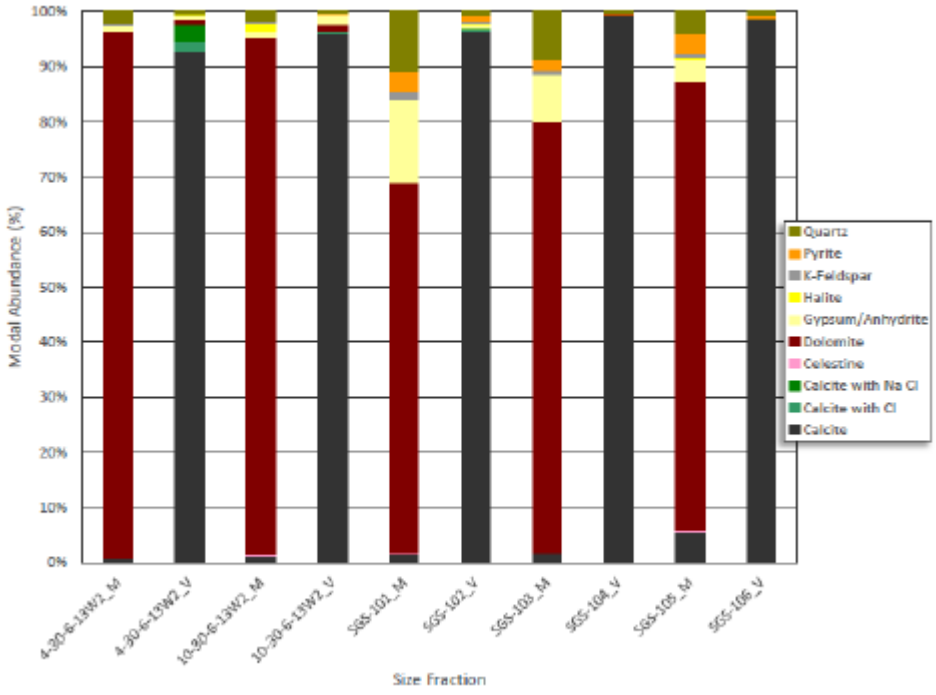

Figure 136 – Modal abundance (weight percent) of minerals analyzed by QEMSCAN

Sample	4-30-6-13W2_M	4-30-6-13W2_V	10-30-6-13W2_M	10-30-6-13W2_V	SGS-101_M	SGS-102_V	SGS-103_M	SGS-104_V	SGS-105_M	SGS-106_V
Calcite	0.93	90.89	1.25	91.86	1.46	94.06	1.76	95.71	5.89	74.43
Calcite with Cl	0.00	1.81	0.00	0.17	0.00	0.19	0.00	0.10	0.01	0.07
Calcite with Na Cl	0.00	2.89	0.00	0.08	0.00	0.21	0.00	0.11	0.00	0.04
Celestine	0.00	0.00	0.22	0.00	0.32	0.00	0.02	0.00	0.04	0.00
Dolomite	95.13	0.80	92.10	1.10	66.48	0.08	78.33	0.03	79.22	0.07
Gypsum/Anhydrite	1.03	0.82	0.98	1.68	14.19	0.74	8.14	0.01	3.76	0.08
Halite	0.02	0.06	2.02	0.00	0.20	0.34	0.10	0.19	0.32	0.12
K-Feldspar	0.54	0.07	0.19	0.02	1.30	0.08	0.95	0.02	1.01	0.10
Pyrite	0.07	0.03	0.12	0.05	2.07	0.62	1.09	0.03	1.97	0.07
Quartz	1.99	0.39	1.67	0.17	11.62	0.61	9.31	0.25	4.04	0.57
Pores	0.29	2.24	1.45	4.87	2.36	3.08	0.30	3.54	3.74	24.44

Table 45 – Modal abundances of minerals in volume percent

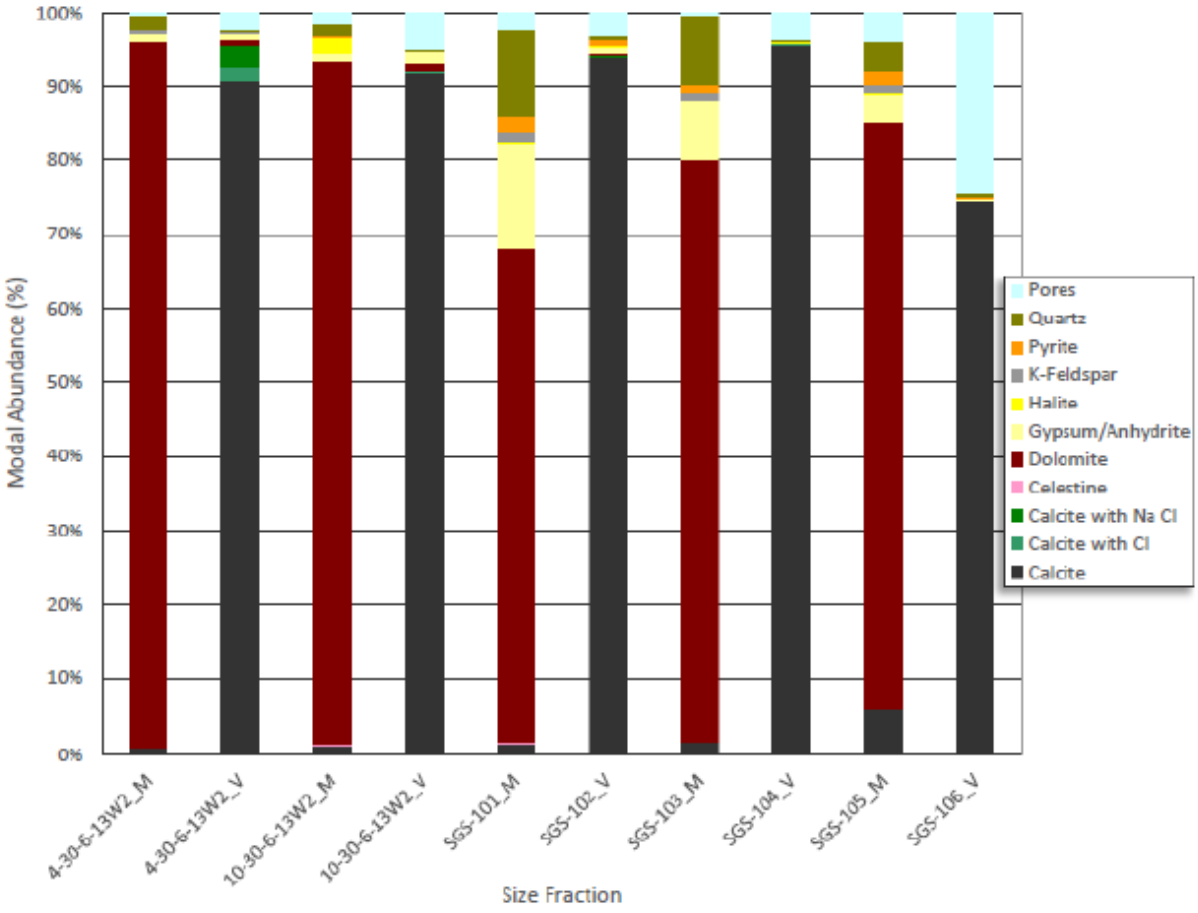

Figure 137 – Modal abundance (volume percent) of minerals analyzed by QEMSCAN

All Marley samples are predominantly dolomite, while all Vuggy samples are predominantly calcite. In the Vuggy samples very small halite inclusions are present, which show as Na and/or CL in the collected spectra. Halite itself was identified in trace amounts in all but sample 10-30-6-13W2_V. Gypsum/anhydrite was observed in all samples from very trace amounts (0.01wt.%) to 15wt.%. Quartz was observed in all samples from very trace amounts (0.2wt.%) to 11wt.%, along with trace amounts of K-feldspar and pyrite. Celestine was observed in minor amounts in the Marley samples 10-30-6-13W2_M, SGS-101_M, SGS-102_M, SGS-103_M and SGS-105_M.

While the Vuggy samples have large internal pore spaces, the Marley samples have a lot of smaller pores, which increase their porosity dramatically.

Observations

The volume of pore space doesn't consistently change from the pre-CO_2 wells to the post CO_2 wells. The variability in pore volume could be contributed to reservoir heterogeneity. The SEM images of the pre-CO_2 wells appear to have a overgrowth on the calcite crystals that are in the Vuggy samples while the calcite crystals in the Vuggy samples on the post CO_2 injection wells do

not have the same overgrowth and appear “clean.” Investigating the internal structure of the calcite crystals will determine if they formed after CO_2 injection or if they were already present. SEM images of the rock samples are provided.

Figures 138 to 147 are the scanned core images of the rock samples; these are provided to illustrate rock and pore texture and framework. Figures 148 to 157 are the false color QEMSCAN images of the cores; this display the lithology present in each sample. Figures 158 to 167 are the Overlain QEMSCAN and scanned core images; these show the location of the lithology on the core samples. Figures 168 to 174 are back-scattered electron images of both Vuggy and Marly core samples; the individual grain sizes and pores can be viewed in these images.

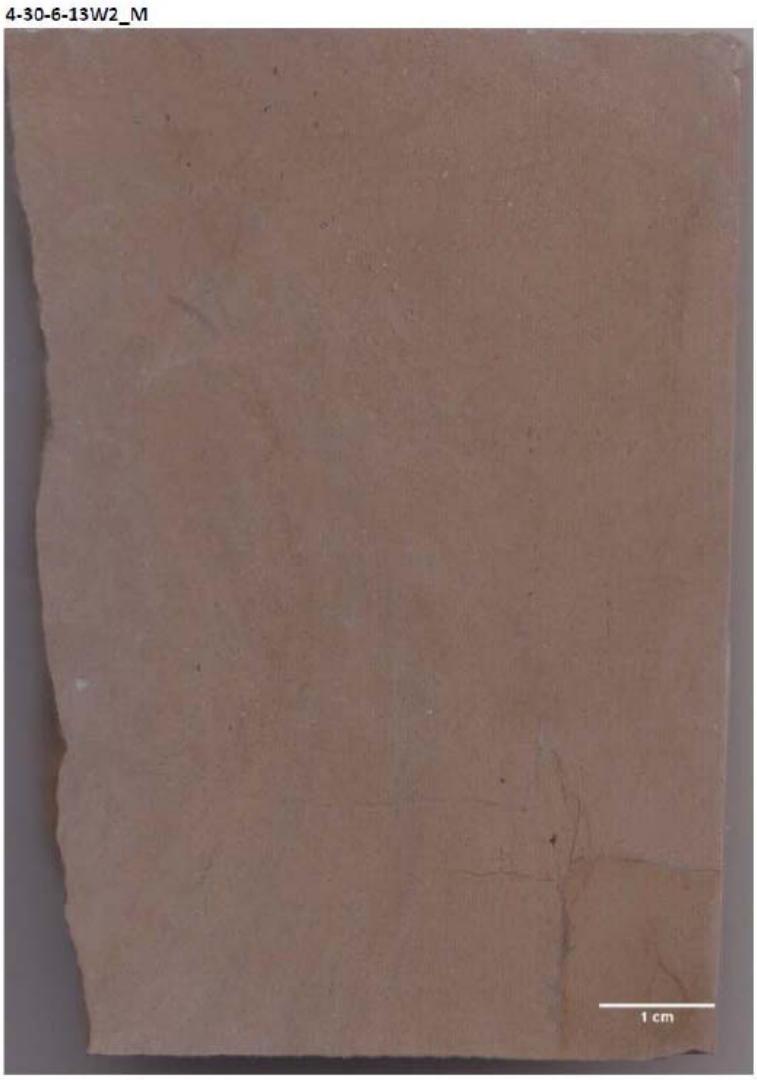

Figure 138 – Scanned core 4-30-6-13W2_M

Figure 139 – Scanned core 4-30-6-13W2_V

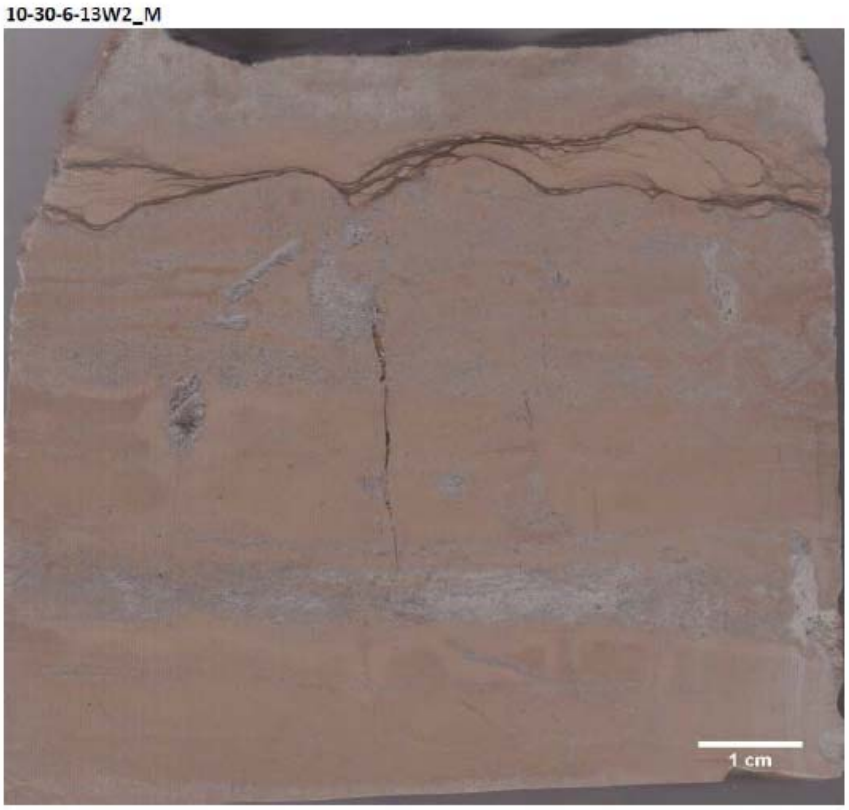

Figure 140 – Scanned core 10-30-6-13W2_M

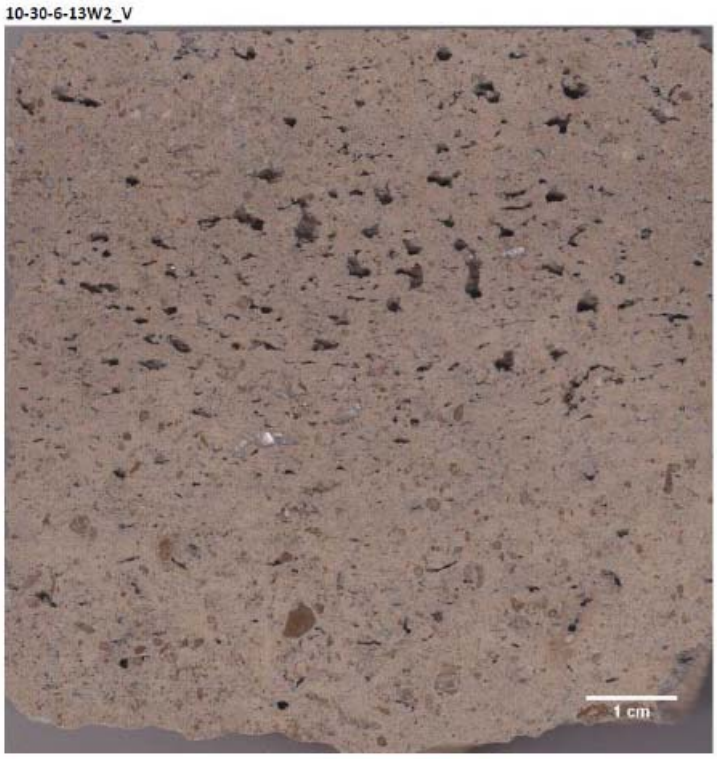

Figure 141 – Scanned core 10-30-6-13W2_V

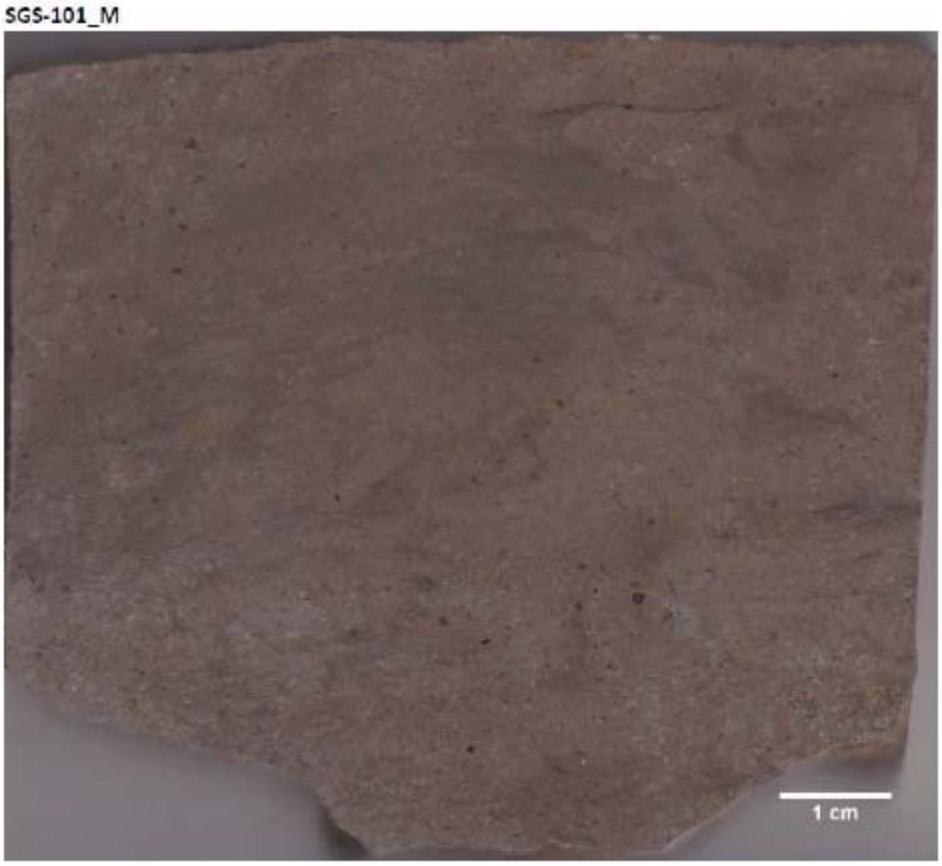

Figure 142 – Scanned core SGS-101_M

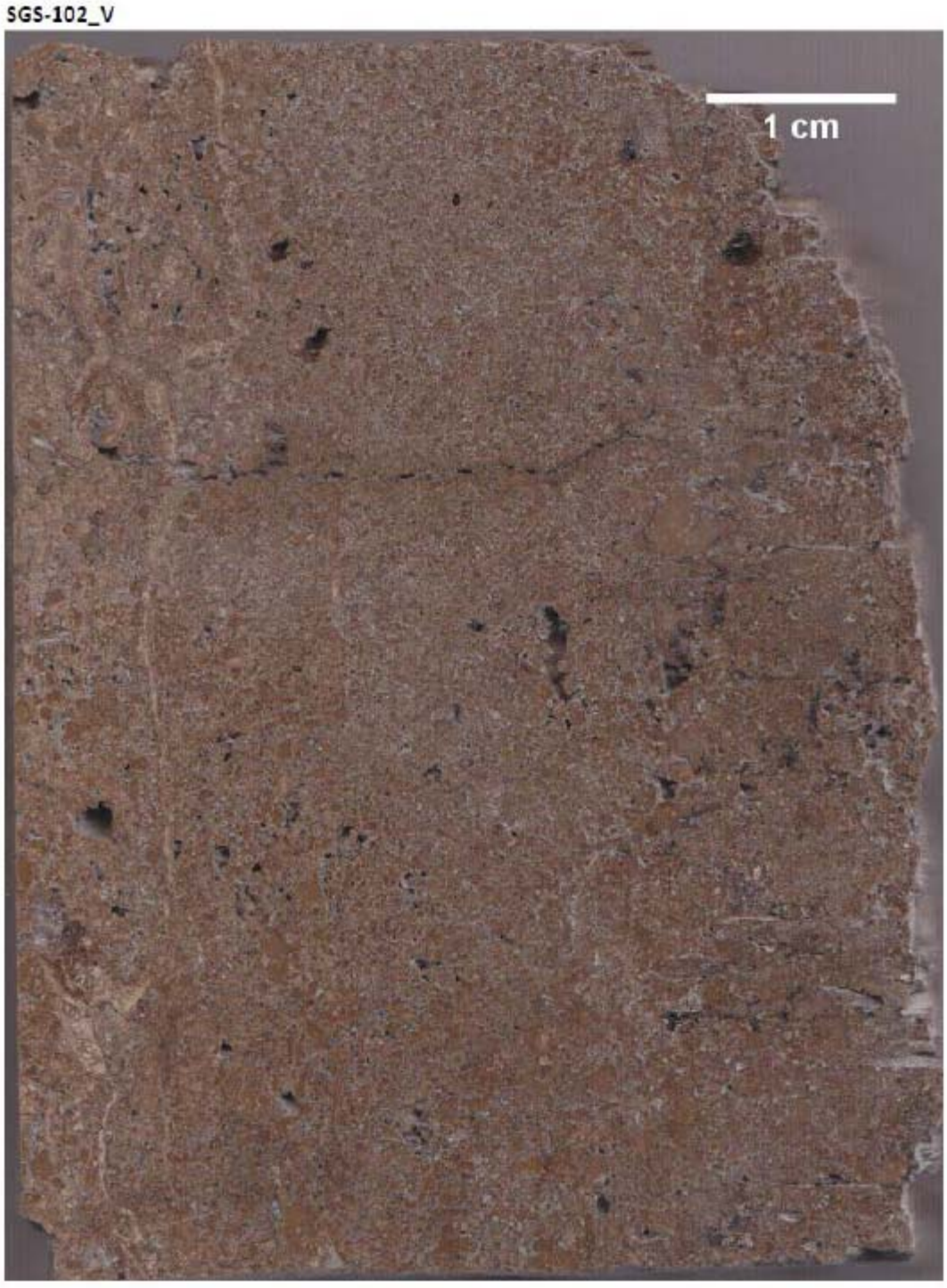

Figure 143 – Scanned core SGS-102_V

Figure 144 – Scanned core SGS-103_M

Figure 145 – Scanned core SGS-104_V

Figure 146 – Scanned core SGS-105_M

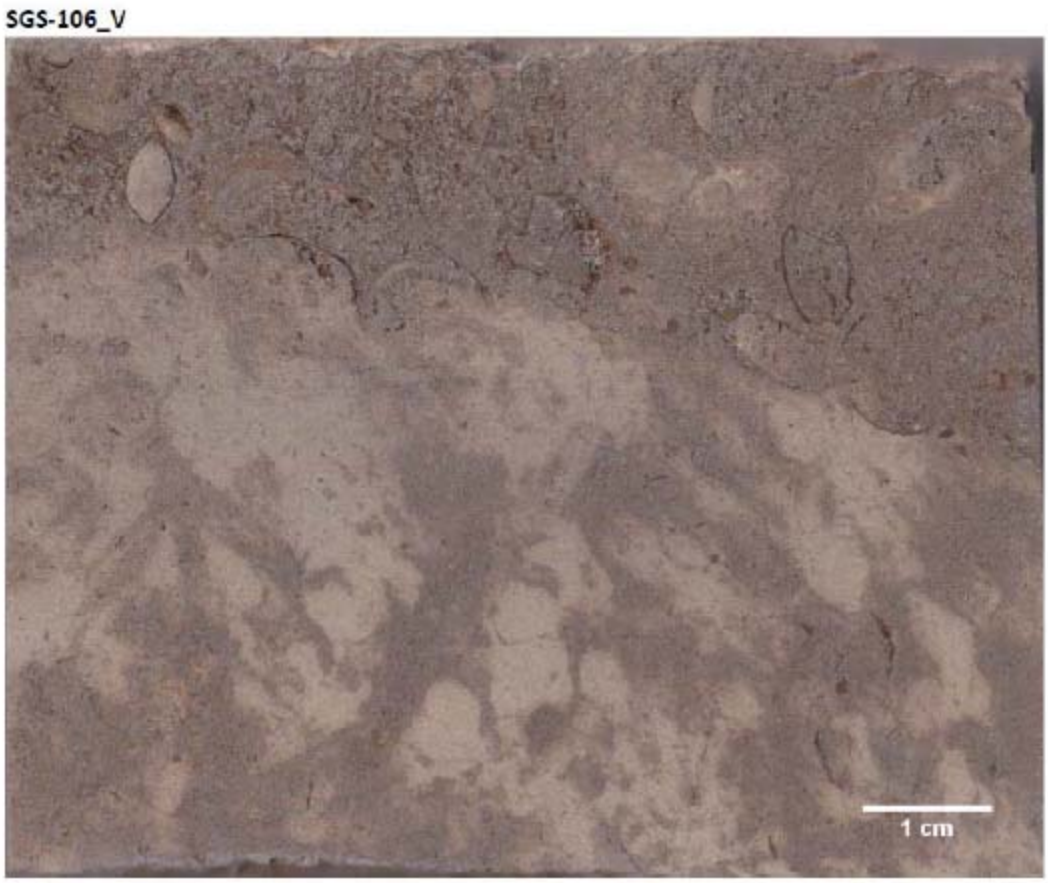

Figure 147 – Scanned core SGS-106_V

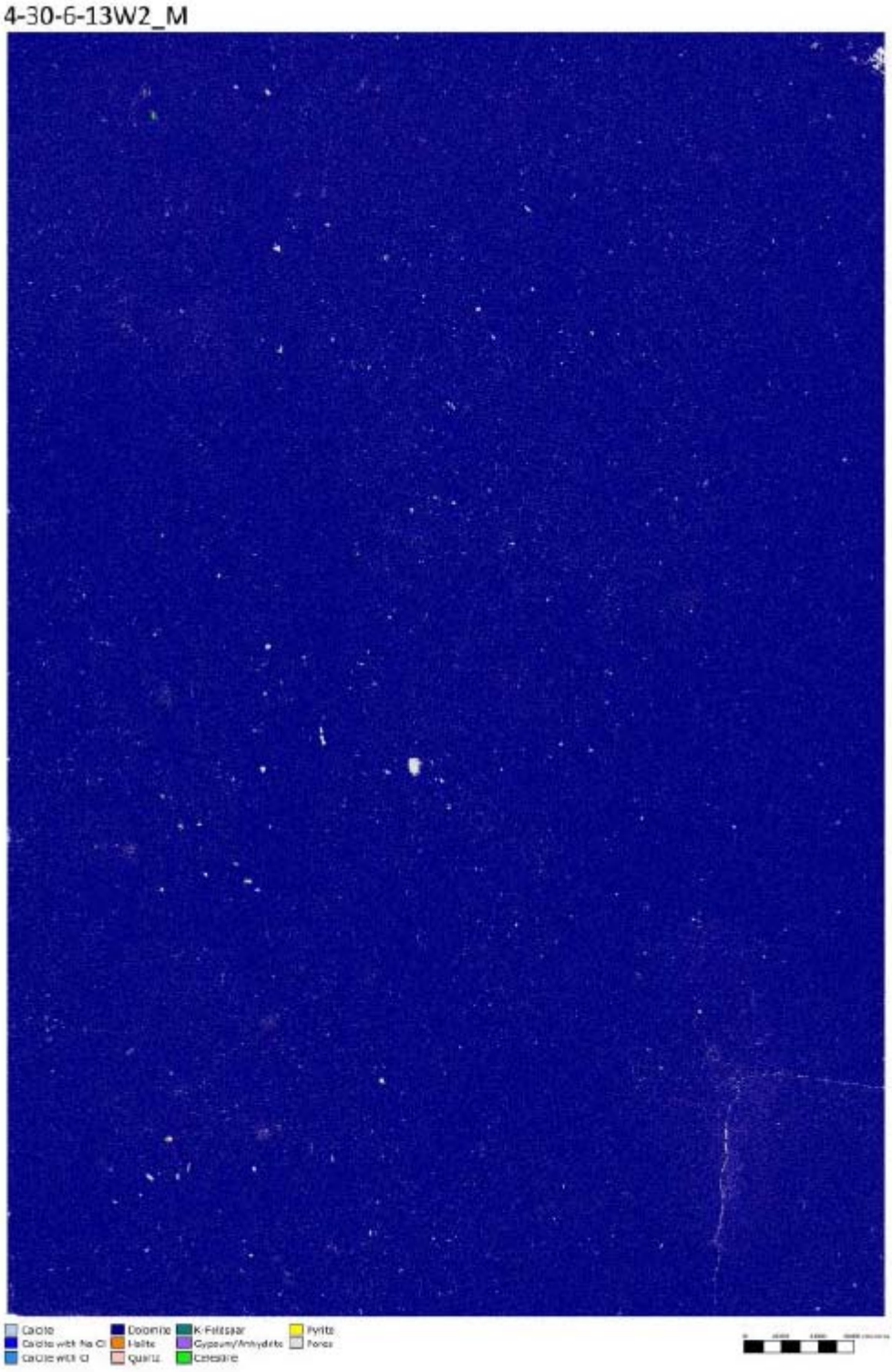

Figure 148 -- False colour QEMSCAN images of core 4-30-6-13W2_M

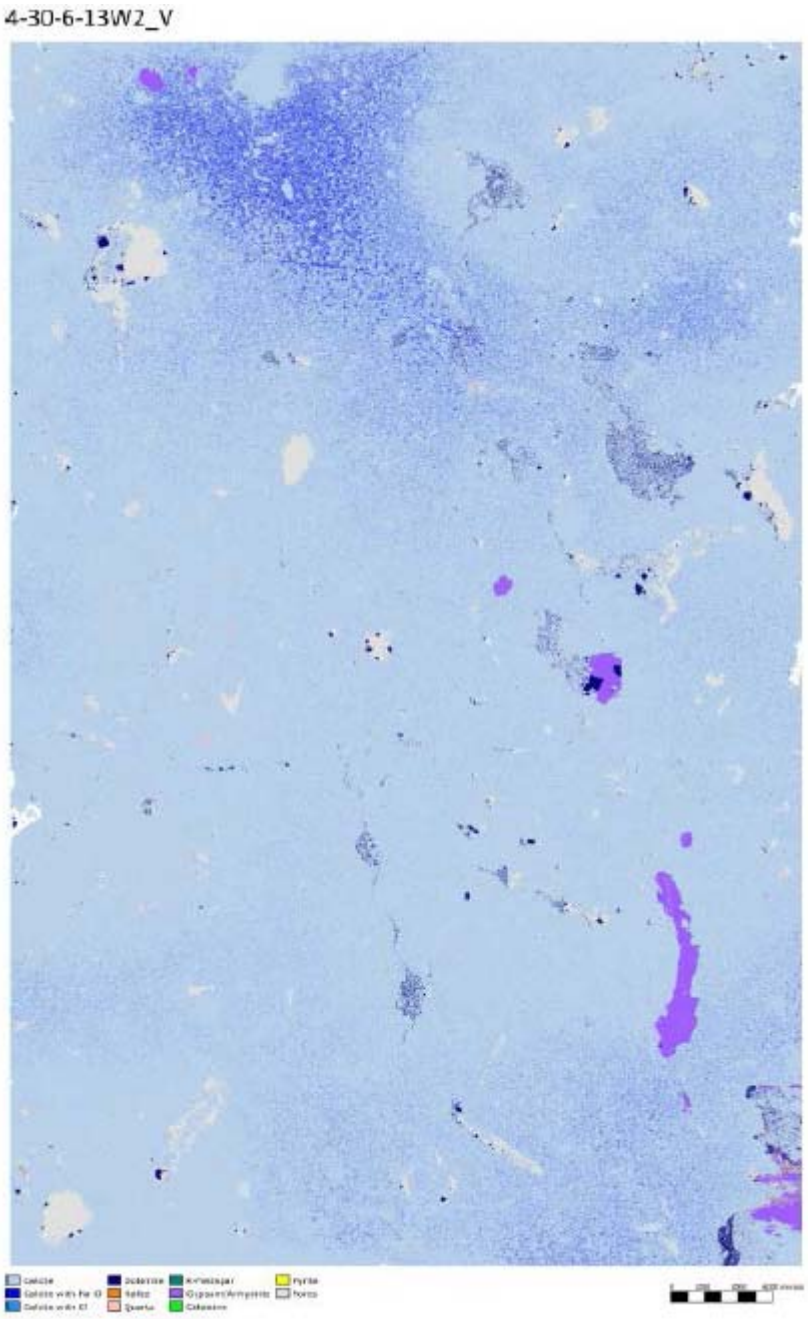

Figure 149 – False colour QEMSCAN images of core4-30-5-13W2_V

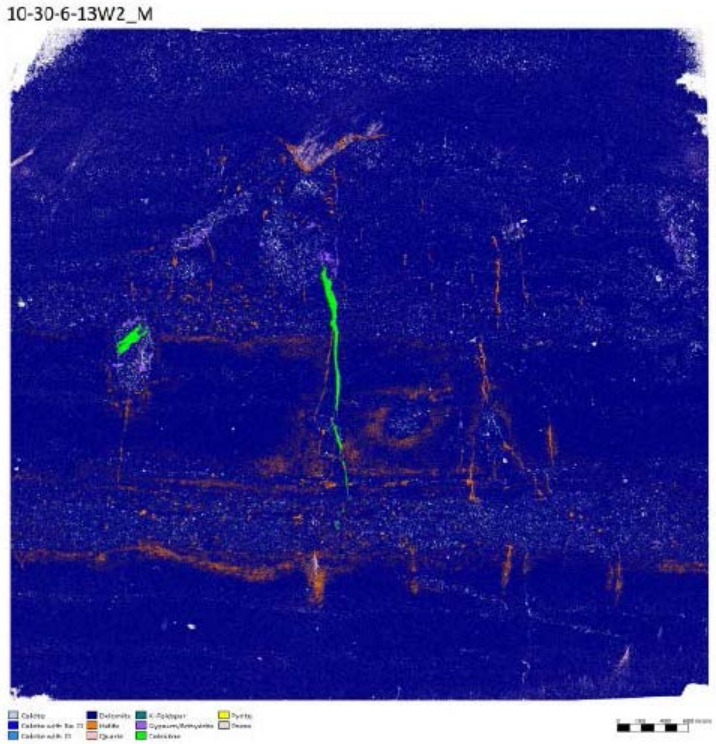

Figure 150 – False colour QEMSCAN images of core 10-30-6-13W2_M

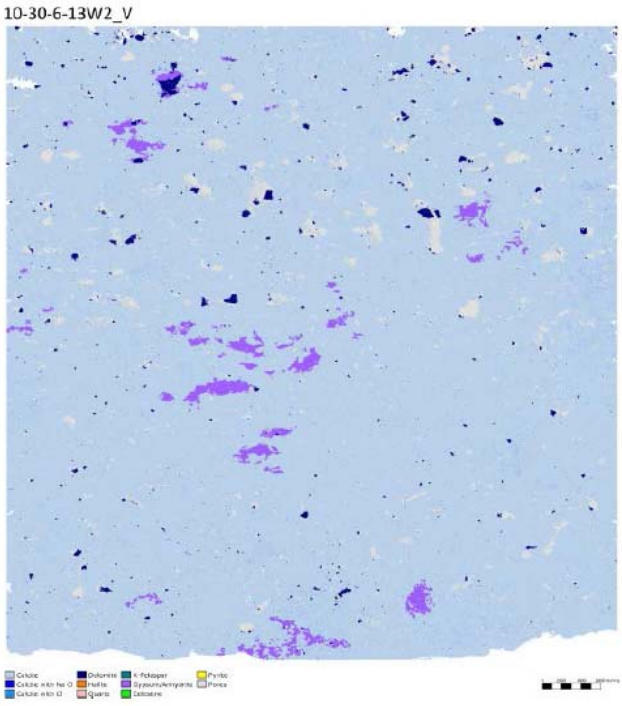

Figure 151 – False colour QEMSCAN images of core 10-30-6-13W2_V

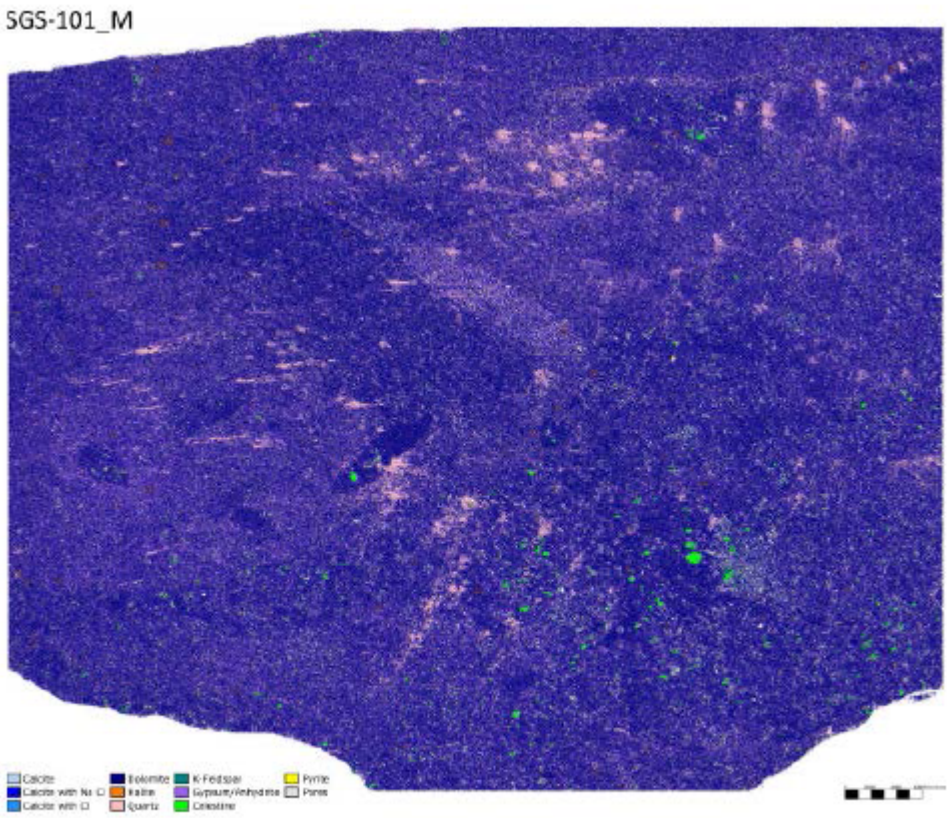

Figure 152 – False colour QEMSCAN images of core SGS-101_M

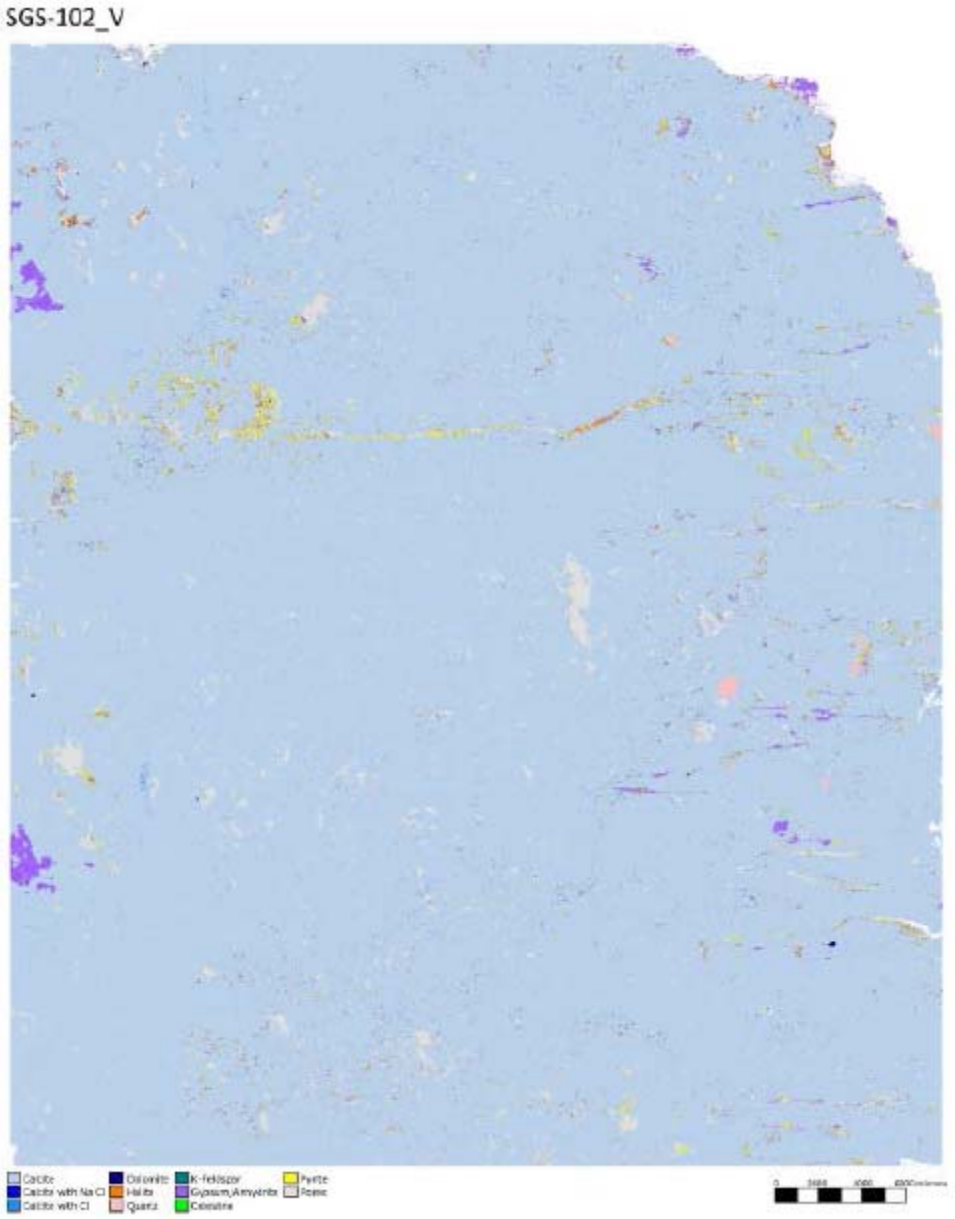

Figure 153 – False colour QEMSCAN images of core SGS-102_V

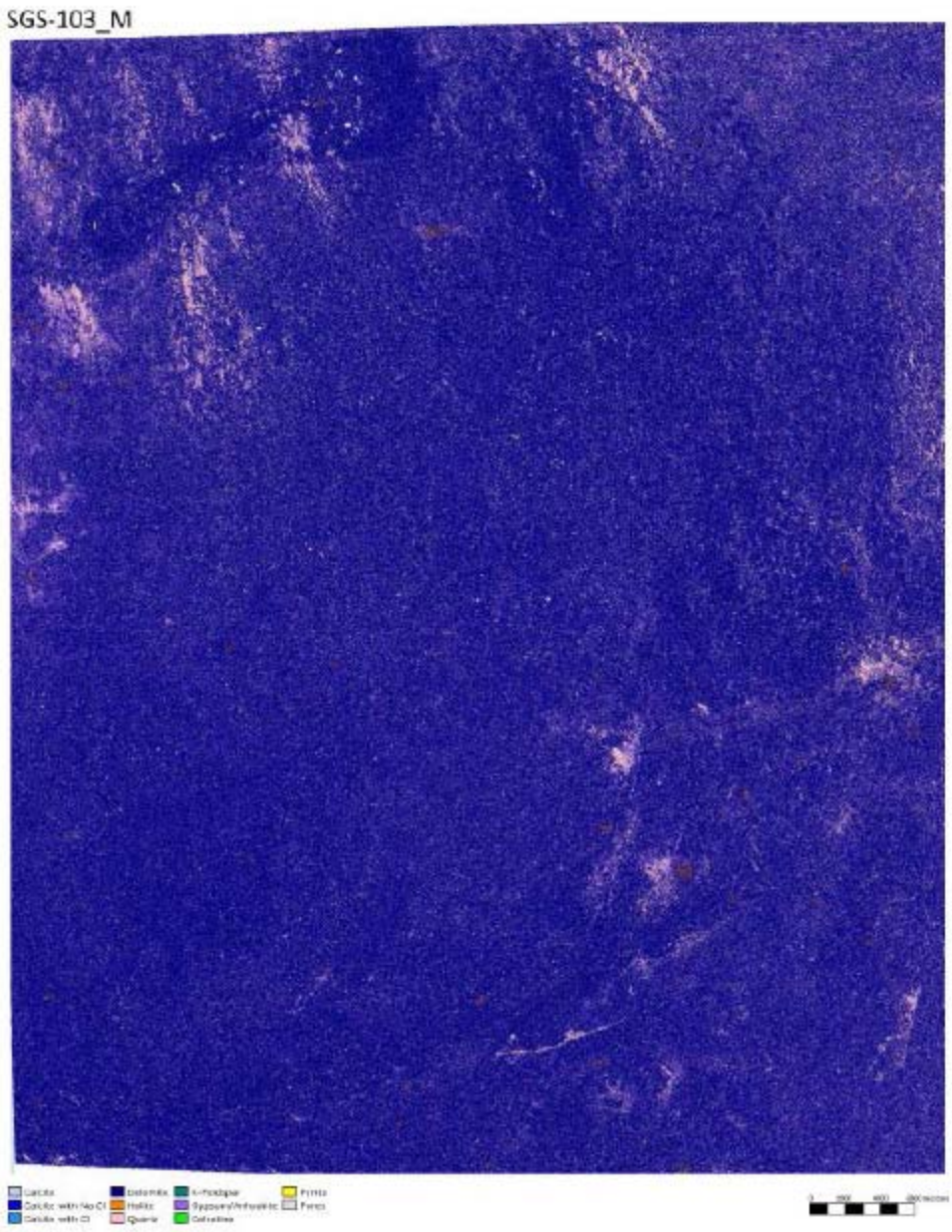

Figure 154 – False colour QEMSCAN images of core SGS-103_M

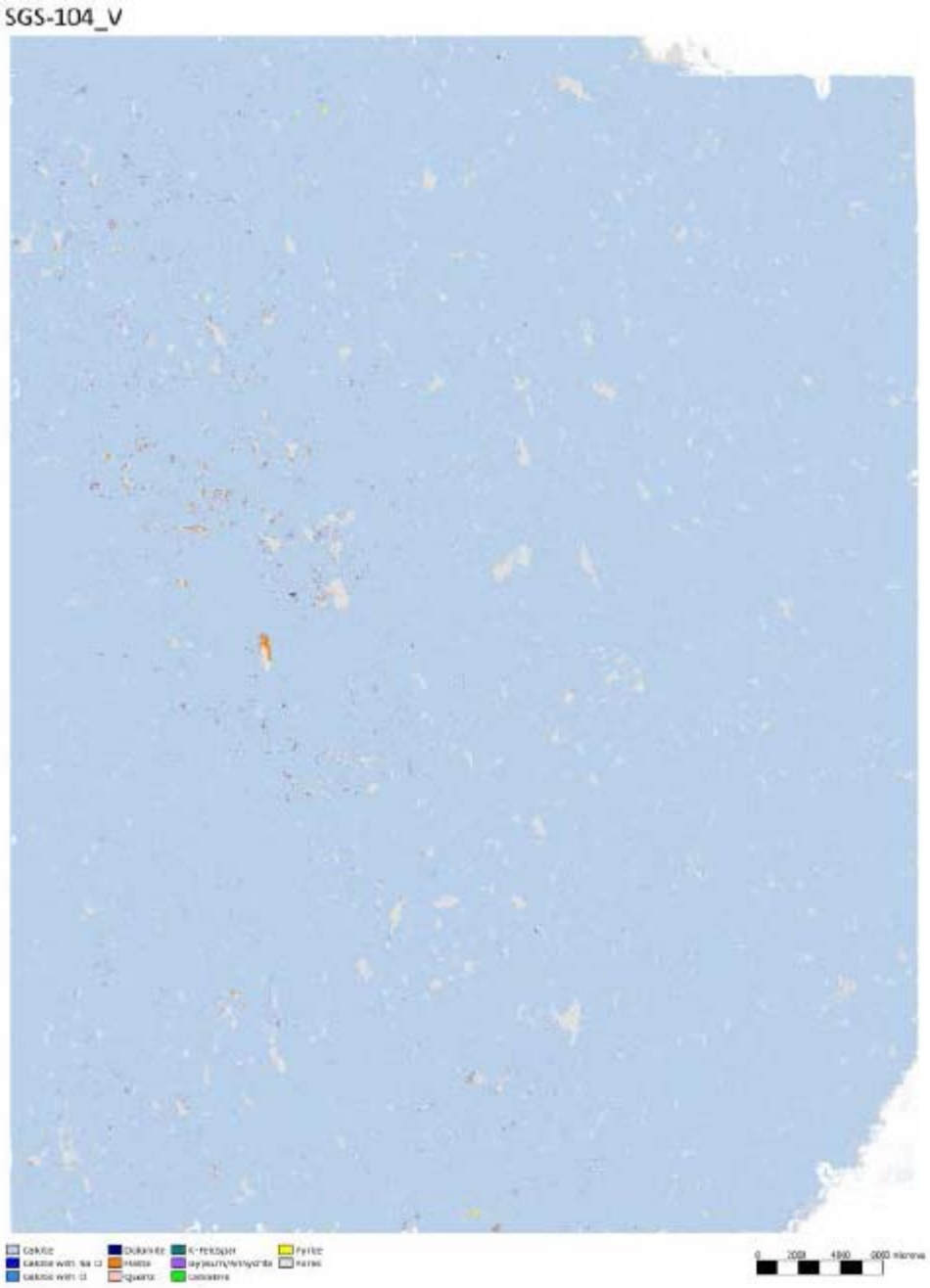

Figure 155 – False colour QEMSCAN images of core SGS-104_V

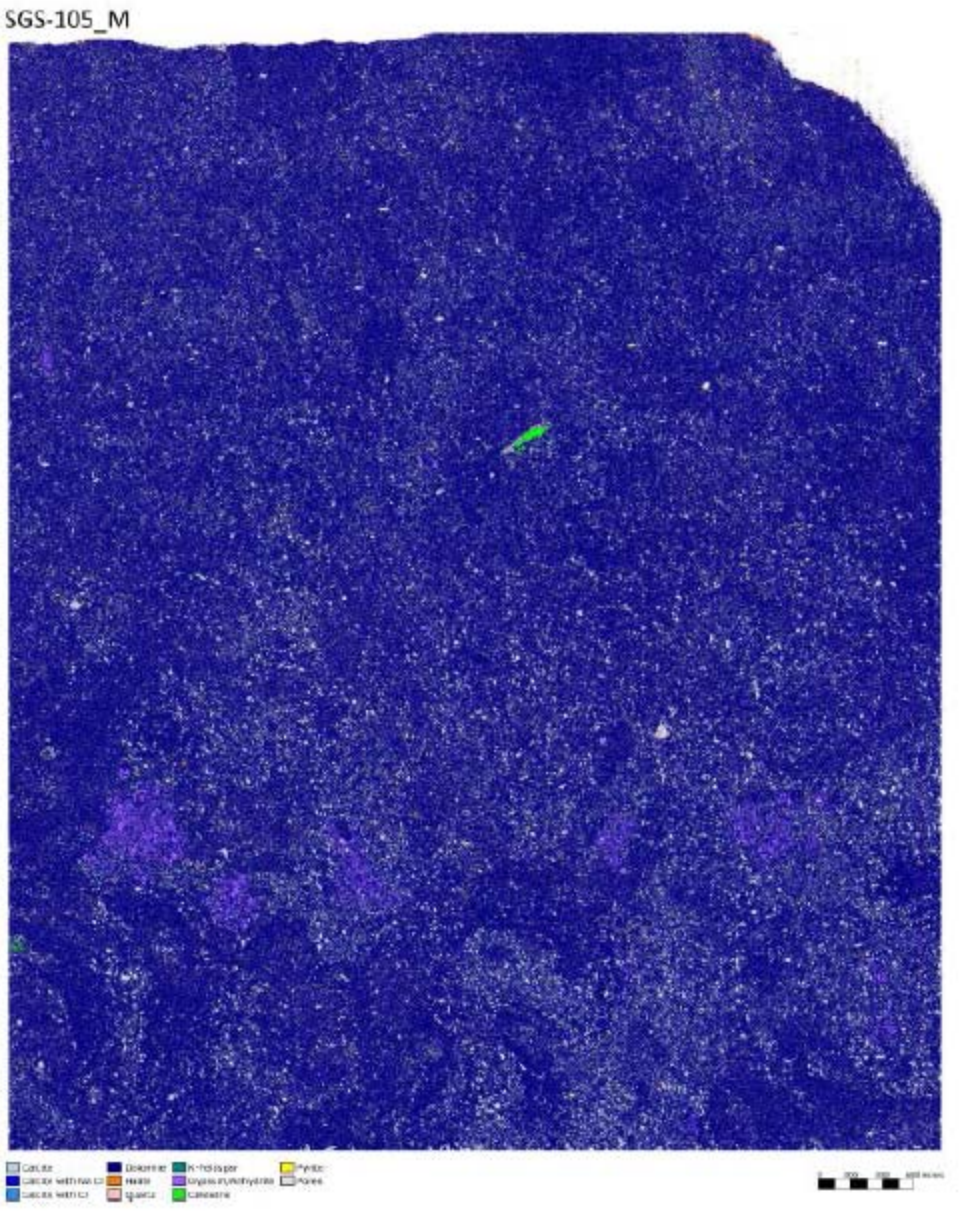

Figure 156 – False colour QEMSCAN images of core SGS-105_M

Figure 157 -- False colour QEMSCAN images of core SGS-106_V

Figure 158 – Overlain QEMSCAN and scanned core images 4-30-6-13W2_M

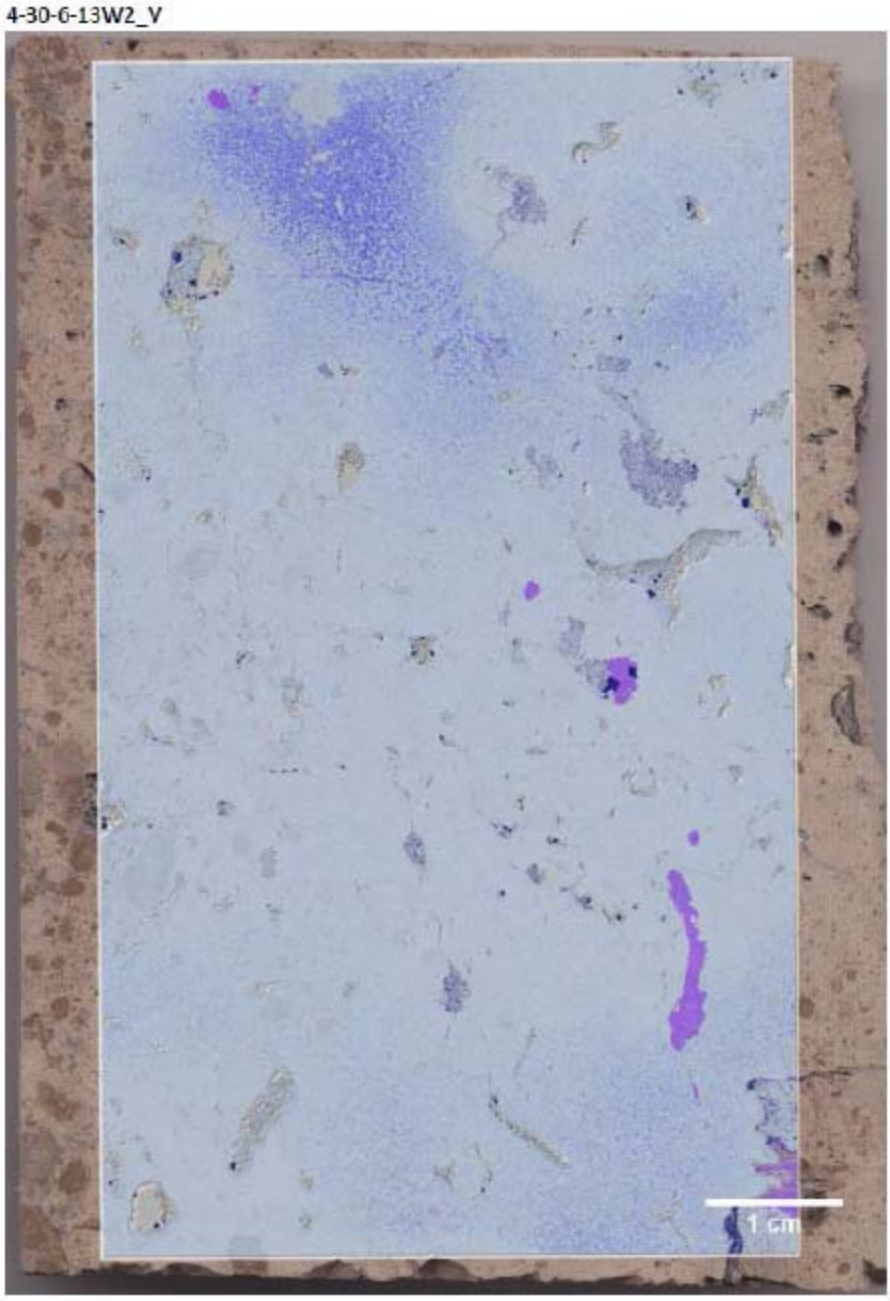

Figure 159 – Overlain QEMSCAN and scanned core images 4-30-6-13W2_V

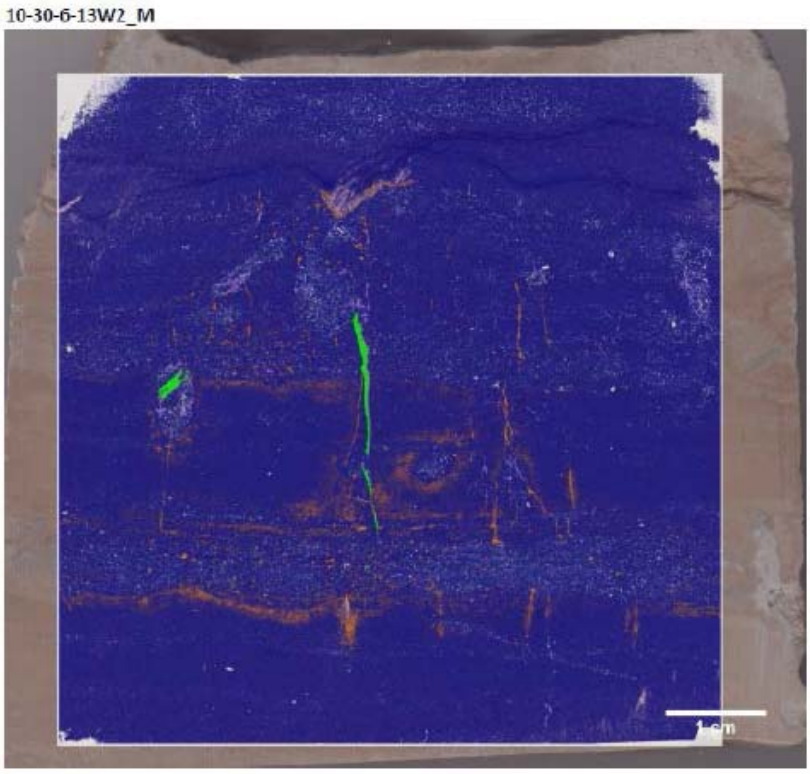

Figure 160 – Overlain QEMSCAN and scanned core images 10-30-6-13W2_M

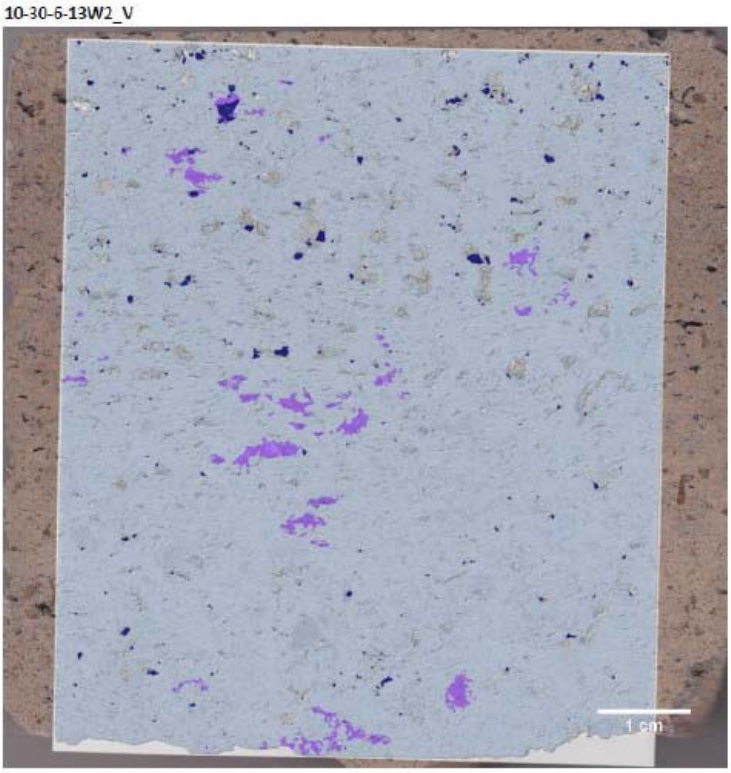

Figure 161 – Overlain QEMSCAN and scanned core images 10-30-6-13W2_V

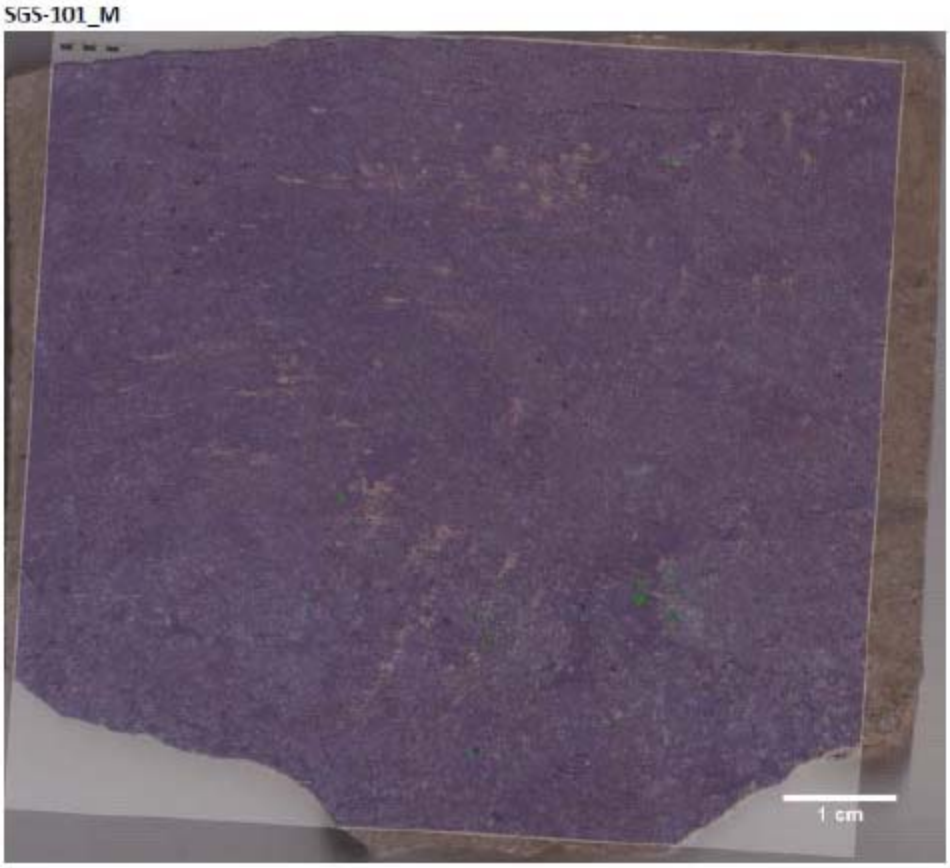

Figure 162 – Overlain QEMSCAN and scanned core images SGS-101_M

Figure 163 – Overlain QEMSCAN and scanned core images SGS-102_V

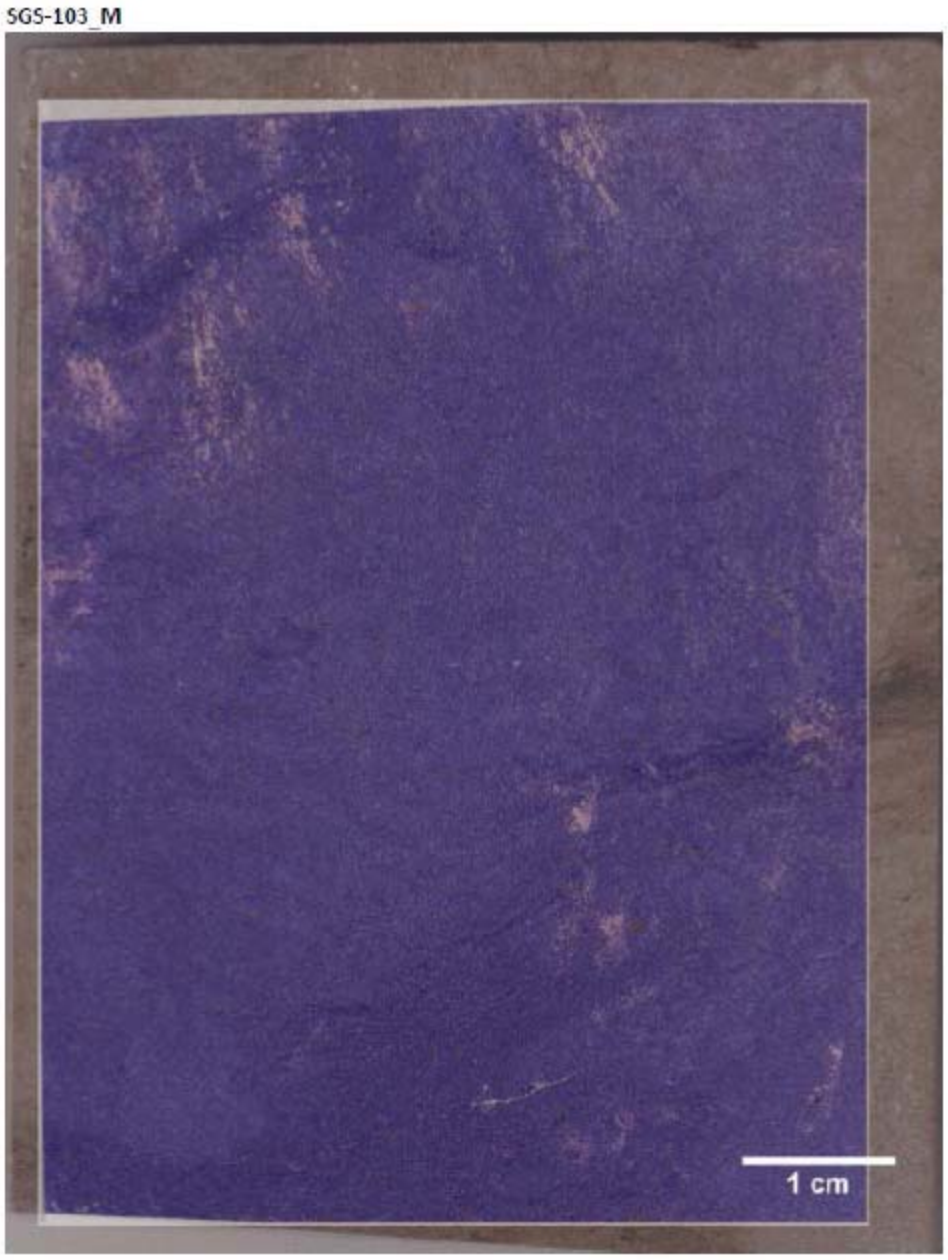

Figure 164 – Overlain QEMSCAN and scanned core images SGS-103_M

Figure 165 – Overlain QEMSCAN and scanned core images SGS-104_V

Figure 166 – Overlain QEMSCAN and scanned core images SGS-105_M

Figure 167 – Overlain QEMSCAN and scanned core images SGS-106_V

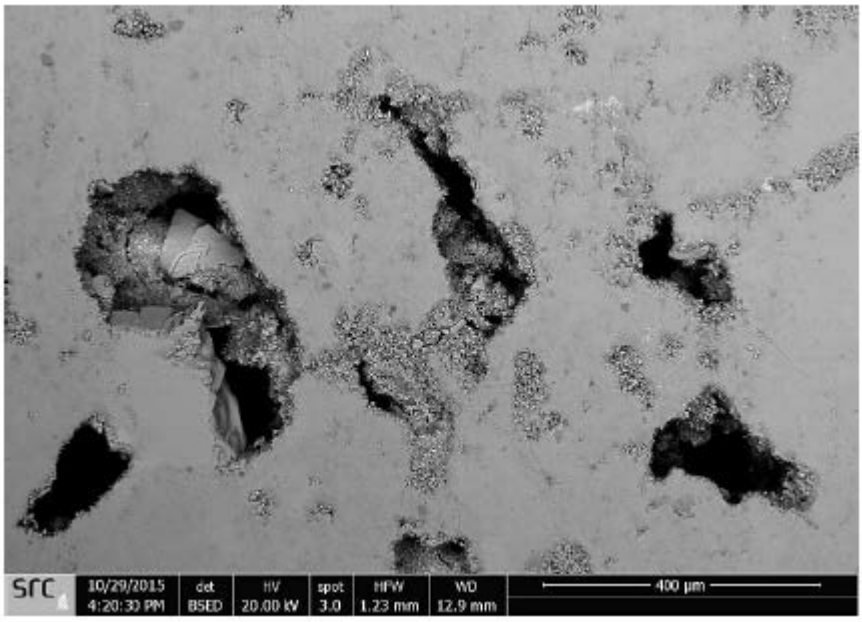

Figure 168 – Unfilled void spaces in Vuggy sample SGS-006

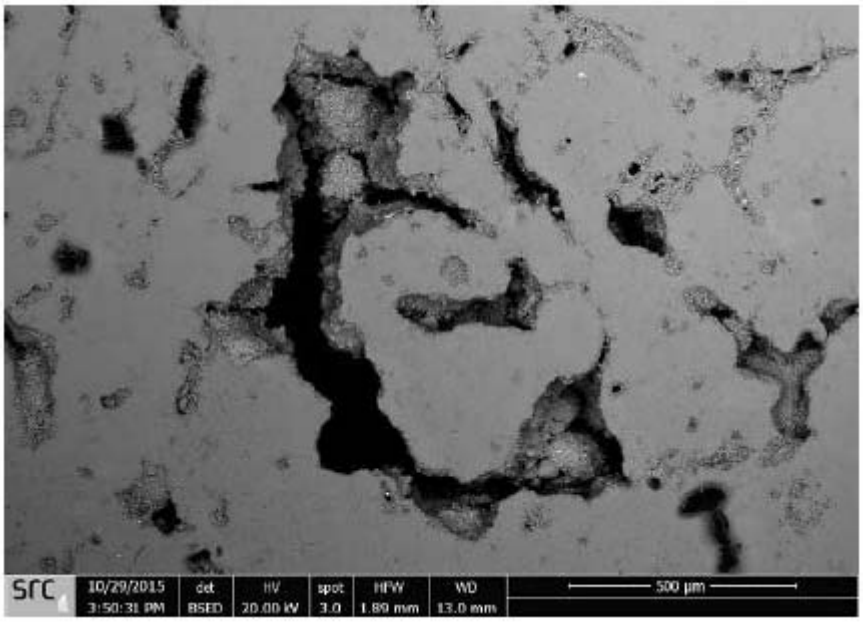

Figure 169 – Unfilled void spaces in Vuggy sample SGS-004

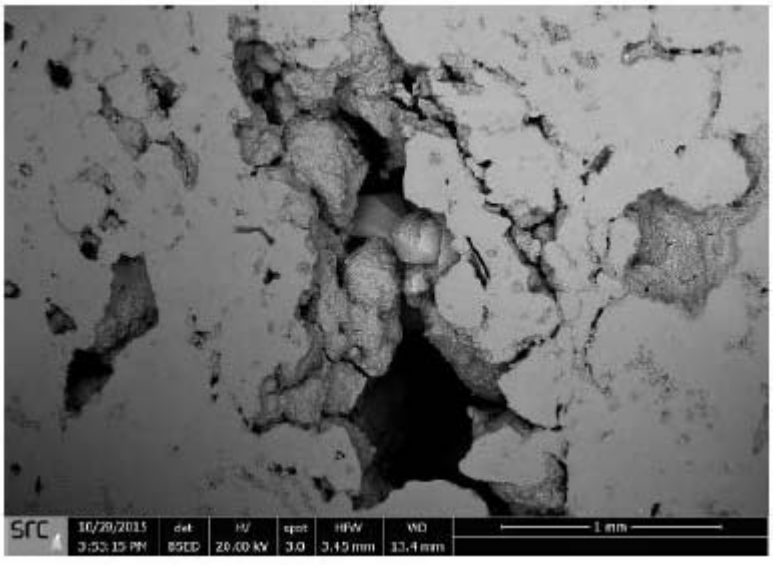

Figure 170 – Unfilled void spaces in Vuggy sample SGS-006

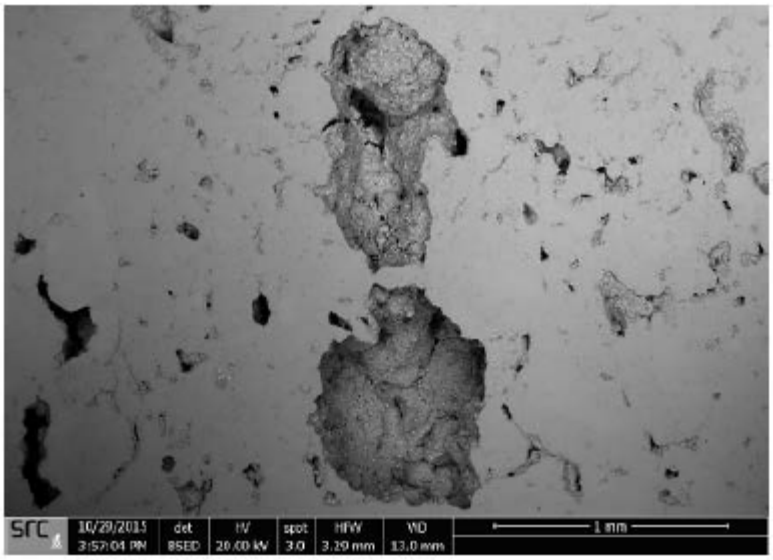

Figure 171 – Unfilled void spaces in Vuggy sample SGS-004

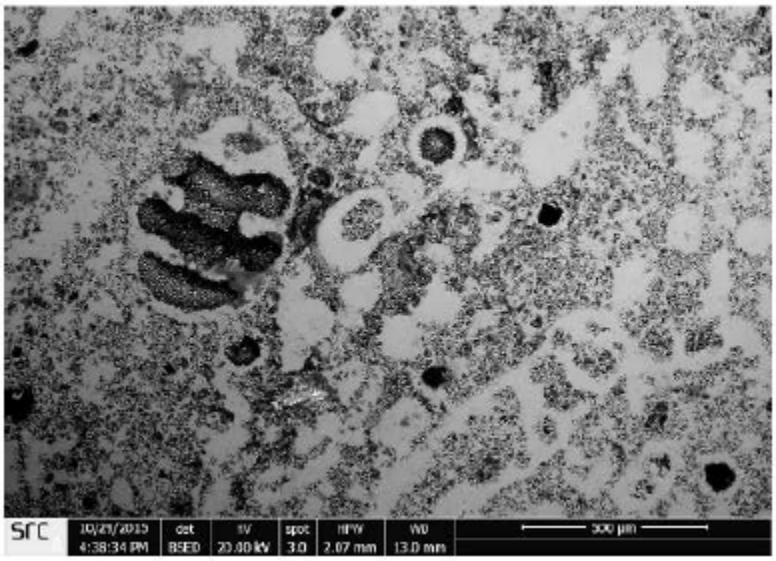

Figure 172 – Microfossils in Vuggy sample SGS-106

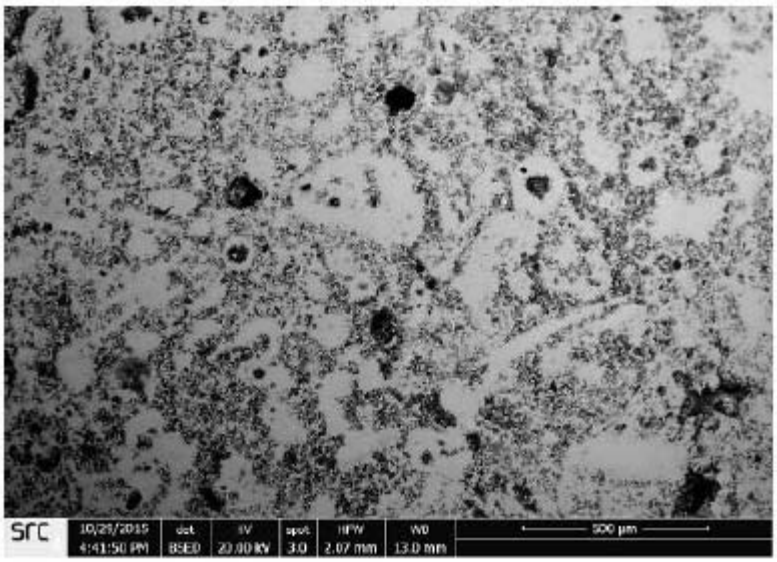

Figure 173 – Microfossils in Vuggy sample SGS-108

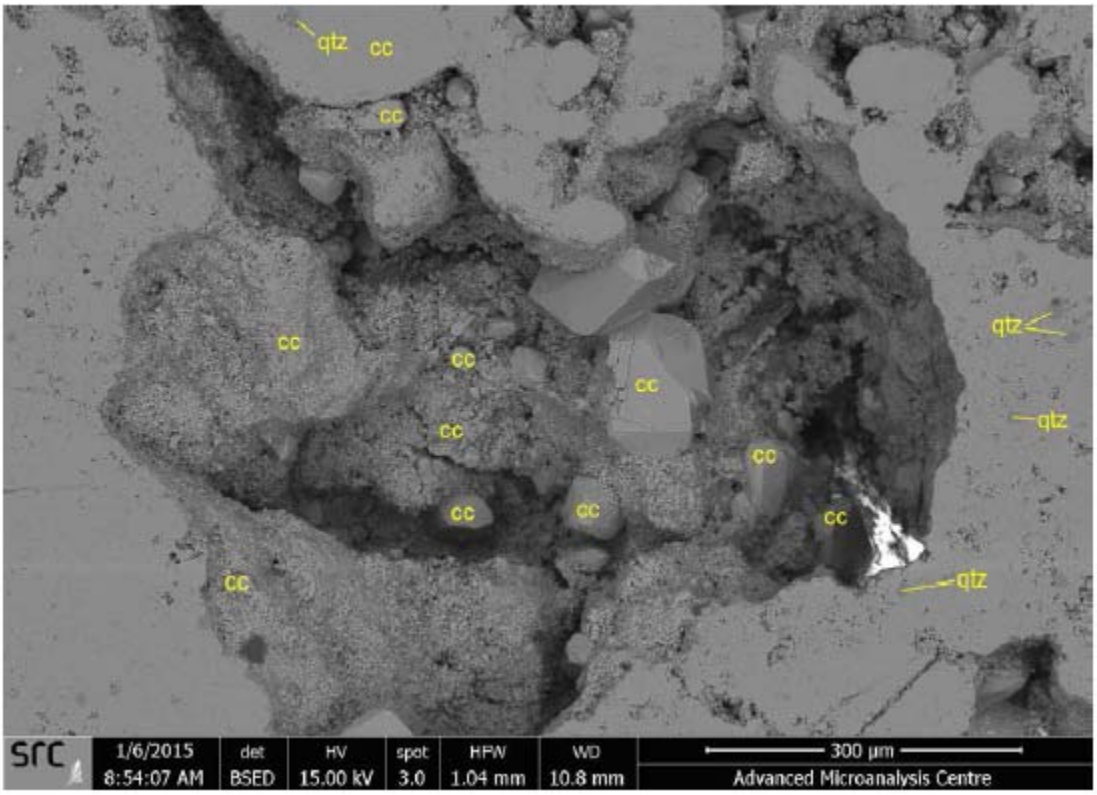

Figure 174 – Pre-CO_2 injection sample, minerals labelled.

13.0 Final Conclusions

The IEAGHG Weyburn-Midale CO_2 Monitoring and Storage project produced perhaps the most comprehensive and important research results related to the safe storage of CO_2 in the subsurface. While the project itself was focussed on storage in a producing oilfield, the research findings have application to most CO_2 storage scenarios in the world, including injection into deep saline formations. With the publication in 2012 of *Best Practices for Validating CO_2 Geological Storage: Observations and Guidance from the IEAGHG Weyburn-Midale CO_2 Monitoring and Storage Project* (Hitchon, 2012), many of those results became publically available to other CO_2-EOR and CCS projects worldwide.

This report has covered research that went into the creation of the BPM (Base Phase) and then goes beyond that publication to present research that demonstrates in a more comprehensive way how CO_2-EOR operations could be transitioned towards credit for long-term storage (Optional Phase of research). This transitioning has been a main area of concern for policy makers and regulators who would like to develop more comprehensive guidelines for giving storage credit to CO_2-EOR operations. The findings reported here on the Base Phase indicate that the integration of project data from four key areas (site characterization/geological integrity; wellbore analyses; storage monitoring; and, risk assessment) effectively demonstrates that long-term storage in oil reservoirs can and indeed has been occurring at the Weyburn field. Such storage potential exists in most other CO_2-EOR operations provided the proper measurement and monitoring is provided during operations, and continues until effective storage has been clearly demonstrated. The Optional Phase of research – entitled SaskCO_2USER – examined seven key areas of interest arising from the Weyburn data collected in the Base Phase to help recommend and identify appropriate measurement, monitoring and verification (MMV) methods, wellbore integrity and corrosion mitigation techniques, and minimum required datasets to confirm CO_2-EOR operations as long-term storage facilities.

Base Phase data helped to inform the SaskCO_2USER research. Site characterization work confirmed the long-term integrity of the containment seal and wellbore integrity work examined an existing, older well in the Weyburn field to illustrate what parts of a well could potentially come into contact with CO_2, and to identify potential areas of wellbore weakness that could be susceptible to leaks. Likewise, the data from geochemical and geophysical analyses was conclusive in proving the containment of CO_2 at the oilfield, and the risk assessment work integrated the available data from the other areas of research to demonstrate that the risk of leakage of CO_2 to the biosphere was minute and well within the acceptable risk scenarios developed for other large industrial projects. These four key research areas did raise a number of questions, however, that helped inform the development of research in the SaskCO_2USER project. There were a large number of technologies and methods used in the MMV program during the Base Phase of research at Weyburn. Going forward, what would be

the minimum MMV requirements for a CO_2-EOR operator to demonstrate safe storage? What wellbore and well casing integrity maintenance measures would an operator need to demonstrate? What technologies would help operators prove the CO_2 has remained in place and is not migrating to other formations above the injection zone?

SaskCO_2USER attempted to answer some of these questions by conducting applied research for commercial applications in high priority areas of CO_2-EOR operations. The research advanced the rich datasets generated from the Weyburn and Midale fields in seven key areas.

Additional work was conducted in overburden monitoring, with the end result being a ranking of the best technologies available for such monitoring, and what components of a storage site (wellbores, caprock, etc.) require the most monitoring to assure long term storage. Pulsed-neutron logging was seen as one of the best tools for determining whether CO_2 leakage is occurring above the formation. Wells remain the highest potential leakage routes, and performing cement bond logs as baselines early in a well's life was determined to be useful for later comparisons as wells age. The most useful imaging for locating CO_2 in the subsurface remains 3D seismic monitoring of the plume. The ranking of technologies offered in this report may aid in the creation of a monitoring plan for other CO_2 storage projects. It affords an operator a method of objectively comparing monitoring technologies to address specific needs related to site-specific risks, regulatory regimes, and economics.

The casing corrosion work looked at two characteristic corrosion scenarios: the first identified corrosion as more prevalent in the lower wellbore near production perforations and the other involved more widespread corrosion closer to the surface. In all cases, the rate of casing corrosion increased near the lower sections of the well near the existing production perforations. While specific mitigation methods were not elaborated upon, the findings suggest that additional research monitoring be done on time-lapse casing corrosion and cement integrity under field conditions that influence corrosion and cement degradation to quantify the rates and probability at which they occur. While several factors influencing wellbore integrity were discovered in this study, completion methods play a critical role in mitigating their impact. More laboratory analyses will be required to fully investigate and pinpoint the key corrosion mechanisms involved.

Passive seismic analyses using an additional year of data from three broadband stations deployed at the Weyburn Midale field was analyzed, and contrasted/compared with earlier seismic readings. No local seismic events were detected during the monitoring period. Of more important consideration for other CO_2-EOR projects was an examination of the in-situ stress conditions at the Weyburn-Midale Field. These conditions were used to estimate the optimum orientation of a fault for it to be reactivated by injection, which suggested a pore pressure increase of 10MPa above hydrostatic to re-activate such a fault. Pore pressures at Weyburn

have not exceeded such values, which may account for the fact that no large, induced events have occurred in this area. Similar comparisons should be done in CO_2-EOR fields in other locations, to identify maximum pressure required to reactivate faults.

The well design work in SaskCO_2USER was perhaps the most compelling work completed in the program, and an extensive set of recommendations were provided on the design and costing of CO_2-EOR wells drilled or converted to injectors. Key well design requirements were identified, along with operational procedures and proper material selection to construct wells in CO_2-EOR and storage reservoir. These recommended designs have a high degree of wellbore integrity for all phases of the well's potential life cycle. For example, operational procedures to maximize fluid containment reliability within the injection zone including tubular connection selection options were developed, and options for future horizontal well designs and investigative techniques of minimizing potential risk of losing seal against sour CO_2 laden fluids were provided.

Minimum dataset recommendations were developed for CO_2-EOR operators through modelling the reservoir flow system, predicting storage capacity, and monitoring CO_2 migration so as to meet a certain level of acceptable risk. The analyses included examining the formation petrophysical properties that are most sensitive to the CO_2 geological storage prediction and migration monitoring; establishing a large spatial range of data acquisition that captures the potential CO_2 migration range, which is normally larger than the storage complex; developing the smallest spatial resolution of sampling measurements, determined from local geologic and petrophysical heterogeneity and anisotropy; and, establishing the smallest temporal span of data acquisition for the purpose of reservoir monitoring.

Additional history matching experiments were conducted using inversion of time-lapse seismic data from the Weyburn field for permeability and porosity. The experiments were conducted on a sector model for a single well pattern carved out of a larger coarse-grid model containing 9 patterns. These additional modelling results show that in all cases the updated models were able to reproduce the synthetic measurements with much greater accuracy than before history matching, with reasonable values for the permeability and porosity updates since the initial modeling done prior to 2012. These history matching experiments compared favourably with earlier reported approaches at Weyburn and suggest continued refinement of history matching models should provide a useful tool for helping to demonstrate the long-term safety of storage at other CO_2-EOR sites.

Finally, examination of core samples from the Weyburn field that have been under long-term exposure to CO_2, provided a means of determining the effect of injected CO_2 on the rock framework and the pore space in the reservoir. Comparing the recently drilled wells to wells that were drilled prior to CO_2 injection revealed the effects of injected CO_2 on the reservoir

matrix. Such examination offers a potential means for CO_2-EOR operators to demonstrate the safety of storage by providing evidence of calcification of the injected CO_2.

Acknowledgements

The IEAGHG Weyburn-Midale CO_2 Monitoring and Storage Project employed over 30 research partners from around the world to perform work and file reports to the PTRC as part of the first 12 years of study. Those researchers have been identified and acknowledged in the BPM (Hitchon, 2012) and cannot all be listed here. However, in this report the PTRC would like to thank the scientists and organizations that were commissioned to provide research in the Optional Phase of the program (SaskCO_2USER), and which were not identified in the BPM. Those organizations and individuals include:

- Jason Laumb, John Hamling, Kurt Eylands, Alexander Azenkeng, Kyle Glazewski, Edward Steadman and John Harju from the Energy and Environmental Research Centre (EERC)
- D.S. Belczewski of Bissett Resource Consultants
- J. Verdon and M. Kendall from Outer Limits Geophysics and University of Bristol
- J-P. Nicot, S. Gao, A. Sun, T.A. Meckel and H.R. Lashgari from the Bureau of Economic Geology at the University of Texas at Austin
- Andrew Duguid (now with Battelle National Laboratory), George El-Kaseeh, Si-Yong Lee, Mark Piercy and Wade Zaluski from Schlumberger.
- O. Leeuwenburgh, S. Meekes, and V. Vandeweijer of TNO (in The Netherlands).
- Gavin Jensen from the Saskatchewan Geological Survey.

Their findings are included in this report and gratefully acknowledged.

References

Aanonsen, S. I., G. Naevdal, D. S. Oliver, A. C. Reynolds, and B. Vallès. (2009). "The Ensemble Kalman Filter in reservoir engineering – a review." SPE Journal, 14(3), 393-412, 2009.

Aarnes, J., and Wildgust, N. (2012). Introduction. In: B. Hitchon (Editor), *Best Practices for Validating CO_2 Geological Storage: Observations and Guidance from the IEAGHG Weyburn-Midale CO_2 Monitoring and Storage Project*. 1–7. Geoscience Publishing, Sherwood Park, AB.

Amaefule, J.O., Altunbay, M., Tiab, D., Kersey, D.G., and Keelan, D.K. (1993). "Enhanced reservoir description: Using core and log data to Identify hydraulic (flow) units and predict permeability in uncored intervals/wells." Paper SPE 26436 presented at the 1993 SPE Annual Technical Conference and Exhibition, Houston, October 3-6.

ASTM International. (2010). G102-89 standard practice for calculation of corrosion rates and related information from electrochemical measurements: West Conshohocken, Pennsylvania.

Bachu, S. (2003). "Screening and ranking of sedimentary basins for sequestration of CO_2 in geological media in response to climate change." Environmental Geology, v. 44, p. 277–289.

Bakun W.H., Stickney M.C., Rogers G.C. (2011). "The 16 May 1909 Northern Great Plains Earthquake" Bulletin of the Seismological Society of America 101, 3065-3071.

Beaubien, S.E., Jones, D.G., Gal, F., Barkwith, A., Braibant, G., Baubron, J-C., Ciotoli, G., Graziani, S., Lister, T.R., Lombardi, S., Michel, K., Quattrocchi, F., Strutt, M.H. (2013). "Monitoring of near-surface gas geochemistry at the Weyburn, Canada, CO_2-EOR site, 2001-2011." *International Journal of Greenhouse Gas Control: The IEAGHG Weyburn-Midale CO_2 Monitoring and Storage Project* Volume 16. Supplement 1 (June): S236-S262. Print.

Bogaert, P. (2002). "Spatial prediction of categorical variables: the Bayesian maximum entropy approach." Stochastic Environmental Research and Risk Assessment 16 (2002) 425–448.

Boness N.L. and Zoback M.D. (2006). "Mapping stress and structurally controlled crustal shear velocity anisotropy in California." Geology 34, 825-828.

Bowden, A., Pershke, D., and Chalaturnyk, R. (2013a). "Geosphere risk assessment conducted for the IEAGHG Weyburn-Midale CO_2 Monitoring and Storage Project." *International Journal of Greenhouse Gas Control: The IEAGHG Weyburn-Midale CO_2 Monitoring and Storage Project* Volume 16. Supplement 1 (June): S276-S291. Print.

Bowden, A., Pershke, D., and Chalaturnyk, R. (2013b). "Biosphere risk assessment for CO_2 storage projects." *International Journal of Greenhouse Gas Control: The IEAGHG Weyburn-Midale CO_2 Monitoring and Storage Project* Volume 16. Supplement 1 (June): S291-S308. Print.

Bowden, A.R. and Rigg, A. (2004). Assessing risk in CO_2 storage projects. The APPEA Journal, 2004, 677-701.

Brondel, D., Edwards, R., Hayman, A., Hill, D., Mehta, S., and Semerad, T. (1994). "Corrosion in the oil industry:" Oilfield Review, v. 6, p. 4–18.

Brown, L. T. (2002). Integration of rock physics and reservoir simulation for the interpretation of time-lapse seismic data at Weyburn Field, Saskatchewan. M.Sc. Thesis, Colorado School of Mines, 149 p.

Canadian Association of Petroleum Producers. (2009a). Best management practice—mitigation of internal corrosion in sweet gas-gathering systems, 2009–0014, June 2009. www.capp.ca/getdoc.aspx?DocId=155645&DT=PDF (accessed April 4, 2014).

Canadian Association of Petroleum Producers. (2009b). Best management practice—mitigation of internal corrosion in sour gas pipeline systems, 2009–0013, June 2009. www.capp.ca/getdoc.aspx?DocId=155644&DT=PDF (accessed April 4, 2014).

Canadian Standards Association. (2012) CSA Z741: Geological Storage of Carbon Dioxide. CSA. 80pp.

Cao, L., Y. Xu, and J. Yu. (2005). "Facies analysis with merged 3D seismic data." 75th Annual International Meeting, SEG, Expanded Abstracts, 739–742

Carle, S. F., and Fogg , G. E. (1997). "Modeling spatial variability with one and multidimensional continuous-lag Markov chains." Mathematical Geology, 29(7):891–918.

Cavanaugh, A. (2013). IEAGHG Weyburn-Midale CO_2 Monitoring and Storage Project: Regional Migration Pathways and Associated Potential Well Risk. Prepared for Petroleum Technology Research Centre. Regina, SK.

Celia, M.A., Bachu, S., Nordbotten, J.M., Gasda, S.E., and Dahle, H.K. (2004). "Quantitative estimation of CO_2 leakage from geological storage—analytical models, numerical models, and data needs." Proceedings of the 7th International Conference on Greenhouse Gas Control Technology, Vancouver, Canada.

Chalaturnyk, R. (2012). In: B. Hitchon (Editor), Risk Assessment. *Best Practices for Validating CO_2 Geological Storage: Observations and Guidance from the IEAGHG Weyburn-Midale CO_2 Monitoring and Storage Project*. 289–320. Geoscience Publishing, Sherwood Park, AB.

Charrad, M., Ghazzali, N., Boiteau, V., and Niknafs, A. (2015). "NbClust: Determining the Best Number of Clusters in a Data Set", https://cran.r-project.org/web/packages/NbClust/index.html last accessed September 2015

Chiles, J-P., Delfiner, P. (2012). Geostatistics: Modeling Spatial Uncertainty, 2nd Edition. 734 pages.

Choi, Y., Young, D., Nesic, S. and Gray L.G.S. (2013). "Wellbore integrity and corrosion of carbon steel in CO_2 geological storage environments: A literature review." *International Journal of Greenhouse Gas Control: The IEAGHG Weyburn-Midale CO_2 Monitoring and Storage Project* Volume 16. Supplement 1 (June): S70-S77 Print.

Choi, Y-S., Young, D., Nešić, S., and Gray, L. G. S. (2013). "Wellbore integrity and corrosion of carbon steel in CO_2 geologic storage environment. A literature review." *International Journal of Greenhouse Gas Control*. 16S (2013) S70–S77. Retrieved from: http://www.icmt.ohio.edu/documents/Journals2013/Wellbore%20integrity%20and%20corrosion%20of%20carbon%20steel%20in%20CO2_Choi.pdf

Cord-Ruwisch, R., Kleinitz, W., and Widdel, F. (1987). "Sulfate-reducing bacteria and their activities in oil production." Journal of Petroleum Technology, p. 97–106.

Crow, W., Carey, J.W., Gasda, S., Williams, B., and Celia, M.A. (2010) "Wellbore integrity analysis of a natural CO_2 producer." International Journal of Greenhouse Gas Control, v. 4, p. 186–197.

Davis, S. D. and C. Frohlich (1993). "Did (or will) fluid injection cause earthquakes? – criteria for a rational assessment." Seismological Research Letters, 64, No. 3-4

Deisman, N., Chalaturnyk, R., Soderberg, H., and Lang, P. (2013). "Cased wellbore tools for sampling and in-situ testing of cement/formation flow properties." *International Journal of Greenhouse Gas Control: The IEAGHG Weyburn-Midale CO_2 Monitoring and Storage Project* Volume 16. Supplement 1 (June): S62-S69. Print.

Duguid, A., Dubois, M., McPherson, B., Hnottavange-Telleen, K., and Lepinski, J. (2010). "Estimating leakage potential based on existing data for EOR-sequestration targets in Kansas." Proceedings of the 9th Annual Conference on Carbon Capture and Sequestration, May 10-13, 2010. Monitor and Exchange Publications and Forum, Washington, D.C.

Duxbury A., White D., Samson C., Hall S.A., Wookey J., Kendall J-M. (2012). "Fracture mapping using seismic amplitude variation with offset and azimuth analysis at the Weyburn CO_2 storage site." Geophysics 77, N17-N28.

Ebanks, W.J. (1987). "Flow unit concept: integrated approach to reservoir description for engineer in projects." AAPG Bulletin, 71(5): 551-552

Emerick, A. and A. C. Reynolds. (2012). "Ensemble smoother with multiple data assimilation." Computers & Geosciences, 2012. http://dx.doi.org/10.1016/j.cageo.2012.03.011.

Enning, D., and Garrelfs, J. (2014). "Corrosion of iron by sulfate-reducing bacteria—new views of an old problem." Applied Environmental Microbiology, v. 80, p. 1226–1236.

Enning, D., Venzlaff, H., Garrelfs, J., Dinh, H.T., Meyer, V., Mayrhofer, K., Hassel, A.W., Stratmann, M., and Widdel, F. (2012). "Marine sulfate-reducing bacteria cause serious corrosion of iron under electroconductive biogenic mineral crust." Environmental Microbiology, v. 14, p. 1772–1787.

Farzadi, P. (2006). "Seismic facies analysis based on 3D multi-attribute volume classification, Dariyan Formation." SE Persian Gulf: Journal of Petroleum Geology, 29, 159–173,

Ferraretti, D., Lamma, E., Gamberoni, G., Febo M., and Raffaele Di Cuia. (2011). "Integrating clustering and classification techniques: a case study for reservoir facies prediction." Emerging Intelligent Technologies in Industry, SCI 369, p. 21–34.

Frohlich C. and Brunt M. (2013). "Two-year survey of earthquakes and injection/production wells in the Eagle Ford Shale, Texas, prior to the MW4.8 20 October 2011 earthquake." Earth and Planetary Sciences Letters 379, 56-63.

Frohlich C., Walter J.I., Gale J.F.W. (2015). "Analysis of Transportable Array (USArray) data shows earthquakes are scarce near injection wells in the Williston Basin, 2008-2011." Seismological Research Letters 86, 492-499.

Gasda, S., Celia, M., Wang J., and Duguid, A. (2013). "Wellbore permeability estimates from vertical interference testing of existing wells." Proceedings of the 11th International Conference on Greenhouse Gas Technologies, Kyoto, Japan, September 2012.

Gendzwill D. and Unrau J. (1996). "Ground control and seismicity at International Minerals and Chemical (Canada) Global Limited." Canadian Institute of Mining Bulletin 89, 52-61.

Hasegawa H.S., Wetmiller R.J., Gendzwill D.J. (1989). "Induced seismicity in mines in Canada – an overview" Pure and Applied Geophysics 129, 423-453.

Hawkes, C. and Gardner, C. (2012). In: B. Hitchon (Editor), Well integrity. *Best Practices for Validating CO_2 Geological Storage: Observations and Guidance from the IEAGHG Weyburn-Midale CO_2 Monitoring and Storage Project*. 255–288. Geoscience Publishing, Sherwood Park, AB.

Hawkes, C., and Gardner, C. (2013). "Pressure transient testing for assessment of wellbore integrity in the IEAGHG Weyburn-Midale CO_2 monitoring and storage project." *International Journal of Greenhouse Gas Control: The IEAGHG Weyburn-Midale CO_2 Monitoring and Storage Project* Volume 16. Supplement 1 (June): S50-S61. Print.

Heidbach O., Tingay M., Barth A., Reinecker J., Kurfeß D., Müller B. (2008). The World Stress Map database release 2008. doi:10.1594/GFZ.WSM.Rel2008.

Heidbach O., Tingay M., Barth A., Reinecker J., Kurfeß D., Müller B. (2010). Global crustal stress pattern based on the World Stress Map database release 2008: Tectonophysics 482, 3-15.

Hitchon, B. (Editor). (2012). *Best Practices for Validation CO_2 Geological Storage: Observations and Guidance from the IEAGHG Weyburn-Midale CO_2 Monitoring and Storage Project.* Geoscience Publishing, Sherwood Park, AB.

Horner R.B. and Hasegawa H.S. (1978). "The seismotectonics of Southern Saskatchewan" Canadian Journal of Earth Sciences 15, 1341-1355.

IEA Environmental Projects Ltd. (2008). "Long term Integrity of CO_2 storage: well abandonment." IEA Greenhouse Gas R&D Programme. Retrieved from: http://decarboni.se/sites/default/files/publications/98891/long-termintegrity-co2-storage-well-abandonment.pdf

IEAGHG. (2015). Retrieved from Monitoring Selection Tool: http://ieaghg.org/ccs-resources/monitoring-selection-tool1.

Intergovernmental Panel on Climate Change. (2005). *Special Report on Carbon Dioxide Capture and Storage*. Cambridge University Press, New York and Cambridge.

Irani, M. (2012). Development and Application of Bow Tie Risk Assessment Methodology for Carbon Geological Storage Projects. PhD. Thesis. University of Alberta, Edmonton, AB.

Jafari, A., S. Talman, and E. Perkins. (2011). "Numerical simulation of four-pattern CO_2-flood EOR in the Weyburn Phase 1B Area." Report prepared by Alberta Innovates Technology Futures for PTRC, Regina, SK.

Jensen, G., Nickel, E., and Rostron, B. (2013). "Refinement of the Weyburn-Midale geological and hydrogeological model: Developing a better framework to determine reservoir response to injected CO_2 movement." *International Journal of Greenhouse Gas Control: The IEAGHG Weyburn-Midale CO_2 Monitoring and Storage Project* Volume 16. Supplement 1 (June): S5-S14. Print.

Jensen, W.B. (2012). "Faraday's laws or Faraday's law?" Journal of Chemistry Education, v. 89, p. 1208–1209.

Jimenez Gomez J.A. (2006). *Geomechanical Performance Assessment of CO_2 – EOR Geological Storage Projects.* Ph.D. Thesis, University of Alberta.

Johnson, J., and Rostron, B. (2012). Geochemical Monitoring. In: B. Hitchon (Editor), *Best Practices for Validating CO_2 Geological Storage: Observations and Guidance from the*

IEAGHG Weyburn-Midale CO_2 Monitoring and Storage Project. 119–154. Geoscience Publishing, Sherwood Park, AB.

Johnson, J., and Rostron, B. (2012). Storage Performance Predictions. In: B. Hitchon (Editor), *Best Practices for Validating CO_2 Geological Storage: Observations and Guidance from the IEAGHG Weyburn-Midale CO_2 Monitoring and Storage Project*. 79–117. Geoscience Publishing, Sherwood Park, AB.

Konogorov, V. (2012). Well Integrity Master Class, Well Cementing. Presentation. Retrieved: www.fesaus.org/webcast/2012/05/MasterClassWellIntegrity/NonMembers/3_Cementing_Konogorov.pdf

Kuhn, M. (2015). "Caret: classification and regression training", https://cran.r-project.org/web/packages/caret/index.html, last accessed September 2015

Kutchko, B., Pike, W., Lang, K., Strazisar, B., and Rose, K. (2012). An Assessment of Research Needs Related to Improving Primary Cement Isolation of Formations in Deep Offshore Wells. National Energy Technology Laboratory. Retrieved from: http://www.netl.doe.gov/File%20Library/Research/onsite%20research/publications/NETL-TRS-003-2012_Cementing-Research-Needs_20121207.pdf

Lane, R.A. (2005). "Under the microscope—understanding, detecting, and preventing microbiologically influenced corrosion." AMPTIAC Quarterly, v. 9, p. 3–8.

Langston, J.R. and Chin J.E (1968). "Rainbow member facies and related reservoir properties, Rainbow Lake, Alberta." Bulletin of Canadian Petroleum Geology, v.16, no.1. p. 104-143.

Leeuwenburgh, O. and R. Arts. (2014). "Distance parameterization for efficient seismic history matching with the ensemble Kalman Filter." Computational Geosciences, DOI 10.1007/s10596-014-9434-y, 2014.

Leeuwenburgh, O., J. Brouwer and M. Trani. (2011). "Ensemble-based conditioning of reservoir models to seismic data" Comput. Geosci. 15: 359-378, DOI 10.1007/s10596-010-9209-z, 2011.

Li, Y. and Geng, L. (2014). "Integrate facies clustering feature Information in Reservoir modeling." In: E. Pardo-Ig£zquiza et al. (eds.), Mathematics of Planet Earth, Lecture Notes in Earth System Sciences, DOI: 10.1007/978-3-642-32408-6_141.

Lomax A., Satriano C., Vassallo M. (2012). "Automatic picker developments and optimization: FilterPicker – a robust broadband picker for real-time seismic monitoring and earthquake early warning." Seismological Research Letters 83, 531-540.

Marroquín, I. D. (2014) "A knowledge-integration framework for interpreting seismic facies." Interpretation, Vol. 2, No. 1, p. SA1–SA9

McDonald, M., Li, X., and Lim, B. (2014). "Formulated silicate-based pre-flush & spacer for improved wellbore cleaning and wetting." Paper No. AADE-14-FTCE-55 presented at the 2014 AADE Fluids Technical Conference and Exhibition, Houston, Texas, April 15-16, 2014. Available at : https://www.google.ca/webhp?sourceid=chromeinstant&ion=1&espv=2&ie=UTF-8#q=A+formulated+silicate-based+preflush

McLellan P.J., Lawrence K.H., Cormier, K.W. (1992). "A multiple-zone acid stimulation treatment of a horizontal well, Midale, Saskatchewan." Journal of Canadian Petroleum Technology 31, 71-82.

McLennan J.D., Hasegawa H.S., Roegiers J.-C., Jessop A.M. (1986). "Hydraulic fracturing experiment at the University of Regina Campus." Canadian Geotechnical Journal 23, 548-555.

NACE International, 2014, Corrosion in the oil & gas industry: www.nace.org/Corrosion-Central/Industries/Oil---Gas-Production/ (accessed March 2014).

Nygaard, R. (2010). "Well design and well Integrity, Wabamun area CO_2 sequestration project (WASP)." University of Calgary, Energy and Environmental Systems Group Institute for Sustainable Energy, Environment and Economy. Retrieved from: https://www.ucalgary.ca/wasp/Well%20Integrity%20Analysis.pdf

Orayith, M.M. (2012). *The Effect on Bentonite on External Corrosion of Well Casings*. Doctoral Dissertation, School of Materials Corrosion and Protection Center, University of Manchester, United Kingdom.

Ossai, C.I. (2012). "Advances in asset management techniques, an overview of corrosion mechanisms and mitigation strategies for oil and gas pipelines." International Scholarly Research Network, ISRN Corrosion, v. 2012, Article ID 570143, p. 10, doi:10.5402/2012/570143.

Popoola, L.T., Grema, A.H., Latinwo, G.K., Gutti, B., and Balogun, A.S. (2013). "Corrosion problems during oil and gas production and its mitigation." International Journal of Industrial Chemistry, v. 4, p. 35, www.industchem.com/content/pdf/2228-5547-4-35.pdf (accessed March 25, 2014).

Ramirez, A., D. White, Y. Hao, K. Dyer, and J. Johnson. (2013). "Estimating reservoir permeabilities using the seismic response to CO_2 injection and stochastic inversion." International Journal of Greenhouse Gas Control, 16S, S146-A159, 2013.

Reinbold D.J. and Gillispe M.D. (1974). Seismicity in the Area of Ft. Peck, Montana 1966-1968. Unclassified Final Report AL-74-2 to the U.S. Army Engineer District, Omaha, Nebraska.

Rincones, J.G., Delgado, R., Ohen, H., Enwere, P., Guerini, A., and Marquez, P. (2000). "Effective petrophysical fracture characterization using the flow unit concept – San Juan Reservoir, Orocual Field, Venezuela." paper SPE 63072 presented at the 2000 SPE Annual Technical Conference and Exhibition, Dallas, October 1-4.

Romanak, K., G.W. Sherk, S. Hovorka, and C. Yang. (December 2013). "Assessment of alleged CO_2 leakage at the Kerr farm using a simple process-based soil gas technique: Implications for carbon capture, utilization, and storage (CCUS) monitoring" Science Direct. Google. http://www.sciencedirect.com/science/article/pii/S1876610213005699 Web. December 8, 2015.

Rostron, B.J., Whittaker, S., Hawkes, C., White, D. (2012). Characterization. In: B. Hitchon (Editor), *Best Practices for Validating CO_2 Geological Storage: Observations and Guidance from the IEAGHG Weyburn-Midale CO_2 Monitoring and Storage Project*. 9–77. Geoscience Publishing, Sherwood Park, AB.

Roy, A., and Marfurt, K.J. (2011). "Cluster assisted 3D unsupervised seismic facies analysis - An example from Osage County, Oklahoma." Oral presentation at AAPG Mid-Continent Section meeting, Oklahoma City, Oklahoma, October 1-4, 2011.

Ryerson, F.J., Lake, J., Whittaker, S., and Johnson, J. (2013). "Natural CO_2 accumulations in the western Williston Basin: A mineralogical analog for CO_2 injection at the Weyburn site." *International Journal of Greenhouse Gas Control: The IEAGHG Weyburn-Midale CO_2 Monitoring and Storage Project* Volume 16. Supplement 1 (June): S25-S34. Print.

Sartore, L. (2013) spMC: modelling spatial random fields with continuous lag Markov chains." The R Journal Vol. 5/2, December 2013.

Sethian, JA. (1996) Level Set Methods: Evolving Interfaces in Computational Geometry. Cambridge, Cambridge University Press. 237 p.

Shenawi, S.H., White, J.P., Elrafie, E.A., and Kilany, K.A. (2007). Permeability and Water Saturation Distribution by Lithologic Facies and Hydraulic Units: A Reservoir Simulation Case Study, SPE 105273.

Sherk, G.W., Romanak, K., Dale, J., Gilfillan, S., Haszeldine, S., Ringler, E., Wolaver, B., Yang, C. (2011). "The Kerr investigation: final report – Finding of the investigation into the impact of CO_2 on the Kerr property" IPAC-CO_2 Research Inc. Print.

Soto, R., Torres, F., Arango, S., and Cobaleda, G. (2001). "Improved reservoir permeability models from flow units and soft computing techniques: a case study, Suria and Reforma-libertad fields, Colombia." Paper SPE 69625 presented at the SPE Latin American and Caribbean Petroleum Engineering Conference, Buenos Aires, March 25-28.

Srinivasan, S., and Sen, M. (2011). “Stochastic modeling of facies distribution in a carbonate reservoir in the Gulf of Mexico.” Geohorizons, December 2009/54

Stork A.L., Verdon J.P., Kendall J-M. (2015). “Assessing the microseismic response at the In Salah Carbon Capture and Storage (CCS) site with a single three-component geophone.” International Journal of Greenhouse Gas Control 32, 159-171.

Sun, Alexander Y., Robert W. Ritzi, and Darrell W. Sims. (2008). “Characterization and modeling of spatial variability in a complex alluvial aquifer: Implications on solute transport.” Water Resources Research, Vol. 44, W04402.

Trium Environmental. (2011). “Site Assessment – SW30-5-13W2M, prepared by TRIUM Environmental Inc.” CENOVUS Energy. November 23, 2011. Web. Accessed December 9, 2015. http://www.cenovus.com/operations/oil/docs/TRIUM-Report.pdf.

Uddin, M., A. Jafari, S. Talman, E. Perkins, and J. Ivory. (2011). “Numerical simulation of single SSWG Pattern 1 (P1612614) – History match from 1956 – 2010 and predictions from 2010-2070” Report prepared for PTRC, Regina, SK.

URS. (2010a). Weyburn Project Biosphere Risk Assessment. Internal Report prepared for Petroleum Technology Research Centre, Regina, SK.

URS. (2010b). Weyburn Project Biosphere Risk Assessment. Internal Report prepared for Petroleum Technology Research Centre, Regina, SK.

Verdon J.P. (2014). “Significance for secure CO_2 storage of earthquakes induced by fluid injection.” Environmental Research Letters 9, 064022.

Verdon J.P. and Kendall J-M. (2011). “Detection of multiple fracture sets using observations of shear-wave splitting in microseismic data.” Geophysical Prospecting 59, 593-608.

Verdon J.P., Kendall J-M., Stork A.L., Chadwick R.A., White D.J., Bissell R.C. (2013). “Comparison of geomechanical deformation induced by megaton-scale CO_2 storage at Sleipner, Weyburn, and In Salah.” Proceedings of the National Academy of Sciences 110, E2762-E2771.

Verdon J.P., Kendall J-M., White D.J., Angus D.A. (2011). “Linking microseismic event observations with geomechanical models to minimise the risks of storing CO_2 in geological formations.” Earth and Planetary Science Letters 305, 143-152.

Verdon J.P., Kendall J-M., White D.J., Angus D.A., Fisher Q.J., Urbancic T. (2010). “Passive seismic monitoring of carbon dioxide storage at Weyburn.” The Leading Edge 29, 200-206.

Walter, D.A. (1997) “Geochemistry and microbiology of iron-related well-screen encrustation and aquifer biofouling in Suffolk County.” Water-Resources Investigations Report 97-4032, Long Island, New York, U.S. Geological Survey.

Watson, T.L., and Bachu, S. (2007). “Evaluation of the potential for gas and CO_2 leakage along wellbores.” Presented at the Society of Petroleum Engineers (SPE) E&P Environmental and Safety Conference, Galveston, Texas, March 5–7, SPE Paper 106817.

Weissmann, G. S., and G. E. Fogg. (1999). “Multiple-scale alluvial fan heterogeneity modeled with transition probability geostatistics in a sequence stratigraphic framework.” J. Hydrol., 226, 45-48

White, D. (2012). Geophysical Monitoring. In: B. Hitchon (Editor), *Best Practices for Validating CO_2 Geological Storage: Observations and Guidance from the IEAGHG Weyburn-Midale CO_2 Monitoring and Storage Project*. 155–214. Geoscience Publishing, Sherwood Park, AB.

White, D. (2013a). “Seismic characterization and time-lapse imaging during seven years of CO_2 flood in the Weyburn field, Saskatchewan, Canada.” *International Journal of Greenhouse Gas Control: The IEAGHG Weyburn-Midale CO_2 Monitoring and Storage Project* Volume 16. Supplement 1 (June): S78-S94. Print.

White, D. (2013b). “Toward quantitative CO_2 storage estimates from time-lapse 3D seismic travel times: An example from the IEAGHG Weyburn-Midale CO_2 monitoring and storage project.” *International Journal of Greenhouse Gas Control: The IEAGHG Weyburn-Midale CO_2 Monitoring and Storage Project* Volume 16. Supplement 1 (June): S95-S102. Print.

Widess, M.B. (1973). “How thin is a thin bed?” Geophysics, vol. 38, p. 1176-1180.

Wildgust, N., Tontiwachwuthikul, P., and Gilboy, C. (2013). “Introduction to a decade of research by the IEAGHG Weyburn-Midale CO_2 monitoring and storage project.” *International Journal of Greenhouse Gas Control: The IEAGHG Weyburn-Midale CO_2 Monitoring and Storage Project* Volume 16. Supplement 1 (June): S1-S4. Print.

Wilson W., Surjik D.L., Sawatzky H.B. (1963). “Hydrocarbon potential of the South Regina area, Saskatchewan.” Saskatchewan Department of Mineral Resources, Report No. 76.

Wilson, M. and Monea M. (2004). *IEA GHG Weyburn CO_2 Monitoring and Storage Project Summary Report 2000-2004, Volume III*. The proceedings of the 7th International Conference on Greenhouse Gas Control Technologies. September 5-9, 2004. Vancouver, BC. Petroleum Technology Research Centre, Regina, SK.

Worth K., White D., Chalaturnyk R., Sorensen J., Hawkes C., Rostron B., Johnson J., Young A. (2014). "Aquistore project measurement, monitoring and verification: From concept to CO_2 injection." Energy Procedia 63, 3202-3208.

Zhang, M., and Bachu, S. (2011) "Review of integrity of existing wells in relation to CO_2 geological storage—what do we know?" International Journal of Greenhouse Gas Control, v. 5, no. 5, p. 826–840, doi:10.1016/j.ijggc.2010.11.006.

Zulqarnain, M. (2012). (*Thesis*) Simulations of the Primary Cement Placement in Annular Geometries During Well Completions Using Computational Fluid Dynamics (CFD). Retrieved: http://www.researchgate.net/profile/Muhammad_Zulqarnain/publication/262911694_Simulations_of_the_Primary_Cement_Placement_in_Annular_Geometries_during_Well_Completion_Using_Computational_Fluid_Dynamics_(CFD)/links/0046353923594395f2000000.pdf

Bibliography

Burrowes, O.G. (2001). Investigating CO_2 storage potential of carbonate rocks during tertiary recovery from a billion barrel oil field, Weyburn, Saskatchewan: Part 2 – Reservoir geology (IEAGHG Weyburn CO_2 Monitoring and Storage Project). *In* Summary of Investigations 2001, Volume 1, Saskatchewan Geological Survey, Saskatchewan energy and Mines, Miscellaneous Report 2001-4.1, 64-71.

Carroll, S., Hao, Y., Smith, M., and Sholokhova, Y. (2013). "Development of scaling parameters to describe CO_2-rock interactions within Weyburn-Midale carbonate flow units." *International Journal of Greenhouse Gas Control: The IEAGHG Weyburn-Midale CO_2 Monitoring and Storage Project* Volume 16. Supplement 1 (June): S185-S193. Print.

Cavanagh, A., and Rostron, B., (2013). "High-resolution simulations of migration pathways and the related potential well risk at the IEAGHG Weyburn-Midale CO_2 Storage project." *International Journal of Greenhouse Gas Control: The IEAGHG Weyburn-Midale CO_2 Monitoring and Storage Project* Volume 16. Supplement 1 (June): S15-S24. Print.

Chalaturnyk, R., Zhou, W., Stenhouse, M., Sheppard, M., and Walton, F. (2004). Theme 4: Long-Term Risk Assessment of the Storage Site. *IEAGHG Weyburn CO_2 Monitoring & Storage Project Summary Report 2000 - 2004*. Volume 3. 211–268. Print.

Edmonds, A.C., and Moroney, A.P.. (1998). Geology. Development and optimization of the Weyburn unit, southeastern Saskatchewan. *In* J.R. Hogg (Editor), *Oil and Gas Pools of the Western Canada Sedimentary Basin*, 1-12. Canadian Society of Petroleum Geologists, Special Publication S-51.

Elkhoury, J., Ameli, P., and Detwiler, R. (2013). ”Dissolution and deformation in fractured carbonates caused by flow of CO_2-rich brine under reservoir conditions.” *International Journal of Greenhouse Gas Control: The IEAGHG Weyburn-Midale CO_2 Monitoring and Storage Project* Volume 16. Supplement 1 (June): S203-S215. Print.

Johnson, J., and White, D. (2012). In: B. Hitchon (Editor), History Matching and Performance Validation. *Best Practices for Validating CO_2 Geological Storage: Observations and Guidance from the IEAGHG Weyburn-Midale CO_2 Monitoring and Storage Project*. 215–254. Geoscience Publishing, Sherwood Park, AB.

Lake, J. and Whittaker, S. (2006). Occurrences of CO_2 within southwest Saskatchewan: Natural analogues to the Weyburn CO_2 injection site. Summary of Investigations 2006, Vol. 1, Saskatchewan Geological Survey, Miscellaneous Report 2006-4.1. <CD-ROM, paper A-5>.

Law, D., Huang, S., Freitag, N., Perkins, E., Wassmuth, F., Dunbar, B., and Arghari, K. (2004). Theme 3: CO_2 Storage Capacity and Distributions Predictions and the Application of Economic Limits. *IEAGHG Weyburn CO_2 Monitoring & Storage Project Summary Report 2000 - 2004*. Volume 3. 149–209. Print.

Li, G., Burrowes, G., Majer E. and Davis, T. (2001). Weyburn field horizontal-to-horizontal crosswell seismic profiling: Part 3 – Interpretation. Society of Exploration Geophysicists 2001 annual meeting, San Antonio, Expanded Abstracts.

Luo, P., Er, V., Freitag, N., and Huang, S. (2013). ”Re-characterizing evolving fluid and PVT properties of Weyburn oil-CO_2 system” *International Journal of Greenhouse Gas Control: The IEAGHG Weyburn-Midale CO_2 Monitoring and Storage Project* Volume 16. Supplement 1 (June): S226-S235. Print.

Ma, J. and I. Morozov. (2010). AVO modelling of pressure-saturation effects in Weyburn CO_2 sequestration. *The Leading Edge* 29, 178-183.

Mayer, B., Shevalier, M., Nightingale, M., Kwon, J-S., Johnson, G., Raistrick, M., Hutcheon, I., and Perkins, E. (2013). “Tracing the movement and the fate of injected CO_2 at the IEAGHG Weyburn-Midale monitoring and storage project (Saskatchewan, Canada) using carbon isotope ratios.” *International Journal of Greenhouse Gas Control: The IEAGHG Weyburn-Midale CO_2 Monitoring and Storage Project* Volume 16. Supplement 1 (June): S177-S184. Print.

McNab, W., Ramirez, A., and Johnson, J. (2013). “Quantifying reactive chemistry along an injected CO_2 flow path at the field scale using a Monte Carlo simulation approach.” *International Journal of Greenhouse Gas Control: The IEAGHG Weyburn-Midale CO_2 Monitoring and Storage Project* Volume 16. Supplement 1 (June): S194-S202. Print.

Meadows, M. (2013).“4D rock and fluid properties analysis at the Weyburn field, Saskatchewan.” *International Journal of Greenhouse Gas Control: The IEAGHG Weyburn-Midale CO_2 Monitoring and Storage Project* Volume 16. Supplement 1 (June): S134-S145. Print.

Meadows, M. and Cole, S. (2013). “4D seismic modeling and CO_2 pressure-saturation inversion at the Weyburn field, Saskatchewan.” *International Journal of Greenhouse Gas Control: The IEAGHG Weyburn-Midale CO_2 Monitoring and Storage Project* Volume 16. Supplement 1 (June): S103-S117. Print.

Njiekak, G., Schmitt, D., Yam, H. and Koffman L.S. (2013). “CO_2 rock physics as part of the Weyburn-Midale geological storage project.” *International Journal of Greenhouse Gas Control: The IEAGHG Weyburn-Midale CO_2 Monitoring and Storage Project* Volume 16. Supplement 1 (June): S118-S133. Print.

Risk, D., McArthur, G., Nickerson, N., Phillips, C., Hart, C., Egan, J., Lavoie, M. (2013). ”Bulk and isotopic characterization of biogenic CO_2 sources and variability in the Weyburn injection area.” *International Journal of Greenhouse Gas Control: The IEAGHG Weyburn-Midale CO_2 Monitoring and Storage Project* Volume 16. Supplement 1 (June): S263-S275. Print.

Sacuta, N. (2014). “What Happens When CO_2 is Stored Underground – Q&A from the IEAGHG Weyburn-Midale CO_2 Monitoring and Storage Project.” Global CCS Institute, Melbourne, AU. (ISBN- 978-0-9871873-3-1) Print.

Sacuta, N., and Mourits, F. (2012). In: B. Hitchon (Editor), Community Outreach. *Best Practices for Validating CO_2 Geological Storage: Observations and Guidance from the IEAGHG Weyburn-Midale CO_2 Monitoring and Storage Project*. 321–329. Geoscience Publishing. Sherwood Park, AB.

Shevalier, M., Nightingale, M. Mayer, B., Hutcheon, I., Durocher, K., and Perkins, E. (2013). “Brine geochemistry changes induced by CO_2 injection observed over a 10 year period in the Weyburn oil field.” *International Journal of Greenhouse Gas Control: The IEAGHG Weyburn-Midale CO_2 Monitoring and Storage Project* Volume 16. Supplement 1 (June): S160-S176. Print.

Talman, S., Perkins, E., Jafari, A., and Shevalier, M. (2013). “Geochemical tracers applied to reservoir simulation of the Weyburn CO_2 EOR field.” *International Journal of Greenhouse Gas Control: The IEAGHG Weyburn-Midale CO_2 Monitoring and Storage Project* Volume 16. Supplement 1 (June): S216-S225. Print.

Uddin, M., Jafari, A., and Perkins, E. (2013). “Effects of mechanical dispersion on CO_2 storage in Weyburn CO_2-EOR field – Numerical history match and prediction.” *International*

Journal of Greenhouse Gas Control: The IEAGHG Weyburn-Midale CO_2 Monitoring and Storage Project Volume 16. Supplement 1 (June): S35-S49. Print.

Wegelin, A. (1987). Reservoir characteristics of the Weyburn field, southeastern Saskatchewan. *Journal of Canadian Petroleum Technology* 26, 60-66.

White, D., Hirsche, T., Davis, T., Hutcheon, I., Adair, R., Burrowes, G., Graham, S., Bencini, R., Majer, E. and Maxwell S.C. (2004). Theme 2: Prediction, Monitoring and Verification of CO_2 Movements. *IEAGHG Weyburn CO_2 Monitoring & Storage Project Summary Report 2000 - 2004*. Volume 3. 73–148. Print.

White, D., Burrowes, G., Davis, T., Hajnal, Z., Hirsche, K., Hutcheon, I., Majer, E., Rostron, B. and Whittaker S. (2004). Greenhouse gas sequestration in abandoned oil reservoirs: The International energy Agency Weyburn pilot project. *GSA Today* 14 (7), 4-10.

Whittaker, S., Rostron, B., Khan, D., Hajnal, Z., Qing, H., Penner, L., Maathuis, H., and Goussev, S. (2004). Theme 1: Geological Characterization. *IEAGHG Weyburn CO_2 Monitoring & Storage Project Summary Report 2000 - 2004*. Volume 3. 15–69. Print.

List of Acronyms and Abbreviations

ANSS – USGS's Advanced National Seismic System

BPM – Abbreviated title for the Best Practices Manual for the Weyburn project; full title is *Best Practices for Validation CO_2 Geological Storage: Observations and Guidance from the IEAGHG Weyburn-Midale CO_2 Monitoring and Storage Project*

CCS – Carbon Capture and Storage

CCUS – Carbon Capture Utilization and Storage

EERC – Energy and Environmental Research Centre

EOR – Enhanced oil recovery

IEAGHG – International Energy Agency Greenhouse Gas Research and Development Programme

MMV – Measurement, monitoring and verification (of stored CO_2)

PTRC – Petroleum Technology Research Centre

SaskCO_2USER – Saskatchewan CO_2 Oilfield Use for Storage and EOR Research (Optional Phase of the WMP)

USGS – United States Geological Survey

WMP – Abbreviated acronym for the IEAGHG Weyburn-Midale CO_2 Monitoring and Storage Project